Universitat Autònoma de Barcelona

Biomarkers detection of global infectious diseases based on magnetic particles

Soledad Carinelli

ADVERTIMENT. L'accés als continguts d'aquesta tesi queda condicionat a l'acceptació de les condicions d'ús establertes per la següent llicència Creative Commons: http://cat.creativecommons.org/?page_id=184

ADVERTENCIA. El acceso a los contenidos de esta tesis queda condicionado a la aceptación de las condiciones de uso establecidas por la siguiente licencia Creative Commons: http://es.creativecommons.org/blog/licencias/

WARNING. The access to the contents of this doctoral thesis it is limited to the acceptance of the use conditions set by the following Creative Commons license: https://creativecommons.org/licenses/?lang=en

Universitat Autònoma de Barcelona

Biomarkers detection of global infectious diseases based on magnetic particles

Doctoral Thesis

Soledad Carinelli

Supervisora: María Isabel Pividori Gurgo

PROGRAMA DE DOCTORAT DE QUÍMICA
Departament de Química
Facultat de Ciències
2019

Thesis submitted to aspire for the Doctor Degree

Soledad Carinelli

Director´s approval:

Dr. Maria Isabel Pividori Gurgo
Departament de Química
Universitat Autònoma de Barcelona

Bellaterra (Cerdanyola del Valles), june 2019

Acknowledgments

The present work has been carried out in the laboratories of the Grup de Sensors i Biosensors of the Departament de Química from Universitat Autònoma de Barcelona and the Laboratory of Cellular Immunology of the Institute of Biotechnology and Biomedicine thanks to the Marie Curie ITN fellowship provided by Universitat Autònoma de Barcelona and the following financial support:

BioMaX, Novel diagnostic bioassays based on magnetic particles, Marie Curie Initial Training Networks (FP7-PEOPLE-2010-ITN)

Ministry of Economy and Competitiveness (MINECO), Madrid (Project BIO2013-41242-R and BIO2016–75751-R)

Generalitat de Catalunya (Projects 2014 SGR 837)

Grup de Sensors i Biosensors
Unitat de Química Analítica
Departament de Química
Universitat Autònoma de Barcelona
Edifici Cn, 08193, Bellaterra

A mis padres y hermanas,
mis cielos, en aquella, mi tierra lejana.

A Airán y Micaela,
mis raíces, en ésta, mi tierra cercana.

Acknowledgments

En primer lugar quiero agradecer a mi directora de tesis, Isabel Pividori, por haberme dado la oportunidad de realizar esta aventura del doctorado en el Grupo de Sensores y Biosensores y cultivar mi amor por la ciencia. Durante estos años, me diste la posibilidad de trabajar en distintos grupos, de aprender muchas técnicas, de participar en congresos y de colaborar en la BANT School. He aprendido mucho a tu lado. Gracias.

A Mercè Martí, por haberme abierto las puertas del laboratorio de Immunologia cel·lular. Por todas las charlas sobre linfocitos, las horas acompañándome en la campana de flujo y mirando células en el microscopio. Gracias por transmitirme tu amor por el trabajo de laboratorio.

To Mats Nilsson, I thank you for your support and warm encouragement. The two months I have spent there, coinciding with the pregnancy of Micaela, have been one of the most enriching experiences I have lived.

El camino del doctorado ha sido largo y con muchos trayectos, pero en cada uno de ellos he conocido gente maravillosa que me ha acompañado y enseñado en los más diversos sentidos.

A la gente del laboratorio, Susi, Tami, Ale, Anna, Delfina, Rey, Ale, Sandra… Gracias por su tiempo para enseñarme, por los "cafés científicos", por los días del chocolate, por las excursiones a la montaña y la playa, y por tantos momentos bonitos compartidos. A Raquel, Jose, Vane, Anna, Silio, Adrià, Alberto, Melania, Luciano, con ustedes la convivencia ha sido más breve, pero siempre haciendo que los días de trabajo sean amenos, y llenos de sonrisas.

A la gente de la planta y de la torre, Julio, Xavi, Cristina, Marta, Joan, Ferdia, Andrea, Angélica, Jùlia, Fran, Andreu, Anna, y muchos más, con los que he compartido charlas y risas de pasillo o comedor.

A NOSOTRAS AHÍ. Montse, Olga, Susi, Tami, AnaMari, Marta, Pilar, Elena, Cata, Sandra, Silvia, Amanda, a nuestros míster David y Joan. Habéis despertado una vocación efímera, porque eran los entrenamientos con ustedes, las concentraciones, los partidos, las charlas de vestuario, y los viajes juntas, las verdaderas razones de este amor por el FÚTBOL.

A las materas, Montse, Olga y AnaMá, primero por haber amado tanto el mate como lo hago yo. Segundo, por todos y cada unos de los momentos juntas. Han sido un gran sostén. Gracias por haber estado al lado mío y haber compartido mis más grandes alegrías y mis más grandes tristezas.

Montse, mi Montse. Primero nos unió los jueves de chocolate en Analítica, luego el fútbol, le siguieron las tardes de mates y a partir de allí desde casas rurales, viajes, bodas, spas, y hasta Rafaela, esa ciudad perdida en Argentina que te llevó hasta mi familia. Todos los trayectos de este doctorado tienen un trocito de ti. Gracias.

Siguiendo por mi “otro lab”, Inmunología. A Cris, porque a pesar de que al principio solo querías enseñarme un montón de cosas y no compartirme con nadie, me regalaste una de las cosas más bonitas que tengo, estar en tu tribu y ser parte de ella.

A los integrantes de esa tribu. Erika, cada vez que pienso en ti solo veo una carcajada. Te has convertido en una de esas personas tan especiales que se nos olvida llamarnos y cuando hablamos parece que no haya pasado el tiempo. A Javi, gracias por tu apoyo incondicional y todo tu cariño, sobretodo, en este último tramo de la tesis. A Iñaki, por las largas charlas sobre ciencia, historia europea y películas argentinas y porque, a pesar de escuchar millones de veces la misma historia, siempre guardas una sorprendente. A Annabel, Manuel, MariCarmen, Anita, Samu, Diego, Pilar, Anna, Carlos, gracias por todo el afecto, por el aguante en estos años y sobre todo gracias por esta tribu hermosa que hemos construido.

A SPEED Group, gracias a ustedes he crecido muchísimo como científica y como persona. Neus, he aprendido tanto de ti!! Y aunque no consigo materializarlo todo, llevo tus consejos y tu filosofía de trabajo siempre presente. A Juan Pablo, Marina, Irene, Perla, Laura, Inci, Dmitry, Sunil porque, además de mi trabajo en el grupo, han soportado este último gran trayecto. Y a la gente del CNM, porque ha sido una gran experiencia formar parte de “la casa” durante poco más de dos años.

A mi pandilla de Argentina: Jime, Luli, Carla, Vero, Ger, Lisandro, Silvi, Quela, Vane. Acá, allá, da igual el lugar, siempre volvemos a ser nosotros mismos sin tapujos, como si el tiempo no pasara.

Y Finalmente a mis seres queridos que les ha tocado acompañarme durante esta Tesis. A Airán, porque haber hecho el doctorado tiene mucho que ver contigo. Porque en todos mis pasos, y en todas mis caídas siempre has estado a mi lado, y porque he llegado al final de tu mano (que seguiré sosteniendo). Te amo.

A Micaela, porque a pesar de que le has robado millones de minutos de mi tiempo a la tesis, en cada uno de ellos he descubierto y aprendido algo nuevo. Te amo tanto, tanto!

A mis padres Luis y Esthella, a mis hermanas Nati y Pato, y a mis mellis Lauti y Francis. Cuánto daría por tenerlos conmigo! Gracias por toda la comprensión y el apoyo, por todos los besos y abrazos en la distancia. Los kilómetros nunca han logrado alejarnos. Los quiero con el alma.

A Francis y Pablo, mi soporte incondicional. Porque siempre han pensado en mi, incluso cuando yo misma me olvidaba de hacerlo.

A Isa, Fer, Iris, Ruiman y Mael, nuestra pequeña familia canaria. Gracias por haber estado (y estar) siempre presentes.

Y a todos aquellos que han contribuido a hacer esto posible (y que he olvidado mencionar) y me han acompañado a lo largo de este camino. GRACIAS!

Table of Contents

List of symbols and abbreviations

§	Section
AU	Absorbance unit
2D	Two-dimensional
3SR	Self-sustaining sequence replication
Ab	Antibody
Ag	Antigen
AIDS	Adquired immune Deficiency Syndrome
antiCD3-MPs	AntiCD3-modified magnetic particles
antiCD3-PerCP	AntiCD3 antibody peridinin chlorophyll protein labelled
antiCD4-biotin	AntiCD4 antibody biotin labelled
antiCD4-FITC	Anti-CD4 antibody Fluorescein Isothiocyanate labelled
antiDIG-HRP	Anti-digoxigenin-peroxidase Fab fragments
antiFLU-HRP	Anti-fluorescein-peroxidase Fab fragments
Anti-TNF	Anti-tumor necrosis factor
ART	Antiretroviral treatment
Au-NP	Gold nanoparticles
Av-GEC	Avidin graphite-epoxy composite
BIO	Biotin
BSA	Bovine Serum albumin
BSL	Biosafety Level
C2CA	Circle-to-circle amplification
CBA	Cytometric Bead Array
CDC	Centers for Disease Control and Prevention
cDNA	Complementary DNA
CMV	Cytomegalovirus
DENV	Dengue virus
DEPC	Diethylpyrocarbonate
DIG	Digoxigenin
DNA	Deoxyribonucleic acid
dsDNA	double-stranded DNA
DTT	Dithiothreitol
EBOV	*Ebolavirus*
EBV	Epstein Barr virus
EDS	Energy dispersive X-ray spectroscopy detector
ELISA	Enzyme-linked immunosorbent assay
ELISPOT	Enzyme-linked immunospot
PBS	Phosphate buffered saline
EU	European Union
EVD	Ebola virus disease
FC	Flow cytometry
FDA	Food and Drug Administration
FET	Field-effect transistors
FLU	Fluorescein
FSC	Forward scatter
GAPDH	Glyceraldehyde 3-phosphate dehydrogenase
gDNA	Genomic DNA
GEC	Graphite-epoxy composite
GP	Glycoprotein
HA	Hemagglutinin
HDA	Helicase-dependent amplification
HIV	Human Immunodeficiency Virus
HQ	Hydroquinone
HRP	Horseradish peroxidase
HRPII	Histidine-rich protein II
IFN-γ	Interferon gamma
IgG	Immunoglobulin G
IgM	Immunoglobulin M
IGRA	Interferon-γ release assay
IL	Interleukin

IMDM	Iscove's Modified Dulbecco's Medium
IMS	Immunomagnetic separation
IUPAC	International Union of Pure and Applied Chemistry
LAMP	Loop-mediated isothermal amplification
LIA	Line immunoassays
LOD	Limit of detection
MARV	*Marburgvirus*
m-GEC	Magneto graphite-epoxy composite
MNP	Magnetic nanoparticles
MP	Magnetic particles
mRNA	Messenger RNA
MW	Molecular weight
NA	Neuraminidase
NASBA	Nucleic acid sequence-based amplification
NAT	Nucleic acid test
NK	Natural killer cells
NP	Nucleoprotein
PBMC	Peripheral blood mononuclear cell
PBS	Phosphate buffered saline
PCR	Polymerase chain reaction
PHA	Phytohemagglutinin
polydT-MPs	PolydT modified magnetic particles
ProtA-GEC	Protein A graphite-epoxy composite
qPCR	Quantitative polymerase chain reaction
q-RT-PCR	Quantitative Reverse Transcription Polymerase Chain Reaction
RCA	Rolling circle amplification
RDT	Rapid diagnostic test
REM	Rapid expansión method
RIN	RNA Integrity number
RNA	Ribonucleic acid
RPA	Recombinase polymerase amplification
RSD	Relative standard deviation
RT	Room temperature
RT-PCR	Reverse Transcription Polymerase Chain Reaction
SD	Standard deviation
SDA	Strand displacement amplification
SEM	Scanning electron microscope
SPE	Screen-printed electrodes
SSB	Single stranded binding proteins
SSC	Side scatter
Strep-Cy5	Streptavidin pentamethine cyanine labelled
StreptAv-MPs	Streptavidin modified magnetic particles
SWV	Square wave voltammetry
TAE	Tris-Acetate-EDTA
Taq pol	DNA polymerase from Thermus aquaticus
TAS	Transcription-based amplification system
TB	Tuberculosis
TCR	T cell antigen receptor
TE	Toxoplasmic encephalitis
Th	T helper
TMA	Transcription-mediated amplification
TMB	3,3',5,5'-Tetramethylbenzidine
tRNA	Transfer RNA
UNAIDS	Joint United Nations Programme on HIV and AIDS
VP	Virion proteins
WHO	World Health Organization

List of Tables

Chapter 1

Chapter 3

Chapter 4

Chapter 5

Chapter 6

List of Figures

Chapter 1

Chapter 3

Chapter 4

Chapter 6

Resumen

Las enfermedades infecciosas suponen una gran amenaza para la salud mundial debido a la rápida diseminación y adaptación de los patógenos, favorecida por el turismo, la migración y los movimientos a través de las fronteras.

El papel principal del diagnóstico clínico es identificar de forma fehaciente una enfermedad en un paciente. La rapidez en el diagnóstico permite que el paciente reciba una terapia antimicrobiana específica, evitando tratamientos empíricos o con fármacos inapropiados. La administración del tratamiento adecuado previene la propagación de la infección, reduciendo la morbilidad y mortalidad. Los dispositivos de diagnóstico rápido permiten detectar enfermedades y monitorearlas de forma confiable en cualquier centro sanitario, reduciendo el coste social y del paciente. Entre estos dispositivos, los biosensores electroquímicos presentan una alta sensibilidad y especificidad así como una instrumentación sencilla, pudiendo expandirse fácilmente a plataformas de detección múltiple. Además, la integración de partículas magnéticas (MPs) en métodos de diagnóstico rápido incrementa la sensibilidad y especificidad debido su capacidad para aislar y preconcentrar una molécula diana cuando éstas son modificadas con elementos de bioreconocimiento específico, tales como anticuerpos u oligonucleótidos. Así, las MPs modificadas pueden unirse específicamente a biomarcadores y concentrarlos de muestras complejas bajo la actuación magnética, eliminando posibles interferencias.

En esta tesis se presenta el desarrollo de estrategias de diagnóstico basados en tecnologías emergentes, asequibles y que requieren un entrenamiento mínimo de los usuarios finales, tales como los biosensores electroquímicos con accionamiento magnético. Estos dispositivos brindan resultados rápidos, y permiten tomar acciones inmediatamente, como por ejemplo la prescripción de un tratamiento adecuado durante la primera visita médica.

En primer lugar, se presentan dos tipos de pruebas diagnósticas para la cuantificación de linfocitos CD4 en sangre entera, usando MPs. Se describen dos formatos, uno que se realiza en microplacas de poliestireno tipo ELISA con detección óptica y otro usando electrodos de grafito-epoxi con biosensado electroquímico. En ambos casos la estrategia de recuento de células CD4 se basa en a) el aislamiento de células CD4 usando MPs modificadas con anticuerpos antiCD3 y su marcación utilizando anticuerpos antiCD4 biotinilados; b) la marcación enzimática con estreptavidina-peroxidasa; y c) la detección basada en la actividad de la enzima. La separación y marcación de los linfocitos se realiza a través de los receptores

de membrana CD3 y CD4. Esta doble marcación no sólo evita interferencias de otras células que expresan alguno de estos receptores, sino que aumenta la especificidad del ensayo. Así, el Capitulo 3 y 4 describe el desarrollo y la evaluación de dichas estrategias para el seguimiento rápido de pacientes con HIV en entornos de bajos recursos.

En el capítulo 5 se describe un ensayo de liberación de interferon-γ basado en la detección electroquímica de dicho trascripto producido por linfocitos T previamente aislados de sangre. Este test utiliza partículas magnéticas para el aislamiento y preconcentración de tres dianas diferentes (linfocitos T, mRNA y ADN doblemente marcado) en el mismo ensayo. En primer lugar los linfocitos T se aislan de la sangre usando MPs modificadas con anticuerpos antiCD3. En segundo lugar, el mRNA de los linfocitos se preconcentra sobre MPs modificadas con polidT mediante unión a la cola de poli(A). Posteriormente se retrotranscribe el mRNA y se amplifica el cDNA mediante PCR múltiplex con marcación doble para la amplificación específica de IFN-γ y gliceraldehído-3-fosfato deshidrogenasa. Finalmente, se inmovilizan los amplicones biotinilados en MPs modificadas con estreptavidina, y se realiza el genosensado electroquímico para la detección de IFN-γ a través del otro marcador del cebador. Esta estrategia se propone como alternativa a los ensayos de liberación de IFN-γ que se usan en la actualidad para la identificación de la Tuberculosis.

Por último, se presenta el diseño de un test de diagnóstico rápido, específico y altamente sensible basado en la amplificación isotérmica sobre MPs con detección electroquímica. Las técnicas de amplificación isotérmicas han surgido como una alternativa a los métodos basados en PCRs para la identificación de microorganismos infecciosos, debido a la barrera que éstos últimos muestran para su implementación en entornos de bajos recursos. El capítulo 6 presenta la detección electroquímica de ADN usando sondas candado con amplificación isotérmica de círculo rodante y amplificación círculo a círculo. Esta estrategia ha demostrado ser una poderosa herramienta para la detección específica y sensible de ácidos nucleicos para su aplicación en el diagnóstico clínico.

De acuerdo con todas las estrategias descriptas, los biosensores electroquímicos representan una gran promesa para la detección de forma más rápida, simple y económica comparado con los métodos tradicionales de diagnóstico de enfermedades infecciosas. Además, las estrategias desarrolladas en esta tesis demuestran un gran potencial para su aplicación en entornos de bajos recursos.

Summary

Infectious diseases are becoming a major threat worldwide due to the fast dissemination and adaptation of pathogens favored by the unrestricted globalization, increasing migration and traveling and moving across the borders.

The primary role of diagnostics is to identify a disease. The rapid identification of a disease allows the patient to be placed on a specific antimicrobial therapy and avoid prolonged management on empiric, potentially inappropriate drug. Moreover, prompt initiation of proper therapy prevents the spread of communicable disease and lead to dramatic reductions of infection-associated morbidity and mortality. Therefore, point-of-care devices that can reliably detect and/or monitor diseases would result in an improved care, reduction of antibiotic prescription, and minimization of patient and societal cost of illness. Among them, electrochemical biosensors have the advantage of high sensitivity/specificity as well as simplicity of instrumentation, and can be easily expanded to multiplex detection platform. Furthermore, the integration of magnetic particles (MPs) in point-of-care tests provides an even increased sensitivity and specificity due to the isolation and preconcentration of the target, whether MPs are modified with a specific recognition biomolecule (antibodies or oligonucleotides). Modified-MPs can thus specifically bind the biomarkers and preconcentrate them from the complex specimen under magnetic actuation, preventing interferents before testing.

Affordable emerging technologies requiring minimal training for final users, such as magnetic actuated electrochemical biosensors, are presented in this dissertation in order to provide rapid results and to enable taking action immediately, for instance the prescription of appropriate treatment at first visit.

Firstly, two simple diagnostic tests for CD4+ T lymphocytes quantification, directly in whole blood, and based on magnetic particles are presented. The assay is performed in polystyrene microplate in an ELISA-like format for the optical detection or using graphite-epoxy electrodes for the electrochemical biosensing strategy. In both cases, the CD4 counting strategy has involved three main steps: a) immunomagnetic separation of CD4+ T cells by antiCD3-MPs and labeling by using biotinylated antiCD4 antibody; b) enzymatic labeling; and c) detection based on the peroxidase activity. The isolation and labeling of lymphocyte is performed using two cell receptors: CD3 and CD4. The dual labeling not only avoids interferences of other cells expressing single membrane receptors, but also increases the specificity of the assay. Thus, the

development and evaluation of magnetic-actuated rapid HIV diagnostic platforms appropriate for their use in low resource settings for the following-up of patients under treatment is demonstrated in Chapter 3 and 4.

Secondly, an interferon-γ release assay based on electrochemical detection for interferon-γ transcript detection produced by isolated T lymphocytes is described. This approach also involves the integration of MPs for the isolation and preconcentration of three different targets (including whole T lymphocytes, mRNA transcripts and double-tagged DNA) in the same test. Accordingly, T lymphocytes are isolated from whole blood using antiCD3-MPs. Secondly, mRNA presenting poly(A) tail is preconcentrated on polydT-MPs from T lymphocyte. Afterward, mRNA is retrotranscripted and cDNA amplified by multiplex double-tagging PCR for the specific amplification of IFN-γ and glyceraldehyde-3-phosphate dehydrogenase. Finally, one of the tags of the primers is used for the amplicons immobilization on streptavidin-MPs as support, while the electrochemical magneto-genosensing for transcript detection is performed using the other tag. This strategy, described in detail in Chapter 5, results in an alternative for IFN-γ release assays, which can be used for identifying infectious states such as Tuberculosis.

Finally, the design of a diagnostic test involving a rapid, specific and highly sensitive procedure based on isothermal amplification on MPs with electrochemical readout is presented. Isothermal amplification techniques are emerging as good candidates to replace PCR for the identification of infectious microorganism, since PCR-based method can be a critical barrier in low resource settings. An electrochemical DNA detection using padlock probes and the subsequent amplification with rolling circle and circle to circle amplification is presented in Chapter 6. This strategy has demonstrated to be a powerful combination for highly specific and sensitive nucleic acid detection that can be applied in clinical diagnosis.

Accordingly, to all these applications, electrochemical biosensors offers considerable promise for obtaining information in a faster, simpler and cheaper manner compared to traditional methods for infectious disease diagnosis. Moreover, the strategies developed in this dissertation possess great potential in many applications, in low resource settings.

Chapter 1

INTRODUCTION

1.1 Infectious diseases

Infectious or communicable diseases are caused by pathogenic microorganisms, including bacteria, viruses, fungi or parasites. Infectious agents can be spread, directly or indirectly, from one person to another. On the other hand, zoonosis diseases are diseases of animals that can cause illness when transmitted to human. However, in normal conditions, some bacteria are usually present in different parts of the body without producing diseases, constituting the normal flora.[1]

An infection results when a pathogen invades a host and begins growing while a disease impairs the normal tissue function as a consequence of a microorganism invasion. The time elapsed between infection and clinical symptoms is called incubation period and it depends on the organism causing the infection. Sometimes, during this period, the microorganism can be transmitted to other people while in other instances, the infected person is not contagious until the illness begins. The signs and the symptoms depend on the pathogenic agent, but often include fever and fatigue. Most of the infections are diagnosed based on the symptoms and further treated with medicines, requiring in some instances hospitalization.

A disease outbreak is defined as the occurrence of illness cases in a large number compared to the normal case number. It can be also considered the appearance of a disease not previously recognized in a specific area or community. During an outbreak, the authorities have to consider actions to limit and control the spread of the disease in order to avoid a pandemic. Social distancing, patient quarantine and, isolation are usually recommended.

The spread of an infectious disease from one place to another is called *Chain of Infection*.[2] This process consists of six different links [3,4] that are connected (Figure 1.1):

Etiologic agent. It is the microorganisms that can cause a disease, including bacteria, virus, fungi or parasites.

Reservoir. It is the habitat in which the infectious agent normally lives, grows and multiplies.

Portal of entry. It refers to the manner in which a microorganism enters a susceptible host. The portal of entry usually includes the mucous membranes, including the skin, the respiratory, and the gastrointestinal tracts.

Portal of exit. It is the path by which a microbe leaves the host. For example, through the nose, mouth by sneezes or coughs, by feces, or through body fluids.

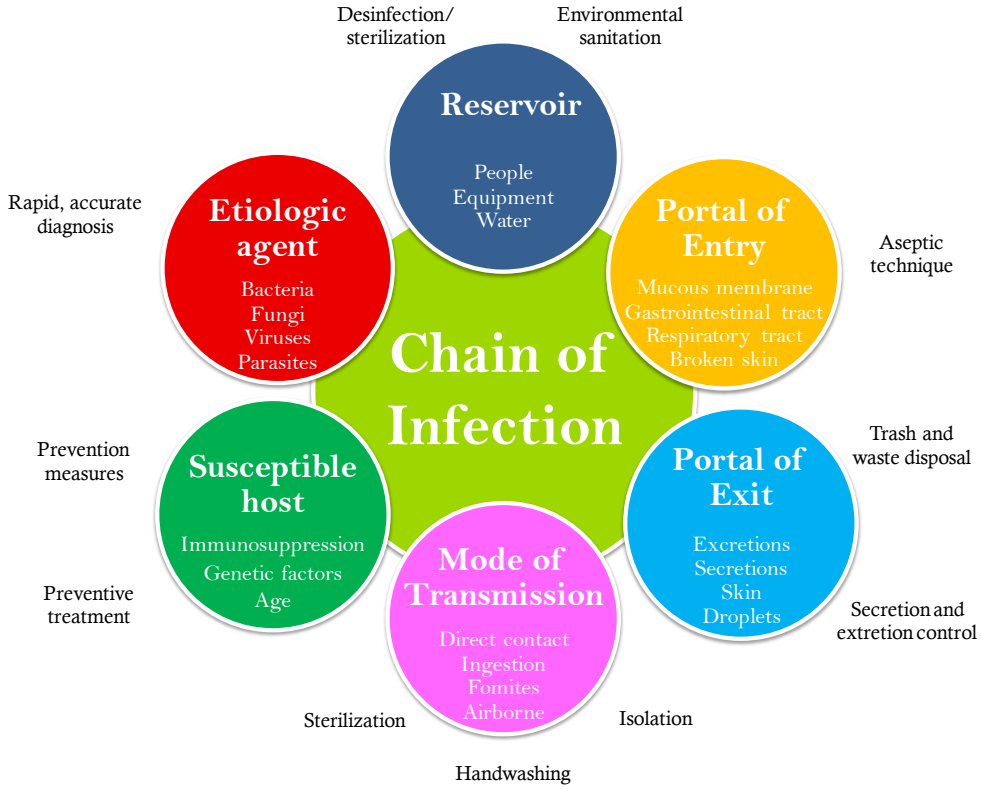

Figure 1.1. The *Chain of Infection* and preventing actions to interrupt the spread of an infection. Figure adapted from Heller and Veach, 2008.[5]

Mode of transmission. It is the vehicle to carry the causative agent from the host to other people or place. The transmission can be direct (by contact with the infectious host) or indirect (through intermediate such as animal vectors, air, food, water, contaminated equipment or other sources).

Susceptible host. It is the final link in the chain of infection. Several factors are related to the susceptibility to infection, including age, genetic factor, the presence of chronic diseases or conditions that weaken the immune system, certain types of medications, malnutrition, and exposure to the infectious agent reservoir.

The infective processes can be interrupted by breaking any link of the chain.[6] For example, the early identification of the causative agent allows the design of preventive action to control the spread of the infection.[5] Figure 1.1 outlines the components of *Chain of infection* and some preventive action to avoid the spread of an infectious process.

1.2 Global impact of infectious diseases

Infectious diseases affect the daily life of million people all around the world, and are responsible for hundreds of thousands of deaths, mostly in the developing countries. Although most of these major infectious diseases are treatable, the early detection of people requiring treatment remains a major issue.[7]

Despite the impact of the biotechnology, nanoscience and information and communications technology in daily life, the burden of infectious disease is still an issue, affecting global health.[8] According to the World Health Organization (WHO) database and the last survey available, in 2016, approximately 6.6 million people died due to infectious diseases, being lower respiratory infection, diarrhea diseases, and tuberculosis the main causes of these deaths. In addition, every year millions of people fall ill due to infectious diseases. In detail, 1.8 million people becoming newly infected of HIV (Human Immunodeficiency Virus), more than 10 million people fell ill with tuberculosis, and there were an estimated 216 million cases of malaria in 2016. The globalization and the population movement have accelerated the spread of infectious disease outbreaks around the world that initially were geographically localized.[9]

Table 1.1 shows the leading causes of death in the World during 2016, including communicable and non-communicable diseases.[10]

Table 1.1. Leading causes of death worldwide. Data taken from *WHO, Global health estimates 2016 summary tables.*[10]

Cause of death	World position	Deaths (x1000s)
All causes		**56,874**
Lower respiratory infections	4	2,957
Diarrheal diseases	9	1,383
Tuberculosis	10	1,293
HIV/AIDS	14	1,012

In most of the cases, early diagnosis and treatment can interrupt the transmission of the infectious agent and prevent the development of long-term complications.

Infectious disease is a matter of national security and has a great impact on public health and the world economy. Access to drugs has improved markedly over the past decade with the advent of drug-access campaigns, mass-treatment programs and public resources promoting by the United Nations Millennium Development Goals.[11] Most global health centers are in

high-income Europe Union countries with strong links with low-income countries,[12] due to the investing support of the European Parliament in research and development for global health. Although global improvements in prevention, early detection, control and treatment are becoming more effective at reducing the number of people infected, infectious diseases still continue to have a huge impact on the quality of life of people worldwide. In addition, economic barriers accentuate this problem in areas with limited resources. For example, 40% of deaths in low-income countries are children under 15 years and only the 20% are older than 70 years, being communicable diseases the main causes of deaths such as lower respiratory infections, HIV/AIDS, diarrheal diseases, malaria and tuberculosis.[13]

The development of novel diagnostic tests is of great importance for the rapid identification of infectious agent and disease prevention. Nevertheless, despite large advances in diagnostic technologies, many patients with suspected infections receive empiric antimicrobial therapy rather than appropriate therapy dictated by the rapid identification of the infectious agent.[14] For instance, several studies document at least 50% of adult and pediatric patients with upper respiratory tract infections receive antibiotics,[15,16] despite the fact that the majority of these illnesses are caused by viruses. As a result, the overuse of effective antimicrobials produces increasing levels of antimicrobial resistance.

Summarizing, infectious diseases continue devastating economies and damaging health systems, especially in the poorest countries. This fact is favored by the fast dissemination and adaptation of pathogens, and promoted by the unrestricted cultural globalization, the increasing migration and travelling, and the moving across the borders. Progress remains irregular and millions of people are not being reached with prevention measures and treatment. The diagnostic tests of these infection diseases affecting global health in the developing world should be simple and affordable in low-resource settings without any lost in the analytical performance. The complexity of a test includes the need for user interpretation, the level of training, the number of manual manipulations, the user intervention steps, and the instrumentation required.[17,18]

1.3 Laboratory techniques for the diagnosis of infectious diseases

The development of robust diagnostic tests for the specific and sensitive detection of biomarkers is one of the biggest challenges in the medical field. The approach of diagnostics based on single biomarkers has changed, and multiplex detection may result in improved detection.[19]

Due to infectious disease can be caused by a wide variety of microorganisms, clinical signs and symptoms are useful to help the practitioner to identify the type of infection, and depending on it, a laboratory test of any fluid can be ordered (blood, urine, sputum, genital secretions, among others). The most common types of methods for the infectious agent identification are described in this section.[20]

1.3.1 Microscopy

This technique provides a morphological evaluation of the infectious agent by identifying their size, shape and cellular structure.[21] The samples are obtained directly from the patient as sputum, blood, urine, among others. The accurate identification of the pathogens depends on the experience of the microscopist and the quality of the equipment.[22]

In many cases, microscopic detection is used in combination with biochemical and/or antibody-based staining. The main limitation of this technique is that microscopy usually requires at least $1\times10^{4\text{-}5}$ organisms per mL, limiting their sensitivity.[1] The preconcentration of the sample by centrifugation and fluorescent stains are strategies usually used to increase the sensitivity.

1.3.2 Microbiological Culture

This technique is considered the gold standard method for most of the pathogenic agent. The microorganism is allowed to grow in a specific growth medium and then detected based on the size, shape, color of the colony and the changes produced by its growth.[23] Cultures generally take from a few days to several weeks depending on the microorganism. For instance, *Mycobacterium tuberculosis* are slow growing and the culture may take up to 2 months to grow, while there are others that result extremely dangerous to culture, such as *Ebolavirus*. In some cases, when a microorganism is cultured and identified, a variety of

antimicrobial drugs can be also added in order to assess its susceptibility to antimicrobial drugs and to determine which treatment will be most effective against that pathogen.[23] This kind of test is known as disk diffusion or Kirby-Bauer test.

1.3.3 Immunological test

This methodology is based on the specific binding of an antibody (Ab) and an antigen (Ag). Antibodies are proteins that are normally produced by the immune system in response to a foreign agent, while an antigen is defined as a molecule capable of inducing an immune response in the host organism.[24] Immunological tests can be designed to detect as a target either the antigen or the antibody. In the first strategy, the pathogenic agent is directly detected as an antigen, by means of a specific antibody produced *in vitro* in the animal host. On the other hand, the specific antibodies (usually immunoglobulin M and G class) naturally produced in the patients against the pathogen can be also detected. Depending on the pathogen, one of these strategies can be more sensitive than the other. The antigen-antibody complex can be thus detected by labeling either the antigen or the antibody. These tests are usually performed on serum samples. Several techniques may be employed, described below.

1.3.3.1 Precipitation tests

It is based on the fact that some soluble antigens can form a lattice-like structure when interact with antibodies, producing visible precipitates. Ouchterlony double diffusion and counter immunoelectrophoresis are examples of precipitation tests. These tests are currently used in fungal infection or pyogenic meningitis. As a positive result requires a large amount of analyte to produce a visible precipitate, the sensitivity is usually poor.[25] Precipitation test can increase its sensitivity by attaching soluble antigens to large carriers such as latex beads, converting precipitation tests in agglutination test.[26]

1.3.3.2 Agglutination test

This test differs from precipitation in the size and solubility of the antigen. The cross-linking reaction between particulate-micro sized antigens and antibodies produces, instead of precipitation, visible clumps.[25] Agglutination is more sensitive than precipitation and it is currently used for virus detection (influenza and Newcastle virus) and in the detection of specific antibodies towards syphilis and *Salmonella* infections.

1.3.3.3 Enzyme-linked immunosorbent Assay (ELISA)

This methodology is usually performed on a polystyrene 96-well microplate, in which one of the immunological pair is immobilized by adsorption. It can be also designed to detect as a target either the pathogens as the antigen or, instead, the antibodies produced by the patient as consequence of an infection.[27,28] An enzyme, usually horseradish peroxidase (HRP) linked to one of the immunological species, is used as a label to achieve the optical readout. The detection is performed by assessing the enzymatic activity. The optical density is correlated with the enzyme activity which is directly proportional to the target concentration present in the sample.

As previously stated, ELISA can be performed, with some modifications, in different formats in order to detect either an antigen or an antibody in case of infectious diseases, as schematically shown in Figure 1.2. The antigens are usually detected using sandwich immunoassay format. This type of assay involves the use of two antibodies, one for the analyte capture and the other one for the detection.[29] The capture antibody is attached to the solid phase. The antigen is then added, followed by the detection antibody, which binds the antigen at a different epitope than the capture antibody. As a result, the antigen is 'sandwiched' between the two antibodies (Figure 1.2, panel A and B).[27] Sandwich ELISA presents higher specificity due to the use of two antibodies to detect the antigen.

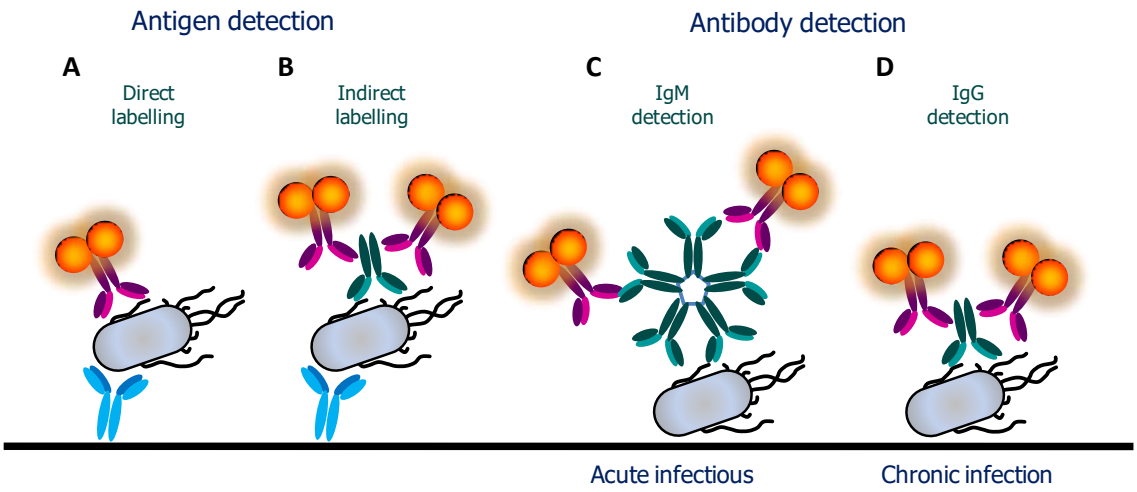

Figure 1.2. Types of ELISA test based on the target immobilization and detection format. A) Direct sandwich ELISA for antigen detection; B) Indirect sandwich ELISA for antigen detection; C) Direct Sandwich ELISA for IgM antibody detection; D) Direct sandwich ELISA for IgG antibody detection.

The detection antibody can be directly attached to an enzyme conjugate, in which case this is referred to as a direct sandwich ELISA (Figure 1.2, panel A).[30] If the detection antibody used is unlabeled, a secondary enzyme-conjugated detection antibody is required. This format is known as an indirect sandwich ELISA (Figure 1.2, panel B). When a secondary antibody is used, there is a signal amplification, which usually increases the assay sensitivity. It is due to more than one labeled secondary antibody can bind the primary antibody. However, indirect ELISA assays is longer than direct ELISAs since an additional incubation step is required.

On the other hand, immunoassay for the detection of antibodies involves the binding of the antigen to the solid surface instead of an antibody.[29] Thus, when the sample is added (usually human serum), the specific antibodies produced as a consequence of infection bind to the antigen coated on the plate (Figure 1.2, panel C and D).

Antibody detection is used to detect the antibodies in response to an infectious agent. After the exposure to a pathogen, the immune response is characterized by an early rise of antigen-specific Immunoglobulin M (IgM). The levels of IgM subsequently decline. However, if the infection is chronic or persistent, or even in case of previous infection, the amount of antibody increases followed by affinity maturation, switching to the production of Immunoglobulin G (IgG) antibodies of increased affinity.[31] Thus, IgM antibody detection is used to identify for primary or acute infection (Figure 1.2, panel C), while IgG antibody indicates previous exposure to the virus or parasite (Figure 1.2, panel D). IgM is commonly used for acute hepatitis A, B, and E infections, dengue, Zika, HIV, Ebola virus, and Chikungunya virus, among others,[32] while IgG is required in order to assess the stage of infection.

Other techniques based on the same concept, but using different labels as readouts, are immunofluorescent assay and radioimmunoassays. In these techniques, antibodies are labeled with fluorescent dyes or radioactive material, respectively, instead of enzymes.

1.3.3.4 Western blot

This method relies on the protein separation by gel electrophoresis on the basis of the molecular weight, followed by the immunological detection.[33,34] The proteins are then transferred to a membrane producing characteristic bands for each protein. Finally, the membrane is incubated with labeled-antibodies specific to the protein of interest.[34] The combination of electrophoresis and enzyme detection confers a very high specificity to the

method being used to confirm a positive result obtained by a screening test. This technique is widely used as confirmatory test for HIV diagnosis as described in *§1.6.6.3*.

1.3.4 Nucleic acid-based diagnostic tests

These methods, described in detail in *§1.4*, are based on the genetic identification of the pathogen by detecting specific DNA (deoxyribonucleic acid) or RNA (ribonucleic acid) sequences. They are also used for assessing the drug susceptibility by identifying resistance genes or mutations. Genital infections caused by *Chlamydia trachomatis* or *Neisseria gonorrhoeae, or* pharyngitis caused by group A *Streptococcus* can be currently detected by nucleic acid test (NAT) with non-amplified samples due to the high concentration of the pathogen in the biological fluids. However, the detection of DNA sequences may require the DNA amplification depending on the infectious agent concentration. Polymerase Chain Reaction (PCR) is the amplification method most widely used to amplify the DNA or RNA target for reliable detection, further described in *§1.4.2.1*. Nevertheless, in the last decades isothermal techniques have emerged as rapid and efficient amplification method that can be performed at a constant temperature without thermal cycling, simplifying the procedure and the equipment required.

1.3.5 Other detection methods

This group of techniques is used for the identification of an organism after its isolation. They involve the classical biochemical testing as well as instrumental methods, such as chromatography or mass spectroscopy. Chromatographic methods are used to identify microorganisms by analyzing and comparing the fatty acid profile in a database, while in mass spectroscopy, the microorganisms are identified by analyzing the protein profile according to their relative mass and abundance. The main advantage of mass spectroscopy is that an organism can be identified in less than 1 h. These techniques are also used for warfare and bioterrorism agents.

1.4 Molecular diagnosis in infectious disease

Molecular detection assays are increasingly becoming routine diagnostic techniques for the identification of microorganisms based either in their genome (genetic material) or in their gene expression level.

1.4.1 Genetics and DNA

Genetic is defined as the study of genes, genetic variation, and heredity in living organisms.[35] In the early twentieth century, the chromosomes were identified as the carriers of genetic material and were described as linear structures with genes located at specific sites along them.[36] Each gene is a sequence of DNA and it is compacted in the nucleic acid constituting the chromosomes. Moreover, DNA holds the code for synthesizing proteins. In this process the DNA is read and transcribed into a messenger molecule of RNA (mRNA) that will serve as a template to produce a protein by assembling aminoacids.

The chemical composition of nucleic acid was determined by Albreacht Kossel by isolating the five nucleotide bases that are the building blocks of DNA and RNA: adenine (A), cytosine (C), guanine (G), thymine (T) and uracil (U).[37,38] This work was awarded the Nobel Prize in Physiology of Medicine in 1910. Later, in 1929, Phoebus Levene showed that the components of DNA were linked in the order phosphate-sugar-base,[39] while Erwin Chargaff reported that in DNA molecule the number of guanine is equal to the number of cytosine units, and the number of adenine units equals to thymine. Thereafter, in 1952, Rosalind Franklin obtained an X-ray diffraction image [40] which was used to formulate the DNA molecular model of double-helix by Watson and Crick in 1953.[41]

1.4.2 Nucleic acid-based amplification method

The development of molecular diagnostic techniques represents a great step towards the sensitive and accurate diagnosis, and follow-up of infectious diseases.[42-44] Molecular diagnostics of low abundance targets require the use of nucleic acid based amplification method. Next sections describe the most used amplification methods for nucleic acid detection.

1.4.2.1 Polymerase chain reaction

The PCR allows the production of billions of copies (amplicons) from the amplification of single or few DNA sequences (also called templates) by two oligonucleotide primers, and performed by the enzyme DNA polymerase. A primer is defined as a short segment of single-stranded DNA (usually from 20 to 30 nucleotides) that determines the beginning and the end of the amplified region. Two primers (forward and reverse) are required, each complementary to one strain of DNA template, as it is depicted in Figure 1.3.

PCR consists in repeated thermal cycles that involve three steps: denaturation, annealing and extension. In denaturation step, the DNA is melted at 94-98 °C for 20-30 sec in order to break the hydrogen bonds holding the two strands of DNA. During the annealing, the temperature is lowered up to 50-65 °C (depending on the primer lengths and composition). In this step, the primer specifically binds to the complementary DNA template. Finally, in the extension/elongation step usually performed at 72 °C, the DNA polymerase synthesizes a new DNA strand complementary to the DNA template by adding deoxynucleotides (dNTPs) in 5´ to 3´direction (Figure 1.3).

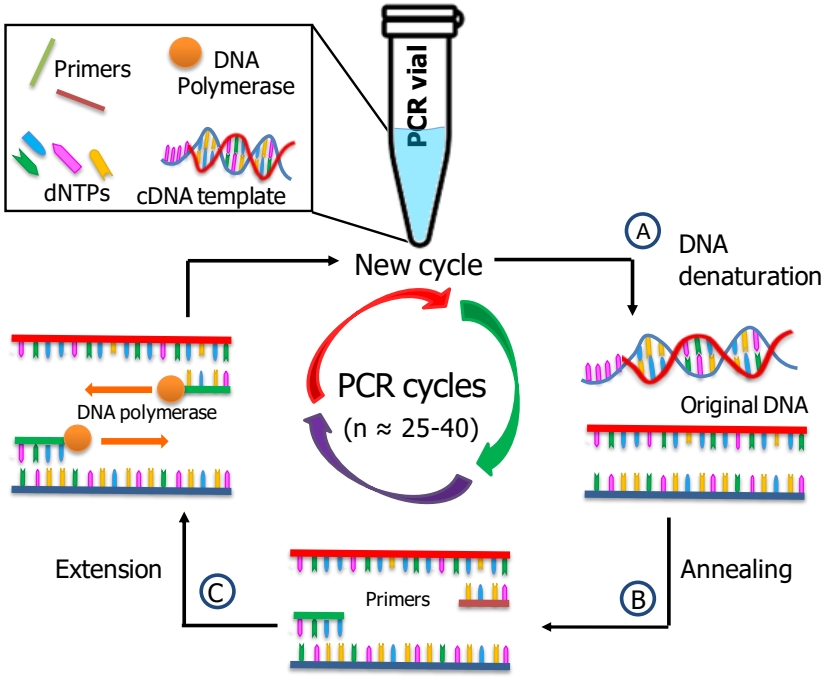

Figure 1.3. Representation of the PCR procedure. Each cycle involves the following three steps: (A) DNA denaturation, (B) primers annealing and (C) DNA extension. When the cycle is repeated several times, the net result is an exponential increase in the number of DNA copies.

In Reverse Transcription Polymerase Chain Reaction (RT-PCR), the RNA is first converted to a complementary DNA (cDNA) by the enzyme reverse transcriptase, and further amplified by PCR.[45] This technique plays an important role in diagnosing RNA virus infections, detecting viable *Mycobacteria* species, and monitoring the effectiveness of antimicrobial therapy. Moreover, RT-PCR provides the possibility to assess gene transcription in cells or tissues. The analysis of mRNA is a useful tool for the study of gene expression. Thus, the expression of some genes is controlled by the environmental changes. For instance, interferon gamma gene is expressed and secreted as a protein during viral infection to activate the specific immune response.

Another approach is the multiplex PCR, in which two or more microorganisms can be detected simultaneously by using two or more sets of primers specific for the different DNA targets. However, multiplex PCR is usually less sensitive. Primers used in multiplex PCR must be carefully designed to have similar annealing temperatures, which often require extensive empirical testing.

The amplicons generated during PCR are usually analyzed by gel-electrophoresis, capillary electrophoresis, or fluorescent probes, among others. Electrophoresis is a technique commonly used to separate charged molecules as DNA, RNA and proteins according their size by applying an electric field to move the charged molecules through a matrix. Large molecules migrate slowly and travel a shorter distance through the gel than smaller ones. This phenomenon is called sieving. The type of gel depends on the analyte to be detected. Thus, agarose gels are usually used for DNA, showing a wide range of separation (from 50 to 20,000 base pairs) while polyacrylamide gels are typically used for proteins and small fragments of DNA (from 5 to 500 base pairs). The identification of the amplified DNA is achieved by adding a dye and visualized with an ultraviolet transilluminator. By using molecular markers, it can be determined the amplified fragment size by their comparison to linear DNA fragments of known lengths. Figure 1.4 shows a schematic representation of a gel loaded with DNA samples into an electrophoretic tank and a picture of typical gel visualization after the exposure to UV light.

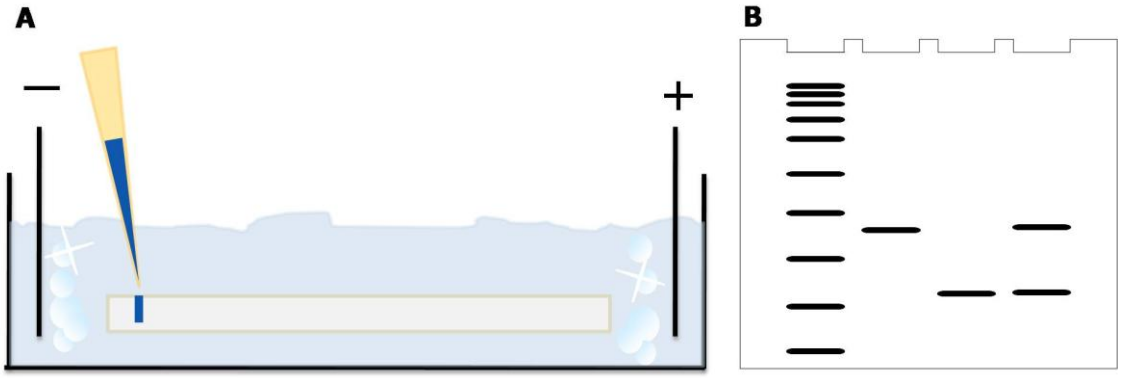

Figure 1.4. Illustration of DNA electrophoresis setup used to separate DNA fragments according its size. (A) A gel sits within a tank of buffer. The DNA samples are placed into wells at one end of the gel and an electrical current passed across the gel. The negatively-charged DNA moves towards the positive electrode. (B) Visualization of the DNA band according their fragment size.

Real-time polymerase chain reaction, also known as quantitative polymerase chain reaction (qPCR), allows not only the amplification, but also the amplicon quantification, avoiding any additional post-PCR processing. qPCR detects the accumulation of amplicons after each thermal cycle (in real time) by using fluorescent probes so that the amount of PCR product correlates to the initial amount of target template. Digital PCR is the most recent PCR-related technique appeared in the market. In this technique instead of recording the degree of amplification, the reactions take place in individual compartments and are treated as binary response, that is, with or without amplification product (‘‘yes’’ or ‘‘no’’ answer).[46]

1.4.2.2 Isothermal techniques

Isothermal amplification of nucleic acid enables rapid and specific amplification of RNA or DNA at constant temperature, avoiding the requirement of thermocycler machines. These techniques have demonstrated to be more resistant to inhibitors in complex samples compared to PCR. This property is conferred by the polymerase enzyme used for the isothermal amplification. Moreover, isothermal amplifications have been satisfactorily used for in situ or intracellular bioimaging and sequencing. There are different isothermal amplification methods, based on a different enzymatic or molecular strategy.[47] The most commonly isothermal techniques are described below.

1.4.2.3 Helicase-dependent amplification (HDA)

This technique mimics the *in vivo* DNA replication process and is based on the same principle of PCR in which two primers are used for the specific hybridization to the 5´and 3´target borders, and a polymerase enzyme extends the annealed primer by adding dNTPs to generate double-stranded products. Here, heat denaturation is replaced by the DNA helicase enzyme that is able to separate double-stranded DNA and generate single-stranded templates for primer hybridization and subsequent extension.[48] The two single strands are maintained separately by the action of single stranded binding proteins (SSB), making possible the template extension at 37 °C (Figure 1.5).

The main limitations of HDA are the low speed and processivity of helicase, and the lack of coordination between the helicase and the polymerase.[49] However, some improvements in the speed and processivity of the polymerase were reported, allowing DNA fragment amplification up to 2.3 kilobase pairs.[50]

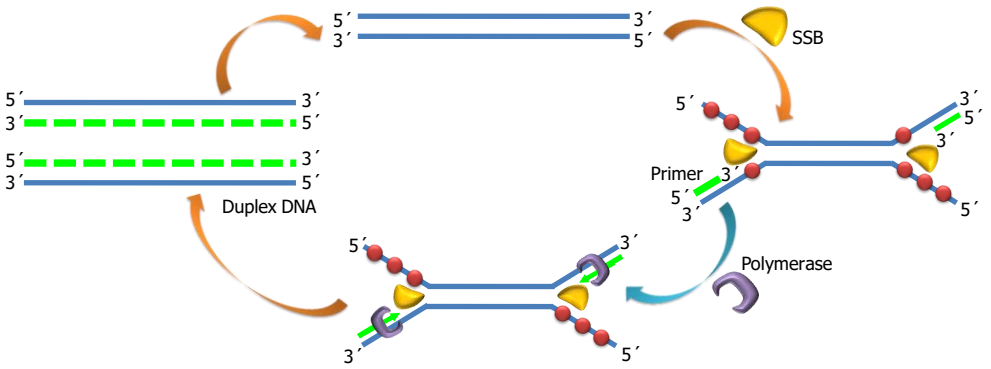

Figure 1.5. Scheme of HDA isothermal amplification. Target DNA is separated by the action of helicase enzyme and stabilized by single strand binding proteins (SSB), allowing primers hybridization. After annealing, it is elongated forming a new strand. Figure adapted from Li and MacDonald, 2015.[49]

1.4.2.4 Recombinase polymerase amplification (RPA)

This method uses DNA polymerases that have strand displacement abilities to generate continuous growing nucleic acid in a self-displacing cycle.[51] Moreover, RPA also employs single stranded binding proteins to separate double-stranded DNA. RPA introduces a recombinase engine for inserting two opposing primers with a template in duplex DNA, a single-stranded DNA-binding protein for stabilizing the displaced strands of DNA, and strand-displacing polymerase for synthesizing DNA where the primers bind to the template DNA (Figure 1.6). All the RPA processes proceed continuously under physiological temperature of 37-42 °C with no other sample treatment to perform the amplification.

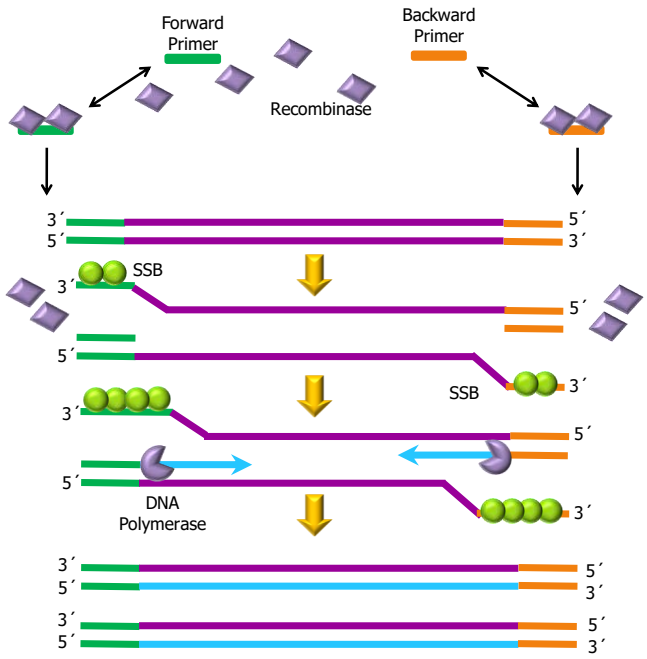

Figure 1.6. Scheme of RPA amplification. Recombinase enzyme binds each primer. When the homologous sequences are located, a strand exchange reaction is performed due to strand-displacement activity of the recombinase. Single stranded binding proteins (SSB) stabilize the displaced DNA. A DNA polymerase initiates the synthesis of the templates forming two DNA molecules. This process is repeated leading to an exponential amplification. Figure adapted from Li and MacDonald, 2015.[49]

1.4.2.5 Loop-mediated isothermal amplification (LAMP)

This method uses loop-forming primers and a strand displacing polymerase to create large, concatemeric amplicons containing multiple copies of the target. LAMP relies on the auto-cycling strand displacement DNA synthesis, which is carried out at 60-65 °C for 45-60 min in the presence of DNA polymerase, dNTPs, specific primers and the target DNA template.[52] This isothermal method employs a set of four primers (two inner and two outer primers) that recognize six distinct regions on(of) the target DNA. The amplification reaction consists of two steps: the non-cyclic reaction which leads to the formation of dual looped DNA strand, and the cyclic amplification and elongation that leads to strand displacement DNA synthesis.[53] The four primers operate in growing amplified DNAs, thus leading to cauliflower-shaped products consisting of alternatively inverted repeats of the target sequence in the same strand (Figure 1.7).[54] The main drawback of LAMP amplification is its tendency to provide false positive results due to nonspecific amplification of non-target DNA sequences.[55]

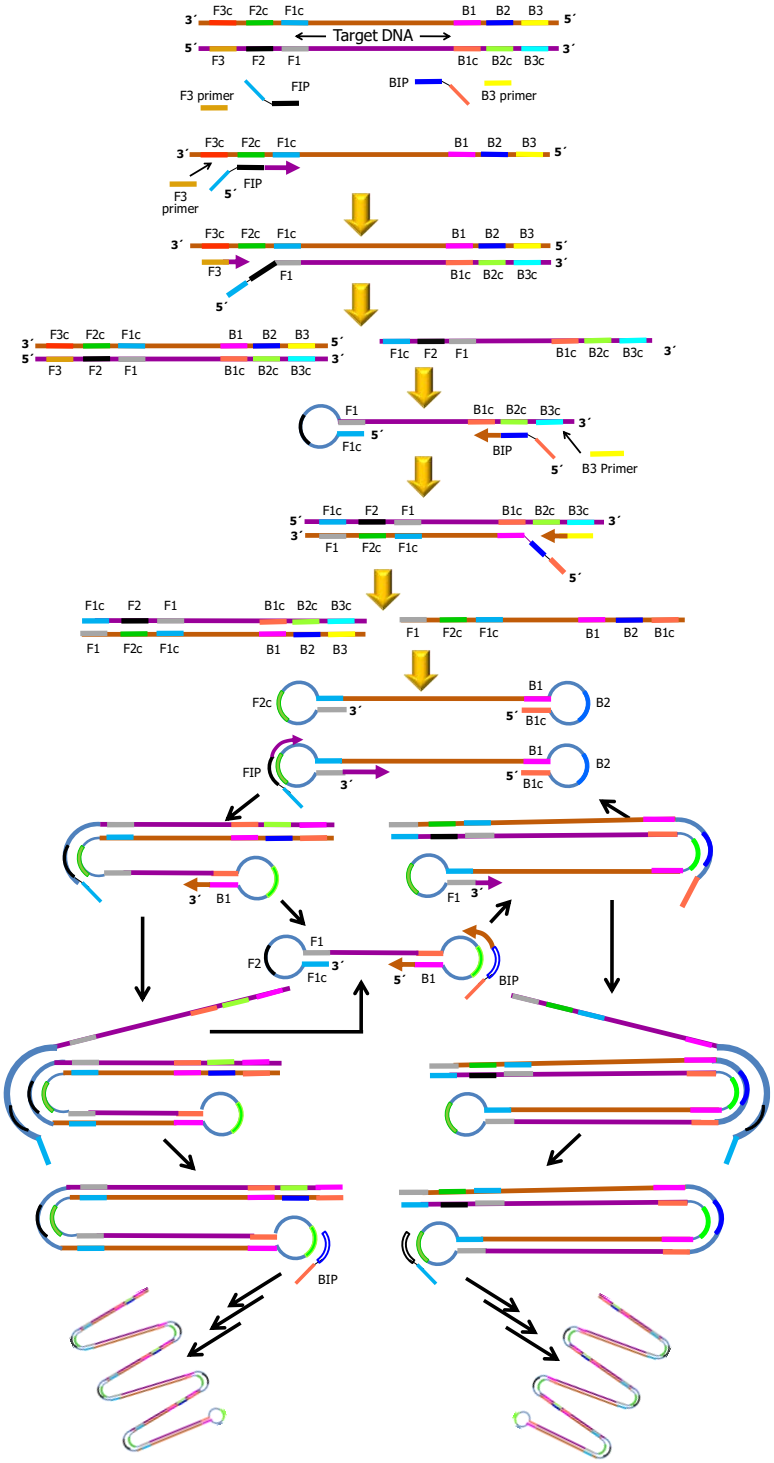

Figure 1.7. Scheme of LAMP amplification. LAMP employs two sets of primers, indicated as FIP and BIP, and F3 and B3. In the non-cycling amplification step FIP primers bind to the target sequence and is elongated by the polymerase. Subsequently, F3 binds on its complementary DNA and a polymerase initiates the synthesis, displacing the newly synthesized DNA. The replaced strand forms loop structures due to its complementarity. Similar reactions are generated with BIP and B3 primers. Dumbbell-like DNA structures are then generated (loops at both ends), being the starting structure in the cycling step. FIP/BIP primer hybridizes to the loops on the product and initiates DNA synthesis. As a result, several sized structures consisting of alternately inverted repeats of the target sequence on the same strand are formed. Figure adapted from Li and MacDonald, 2015.[49]

1.4.2.6 Strand displacement amplification (SDA)

Similar to LAMP, SDA employs a set of four primers. Two of them consist of complementary sequences to the DNA target at their 3' end and restriction enzyme sites at their 5' end. The other two primers are the conventional ones. This method requires a pre-heating step to denature the double-strand DNA, while the rest of the reaction is performed at 37 °C. As shown in Figure 1.8, the amplification reaction consists basically of two steps: a template generating extended strands and a cycling step, which occur in tandem to produce an exponential amount of double-stranded DNA. The new double-strand DNA starts another round of enzyme nicking, extension and displacement.[56,57]

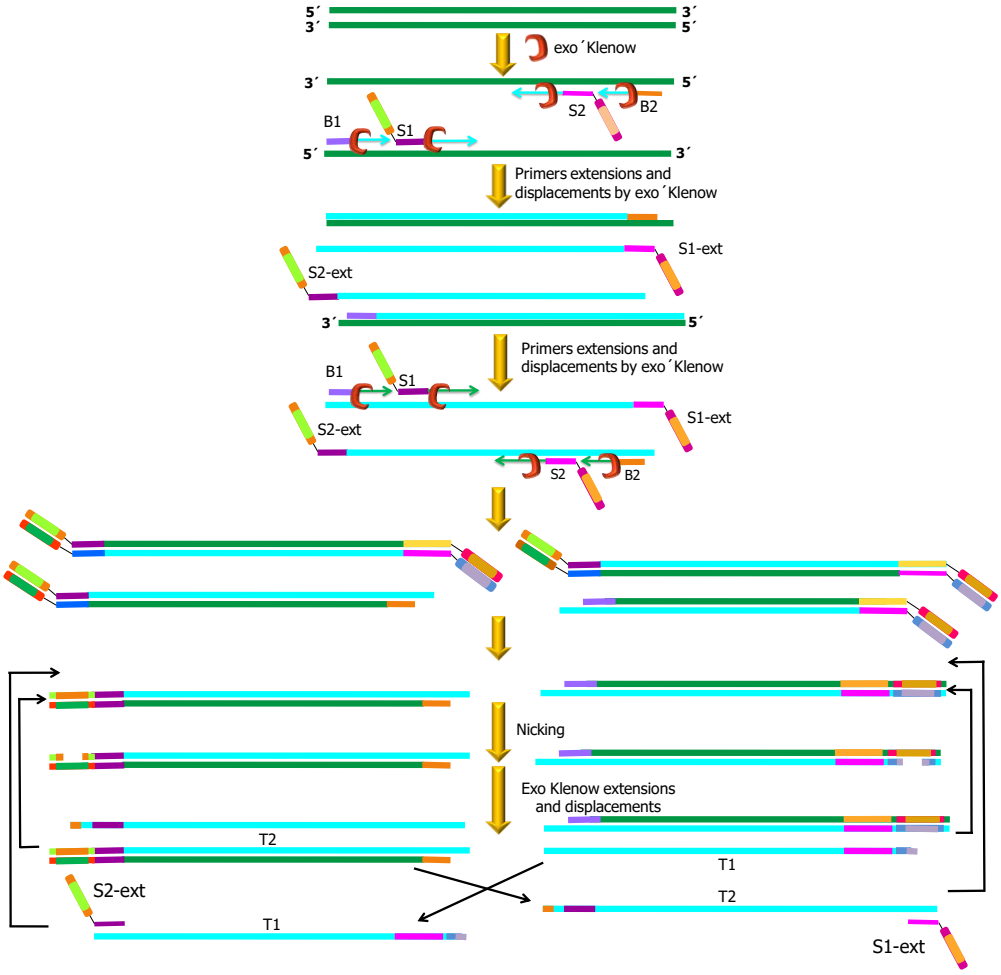

Figure 1.8. Scheme of SDA reaction. After DNA denaturalization, the four primers (S1, S2, B1 and B2) bind its complementary sequence. Exo Klenow polymerase extends S1 and S2 generating extended products, and its products are displaced by the extension of B1 and B2 primers. Subsequently, primers bind again and are extended and displaced in the same way. Primers S1 and S2 have restriction sites, generating nicking sites. After the nicking, Exo Klenow elongates this strand producing a new amplified product and displacing the template that can be re-annealed by S2 or S1 primer. The new double-strand DNA starts another round of enzyme nicking, extension and displacement. Figure adapted from Li and MacDonald, 2015.[49]

1.4.2.7 Transcription-based amplification system (TAS)

This amplification mimics the retroviral strategy of RNA replication *via* cDNA intermediates, and is especially suitable for RNA detection. Variations on this process are referred to as nucleic acid sequence-based amplification (NASBA),[58] self-sustaining sequence replication (3SR),[59] or transcription-mediated amplification (TMA).[60] This exponential amplification system uses three enzymes: reverse transcriptase, RNase H, and T7 DNA-dependent RNA polymerase.[58] In Figure 1.9 NASBA amplification mechanism is shown. The amplification steps involve A) the formation of DNA-RNA hybrids with reverse transcriptase using primers containing a RNA polymerase binding site, B) the degradation of RNA strand within the hybrid using RNase H, C) creation of double-stranded DNA with reverse transcriptase, and D) the generation of many copies of single-stranded RNA using T7 RNA polymerase. The reaction requires temperature of 65°C for first primer annealing, while the rest of the reaction is performed at 41 °C.[58] There are some commercial systems based on this type of amplification such as NucliSENS EasyQ System developed by BioMerieux that incorporate NASBA for detection and quantification of the HIV-1 RNA in human plasma.[61]

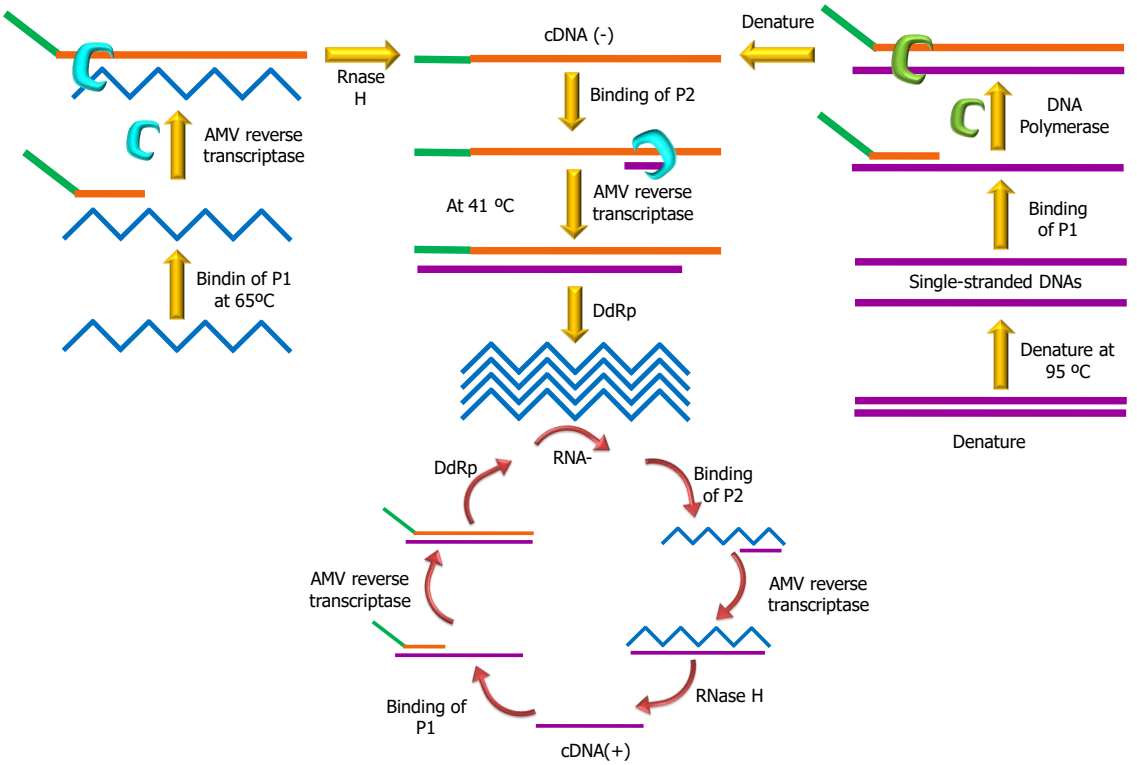

Figure 1.9. Scheme of NASBA amplification. P1 primer binds to the target RNA and is elongated by reverse transcriptase (AMV-RT) forming a RNA/DNA hybrid. P1 primer contains a polymerase promoter sequence. RNase H hydrolyzes the RNA strand of the hybrid. Then, P2 is annealed to single stranded DNA and elongated, generating the polymerase promoter sequences that are recognized by the polymerase. Multiple copied of RNA are generated, starting again the cycle. DdRp: DNA dependent RNA polymerase. Figure adapted from Li and MacDonald, 2015.[49]

1.4.2.8 Rolling circle Amplification (RCA)

Rolling circle amplification is a linear amplification method based on the circular genome replication of plasmids and bacteriophages that employs a circular single-strand DNA template for initiating the template extension by phi29 polymerase.[62] The most distinctive aspect of RCA is the requirement of circular single-stranded templates, which makes RCA uniquely well-suited for the amplification of circular DNA molecules such as plasmids and certain virus genomes (Figure 1.10, panel A).[62-64] However, RCA is not only limited to employ circular DNA, but also can use circular primers, called padlock probes, as template for RCA (Figure 1.10, panel B). The amplification takes place when the DNA polymerase replicates a circular DNA template over and over again, building a long single-stranded tandem repeated product. Due to the circle size template is too small to form a double strand around the circle, the newly DNA is force to unwind.[55,65]

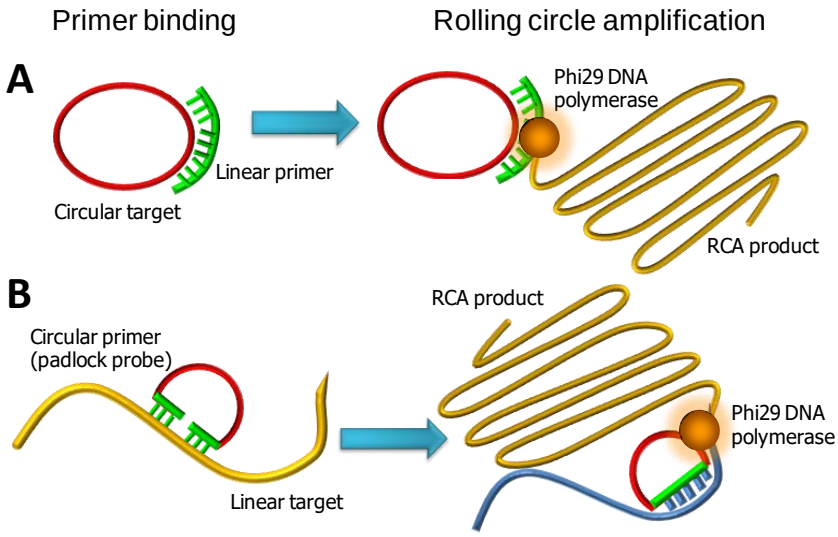

Figure 1.10. Scheme of Rolling circle amplification (RCA). A) RCA of a circular template using linear primers; B) RCA of a linear template using circular primers.

One of the most important advantages of RCA is that it is a very simple procedure.[66] The technique is inexpensive, highly sensitive and provides high multiplexity for diagnostic methods. RCA has also some disadvantages. Special attention must be taken to prevent false positives and possible contamination. Nevertheless, the use of endo and exonucleases in the experiment can avoid these problems.[67,68]

In order to extend the application of this strategy to linear DNA targets, padlock probes are usually used. Padlock probes are linear oligonucleotide, typically 70-100 nucleotides in length, specifically designed for target recognition sequences by both 5´- and 3´- ends (Figure 1.10,

panel B). A padlock probe consists of three segments: two target-complementary end sequences and a non-target-complementary element that links the end sequences together. The target-complementary segments are typically in the range of 15–22 nucleotides in length and the linking segment present sequences for identification and amplification of the RCA amplified product.

The padlock probe design is such that the ends of the probe hybridize head to tail on the single-stranded target molecule, forming a nicked DNA duplex that can be joined by a DNA ligase. Hence, the hybridization of the padlock probe to the DNA target joins the two end segments (padlock probe arms) and closes the padlock probe forming a circle. The requirement for dual hybridization of two different segments (ends) to target molecules provides high specificity of identification/detection in complex populations of nucleic acids. Moreover, the ligation reaction guarantees selectivity among similar target sequence variants, because of the impairment of the ligases to covalently join oligonucleotides that are mismatched.

Due to the intra-molecular nature of the ligation reactions, problems with cross-reaction between padlock probes are minimized. As a result, large sets of padlock probes can be combined in the same reaction. A large number of circularization probes can therefore be combined in multiplexed assay without problems of interference. Furthermore, padlock probes are also used for mutagenesis detection. The location of the mismatch in the padlock is used to detect punctual mutagenesis.

1.4.2.9 Circle-to-circle amplification (C2CA)

It is an isothermal amplification based on a double RCA. Here, the resulting amplicons are the multiple repeats of the circular template, which are subsequently digested by enzymes into each individual short oligonucleotide. Each segment is circularized again and a new round of rolling circle amplification is performed (Figure 1.11). C2CA protocol is a very powerful and sensitive technique for amplification and analysis of DNA targets at very low concentration range. Moreover, multiplexed genotyping of polymorphic loci and quantitative DNA analysis are the two major areas of application described for C2CA in solution.[11]

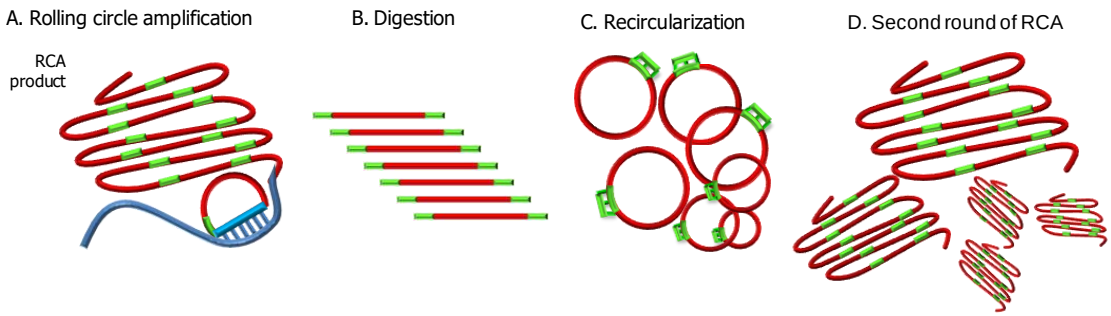

Figure 1.11. Scheme of Circle-to-circle amplification (C2CA). A) RCA of a template; B) Digestion of the tandem repeated product; C) Recircularization on the circle using a primer; D) Second round of rolling circle amplification.

Rolling circle products can not be identified by gel electrophoresis, yielding a broad smear of high molecular weight DNA.[62] Interestingly, the long DNA threads produced in the RCA collapse into a random coil with a diameter of about 700 nm.[69] A local enrichment of fluorescence can be achieved by hybridizing fluorescence probes to a repeated sequence in the rolling-circle product, resulting in bright fluorescent blobs that are easily visualized using standard fluorescence microscope. Digital quantification of RCA products was described by the first time in 2006.[70] This method was based on the use of a microfluidic channel mounted in a confocal microscope across a flow channel. Thus, the RCA products are labelled with a fluorescent tags and visualized like bright dots by pumping the rolling circle products through the microchannel.

1.5 Biosensors

1.5.1 Definition and classification of biosensors

Since the concept of biosensor was described for the first time by Leland C. Clark in 1962, the number of publication has been increasing year by year.[71] Clark´s biosensor consisted on the immobilization of the glucose oxidase enzyme on an oxygen electrode using dialysis membrane.

Surprisingly, the first biosensor described in the literature has become the most successful commercialized device. Currently, glucose sensor dominates the market for diagnostic companies, being Roche, Johnson & Johnson, Abbot and Bayer, the ones that controlled the 90% of the sales.[72,73] Other commercial device in this area includes cholesterol, lactate, triglycerides and creatinine biosensors.[74]

A biosensor is defined by the IUPAC (International Union of Pure and Applied Chemistry) as "a device that uses specific biochemical reactions mediated by enzymes, immunosystems, tissues, organelles or whole cells to detect chemical compounds usually by electrical, thermal or optical signals".[75] When the recognition element is a chemical compound, the sensor is referred to be a chemical sensor, while the recognition element is a biomolecule, it is known as a biosensor. Thus, a biosensor converts a biological event into an electrical signal by the integration of two main components: a bioreceptor or biorecognition element, which interacts with the target analyte producing a physical change and a transducer which converts the recognition event into a measurable electrical signal (Figure 1.12).[76] The specificity for the analyte depends on the biological recognition element, whereas the sensitivity of a biosensor is determined by the transducer properties.[77]

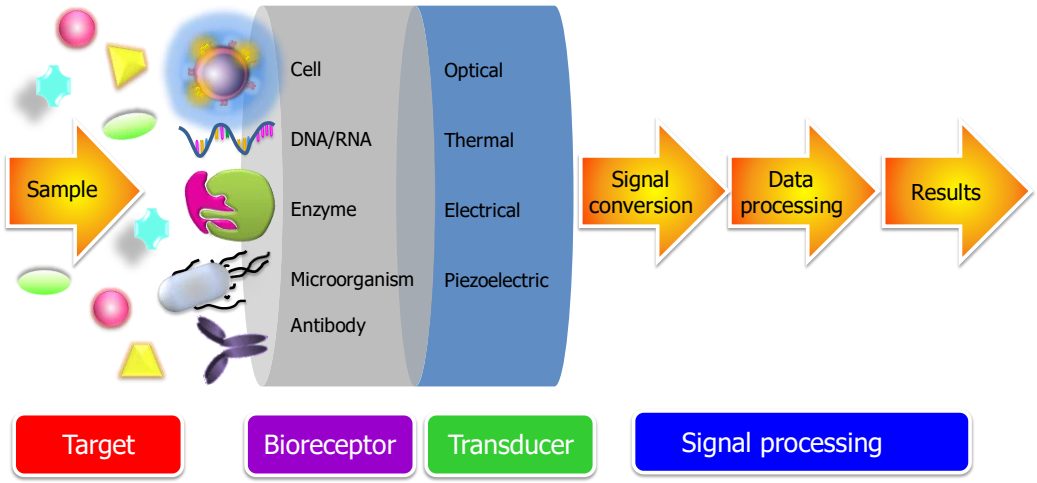

Figure 1.12. Schematic representation of the biosensor components. The target is recognized by the bioreceptor and produces a change in any physical property that is registered by the transducer, which converts it in a digital data.

The biosensors can be classified according to the nature of the recognition event as follows:

Catalytic devices. This kind of biosensors uses an enzyme to recognize the target substrate. The biosensor is based on a reaction catalyzed by macromolecules, which are present in their original biological environment, have been isolated previously or have been manufactured. Thus, a continuous consumption of substrate(s) is achieved by the immobilized biocatalyst incorporated into the sensor. Transient or steady-state responses are monitored by the integrated transducer.

Affinity devices. The recognition event of this type of biosensors relies on the selective binding of target analyte to a ligand partner (e.g., antibody, oligonucleotide, DNA, biomimetics molecules mimicking biological analogues or others affinity receptors). The equilibrium is usually reached and there is no further net consumption of the analyte by the immobilized biocomplexing agent. Since, in some cases, this binding cannot be detected itself, the biocomplexing reaction can be monitored using a complementary biocatalytic reaction.

The biosensors can be also classified according to its bioreceptor, as follow:

Enzyme biosensors. It uses enzymes to measure the selective catalysis or inhibition of it towards a specific target. Enzymes are proteins with high catalytic activity and selectivity towards substrates. There are some limitations such as pH, ionic strength, chemical inhibitors, and temperature because these parameters affect the enzymatic activity. An example of enzyme based biosensor is glucose biosensors. In most cases enzymes are used also as labels by their conjugation to antibodies or antigens.

Immunosensors. They are biosensors that use antibodies as biorecognition element. The large binding capability of the antibodies toward its target confers to the immunosensors high specificity to the analyte of interest.[78]

Biosensors based on DNA, RNA and peptide nucleic acid. It use nucleic acid as bioreceptor and its specificity is based on the base pair affinity between a target nucleotide strand to a complementary strand.[79] Nowadays, mainly synthetic oligodeoxyribonucleotides (ODNs) are used as probes in the DNA sensors. DNA biosensors are used for the diagnosis of genetic diseases, among others.

Cells biosensors. These biosensors use entire cell/microorganism or a specific cellular component that is capable of specific binding to certain species or based on the measurement of their metabolism. The advantages of these biosensors rely on their low cost, stability and their ability to carry out several complex reactions involving enzyme and cofactors. Example of cell based sensor is Cellsense that uses *Escherichia coli* bacteria for rapid ecotoxicity analysis.

Molecular imprinted polymer-based biosensors. Molecular imprinted polymers are biomimetic receptor molecule capable of binding a target with high affinity and specificity. The technique of molecular imprinting allows the formation of specific recognition sites in synthetic polymers through the use of templates or imprint molecules. These recognition sites mimic the binding sites of biological receptor molecules such as antibodies and enzymes.[80]

The biosensors can be also classified accordingly to the transducers, as follows:

Optical. This transducer measures the changes in the light properties such as absorbance, fluorescence, optical diffraction, among others. Fiber-optic biosensors use optical fibers for signal transduction, and are dependable only on optical transduction mechanisms for detecting target biomolecules. Surface plasmon resonance biosensors are based on the measurement of the refractive index of a very thin layer of material absorbed on a metal to monitor interactions between an analyte in solution and the bioelement immobilized on the sensor surface. The main advantage of this type of biosensors is the label-free technology.[81]

Piezoelectric (mass-sensitive). These biosensors are based on the coupling of the bioelement with a piezoelectric component, usually a quartz-crystal coated with gold electrodes. These crystals can be made to vibrate at a specific frequency with the application of an electrical signal. The frequency of oscillation is dependent on the electrical frequency applied to the crystal as well as the mass of the crystal. Thus, an increasing of the mass due to binding of molecules produces an oscillation frequency of the crystal that can be measured and finally used to determine the additional mass of the crystal.

Calorimetric (thermometric). This type of biosensor is based on the fundamental properties of biological reactions, namely absorption or production of heat, which in turn changes the temperature of the medium in which the reaction takes place. These biosensors are constructed by combining immobilized biomolecules with temperature sensors. When the analyte is in contact with the bioelement, the heat reaction is measured and is calibrated against the analyte concentration. The total heat produced or absorbed is proportional to the molar enthalpy and the total number of molecules in the reaction. The main advantage of this transducer is that they do not need of frequent recalibration.

Electrochemical biosensors. The principle of this class of biosensor involves the production or consumption of ions or electrons when a biomolecule interacts with its target. These changes affect the electrical properties of the system and can be measured by electric current or potential.

Nowadays, electrochemical biosensors are considered a very powerful analytical tool thanks to their excellent features and their capability to be implemented at point-of-care. These characteristics make them highly attractive as rapid detection methods in medicine, food safety, industries processes, security and defense, among others.[82]

In the present thesis, electrochemical biosensors were used as analytical devices for clinical diagnosis. For this reason, the next sections are focused on this kind of biosensors.

1.5.2 Electrochemical biosensors

In the last year, electrochemical biosensors have shown a huge impact in the analytical determination field because they are robust, easy to use, and amenable to miniaturization. This type of device is simple, provides rapid response, and allows the measurements in complex samples.[83] Electrochemical sensors can be classified according to the electrochemical property that is measured [79]:

Potentiometric. This transducer measures difference in potential that is generated in an ion-selective membrane separating two solutions at zero current flow.

Surface charge using field-effect transistors (FETs). The electric field is used to control the conductivity of a channel between two electrodes in a semiconducting material.

Conductimetric. This transducer measures the change in electrical conductance/resistance of the solution when ions or electrons are produced during the course of biochemical reaction.

Amperometric. This kind of transductors measures a change in the current produced as consequence of the oxidation or reduction of an electroactive species at a fixed potential.[84] When the current is measured at a constant potential, it is referred to as amperometry. However, when the current is measured during a potential scanning, it is referred to as voltammetry.[85] Amperometric biosensors can use for their biochemical reaction molecules which are able to transfer electrons, called mediators. Mediators can participate in the redox reaction with the biological component assisting in the faster electron transfer process. A mediator can be defined as a low molecular weight redox couple, which shuttles electrons from the redox centre of the enzyme to the surface of the electrode.[86] As a result lower potentials can be used, thus the influence of interferents is reduced. Most of the amperometric biosensors require the use of labels such as enzymes since the majority of the biological samples are not intrinsically electroactive.

The electrochemical cells for amperometric determinations are performed in a three-electrode setup: working, reference and auxiliary electrode. The current flow is measured on the working electrode, once the redox reaction of interest occurs. The reference electrode is used to keep constant the potential applied between the working and auxiliary electrode. The auxiliary electrode acts as a counter electrode to close the electric circuit. The proper election of the potential reaction provides selectivity to the system, allowing the selective oxidation or reduction of one or another chemical species present in the sample.[87]

The resulting current (reduction or oxidation) is described by Faraday's law (in its differential form) as:

$$I = n\,x\,F\,x\,\frac{\delta C}{\delta t}$$

In which n is the number of electrons implied in the process, F is the Faraday's constant and $\delta C/\delta t$ is the reaction rate (oxidation or reduction of the analyte) expressed as mol s^{-1}. In the equation, the electric current is directly proportional to the electron transfer reaction occurring at the electrode-solution interface.

In the present thesis, amperometric biosensors were used as analytical tools for clinical diagnosis.

1.5.3 Working electrodes in amperometric biosensors

The choice of the transducer used for an electrochemical determination is crucial because it will be responsible of the sensitivity of the biosensing process, the cost of the assay, the immobilization procedure, the need of activation pretreatment, and surface regeneration, among others factors.

A wide variety of materials are used as transducer in the working electrode. The most popular involves mercury, carbon or noble metals. In 1959, the Nobel Prize in Chemistry was awarded to Heyrovský for his discovery and development of polarographic methods.[88] Due to its very attractive electrochemical behavior, high reproducibility, renewable and smooth surface, mercury was the most fashionable electrode material for many years. However, mercury electrodes have been losing popularity due to its toxicity. Currently, carbon-based electrodes are extensively used in the field of electroanalysis, primarily because of its broad potential window, low background current, rich surface chemistry, low cost, and chemical inertness. In contrast, electron-transfer rates observed at carbon surfaces are often slower that those observed at metal electrodes. Some examples of carbon-based electrodes are glassy carbon, carbon paste, carbon fibers, carbon composites, graphene, carbon nanotubes, among others.[89] Those materials appear in the literature in different configurations, being the most used cylindrical and screen-printed electrodes. The latter kind of electrode arose in response to the need for miniaturization and involved reduction in workload and waste, and gave characteristics of portability and cost effectiveness.

1.5.3.1 Screen-printing electrodes

The incorporation of screen printing technology in the design of enzyme electrodes, by the MediSense team in the early 1980´s, proved to be a decisive element in the commercialization of the home blood glucose.[90] Today, approximately half of the electrodes used in disposable glucose sensors are screen printed using curable polymer inks. This kind of electrode results very attractive thanks to its compatibility with mass production and portable analyzer, simple fabrication, and minimal sample and waste. These screen-printed electrodes (SPEs) consist in a solid substrate where a working electrode, counter electrode and (pseudo)reference electrode are printed on it. The miniaturization of the common SPEs to the micrometer-scale can offer advantageous features attributed to microelectrodes, such as improved signal-to-noise ratios, independence of forced convection, a low ohmic drop and a faster mass-transport rate than conventional electrodes.[91,92]

The screen-printing technique uses a mould template through which a roller or squeegee deposits ink or any printable material on the open areas of the mould. Generally, different moulds are prepared to print the different parts of the electrode. The ink has to be solidified onto the support/substrate by thermal treatment.[93] Finally, protective ink coating is used to isolate the conductive connection area of the electrodes.

The most popular ink used are silver as conductive track, and gold or carbon as working electrode. However, due to the higher cost of gold, carbon-based screen printed electrodes are more common. To improve the electron transfer a widespread variety of materials were incorporated in working electrodes by mixing carbon ink with, for example, manganese and bismuth oxide, carbon nanotubes, among others.[94,95]

1.5.3.2 Electrochemical electrodes based on graphite-epoxy composites

Rigid conducting graphite-epoxy composites (GEC) have been extensively used in our laboratory for genosensing and immunosensing approaches with analytical applications such as environmental, foodborne safety, medical diagnostic, etc.[96] Composites result from the combination of two or more dissimilar materials, in which each retains its original properties, while conferring distinctive chemical, mechanical, and physical properties. Carbon materials are ideal conducting phases to be used in composites because they have low electrical resistivity, as well as all the advantages described above.[97]

In this work, graphite-epoxy composites were built by combining a non-conductive commercially available epoxy resin (binder matrix) where graphite serves as the conductive

material. The resulting paste was hardened by curing the material by heating conferring robustness and rigidity to the electrode. As it will be described in the following sections, the graphite-epoxy electrodes are sensitive, robust and cheap transducers that can be used for biosensing.

The carbon surface can be easily modified by dry and wet absorption of the bioreceptor (DNAs, oligonucleotides, enzymes, aptamers, antibodies, etc.),[98] yielding a reproducible and stable layer of bioreceptor on the electrode surface.[99] In our group, the inclusion in the formulation of affinity proteins such as avidin (Av-GEC) [100,101] or protein A (ProtA-GEC) [102] as well as the integration of nanomaterials such as metal nanoparticles[103,104] and carbon nanotubes[105] have been previously described.

In the recent years, the integration of magnetic particles in analytical applications has increased enormously. In our work the magnetic particles (MPs) are incorporated in the detection strategy not only for the sample capturing and preconcentration processes, but also for reducing the assay time, minimizing the sample handling, reducing the matrix effect and facilitating the washing steps. Moreover, the MPs make possible the immobilization of the sample on the graphite-epoxy composite by the introduction of a neodymium magnet inside the GEC electrodes (m-GEC) (Figure 1.13, panel e and f). In Figure 1.13 the construction of m-GEC electrodes is schematically depicted. These electrodes, designed in our laboratory, are conventional GEC electrodes in which a small magnet is incorporated in the body of the electrode as detailed in Chapter 4, 5 and 6.

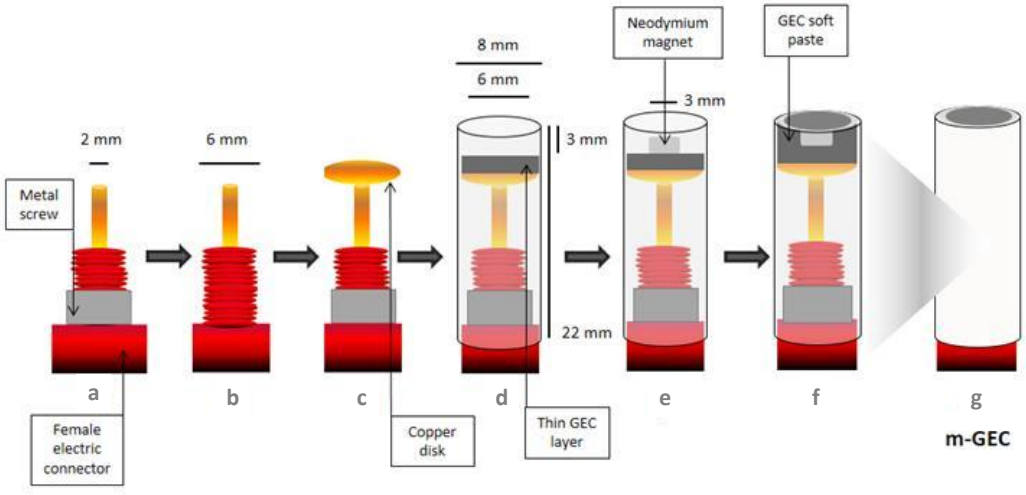

Figure 1.13. Schematic representation for the m-GEC electrodes construction.

1.5.4 Magnetic particles in biosensing

The integration of micro- and nano- magnetic particles has provided and remarkable progress in biosensing devices improving their analytical performance. The size of these beads varies from nanometers to few micrometers and their composition include pure metal particles such as iron, cobalt, nickel, among others, as well as metal oxides such as manganese oxides, nickel oxides, iron oxides, and cobalt oxides. However, among these particles, metal oxides are often preferred over pure metals because they are more stable to oxidation, being ferrous or ferric oxide (magnetite Fe_3O_4 and maghemite γ-Fe_2O_3) one of the main constituents used to synthesized magnetic particles for biomedical applications.[106]

The magnetic properties of core are strongly dependent on the synthetic method, chemical composition and their size, which plays an essential role in their behavior under the application of an external magnetic field. On the other hand, the magnetic core can be embedded in a polymer matrix such as polystyrene, polyacrylamide, dextran, alginate, silica, among others. The coating of the magnetic core is crucial for protection against oxidation, their stabilization and particle aggregation.[107] Additionally, the functional groups of the polymer are used for tuning the particle surface for a desired application.

The magnetic particles can be conjugated by surface chemistry to various biomaterials such as proteins, enzymes, antibodies, or oligonucleotides. The functionalization of the particles with specific ligands makes possible their use for many *in vivo* applications including magnetic resonance imaging contrast enhancement, hyperthermia, drug and gene delivery, photodynamic therapy, among others.[108]

Magnetic particles bring several advantages to detection assay or *in vitro* applications due to their large surface:volume ratio that facilitates higher capture efficiencies than two dimensional surfaces. Moreover, easy washing procedure can be applied with relatively high speed and simplicity. Superparamagnetic particles are especially attractive due to their magnetic behavior when an external magnetic field is applied. Thus, superparamagnetic particles can magnetize under an external magnetic field. This property can be easily applied *in vitro* application such as microorganism, cell, as well as nucleic acid purification and preconcentration.

Among the main advantages of integrating magnetic particles in biosensing strategies is the ability to concentrate biomolecules and minimize the effect of the sample matrix; the fast kinetics and high binding capacity, which reduces the total assay time. Moreover, their use as solid support in bioassays has shown to greatly improve the performance of the biological

reactions. Thus, improvements in the sensitivity of assays using antibody-coated magnetic particles have also reported for the detection of biomarkers. The integration of magnetic particles in different fields of assays for the detection of clinical biomarkers is reviewed in *§1.8*.

1.6 Acquired immune deficiency syndrome

Acquire Immune Deficiency Syndrome (AIDS) is caused by the human immunodeficiency virus (HIV). AIDS is the last stage of the HIV infection, since during the course of the disease, the virus attacks the cells involved in the immune response. A primary target of HIV is CD4 T lymphocytes which are preferentially depleted during the course of the disease.

The first cases of AIDS were reported in United State in 1981, and they were described as rare cases of pneumonia.[109,110] In 1983, the HIV was identified as the true cause of AIDS, although it was called T-lymphotrophic virus.[111] This syndrome became the first pandemic of the XXI century.

In 1985, a blood test based on ELISA was firstly developed for HIV diagnostic to detect HIV virus, commercialized by Abbott in United State and Europe. This test was approved by the FDA (Food and Drug Administration) for detection of antibodies produced in response to exposure to HIV.[112] Two years later, in 1987, a Western blot test was approved by the FDA for HIV antibody detection as the gold standard test for the presence of HIV antibodies, at the same time the first antiretroviral drug zidovudine was approved in the United State.[113, 114]

In 1992, the first rapid HIV test was authorized to be commercialized while in 1994 the first oral HIV test (non-blood-based antibody test) was approved.[115] Almost fifteen years after the first HIV test, in 2001, a nucleic acid test for screening of blood and plasma was licensed. In 2010, ten years later, the first test that detects both antigen and antibodies was approved while the first rapid test based on the same detection appeared in 2013.[116]

The development of new methods of HIV detection continues to be a key in the fight against this disease. HIV infection constitutes a big public health concern because of the huge number of people affected and the limitation of the treatment in low-income countries.

1.6.1 The immune system

The immune system is a network of proteins, cells, tissues, and organs that work together to defend the body against attacks of foreign invaders upon infection, the pathogens exhibit foreign biomolecules named as antigens that are not normally present in the body.[117]

There are two different immune responses against pathogens [118,119]:

Innate response. It is a nonspecific defense mechanism and not antigen-dependent response that takes place without previous exposure to the antigen. This response is very important in controlling an infection during the first few days after the exposure to a microorganism.

Acquired response. This kind of response is specific and improves under repeated exposure to a given antigen. The response involves the proliferation of antigen-specific B and T cells (also called lymphocytes), which occurs when the surface receptors of these cells bind to antigen. B cells secrete immunoglobulins, the antigen-specific antibodies responsible for eliminating extracellular microorganisms. T cells assist the B cells to make antibodies and can also activate macrophages.

1.6.2 The Human immunodeficiency virus

The human Immunodeficiency virus belongs to the retroviridae family, specifically lentivirus subfamily,[120] and is characterized by a single-stranded RNA genome. Viral RNA is replicated by a reverse transcriptase enzyme that makes the reverse transcription of RNA to DNA. Viral DNA gets integrated into the host genome as protovirus.

The HIV virus is an enveloped virus with icosahedral shape of about 80-120 nm in diameter. The different parts of the structure (Figure 1.14), from inner to outer, are[121] :

Viral core. It comprises the whole machinery for the HIV replication, including two copies of positive-sense single-stranded RNA, the enzymes (reverse transcriptase, ribonuclease, integrase, and protease) the regulatory proteins, coated by the nucleocapsid, and p24 protein that composed the casid.

HIV matrix proteins. It consists in a layer of p17 protein, which is placed between the envelope and core, ensuring the integrity of the virion particle.

Viral envelope. It is the outer coat of the virus and consists in a lipidic double-layer membrane where different viral proteins, such as gp120 and gp41, are embedded. These

glycoproteins play an important role in the virus attachment to the target cells to initiate the infectious cycle. The viral envelope presents also host protein taking from the host membrane during the budding process (formation of new particles).

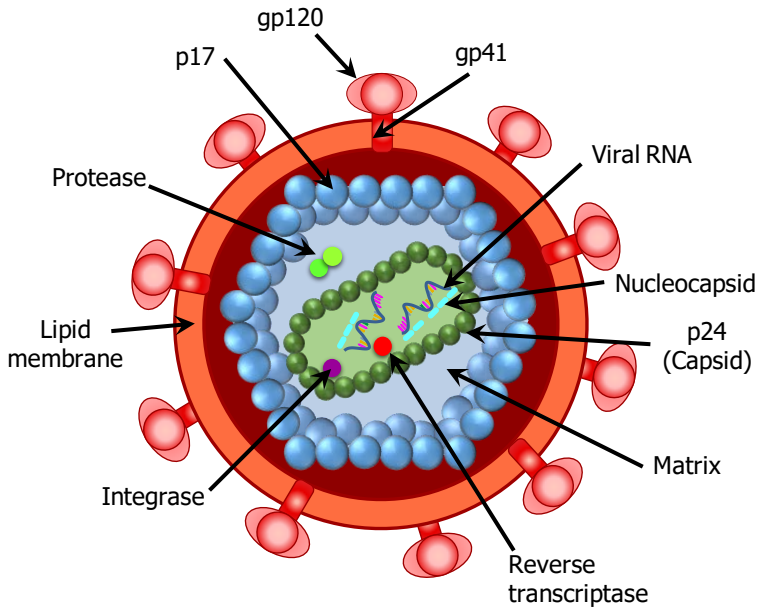

Figure 1.14. Structure of the HIV virus. Figure adapted from Rajarapu, 2014.[122]

1.6.3 Human immunodeficiency virus infection

The HIV transmission from person to person occurs when blood, blood products, semen, vaginal fluids or breast milk from an infected person enters the bloodstream of another person via injection or across breaks or small abrasions of the skin or mucous membranes. Virtually all transmission occurs through sexual, parenteral (injection with contaminated equipment, blood or blood products), or vertical (to the child during pregnancy or breast feeding) route. HIV is present in other body fluids such as tears, urine, amniotic fluid, bronchoalveolar. Nevertheless, the transmission via exposure to these fluids has not been reported.

For cell infection, HIV introduces the viral RNA into the cell target cytoplasm. HIV entries to the cell by the attachment of the gp120 and gp41 proteins to the CD4 (cluster of differentiation 4) host membrane cell receptor.[123,124] Once the viral protein interacts with the CD4 receptor, gp120 is activated and makes contact with CCR5 or CXCR4 chemokine (a multipass membrane protein).[32,125] Protein interactions lead to the fusion of viral envelop with the cellular plasma membranes that allows the internalization of the HIV viral core. Thus, two viral RNA genomes and viral enzymes such as reverse transcriptase, integrase and

protease are release to the host cytoplasm. The last step of the virus infection is the integration of the viral RNA to the host-cell genome. Reverse transcriptase enzyme copies viral RNA into double-stranded DNA (dsDNA), which is integrated as provirus by the integrase enzyme action into the host genome. The provirus acts as a template for viral genomic and messenger RNA transcription when the host cell replicates.[126]

1.6.4 Clinical stages of the HIV infection

After HIV infection, the virus infects cells that present CD4 receptor on its membrane, mainly CD4 T lymphocytes. HIV produces new copies of itself, which can then infect other cells. Over time, HIV infection leads to a severe depletion in the number of CD4 T lymphocytes, turning the host susceptible to opportunistic infections or tumors. The HIV progression can be divided in stages that are depicted in Figure 1.15.[127] However, the progression of the disease varies from person to person and also depends on several factors, including genetic factors, the clinical condition before HIV infection, early diagnosis, care and treatment, among others.

1.6.4.1 Acute/primary HIV Infection

This first stage is characterized by the development of flu-like symptoms or mononucleosis syndrome which includes fever, headache, sore throat, and rash.[128] During this period, the virus multiplies and spread rapidly throughout the body, reaching a high level of viremia. For this reason, the risk of transmission is higher during this stage. At the very first beginning of the infection, the virus not only infects, but also destroys the CD4 T lymphocytes, until the immune system is able to stop the HIV replication. This fact leads to a stable level of virus, named viral set point. The immune system takes from one week up to three months to develop an immune response against the HIV, by producing antibodies, cytotoxic, and CD4 T lymphocytes. This process is known as seroconversion. Up to this stage, the diagnosis based on HIV antibody test might produce false negative results.

1.6.4.2 Clinical latency or asymptomatic HIV infection

This period varies from 2 up to 15 years.[129] During this stage, the HIV multiplies but at very low rate. This latency period is characterized by no clinical symptomatology, although a continuous decrease in the CD4 T lymphocyte level is observed. The rate of lymphocyte depletion is more rapid as the patient approaches the last stage of the disease. Although the

HIV level in peripheral blood is low, the virus remains infective and it can still spread to other people. The active presence of HIV in the lymph nodes keeps the immune system in activity.[130] It is recommended to start the antiretroviral treatment (ART) during this stage. In order to keep the virus in check and to delay the entry to the last stage of the disease. During this period, the disease can be diagnoses by the detection of antibodies, viral load or any other laboratory tests. The levels of both the CD4 count and viral load in the early asymptomatic stage are highly predictive of the disease progression.[131]

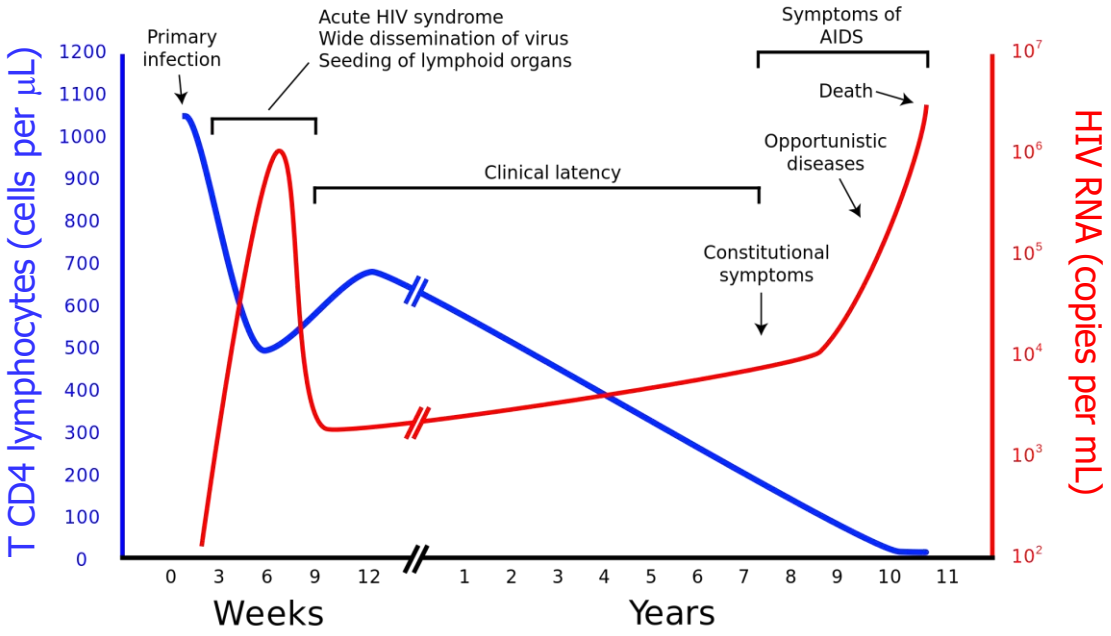

Figure 1.15. Timeline scheme showing the relationship among the stages of HIV infection and the clinical stages describes as CD4 T lymphocyte and HIV virus progression upon HIV infection in untreated HIV patients. Figure adapted from Pantaleo *et al.*, 1993.[127]

1.6.4.3 Acquire Immune Deficiency Syndrome (AIDS)

It is the last stage of HIV infection and starts when the CD4 count is lower than 200 cells per microliter. This period is characterized by a severe damage of the immune system since the lymph nodes and other immune tissues become damaged due to the years of continuous activity. Moreover, the HIV can mutate, increasing the pathogenicity. Beside this, the body is unable to replace the damaged T lymphocytes. In this period the patient is defenseless against the opportunistic infections. These infections are caused by microorganisms that normally do not cause disease but become pathogenic when the immune system is impaired and unable to fight off infection.[132] In low resource countries, where no disease monitoring is available, a

patient is considered to be in the last stage of HIV infection when is affected by one or more opportunistic infections.

1.6.5 Laboratory biomarkers for HIV infection diagnosis

Early HIV diagnosis and continuous monitoring allows health-worker to offer optimal care, effective treatment and the assistance to patients. Moreover, recognizing a HIV patient in the earliest stage of the infection helps to initiate a responsible care and control and avoid further transmission.

Laboratory HIV test are based on the appearance of different HIV biomarkers upon infection. In terms of laboratory biomarkers, after HIV infection, although low levels of viral RNA are present in plasma, no viral biomarkers can be detectable.[133] It takes around 10 days after infection to be able to detect HIV RNA by nucleic acid test.[134,135] Furthermore, as the virus starts to replicate, p24 antigen (capsid) is highly expressed and it can be detected by immunoassays within 4 to 10 days after the detection of HIV RNA (2 to 3 weeks after HIV infection) (Figure 1.16).[136] However, and due to the appearance of antibodies as the response to HIV infection, these antibodies bind to the p24 antigen forming antigen-antibody complexes and interfering with the p24 assay detection.[137] Next, the appearance of antibodies against the virus can be detected. Firstly, IgM antibodies are produced and can be detected by immunoassays from 3 to 5 days after p24 antigen is being detected, and over 10 to 13 days after viral RNA appearance.[138] Finally, IgG antibodies emerge due to immunoglobulin class switching and persist for the lifetime. IgG are detectable by immunoassays from 18 to 38 days since the initial viral RNA detection.[139]

Figure 1.16 illustrates a timeline scheme showing the HIV biomarker appearance and their corresponding laboratory test. Furthermore, in all laboratory tests used not only for HIV diagnosis but also for HIV follow-up are described in detail in next sections.

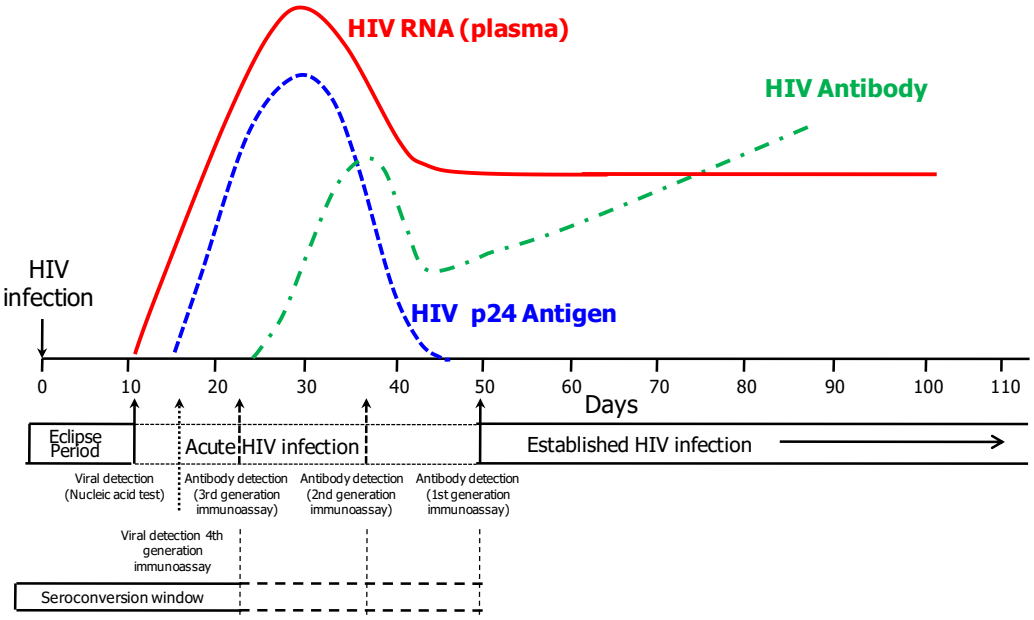

Figure 1.16. Timeline scheme showing the appearance of laboratory biomarkers and laboratory test upon HIV infection. Figure adapted from Branson *et al.*, 2014.[140]

1.6.6 Early diagnosis of HIV infection

There are a wide number of tests available for HIV diagnosis for individuals, as well as for the serosurveillance of blood banks to ensure the safety of blood transfusion and organ donation. It includes HIV antibody test, p24 antigen test and nucleic acid test. The medical guidelines for HIV diagnosis relies on a screening test for triage, followed by the verification of a HIV-positive diagnosis by a confirmatory test.[141] In a screening test, sensitivity is the highest priority in order to completely avoid false negative results and to correctly identify infected individuals, while in the confirmatory test, specificity is the highest priority, in order to avoid false positives results to identify non-infected individuals.[142]

1.6.6.1 HIV screening tests

Screening test include the detection of antibodies, the p24 antigen, or the viral nucleic acid. Thus, HIV infection can be detected by ELISA, particle agglutination, and chemiluminescent immunoassay.

The ELISA is the screening test most widely used for HIV detection. The surface of the microwells is coated with HIV antigen(s) or antibodies and the serum or plasma is added on it.

ELISA test are classified in generation according to the principle used in the assay as well as the type of antigen used. Thus, 1st generation used purified HIV lysates as source of antigen,

2nd generation are based on recombinant proteins or synthetic peptides, 3rd generation assays (or sandwich ELISA) use recombinant proteins and labeled antigen as conjugate increasing the sensitivity and reducing the window period. And the 4th generation assays detects both HIV antibody and antigen, increasing even more the sensitivity and allowing the earlier HIV diagnosis.[143] Several immunoassays to detect HIV antibodies are commercially available as kit format such as Enzygnost Anti-HIV 1/2 Plus (Dade Behring Marburg GmbH, Marburg, Germany); ICE * HIV-1.O.2 (Murex Biotech Ltd. Dartford, U.K.); Vironostika HIV Uni-Form II plus O (Organon Teknika nv Boxtel, The Netherlands); GENSCREEN HIV 1/2 (Bio-Rad, Marnes la Coquette, France); HIVA TEST (Lupin Laboratories Ltd. Mumbai, India); Genedia® HIV Ag-Ab ELISA (Green Cross Life Science Corporation); and Ortho HIV1/HIV2 Antibody Capture ELISA (Ortho Clinical Diagnostics, USA).

The p24 antigen is also detected by ELISA by specific antibodies produced in an animal host as an immune-complex. This method is cheaper than PCR, easy to perform and shows a high sensitivity. However, the p24 antigen appears early in the course of the HIV infection, being only detectable for 1-2 weeks after infection, and then disappears or falls to very low levels until the onset of the clinical illness.

1.6.6.2 Rapid HIV testing

Rapid test is recommended when immediate information is required for the initiation of prophylaxis. Rapid test is especially useful in rural area in which the patient is unlike to return for a follow-up visit. There are commercial available rapid diagnostic test (RDT) for the diagnosis of HIV based mainly on immunochromatography (or lateral flow assays, similar to the pregnancy test), dot immunoassay (or vertical flow assays) and latex agglutination (similar to the detection of the blood typing test). In all cases, they provide visual readout that can be detected in only minutes with just a drop of sample (serum/plasma, venous or capillary whole blood). These tests are easy to perform and can be used outside the laboratory facilities. Nevertheless, they are extensively used not only in the private practitioner consultation, but also in public health centers, as screening test due to the simplicity and easy interpretation of the results. Moreover, and due to the ability of such test to provide presumptive results in few minutes; it is an irreplaceable tool in emerging areas.[144]

The commercially available tests are listed below being some of them already approved by the FDA, as indicated:

Immunochromatography. OraQuick® Rapid HIV-1/2 Antibody Test (OraSure Technologies, Inc., USA, FDA approved); Uni-Gold Recombigen® HIV Test (Trinity BioTech, Ireland, FDA approved); Alere Determine™ HIV-1/2 (Alere Medical Co. Ltd, Japan, FDA approved and CE marked), SURE CHECK HIV ½ Assay (BioSURE United Kingdom Ltd., UK, CE marked).

Dot immunoassay. Multispot HIV-1/HIV-2 Rapid Test (Bio-Rad Laboratories, USA, FDA approved); Genie II (Bio-Rad Laboratories, USA CE marked), Reveal™ Rapid HIV-1 Antibody Test (MedMira, Canada, FDA approved), INSTI HIV Self test (BioLytical Laboratories, Canada, CE/FDA approved), DPP HIV1/2 Assay (Chembio Diagnostic Systems Inc., USA, FDA approved).

Agglutination. CAPILLUS™ HIV-1/HIV-2 (Trinity Biotech PLC., Ireland).

1.6.6.3 HIV confirmatory tests

HIV infection is typically confirmed by Western blot. This assay involves the separation and identification of the viral proteins. Western blot results can be positive, negative, or indeterminate. However, due to the large number of tests showing indeterminate results and the good performance obtained with the RDTs, they are currently losing popularity.

Due to, under some conditions, Western Blot can produce a relatively large number of indeterminate results, and the fact that these tests are expensive and technically demanding, similar assays were developed to overcome this issue. One of these assays is the Line immunoassays (LIAs) that are based on recombinant proteins and/or synthetic peptides capable of detecting antibodies to specific HIV-1 and/or HIV-2 proteins. Examples of this new technology include the INNOLIA, Pepti-Lav and RIBA assays.[143]

According to WHO and Joint United Nations Programme on HIV and AIDS (UNAIDS) recommendation, the combination of ELISA and/or simple/rapid assays provide results as reliable as the tradition ELISA/WB at a much lower cost.[145,146]

1.6.6.4 HIV Nucleic Acid test

The nucleic acid tests, based on the amplification by PCR of DNA and RNA, has become the most widely used assays for diagnosis of HIV especially during infancy.[147] Moreover, these assays are used for screening of blood products, diagnosis of acute HIV-1 infection and therapeutic monitoring for determining the initiation of antiretroviral therapy and the follow-up of patients under therapy.[148,149] The Aptima HIV-1 RNA Qualitative Assay (Hologic, Inc., San Diego, USA) is the only FDA-approved test for detecting acute HIV infection.

Both DNA and RNA technologies are complex, requiring special equipments and facilities and trained technicians. The detection of DNA by PCR on blood is generally considered the standard method. However, RNA detection provides quantitative information on virological status. This methodology provides a limit of detection of around 300 copies mL^{-1}. Nevertheless, although prices have lately decreased, NATs remain expensive (US$20-30 per test). In settings with limited laboratory facilities, p24 antigen detection can be considered a good alternative to DNA or RNA detection for the diagnosis of HIV-1 in infants and children.[150,151]

Other methodologies such as NASBA based on isothermal amplification and fluorescent-labeled probes for nucleic acid detection, branched-chain DNA, relying on viral RNA capture by complementary probes, and chemiluminiscent detection with signal amplification by DNA amplifier probes, and transcription-mediated amplification for RNA or DNA detection with similar NASBA principle are also important technologies developed to detect and/or quantify HIV RNA (described in *§1.6.7.1)*.

1.6.6.5 The special case of the diagnosis in newborns

Since the IgG in the fetus and the newborn is derived solely from the mother, the HIV antibody test in infant are not recommended because they can provide false positive results in uninfected children who are born to HIV-infected mothers. The antibodies of the mother can cross the placenta and are present in the newborns until the age of 18 months.[152,153] For this reason, the diagnosis in children under 18 months old is recommended by nucleic acid test or p24 antigen detection.[154]

1.6.7 Follow-up of HIV patients

After a positive confirmatory HIV test, the progression of the disease should be routinely monitored by three laboratory tests: a) viral load for determining the level of viremia, b) CD4 count for evaluating the immunological status of CD4 T lymphocytes, and c) microbiological test for controlling opportunistic infections.

1.6.7.1 Viral load

The measurement of the number of RNA viral copies per milliliter of plasma (commonly known as viral load) is a useful tool not only for the monitoring of the disease progression, but

also to assess the effectiveness of the ART. High values of viral load are related to progression towards AIDS. Periodic monitoring is essential every 6-12 months before starting the ART. The assessment should provide undetectable viral load from 4 to 6 weeks after ART.[155,156]

Current viral load methods include quantitative RT-PCR, branched DNA technology and NASBA. As it was described in *§1.4.2*, this kind of tests are technically demanding, being considered as complex assays because require the use of molecular techniques in biosafety cabinets, experienced technicians, and concerns over contamination. Moreover, this technology is costly and may not be affordable in the developing countries.[157] A large number of commercial kits are currently available based on:

RT-PCR. COBAS® Taqman v 2.0 (Roche Molecular Systems), Abbott RealTime HIV-1, VERSANT® HIV RNA 1.0 (kPCR) (Siemens Healthcare Diagnostics), and artus™ HIV-1 QS-RGQ (Qiagen N.V.);

NASBA. NucliSENS EasyQ® HIV-1 v2.0 (bioMérieux);

BranchedDNA. VERSANT® HIV-1 RNA v3.0 (Siemens Healthcare Diagnostics);

Non-nucleic acid based technologies. ExaVir™ Load version 3.0 (Cavidi AB), HIV-1 p24 Ultra ELISA (PerkinElmer) (RUO).

The average price of these tests is ranged from 5 to 40 dollars per assay (roughly four times more expensive than CD4 count). As a consequence, the implementation of viral load in low resource settings is relatively limited.

1.6.7.2 CD4 count

The progressive CD4 T lymphocyte depletion is a hallmark for HIV monitoring, since lower numbers of circulating CD4 T lymphocytes imply a more advanced stage of HIV disease and less competent defense mechanisms. The cluster of differentiation is a protein expressed on the surface of some cells. The expression of these proteins is used in lymphocyte nomenclature. These proteins are often associated with the specific function of the cells. Cells with different functions express different CD molecules (for instance, total T lymphocytes are CD3+ cells, T helper cells are CD4+ T lymphocytes, cytotoxic T cells are CD8+ T lymphocytes, and B cells are CD19+ lymphocytes).

T lymphocytes are a subset of white blood cells while CD4 is a type of protein found on the membrane of certain immune cells like T lymphocytes, macrophages, and monocytes. CD4 T lymphocytes play a role triggering the body´s response to infections but not neutralizing

infections. They provide help to B cells for the production of antibody, as well as in enhancing cellular immune response to antigens. Because of that they are also called T "helper" lymphocytes. During infection, HIV attaches to these cells, and kill them. In that way, the ability to trigger an immune defense is gradually depleted. Thus, the number of CD4 T lymphocytes shows the status of the immune system of a patient. A normal count of a healthy adult is typically around 500 to 1500 cells per microliter. The CD4 count varies according to the age, population, among other factors. This test is a major laboratory indicator for assessing the damage of the immune system during the progression of the disease, especially during the clinical latency. It is used for HIV disease classification and AIDS definition (Table 1.2), and for designing the clinical trial. Together with viral load, CD4 count is also a good indicator of disease prognosis. Moreover, CD4 count is one of the key factors in determining both the urgency of antiretroviral therapy initiation and the need for prophylaxis for opportunistic infections.[158] It is also the best predictor of disease progression and survival, according to clinical trials and cohort studies. In children aged less than 5 years, the CD4 count is considered the more reliable biomarker for assessing the immune competence.

For all these reasons, regular CD4 count is essential for the monitoring of HIV infections.[159] In untreated patient, CD4 counts should be monitored every 3 to 6 months to assess the urgency of ART initiation and the need for opportunistic infection prophylaxis. Finally, under ART, regular monitoring is necessary to provide information regarding the magnitude of immune reconstitution.

Table 1.2. CD4 count values and clinical status

CD4 level (cell μL^{-1})	Medical value
1200 -600	Normal value in healthy people
500	Start monitoring every 6 months
>300	Very few HIV-related problems, except cancers. Reduced response to vaccinations.
200-300	Water and foodborne pathogens infections (microsporidia, crytosporidia) and skin problems
200	AIDS diagnosis
<200	Pneumocystis pneumonia
<100	Mycobacterium, toxoplasmosis
<50	*Cytomegalovirus* and increased risk for any other disease

1.6.7.3 Microbiological Test

During the progression of the disease, opportunistic infections are responsible of the morbidity and mortality in AIDS patients. Among the opportunistic infections, bacterial enteric and respiratory disease, candidiasis, pneumonia, mycobacterium tuberculosis, cytomegalovirus disease, and Kaposi's sarcoma are the most important to be diagnosed.

1.6.8 CD4 counting by flow cytometry

Flow cytometry (FC) is currently considered the gold standard for CD4 count and also the first choice if a large throughput of samples has to be processed.

Flow cytometry is a complex technology known as automated analytical and quantitative cytology. As the term implies, it measures the properties of the cells, one-by-one, as they flow in a liquid stream, being able to detect any particle ranging from 0.2 to 100 µm at very high rate (10 to 1000 entities/second). The events/particles are illuminated individually as they pass through a laser source, and the light that is scattered and emitted by the cells is then separated into their constituent wavelengths by a series of optical filters and mirrors. The separated optical light falls on individual photodetectors and converted into an electrical pulse, and subsequently to a digital signal.[160] There are three types of phodetectors: forward scatter (FSC), side scatter (SSC) and fluorescence detector.

The properties measured by this technique include the particle size, the granularity or internal complexity and the fluorescence intensity.[161] Each of these characteristics is related with one of each detector. Thus, the light intensity that is scattered in the forward direction (FSC) is roughly equates to the particle size, while light intensity that is scattered in the side direction (SSC) provides information about the granular content within a particle.[162] Both FSC and SSC are unique for every particle, and a combination of the two are used to differentiate cell types/entities in a heterogeneous sample. Moreover, the use of antibody technology in FC has facilitated the phenotypic characterization of cell population. Fluorochromes can be easily attached to specific antibodies or proteins for identifying or studying the expression of different proteins in the cell surface. In each single assay, different fluorochromes can be used for multiplex cell surface biomarkers determination.

Absolute CD4 T lymphocytes count is an immunofluorescence analysis that can be performed using dual- or single-platform methods by employing a biparametric analysis after

the labeling of the sample with fluorescent antiCD3/antiCD4 antibodies or antiCD45/antiCD14 antibodies, according with the gating strategy used.

1.6.8.1 Dual-platform flow cytometry approach for CD4 cell count

In this approach, absolute CD4 count is generated by the combination of two instruments: a haemocytometer or haematology analyzer to enumerate the absolute lymphocyte number, and a flow cytometer, to obtain CD4 T lymphocyte percentage. The absolute CD4 counts are calculated by multiplying the percentage of CD4 cells by the absolute lymphocyte count. In this analysis, variation in the total white blood counts results in a great variability in the % of CD4 cells. This problem is increased in leucopenic patient where the cell number is lower than the sensitivity of the haematological analyzer.

1.6.8.2 Single-platform approach for CD4 counts

This technique enables the absolute CD4 count in an accurate sample volume or by using a known number of fluorescent beads, without the need of coupling a haematological analyzer.

In this dissertation, absolute CD4 counts was performed in a single-platform method using Perfect-Count Microspheres that combines the advantages of direct flow cytometry for cell phenotyping with the use of two different fluorescent microspheres (A and B beads) for absolute counting. Fluorescent CD4 and CD3 antibodies are used for specifically detecting CD4 T lymphocytes. This receptor, as previously stated, is present not only on the membrane of all mature T-cells, but also in other immunological cells such as monocytes, macrophages, and dendritic cells. The use of a second marker such as CD3 avoids interferences of other expressing CD4 receptor cells. While a number of blood cell types may express either CD4 or CD3 antigens (i.e. monocytes and thymocytes, respectively), only -helper lymphocytes express both CD4 and CD3 simultaneously.

For absolute cell counts, a known volume of the Microsphere beads suspension is added to a known volume of stained sample, so that the ratio of sample volume/beads volume is known. Thus, the absolute cell count (as the number of cells per microliter) is obtained by relating the number of cells with the total number of fluorescent microsphere events. The A and B beads ensure the accuracy of the assay by verifying the proportion of both types of microsphere during the analysis.

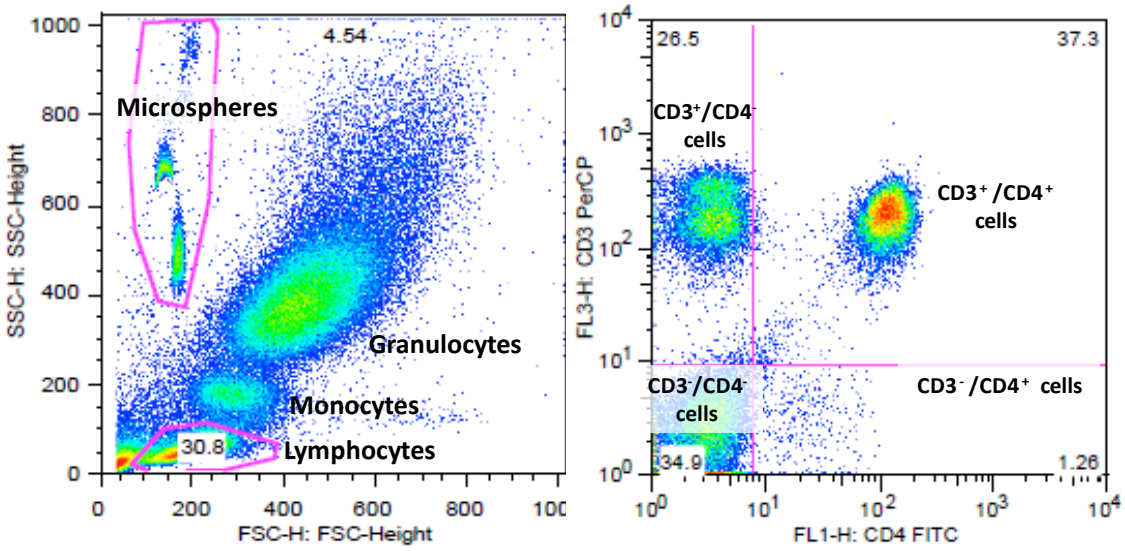

Figure 1.17. Flow cytometry analysis of whole blood for CD4 absolute counts using antiCD3 and antiCD4 label with (fluorescent dyes) antibodies. Left: FSC vs SSC dot plot, in which lymphocyte and microsphere are gated. Right, CD3/CD4 receptor expression analysis of lymphocytes gate from whole blood.

The Figure 1.17 (left panel) shows the typical dot plot graph of FSC vs SSC obtained from whole blood where lymphocytes and microspheres were gated. Right panel of Figure 1.17 shows the CD3/CD4 receptor expression analysis of the lymphocyte gate (left panel). In this panel, three different populations of T cells are shown: CD3-/CD4-which correspond to B lymphocytes, CD3+/CD4- which correspond to CD8 lymphocyte, CD3-/CD4+ which correspond to macrophages, while CD3+/CD4+ correspond to CD4 T lymphocytes.

1.7 Ebola virus disease

Ebola virus is the causative agent of a hemorrhagic fever being the fever and bleeding the major symptoms during this infection. There are five identified Ebola virus species, four of them are known to cause disease in humans: Zaire virus (*Zaire ebolavirus*); Sudan virus (*Sudan ebolavirus*); Taï Forest virus (*Taï Forest ebolavirus*, formerly *Côte d'Ivoire ebolavirus*); and Bundibugyo virus (*Bundibugyo ebolavirus*). However, only a single human case were reported for Tai Forest Ebolavirus.[163] The fifth, Reston virus (*Reston ebolavirus*), produces disease only in nonhuman primates.

After the Ebola virus was identified, 33 sporadic outbreaks worldwide, including 23 human-to-human transmission epidemics, three laboratory-induced outbreaks, and seven animal-to-

human transmission outbreaks.[164] *Zaire ebolavirus*, *Sudan ebolavirus* and *Bundibugyo ebolavirus* are transmitted human-to-human and they are the responsible of the different Ebola outbreaks resulting in different geographic extensions and case fatality rates.[165,] Zaire and Sudan species are responsible for most of the Ebola outbreaks since the first case reported in 1976.

The first case of filoviral hemorrhagic fever were reported in August 1967 in Marburg (Germany) after three laboratory workers got ill by processing organs of infected primates imported from Uganda. In the same year, other case was reported in Belgrade (Yugoslavia). The causative agent was identified as Marburg virus.[166] Almost ten years later, in 1976, Ebola virus was identified in two separate outbreaks occurring simultaneously in Sudan and Zaire (now Democratic Republic of Congo).[167] Ebola virus got its name due to the Ebola River located in the Democratic Republic of Congo, close to the first outbreak. Epidemic studies after the outbreaks resulted in the identification of two distinct species: *Zaire* and *Sudan ebolavirus*.[168]

In 1989, a new strain of Ebola virus was discovered in Reston, Virginia, during the investigation of hemorrhagic casualties in monkeys (*Macaca fascicularis*) imported from the Philippines. Subsequent outbreaks in the United State and Italy due to this strain were reported and in all cases due to infected primates imported from the Philippines.[169] Nevertheless, the Ebola Reston strain possesses low pathogenicity to humans.

Cote d´Ivoire Ebola virus was first reported in 1994 in Ivory Coast, Africa. The virus was isolated from a worker infected during a chimpanzee autopsy.[170] Finally, the last specie was discovered in 2007, in Bundibugyo District, Western Uganda. This strain was reported to have the lowest fatality rate (34%) compared to the others Ebolavirus strains.[171]

1.7.1 Ebola virus

Ebola virus belongs to the *Filoviridae* family of RNA viruses which consists of two genera: *Ebolavirus* (EBOV) and *Marburgvirus* (MARV).

Filovirus virions present a long filamentous shape with uniform diameter of 80 nm but showing variable length. Besides, the viral particles can be branched, circular or U-shaped (Figure 1.18, panel A).[94,172] This morphology is unique among virus and has been decisive for their classification. Ebola virions have a central core formed by a ribonucleoprotein complex (RNP) surrounded by a lipid envelope derived from the host cell plasma membrane

(nucleocapsid) and a transmembrane surface protein composed of trimers of the viral glycoprotein (GP).[173,174] The RNP is composed of a single molecule of linear RNA and four of the seven virion structural proteins: nucleoprotein (NP), virion structural proteins 35 (VP35) and 30 (VP30), and the L-polymerase protein. Two additional viral proteins, VP40 and VP24, are present in the membrane (Figure 1.18, panel B). The nucleocapsid contains a negative-sense, linear single-stranded RNA molecule of 19 kilobases. The negative sense virus is not infective by itself, as it needs to be converted to a positive sense RNA by a RNA polymerase for transcription and replication.

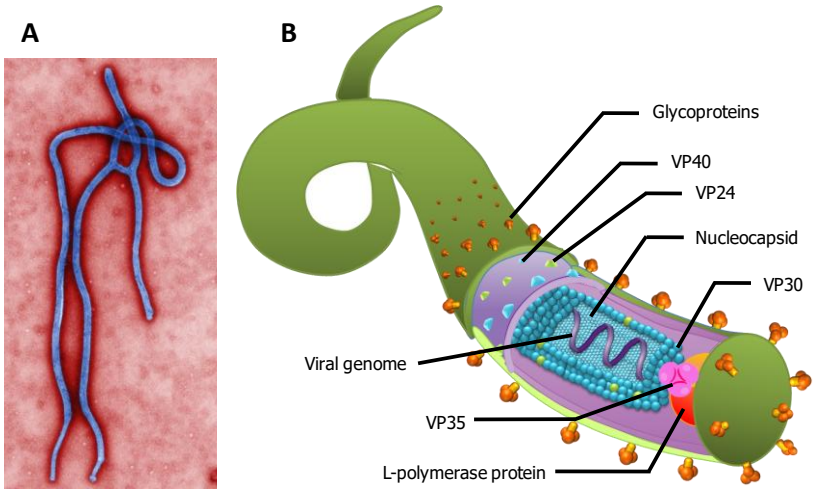

Figure 1.18. Structure of Ebola virus. A) Electron microscopy of the Ebola virus; B) Molecular structure of the Ebola virus.

The Ebola virus genome is organized in seven sequential genes with in-between noncoding regions in the following order: 3´NP gene- VP35 gene – VP40 gene – GP gene –VP30 gene – VP24 gene – L gene – 5´ (Figure 1.19). NP, VP35, VP30 and L-polymerase proteins are involved in formation of the viral ribonucleoprotein complexes (basic unit for viral replication).

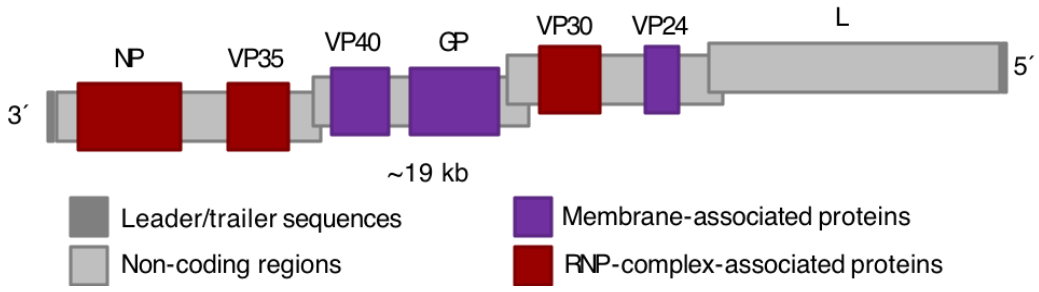

Figure 1.19. Schematic genome organization of *Zaire Ebolavirus* of a representative member of the *Filoviridae* family of viruses.

1.7.2 *Ebolavirus* infection

Transmission of *Ebolavirus* from human-to-human requires close proximity, such as direct contact with blood or body fluids leading to mucous membrane exposure.[175] The transmission was only documented in patient exhibiting symptoms of the disease and is not likely occurred during the incubation period.

During the outbreaks, the first transmission to humans are usually linked to a zoonotic transfer by an animal host, including bats[176,177] or primates[170,178] (gorilla and chimpanzees) exposure. Further infections occur from close contact with relatives, medical staff or contact with corpses. Sometimes, the spread of the disease is strongly associated with treatment seeking of patient from rural villages to urban centers with central medical facilities.[179] Moreover, hospitals occasional serve both as focus and amplifier of the infection as it happened in Maridi in 1976 (213 cases). Finally, an outbreak usually ended when the person-to-person transmission is inefficient. Because of that, patient isolation or quarantine is a critical barrier to interrupt the dissemination of the disease.[180,181]

1.7.3 Clinical stages of the *Ebolavirus* infection

Ebola virus disease (EVD) presents a very high case fatality (mortality ranging from 23% to 90%). The absence of a treatment or vaccination makes it an important pathogen for global health.[182] Filoviruses are classified as Biological Level 4 agents (WHO; Risk Group 4) based on their high mortality rate, person-to-person transmission, potential aerosol infectivity, and the lack of vaccines for prevention and treatment.

The *Ebolavirus* infection is broadly classified in 3 phases:

Onset. The first phase involves the incubation period, which takes from 2 to 21 days after infection. The clinical symptomatology starts with non-specific flu-like symptoms in the 0-3 days, involving fever, fatigue, body ache, sore joints, nausea, vomiting and diarrhea. The most common symptoms are fever in combination with a maculopapular rash around the face, neck, trunk, and arms usually appearing by day 5-7 of the illness.[183]

Bleeding. In the second phase, symptoms often include lethargy, nausea, vomiting, abdominal pain, anorexia, diarrhea, coughing, headache, and hypotension. EVD patients are often dehydrated due to severe diarrhea and vomiting, which frequently leads to acute renal failure. Electrolyte disturbances are also common, including life-threatening hypokalaemia.[184] Hemorrhagic manifestations do not occur in all cases, varying in severity from patient-to-

patient. It was reported that patient with higher incidence of diarrhea, electrolyte disturbances or high viral load are associated with a higher mortality. Mucosal hemorrhage, petechiae, and ecchymosis can be observed in patients with EVD, while massive hemorrhage is usually observed only in fatal cases.

Recovery/Death. The final phase (convalescent or deterioration) (≥ 10 days) involves gastrointestinal hemorrhage, secondary infections, meningoencephalitis, shock and hypotension.[185,186] Moreover, high viral load is closely associated with higher case fatality.[187] Survivors also have higher levels of virus-specific antibodies compared with fatal cases, which have little or no detectable antibody responses before death. Fatal cases progress to more severe symptoms by days 7 to 14 after the onset of disease; death is generally imminent shortly after the onset of coma and shock. Patients who survive from Ebola infection have been reported to show clinical improvement by the middle of the second week.

1.7.4 Laboratory test for Ebola Virus diagnosis

The priority in controlling this epidemic is to promptly identify and isolate infected individuals. Misdiagnosis of Ebola may bring a huge impact on the society. False-positive results put an individual patient in risk of infection by placing him in an Ebola treatment center such as an isolation ward or other Ebola-related health facility. Moreover, a false negative will allow an infected person releases and spreads the disease into the community. Given the consequences of misdiagnosis, WHO highly recommends that only diagnostics that have undergone independent, compressive assessment of quality and safety are used in diagnosing infection with Ebola virus.

Rapid diagnostic methods are essential in control of Ebola outbreaks and lead to a rapid isolation of cases and improved epidemiologic surveillance. The development of new test that replace the used of blood samples by non-invasive samples including, for instance, oral fluid, is still a big challenge due to the strong cultural objections that face medical staff at diagnostic or autopsy. Early Ebola diagnostic test should be done to a mobile biological safety laboratory (BSL) in order to accurately determine its diagnosis. The need of BSL-4 facility to perform Ebola detection and diagnostics using these methods is an additional limitation in Ebola disease management. Nevertheless, only a few international reference laboratories have the level of contingency for Ebola manipulation analysis. In Spain, there is not any BSL-4 laboratory. In Africa there are only two BSL-4 laboratories placed in Gabon and South Johannesburg. Thus, sample collection and transport of the patient blood to BSL-4 laboratory requires specialized

biosecurity laboratory training.[188,189] Lack of routes that connect rural to urban areas represents another obstacle in the management of the disease.

The diagnosis of Ebola infected people is firstly based on the clinical symptomatology. However, many infectious diseases which are epidemic in Africa show the same preliminary non-specific clinical symptoms, including Malaria, typhoid fever, yellow fever, Chickungunya fever, among many others. When a patient shows the non-specific clinical symptoms and is suspected to be infected by Ebola, containment procedures have to be initiated as well as the clinical test.

According to the WHO guideline,[190] detection of the viral antigens or viral RNA is recommended for Ebola diagnosis in the early stage of the illness, while serological diagnosis by detecting specific IgM and IgG antibodies is suitable for late stage of the disease. The diagnosis cannot be based on a single detection method. Thus, a laboratory result should be confirmed before discharging a symptomatic patient from the hospital. Antigen ELISA and quantitative RT-PCR (q-RT-PCR) are the primary test commonly used for acute case diagnosis because its combination provides a rapid and sensitive testing with the fewest resources. When alternative confirmatory tests are not available, molecular diagnostics based on an independent target gene can be used for the confirmation.

The most common laboratory diagnostic tests for Ebola detection/identification are described below. These methods include cell culture, specific antibody/antigen detection test, molecular tests and immunostaining.[191]

1.7.4.1 Cell culture and electron microscopy

In early studies, cell culture and electron microscopy was an important technique to identify these microorganisms and to diagnose pathogen. Ebola virus was discovered in 1976 via traditional viral culture techniques and electron microscopy. The detection of Ebola by these methods is definitive, however, it requires biosafety level 4 containment and they are restricted to research and public health laboratories.[191]

1.7.4.2 Antibody/antigen detection test

Antigen detection by ELISA is used in symptomatic patients during early stage of illness where the high titers of virus are present in blood. Antigen-capture ELISA test uses a pool of

antibodies against the Ebola virus particle for capturing and detecting the viral particles. The main viral targets are the NP, VP40 and GP proteins.[192-195]

For diagnosis based on the detection of antibodies, several immunofluorescent assays were developed. This test is recommended during early convalescence or in seroepidemiological surveys. The assay sensitivity is strongly associated with the antigen of Ebola virus used for IgG or IgM detection. However, ELISA offers a faster, higher-throughput system for serologic test. Moreover, ELISA is compatible with gamma irradiation, allowing the sample processing under BSL-2 conditions, while BSL-4 facilities is required to prepare authentic Ebola antigens.[196-198] Some commercially available Ebola IgM and IgG ELISA kit that utilized recombinant viral proteins has been employed in recent clinical research.

1.7.4.3 Molecular test

Several PCR-based methods were developed for Ebola diagnosis bases in the identification of GP, filo L, or NP conserved sequences followed by sized-based amplicon detection via gel electrophoresis.[199-202] One of the main advantages of this kind of test is that chemical inactivation of the virus can be performed during RNA extraction steps. Despite its diagnostics advantages, molecular test requires electrical power, laboratory infrastructure, and technical expertise, among others. However, in the last outbreaks, expertise in mobile laboratories with molecular testing capacity was gained.

Real–time RT-PCR using fluorogenic probes have become the standard methodology for diagnosis of acute Ebola virus test. Other kind of molecular test such as nested PCR was widely used in the Ebola outbreak in 2000. This test was based on a set of primers specifically designed for nucleoprotein region.

Currently, several diagnostic test with WHO or FDA status presents emergency use authorization. In detail, RealStar® Filovirus Screen RT-PCR Kit 1.0 (Altona Diagnostics GmBH, WHO authorization, L gene RNA), RealStar® Ebolavirus RT-PCR Kit 1.0 (Altona Diagnostics GmBH, FDA authorization, L gene RNA), EZ1 Real-Time RT-PCR Assay (U.S. DoD, FDA authorization, GP gene), CDC Ebola virus NP real-time RT-PCR assay (CDC, FDA authorization, NP gene RNA), CDC Ebola virus VP40 real-time RT-PCR assay (CDC, FDA authorization, VP40 gene RNA), LightMix® Ebola Zaire rRT-PCR Test (TIB MOLBIOL Syntheselabor GmBH, FDA authorization, L gene RNA), Liferiver Ebola virus real-time RT-PCR kit (Shangai ZJ BioTech, WHO authorization, NP gene RNA), FilmArray NGDS BT-E assay (BioFire Defense, FDA authorization,

L gene RNA), FilmArray Biothreat-E Test (BioFire Defence, WHO and FDA authorization, L gene RNA), and XperEbola assay (Cepheid, WHO and FDA authorization, NP, GP gene RNA).

1.7.4.4 Rapid detection test

During the last outbreak, lateral flow immunoassays represented a powerful tool for rapid antibody for rapid test that can be performed at point of care. Thus, three *Ebolavirus* rapid diagnostics, based in lateral flow immunoassay, have received WHO and/or FDA status to be use at point of care. ReEBOV Antigen Rapid test (Corgenix) was the first rapid test that obtained WHO and FDA status. This kind of test can be used bedside with only a drop of fingerstick blood of the patient. Specific antibodies to VP40 protein are immobilized on the test strip. If the virus is present in the sample, immunocomplex are bind in a specific localization on the test. After 15-25 min the result can be visualized. Other two tests, OraSure Ebola Rapid Antigen test (Orasure Technologies, WHO and FDA authorization) and SD Q Line Ebola Zaire Ag (SD Biosensor, WHO authorization), detect VP40 protein and NP, GP and VP40 respectively.

1.8 Biomarkers detection of global infectious diseases based on magnetic particles

Infectious diseases affect the daily life of million people all around the world, and are responsible for hundreds of thousands of deaths, mostly in the developing world. Although most of these major infectious diseases are treatable, the early detection of people requiring treatment remains a major issue. The incidence of these infectious diseases would be reduced if rapid diagnostic tests were widely available at the community and primary care level in low-resource settings. Strong research efforts are thus being focused on replacing standard clinical diagnosis methods such as the invasive detection techniques (biopsy or endoscopy.) or expensive diagnosis and monitoring methods for affordable sensitive tests based on novel biomarkers. The development of new methods that are needed includes solid-phase separation techniques. In this context, the integration of magnetic particles in bioassays and biosensing devices is very promising since they greatly improve the performance of a biological reaction. The diagnosis on clinical samples with magnetic particles can be easily achieved without any pre-enrichment, purification or pretreatment steps, which are usually required for standard methods, which simplifies the analytical procedures. The biomarkers can be specifically isolated and preconcentrated from complex biological matrixes by magnetic actuation, increasing the specificity and the sensitivity of the assay. This review addresses these promising features of the magnetic particles for the detection of biomarkers in emerging technologies related with infectious diseases affecting global health such as malaria, influenza, dengue, tuberculosis or HIV.

1.8.1 Introduction

Despite the impact of the biotechnology, nanoscience and information and communications technology in daily life, the burden of infectious disease is still an issue, affecting global health. Annually, just under 5 million people die from AIDS /or complication related to AIDS and tuberculosis, 2.9 million from enteric infections and 1 million from malaria.[8] The globalization and the population movement have accelerated the spread of infectious disease outbreaks around the world that initially were geographically localized.[9] In most of the cases, early diagnosis and treatment can interrupt the transmission of the infectious agent and prevent the development of long-term complications.

This review article has been published in the journal New biotechnology, 2015, 32(5), 521-532.

Infectious diseases are treatable, and access to drugs has improved markedly over the past decade with the advent of drug-access campaigns, mass-treatment programs and public resources promoting by the United Nations Millennium Development Goals towards Global Health. It was also defined as 'public health without borders'.[11] Most global health centers are in high-income European Union (EU) countries with strong links with low-income countries,[12] due to the investing support of the European Parliament in R&D for global health. However, and despite this major initiative, the need for early detection of people requiring treatment remains a major issue to disease control, since the incidence of infectious disease could be substantially reduced if appropriate diagnostic tests were more widely available at the community and primary care level in low-income countries.[8] The diagnostic tests of these infection diseases affecting global health in the developing world should be simple and affordable in low-resource settings without any lost in the analytical performance. The complexity of a test includes the need for user interpretation, the level of training necessary, the number of manual manipulations, the number of user intervention steps required, and the instrumentation requirement.[17,18]

Gold standard techniques in infectious diseases diagnostics include microscopy, tissue culture, nucleic acid-based techniques and, in some instances, ELISA. Conventional microbial identification methods usually include a morphological evaluation of the microorganism as well as tests for the organism's ability to grow in various media under a variety of conditions, which involve the following basic steps: a) preenrichment, b) selective enrichment, c) biochemical screening and d) serological confirmation. These growing and enrichment steps are relatively time-consuming having a total assay time of up to 1 week in certain pathogens. Moreover, some of them are slowly growing microorganisms or extremely dangerous. In these instances, the identification is determined by the serological detection of the immunological response (antibodies) against the infectious agent of the immune response. ELISA is widely used in clinical diagnostics due to their relatively robustness, versatility and high-throughput. However, the good performance of this assay depends on the operator's skills.

The development of molecular diagnostic techniques represents a great advance in the diagnosis and follow-up of infectious diseases.[44,203,204] Nucleic acid-based detection may be more specific and sensitive than immunological-based detection. Furthermore, the polymerase chain reaction can be easily coupled to enhance the sensitivity of nucleic acid-based assays, especially for slowly growing or hazards microorganisms. Reverse transcriptase polymerase chain reaction has also played an important role in diagnosing RNA-containing virus infections.

However, new methodologies are needed accordingly to the *ASSURED* recommendation published by World Health Organization (WHO), being this acronym defined by (A) *A*ffordable, (SS) *S*ensitive, *S*pecific, (U) *U*ser-friendly, (R) *R*apid and *R*obust, (E) *E*quipment free, and (D) *D*eliverable to those who need it.[18] The development of novel diagnosis platforms to meet the World Health Organization requirements should be focused thus on: *(A)* Cost-effective emerging technologies such as biosensors, lateral flow and agglutination tests, appropriate for application at community and primary-care level as well as in low resource settings; *(SS)* Novel diagnostic targets and disease biomarkers development, to achieve specificity (no false positives) and sensitivity (no false negatives); *(U)* Analytical simplification in order to minimize pipetting, washing steps and manipulation of reagents to provide analytical tools requiring minimal training for final users; *(R)* Robust tests, portable and stable at room temperature, able to provide rapid results and to enable taking actions immediately such as treatment at first visit; *(E)* Bench-top and high cost instrumentation should be avoided, and visual detection should be prioritized; (D) The biomarkers should be selected among the major problems facing the global health, including pathogenic bacteria occurring in food outbreaks, in order to ensure safety in food and water supplies in low resources settings, as well as major global infection disease in low-incomes countries, such as AIDS, malaria, dengue, influenza, and tuberculosis. It is important to highlight that the technology derived from these guidelines would be also transferable to other novel biomarkers related with developed countries for personalized medicine as well as for point-of-care diagnosis in the developed world.

To meet these demands, the preeminent formats under development are lateral-flow, microfluidic devices, lab-on-a-chip and biosensors. However, lateral flow assays show in general poor sensitivity, being a limitation for the detection of novel biomarkers present at low concentration levels.[205] The cost of production of microfabricated devices, requiring in most of the cases bench-top equipments for the readout, still constitute a bottleneck and may put them out of range for end users in the developing world. Biosensors are compact analytical devices, incorporating a biological sensing element, either closely connected to, or integrated within, a transducer system. Despite the massive use of glucose biosensor with electrochemical transduction, examples of other application including diagnosis of infection diseases are currently very limited. As complexity in the methodology increases, from agglutination,[206] lateral flow,[207] ELISAs,[208,209] and PCR-based assays,[210] the analytical performance in terms of sensitivity and specificity also increase. Unfortunately, the total assay time and the need of complex instrumentation requiring costly maintenance also increase.[211]

The main challenge in bioanalysis is thus to provide affordable methods with any loss in the analytical performance.[8]

Novel development in clinical diagnosis that is needed involves preconcentration procedures in solid supports which can be easily integrated in emerging technologies. The biomarkers in complex clinical samples can be thus preconcentrated while the interfering matrix is being eliminated at the same time, increasing the sensitivity and the specificity of the test. One of the most prominent materials to meet this challenge is magnetic particles (MPs).[212] The MPs can be tailored modified to specifically bind the biomarkers and concentrate them from the complex specimen under magnetic actuation, avoiding interferences before testing.[213-215] Magnetic particles (MPs) are synthesized containing a magnetic element in its core such as iron, nickel, neodymium or magnetite. Nowadays several companies offer a wide range of product based on magnetic particles, such as Adembeads®,[216] Dynabeads®,[217] BioMag®,[218] SiMAG®,[219] Miltenyi,[220] among many others.

Although there are commercially available MPs already functionalized with biomolecules for a variety of bioanalytical and biotechnology applications, they can be also tailored modified with specific receptors, using surface chemical groups such as tosyl, amine, carboxyl or epoxy, for the identification/isolation of novel biomarkers including whole organisms, proteins and peptides, antibodies, DNA, among others.[221] With this purpose, recent advances are focused on the use of magnetic particles in magneto-actuated rapid diagnostic tests (RDTs). The integration of magnetic particles can thus simplify the analytical procedure, avoiding the use of classical centrifugation or chromatography separation strategies, since no pre-enrichment, purification or pretreatment steps, which are normally used in standard analytical methods, are required.

Moreover, their use as solid support in bioassays has shown to greatly improve the performance of the biological reactions.[222] Moreover, magnetic particles are used not only as a solid support, but also as a label for detection of a biorecognition event.[223]

Beside the progress in emerging technologies for diagnosis, the study of novel biomarkers for the early detection of infectious diseases is a worldwide challenge.[224] The World Health Organization has defined a biomarker as “almost any measurement reflecting an interaction between a biological system and a potential hazard, which may be chemical, physical, or biological”.[225] The measured response may be functional and physiological, biochemical at the cellular level, or a molecular interaction.[222] The identification of novel biomarkers represents a challenge not only for the improvement of early diagnostics, but also for the patient

monitoring and for the evaluation of the efficiency of a therapeutic strategy. Biomarkers are also very promising candidates in achieving the customization of the healthcare for personalized medicine.

This review describes recent advances in infectious diseases diagnosis using magnetic particles and magnetic-actuated RDT, with special focus on the current trends and perspectives for magnetic separation, magnetic labels, and magnetic detection of biomarkers related with infectious agents affecting global health, such as HIV/AIDS, Tuberculosis, Influenza, Malaria and Dengue.

1.8.1.1 HIV diagnosis and AIDS monitoring based on magnetic particles

The Human Immunodeficiency Virus (HIV) is a retrovirus which infects cells of the immune system, primarily CD4+ T lymphocytes. Progression to Acquired Immune Deficiency Syndrome (AIDS) occurs as a result of chronic depletion of CD4 cells, when the count falls below 200 cells μL^{-1} of blood, at a functional level where opportunistic infections and malignancies cannot be controlled.[226,227]

The HIV infection is commonly diagnosed through blood test detecting antibodies against HIV virus, followed by a confirmatory assay.[228] The serological tests for detection of HIV antibodies are generally classified as screening and confirmatory, being ELISA and Western blot, respectively. A variety of simple, instrument-free, rapid test including agglutination, immunofiltration, immunochromatographic and dipstick test, for instance OraQuick® Advance Rapid HIV-1/2, Reveal™ G-2 Rapid HIV-1 Antibody, Uni-Gold Recombigen® HIV, Multispot HIV-1/HIV-2 Rapid are commercially available.[229] HIV cannot be diagnosed in children by anti-HIV antibody based-test because the maternal antibodies are able to cross the placenta giving false positive results. In this case, virological test based on virus or viral component such as HIV RNA or HIV DNA or ultrasensitive HIV p24 antigen detection, is recommended. After HIV diagnosis, the disease progression should be monitored through viral load based on viral nucleic-acid detection or through the enumeration of CD4 cells by flow cytometry. Nucleic-acid-(amplification) test are laborious strategies, requires dedicated equipment and trained technicians. On the other hand, flow cytometry requires complex and expensive equipment that needs regular maintenance and well trained personnel not only for data analysis, but also for the results interpretation. Currently, there are only few cheaper alternatives to the flow cytometer and they are mostly based on fluorescent labeling, requiring thus costly imaging equipment to achieve detection or, instead, on manual counting with light microscopes.[230-232]

Although RDTs are commercially available for the diagnosis of HIV infection CD4 counting is not available in the areas mostly affected by the HIV[227, 233- 236] being this control imperative for assessing the degree of immune deterioration and speed of progression towards AIDS, and also for initiating the treatment.[237] Recent advances involve the integration of magnetic particles in bioassays for both diagnosis of HIV infection, as well as for the progression and follow-up of AIDS.

RDTs based on magnetic particles for the early detection of HIV infection involving the HIV-1 p24 antigen as biomarker was reported.[238] The magnetic particles were integrated as labels and magnetic readout was used for the detection of HIV infection.[239] In this instance, superparamagnetic particles were integrated in a magnetic immunochromatographic test (MICT) for the HIV-1 p24 antigen determination. The magnetic nanoparticles were used as an alternative to colloidal gold markers usually involved in lateral flow tests for optical readout. In this approach, antibody modified magnetic nanoparticles were incubated with the sample and added to a cassette. The reaction line was read using a magnetic assay reader system that detects the magnetic moment of the superparamagnetic particles bound to the sample. MICT was demonstrated to be a good alternative for rapid HIV test taking advantages of lateral flow test such as simplicity and speed while the use of magnetic nanoparticles and magnetic reader conferred quantification properties to the assay. In other example of HIV infection detection based on HIV-1 p24 antigen, a magneto-actuated amperometric immunosensor based on the integration of gold magnetic nanoparticles (MNPs) was described. This MNPs were coated with multiwalled carbon nanotubes and functionalized with an anti-p24 antibody on the surface of a disposable screen-printed electrode for the p24 electrochemical detection in a one-step format.[240] Due to the integration of MPs in the assay, the immunocomplex could be eliminated by removing the magnetic field, conferring a very easy way to renew the electrode surface by desorption.

The integration of magnetic particles in DNA and RNA-based approaches for the separation and detection of sequences related with HIV was also reported. For instance, polyvinyl alcohol-based magnetic particles were used as viral nucleic acid preconcentration method in combination with detection by reverse transcriptase -polymerase chain reaction (RT-PCR) in one-step.[241] This protocol was applied to screen blood donation with the objective of reducing blood-born transmission of HIV in blood blank. Furthermore, the utility of the bar-code based amplification assay (BCA) in HIV was also demonstrated. This chip-based technique combines gold and magnetic nanoparticles to achieve PCR-like sensitivity.[242,243] The general principle of the bar-code is well known, and involved the ssDNA/RNA target capture

throughout hybridization using a complementary oligonucleotide modified magnetic particle. Target-specific gold nanoparticles loaded with bar-code oligodeoxynucleotide (ODN) probes sandwiched the target. The genetic material acts as a bridge to join the gold NPs bar-code probe with the magnetic particles. After capturing and labeling the DNA target, a magnetic field separated the complexes from the sample. Afterward, the sample was heated to achieve denaturation of the bar-code ODN probes which amplify the signal using a scanometric detection method. With this approach, the multiplexed detection of four synthetic genetic DNA sequences representing the Hepatitis B, Variola, Ebola and HIV viruses were demonstrated.[244] The limitation of this method is that requires the use of detectors such as the Verigene ID^{TM} system to measure the scattered light from the nanoparticles, which is an expensive and complex bench-top instrument.

The multiplex detection of synthetic DNA sequences related with HIV, Ebola and Influenza viruses was demonstrated using a flow injection analysis with electrochemical detection coupled with magnetic particles for DNA isolation.[245] Paramagnetic particles modified with oligo dT sequences were used in this instance to isolate synthetic ODN related with the viral sequences. The preconcentrated synthetic polyA sequences related with the mRNA viral sequences were then hydrolyzed to the monomeric units by applying microwave digestion. The detection was performed in a microfluidic approach on glassy carbon electrode modified with Cu(II)/or CuS nanoparticles to enhance the sensitivity for adenine determination. In this approach, the integration of MPs was used for the elimination of undesirable biomolecules than could affect the specificity and sensitivity of the assay.

Although there are many commercially available for POC HIV diagnosis, there still the need for novel affordable alternatives to flow cytometry for CD4 count in order to monitor the AIDS disease and the treatment in low resource settings. For instance, a microfluidic platform coupling to magnetic particles was described for CD4 cell counting.[246] In this approach, the sample was moved by using magnetic force that pulls the beads thought different chambers. This microfluidic chip was used in an ELISA-like format in a fully automated manner for CD4 cell count. The chip was divided in three compartments. In the first one, the sample collection was performed. The second compartment was the micro-ELISA based chip. Here, the sample was capture using magnetic particles conjugated to anti-CD4 antibody and, further labeled with and anti-CD3 antibody conjugated to peroxidase enzyme (HRP). The enzymatic substrate was also added in this platform. Imaging and data analysis was performed in the third section using a cell phone-based colorimetric detection system. Although this approach presented some

technical limitations, the main achieve of this chip is that MPs were used for non-fluidic transport avoiding high shear stress of the sample.

Finally, Dynal developed a commercial test (T4 Quant Kit) for CD4 cell counting that employs magnetic bead coated with CD14 antibody to bind monocytes that are captured before lymphocyte isolation. Monocyte depletion is performed since they also shared CD4 receptor on its membrane being interference for CD4 counting. After depletion, antiCD4-MPs were used for the specific CD4+ lymphocyte isolation follow by their cellular lysis. CD4 cell nuclei are stained and counted under light microscopy (Figure 1.20).[247] This technique presents the disadvantage of being limited to 10-15 tests per technician due to 'fatigue factor' being also prone to subjective interpretation. However, it shows excellent correlation with the results obtained by flow cytometry, being a good alternative test for its application in the developing world.

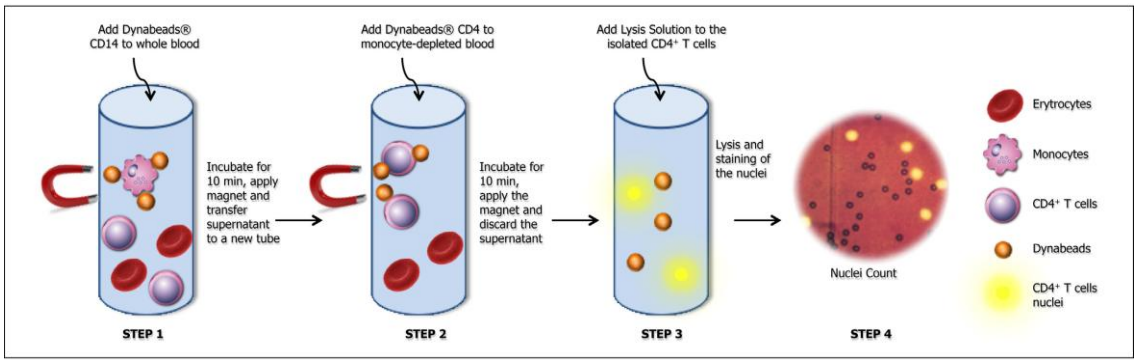

Figure 1.20. T4 Quant principle of positive isolation of CD4+ T cells with pre-depletion of monocytes for reliable CD4+ T cell nuclei counting. Step 1: Depletion of monocytes from whole blood using antiCD14-MPs. Step 2: Immunomagnetic separation of CD4 T lymphocytes using antiCD4-MPs. Step 3: Lysis of the CD4 cells nuclei and staining. Step 4: CD4 count under light microscopy. Adapted from http://www.lifetechnologies.com. Catalog product number 11321D.

1.8.1.2 Separation and detection of Mycobacterium based on magnetic particles

Tuberculosis (TB) is caused by the bacillus *Mycobacterium tuberculosis*. *M. tuberculosis* affects the lungs, forming hard nodules in the respiratory tissues and cavities in the lung, causing the infected person to cough up bright red blood. Active tuberculosis is diagnosed by chest radiology or by sputum collection and microbiological culture.[248] Radiology shows low sensitivity and requires trained staff to operate the imaging system. The reliability of sputum smear microscopy depends mostly on the expertise of sanitary personnel performing the

test[249,250] while the efficiency decreases in HIV-positive patient and children.[251] The culture of sputum is still the gold standard method for TB confirmation. However *Mycobacterium tuberculosis* is a slowly growing microorganism taking as long as six weeks to yield a conclusive result.[252] Since TB is a highly contagious bacteria that can quickly spread, an additional issue is the requirement of a level 3 biosafety facilities for growing the cultures, which is inappropriate for the developing world.[253,254] For latent tuberculosis, tuberculin skin test is widely used. This test is based on the immune response to the purified proteins from a mixture of tuberculosis antigens as the presence or absence of localized inflammation.[255] The test is inexpensive and non-invasive but shows false positive results in patients previously vaccinated with the Bacillus-Calmette–Gurin (BCG) vaccine, and false negative results in patients with sarcoidosis, Hodgkin's lymphoma, malnutrition or co-infected with HIV who have low T-cell counts.[256,257] Despite the availability of highly efficient treatment, TB remains as the second greatest killer worldwide after HIV.[258] In 2010, it was reported around 1.3 million death from TB including HIV patients. Over 95% of these deaths happened in low- and middle-income countries.[259]

Magnetic particles demonstrated to be a promising tool in *M. tuberculosis* for both separation and preconcentration from complex clinical specimens as well as for integration in RDTs. For instance, the hazardous standard centrifugation protocol of sputum specimens prior to culture *M. tuberculosis* can be replaced by an alternative method, which involves the incubation of sputum with magnetic particles (TB-beads, Figure 1.21, panel A) for its preconcentration followed by the mycobacteria release for their further culturing (Figure 1.21, panel A1 and A2). This procedure avoids the exposure of the laboratory staff to the infectious aerosols.[260] The combination of TB-Beads technology [261] for sample isolation and fluorescence microscopy detection was also reported (Figure 1.21, panel A3).[262,263] TB-Beads are paramagnetic particles coated with a polymeric ligand consisting of both charged and hydrophobic chemical groups that are believed to have a high affinity for lipoarabinomannan and mycolic acids presents on the mycobacterial cell surface. The advantage of using this ligand for isolation of mycobacteria is its resistance to proteases.[70] Moreover, alkaline conditions did not affect the high-affinity binding of the TB to the beads, and thus they can be used in alkali-treated sputum compared to antibody-coated beads.[264] However, this methodology showed lower specificity and sensitivity compared with the direct smear methods. *M. tuberculosis* magnetic immunoseparation was also reported. In this approach, magnetic particles coated with polyclonal antibodies towards *M. tuberculosis* were used for the specific capturing of the bacillus. Mycobacteria detection was performed using a specific antibody which recognizes a minor Mycobacteria secreted antigen. This approached showed

to be more sensitive than microscopy.[265] The versatility and the capability to modify its surface with a wide range of biomolecules confer to magnetic particles excellent properties for developing new alternative concentration methods.

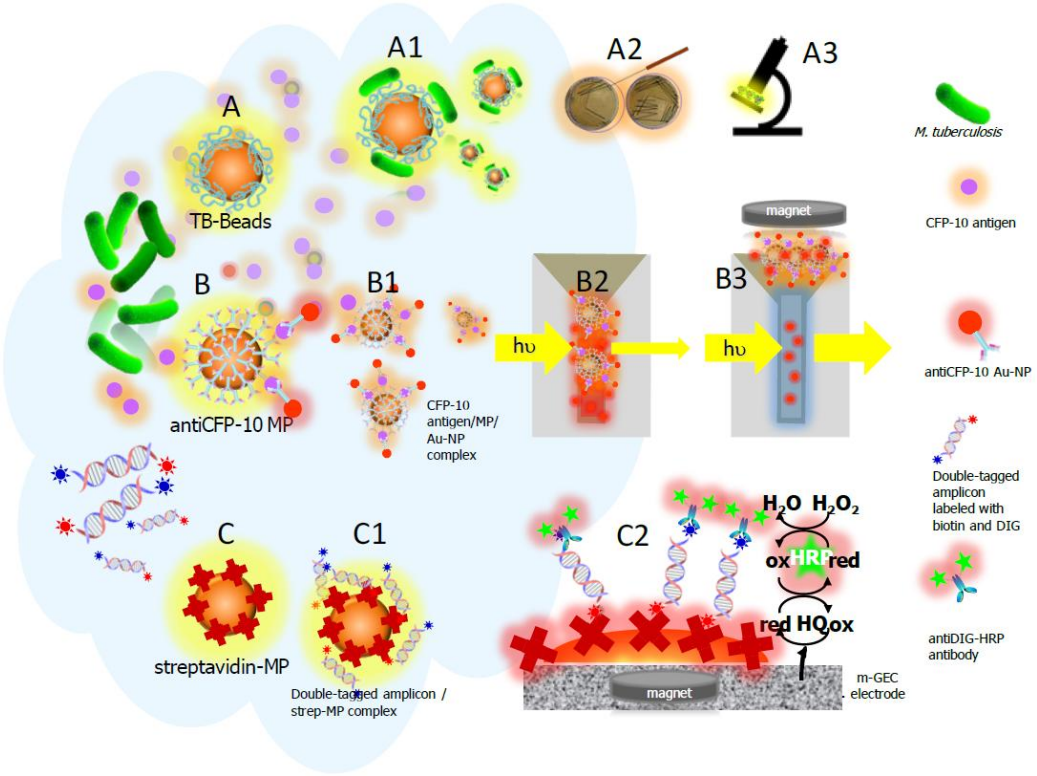

Figure 1.21. Representation of different strategies based on magnetic particles for *M. Tuberculosis* detection. Panel A shows the strategy of preconcentration of *M. Tuberculosis* (A1) using TB-beads for further culture (A2) or staining for microscopy (A3). Adapted with permission from ref [260,262]. Copyright 2011. BioMed Central. Panel B shows the magnetophoretic immunoassay (MPI) strategy for the detection of the TB secreted antigen CFP-10, based on Au-NPs and magnetic particles modified with the anti-CFP-10 antibody (B1). The readout was based on the UV-vis absorbance decrease due to the removal of the Au-NPs with the magnetic particles (B2 and B3). Adapted with permission from ref [266]. Copyright Elsevier. Panel C shows the double-tagging PCR integrated on magnetic particles and magneto-electrodes for the electrochemical genosensing of *M. bovis*. In this approach, double-tagged amplicons were capture with streptavidin-MPs (C1), and preconcentrated by magnetic actuation on the surface of the electrode for the electrochemical readout (C2).Adapted from ref [267]. Copyright 2010. Spanish Society for Microbiology.

Other example in which magnetic particles were used for the detection of tuberculosis, based on the TB secreted antigen CFP-10 as biomarker, in a sandwich-type magnetophoretic immunoassay (MPI) with colorimetric detection (Figure 1.21, Panel B).[266] This approach involved the use of gold nanoparticles (Au-NPs) and magnetic particles, both modified with the anti-CFP-10 antibody (Figure 1.21, Panel B1). The magnetic particle acted as a magneto-actuated carrier, while the Au-NPs as an optical transducer. After the incubation with the

sample, the secreted CFP-10 antigen was sandwiched between the MPs and the Au-NPs, and the complexes were removed by applying an external magnet. The readout was then based on the UV-vis absorbance decrease due to the removal of the Au-NPs with the magnetic particles (Figure 1.21, Panels B2 and B3). In this approach, the advantage of magnetic particles relies on the minimization of the total time of the assay.

The last example involves the use of magnetic particles for the immobilization of double-tagged amplicons on the surface on magneto-actuated electrodes for the detection of *Mycobacterium bovis* in milk (Figure 1.21, panel C).[267] In this approach, a double-tagging PCR amplification of the specific IS6110 gene was achieved, by modifying the amplicon during amplification with biotin (for magnetic capture on streptavidin-MPs) and digoxigenin (for the electrochemical readout based on electrochemical reporter). After reaction with streptavidin-MPs (Figure 1.21, panel C1), the DNA-MPs complexes were captured by magnetic actuation on the surface of the electrode for the electrochemical readout (Figure 1.21, panel C2). This device showed promising features for the detection of *M. bovis* known as a major zoonosis agent involving farm workers and the consumption of contaminated dairy products, on dairy farms by screening for the presence of the bacterium's DNA in milk samples. In this example the MPs were used to preconcentrate and immobilize the target on the surface of the transducer. It was clearly demonstrated the advantages in term of the biosensors sensitivity of using the magnetic particles immobilized on the surface of the magneto-electrode instead of conventional surface modification of the electrode.

1.8.1.3 Immunomagnetic separation and detection of genetic sequences related with Influenza virus

Influenza A are negative-sense, single-stranded, segmented RNA viruses. There are different subtypes of *influenza A* virus and the classification depends on their surface glycoprotein, the hemagglutinin (HA) and the neuraminidase (NA). While many genetically distinct subtypes, only three HA (H1, H2, and H3) and two NA (N1 and N2) subtypes have caused human epidemics.[268] Although most people recover from influenza symptoms within a week without requiring medical care, this virus can also cause severe illness or death especially in those with high risk. Every year, there are about of 3-5 million of new cases of severe illness and about 500,000 death.[269] Because of the high frequent genomic changes and viral mutations of the viruses, WHO Global Influenza Surveillance and Response System continuously monitors the influenza viruses circulating in humans.

Several influenza identification tests using magnetic particles were described, most of them based on the integration of magnetic particles with specific surface functionalization towards influenza. For instance, a method for the identification of H5N1 and Newcastle disease virus using magnetic gold particles for the virus preconcentration followed by PCR amplification and electrophoresis was described.[270] In this approach, the virus was immunocaptured by magnetic gold particles, and then sandwiched with a biotinylated antibody. This complex was then labeled with a biotinylated reporter ODN by its reaction with streptavidin, which actually acted as a linker to join the biotinylated antibody and the biotinylated ODN reporter. The ODN reporter was released, amplified, electrophoresed and visualized. This detection method provides a platform with a high capability to trace levels of Influenza and Newcastle virus simultaneously as a rapid screening method. Another example is based on the immunomagnetic separation and bienzymatic amplification of the H9N2 virus with electrochemical readout.[271] In this approach, the virus was captured by immunomagnetic separation and detected by using a biotinylated antibody. Oxydase-avidin complex was the electrochemical reporter and the immunocomplex-coated magnetic particles were accumulated on home-made electrodes by layer-by-layer assembly technique. The use of magnetic particles allowed the easy electrode surface regeneration, avoiding electrode fouling.

The integration of magnetic particles in microfluidic systems was also described for Influenza diagnosis. In this approach, magnetic particles were used not only for the viral immunomagnetic separation but also for its transport into a microfluidic system where the fluorescence labeling was performed. The fluorescence was monitored in an optical detect-ion module (Figure 1.22). This system was able to successfully distinguish between H1N1 and H3N2 [272] or between influenza A and B using a single chip test within 15 minutes.[273]

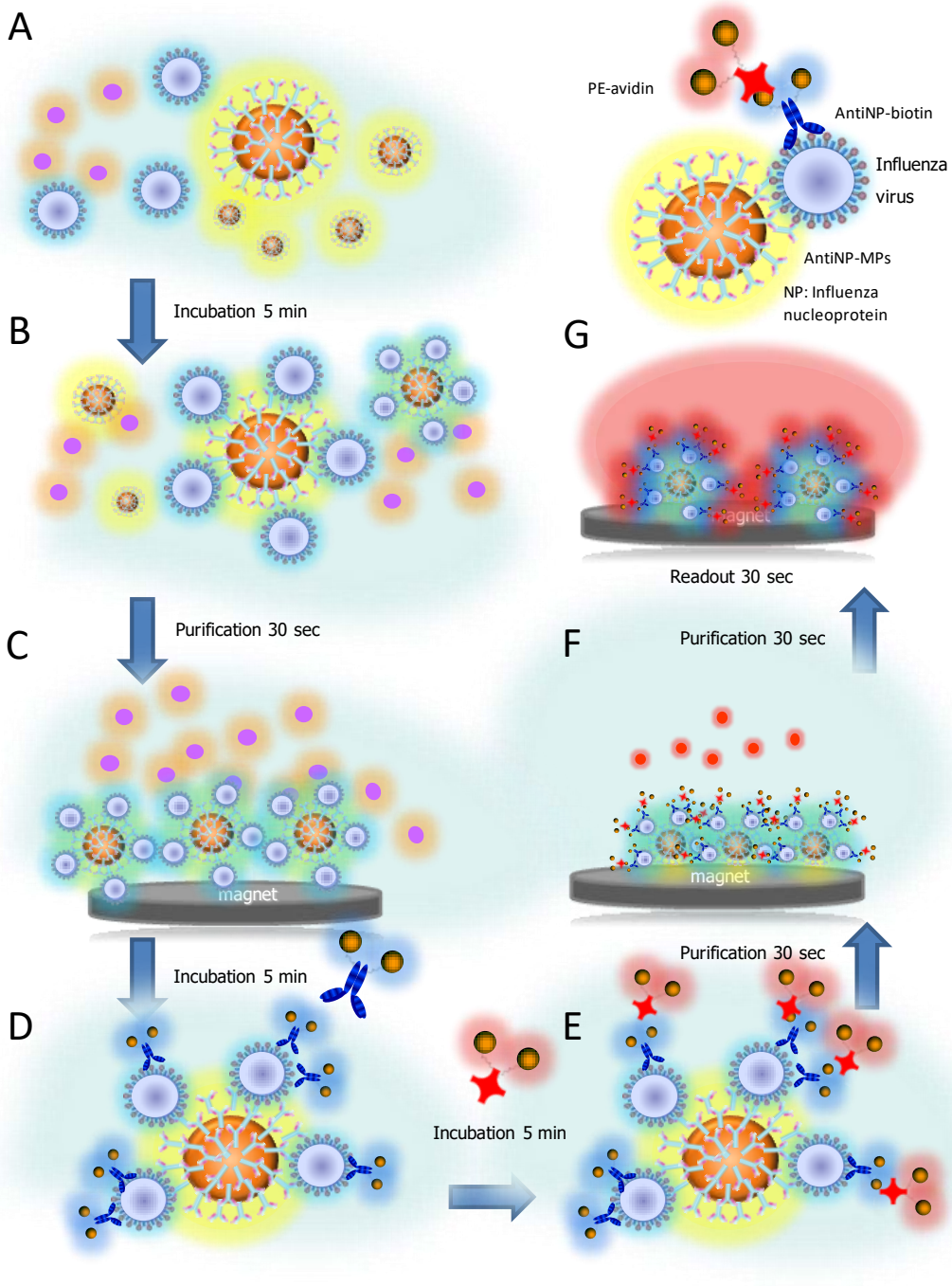

Figure 1.22. Immunomagnetic bead-based microfluidic system with optical detection for Influenza A virus identification. Adapted with permission from ref [272]. Copyright 2011. Elsevier.

In other approaches, the magnetic particles were used as solid support for DNA/RNA isolation of influenza synthetic sequences. For instance, the H5N1 DNA detection was coupled to paramagnetic particle-based isolation protocol. A synthetic PolyA-modified H5N1 oligonucleotide were isolated by using oligo(dT)-MPs and hybridized with a labeling ODN-CdS.[274] In this case, CdS quantum dots were used as electroactive labels, based on cadmium

(II) ions, which are detected by differential pulse voltammetry. A similar approach was also described, but in this instance it was applied for the multiplex oligonucleotide detection of different influenza subtypes (H1N1, H3N2 and H5N1) using QDs made of zinc, cadmium and lead.[275] In other study, a magnetic electrochemical bar code array for detection of single point mutations in H5N1 neuraminidase gene was also described.[276] The mutations in this gene are associated with antiretroviral drug resistance in Influenza strains and the mutation identification is helpful for diagnosis and treatment purposes. Similar to the previous example, multiple mutation sequences based on QDs-labeling were electrochemically detected. The same principle was reported for the detection of oligonucleotide specific sequences of life-threatening viruses (HIV, Influenza and Ebola).[245] All these works reported a high specificity and efficiency in the target isolation due to the use of magnetic particle which avoided the presence of interfering compound during the electrochemical readout.

Another application of magnetic particles was an influenza screening method in which the spectrometric analysis was performed on beads.[277] Magnetic particles were conjugated to anti hemagglutinin antibody and, after lysis of the virus, capsid proteins of virus were immunomagnetic separated and analyzed by mass spectrometry. This rapid and simple on-bead analysis reported to be one order more sensitive that SDS-PAGE gel electrophoresis, as shown in Figure 1.23.

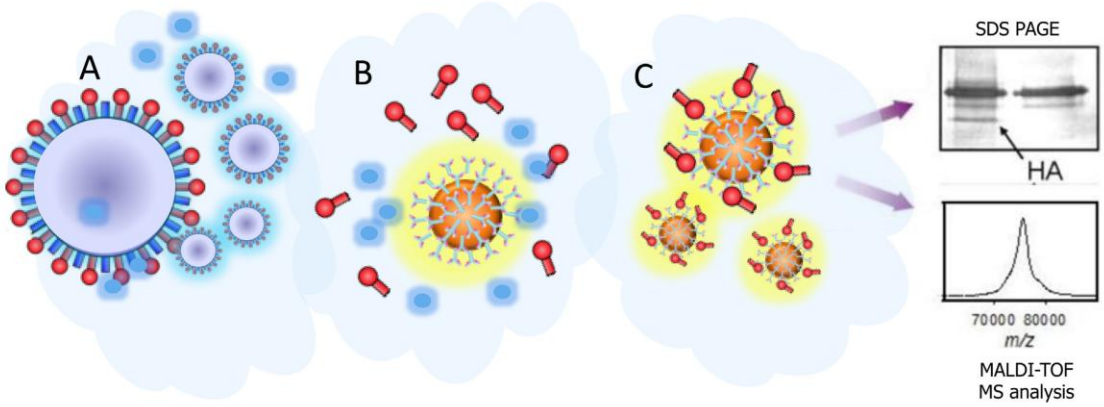

Figure 1.23. Schematic representation of the isolation of H5N2 viral protein (A) after lysis (B) using magnetic nanoparticles (C), followed by the detection by SDS-PAGE and mass spectrometry (MALDI-TOF MS). Adapted with permission from ref [277]. Copyright 2011. BioMed Central.

1.8.1.4 Diagnosis of Malaria biomarkers based on magnetic particles

Malaria is an infectious disease caused by the *Plasmodium* parasite. This disease is transmitted by the bite of *Anopheles quadrimaculatus* (mosquito vector). Four parasite species can cause Malaria in human: *Plamodium falciparum, P. vivax*, *P. malariae* and *P. ovale,* being the first one the most deadly specie.[278] Malaria symptoms are characterized by fever, vomiting, anemia, being often related with fatal complications. The disease targets the liver and red blood cells and has a latent phase in the liver which can result in recurrence after many years.[279]

According to the World Health Organization report, about 200 million of people contract malaria in 2012 and near to 630,000 died of this disease.[280] Africa is the most affected area, counting one death every minute, most of them in children. Malaria is considered one of the major tropical parasitic disease and it is among the three most deadly communicable diseases.[281]

In the absence of diagnostic tests, patients in low-resource settings are often treated based on clinical symptoms and local prevalence of disease. Whereas this approach captures most patients requiring treatment, it also unnecessarily treats patients who do not require treatment. Equally important, this latter group of patients is not being treated for their specific disease due to misdiagnosis. This syndromic management of disease may also increase drug resistance. Recently, strains of *Plasmodium falciparum* resistant to chloroquine, the most useful antimalarial drug, have spread rapidly. Taking into account that other malarial treatments are significantly more expensive, the correct diagnosis of infected people seems to be a cheaper strategy, rather than the treatment of all people with similar symptoms.[8] Moreover, the most ethical policy is to ensure that the new generation of drugs are only used for true cases of malaria to avoid the appearance of resistant strains.[282]

Since the first microscopic observation of malarial parasites in human blood by Laveran in the 1880s, light microscopy is considered to be the gold standard method for malaria diagnosis, and it is generally available in hospitals. The test is very simple to perform: a drop of blood from a finger prick is fixed with methanol on a glass slide and stained with dyes to visualize the parasite by light microscopy. Unfortunately, limited infrastructure in low-resources settings results in extremely poor performance of microscopy as a diagnostic tool for malaria, with shows an accuracy of only 70-75%. Moreover, microscopic diagnosis requires highly trained and experienced staff, being thus in some instances not suitable for routine use at the community level. Modern methods for malaria diagnosis include fluorescent

microscopy, flow cytometry, automated blood cell analyzers, antibody detection, molecular methods, and laser desorption mass spectrometry. The main disadvantage, in most of the cases, is their high cost.[283]

Only very few examples of the integration of magnetic particles for malaria diagnosis were reported. The prevalence of malarial drug resistance is evaluated by polymorphism studies. A multiplex detection of allele sequences was designed using Luminex technology.[284,285] DNA was extracted from dried blood, and a specific sequence was amplified. The sample was immobilized on magnetic particles and labeled with different specific allele oligonucleotide-modified fluorescent of magnetic beads. Every allele was modified with particular beads that presented a spectral distinction from the other ones. Thus, the discrimination of allele sequences was based on the magnetic bead fluorescence. This methodology offers similar accuracy to restriction fragment length polymorphism analyses in which the amplified sequence is treated with polymorphism-specific restriction endonucleases and subsequently analyzed by agarose gel electrophoresis.

The magnetic particles were also used for the selective preconcentration of the protein biomarker HRPII (histidine-rich protein II) for *Plasmodium falciparum*. A rapid and simple magneto immunoassays, which can be coupled with both optical or electrochemical readout for the detection of HRPII was reported (Figure 1.24).[286] The method involved the covalent immobilization of anti-HRP2 IgM monoclonal antibody on magnetic nanoparticles (Figure 1.24, panel A), followed by the reaction with an anti-HRP2 IgG antibody labeled with peroxidase (Figure 1.24, panel B), which could be used as electrochemical or optical reporter (Figure 1.24, panel C). In the magneto immunosensor, the MNPs were used to preconcentrate the biomarker from the clinical sample, to eliminate interferences from the matrix and to immobilize the biomarker in close contact to the electrode surface, increasing thus the limit of detection.

The HRPII protein was also detected after the selective isolation and preconcentration in an extraction cassette.[287] Nickel-modified MPs were added to the sample within the loading chamber of the extraction cassette. The sample was easily transported by an external magnetic field through washing solutions to remove the interfering agents. The protein was eluted at the end of the cassette and subsequent analyzed by SDS-PAGE gel. The simplicity of this technology has demonstrated its application in POCs diagnostic technique as an automated sample concentration device. However, the extraction efficiency (70%) should be improved.

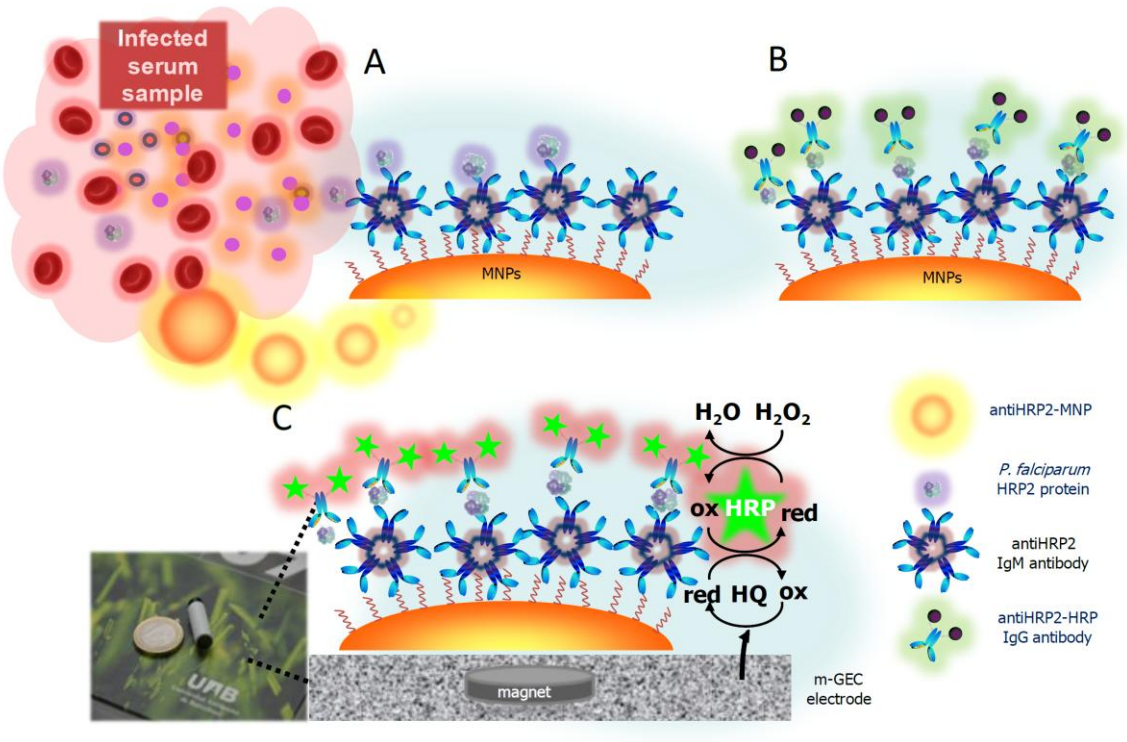

Figure 1.24. Schematic representation of the sandwich magneto-immunosensor for Malaria detection performed on magnetic beads. Adapted from ref [286]. Copyright 2011. American Chemical Society.

1.8.1.5 Magnetic particles-based approaches for Dengue virus diagnosis

Dengue virus (DENV) is transmitted to humans by *Aedes* sp. mosquitoes.[288] In recent years, dengue fever or its severe forms, dengue hemorrhagic fever and dengue shock syndrome, have emerged as a major public health problem.[289] Due to the presence of four distinct serotypes, people living in epidemic areas may suffer up to four infections in their lifetimes, and it is not unusual to find more than one serotype in an area. Every year, about 50-100 million people are affected with dengue but only about 500,000 persons require hospitalization for dengue hemorrhagic fever and 2.5% of cases are fatal.[290] Viremia and antigenemia are good early-fever-onset markers for disease diagnosis of dengue infection. Currently, the dengue diagnostic is performed using ELISAs that detect the presence of immunoglobulin M (IgM) or G (IgG) antibodies against the virus. This type of assays suffer three limitations: antibodies are not detectable after 5 days of infection, some patients do not show IgM in the secondary infection, and they are prone to false positives.[291] For instance, flavivirus producing yellow fever share similar protein structure with dengue. Due to these major limitations in dengue diagnosis, new tests and biomarkers should be further developed.[292] A magnetic nanoparticle-based immunoassay for the detection of dengue

specific antibodies in serum samples was developed. Dengue peptides were screening by phage display, i.e., dengue peptides expressed on M13 bacteriophage that were most specifically recognized by dengue positive antibody were selected. In this approach, the antibodies of the patients were captured on the surface of the protein G-MPs, so the Fab region of antibodies was correctly exposed and incubated with the selected peptide-bacteriophage. The specific antibody was finally identified by a secondary antibody anti-M13 conjugated with HRP for the optical readout in an ELISA-like format.[19] This assay was used for quantification of specific antibodies in patient sera.

A second approach, in which magnetic particles were coated with bacteriophage expressing specific dengue peptide on its surface, was used for the detection of circulating antibodies in positive sera by HRP-conjugated human anti-IgM. The incorporation of magnetic particles not only improved the efficiency of antigen-antibody binding but also avoided the non-specific binding increasing the detection sensitivity. On the other hand, the use of a secondary antibody-HRP towards the M13 bacteriophage protein (which presents a large surface formed by thousands coat protein of pVIII copies), resulted in an additional signal amplification.

Non-specific capturing of virus based on magnetic particles coated with anionic polymers have demonstrated a very high isolation efficiency, for instance for human[293] and avian[294] influenza viruses and HIV virus.[295] In a similar way, poly(methyl vinylether-maleic anhydrate) magnetic particles (Viro-Adembeads, Ademtech, Pessac, France) were used for preconcentration of Chikungunya and dengue virus.[296] This non-destructive method was able to isolated low amount of infectious virus. However, human serum inhibited the virus isolation by saturation of the magnetic particles.

Several studies reported the integration of magnetic isolation in viral detection method. For instance, a the dengue virus was separated by magnetic immunoseparation followed by analysis of the capsid viral protein by matrix-assisted laser desorption/ionization time of flight mass spectrometry (MALDI-TOF MS).[297] in a very similar way that in the case of influenza described in Figure 1.23.[277]

In other approach, a magnetophoretic device with fluorescence readout was developed to rapidly detect dengue virus in serum.[298] This methodology involved the reaction of the virus with superparamagnetic and fluorescent microparticles functionalized with specific dengue antibodies. The magnetic particles were magnetically separated and the dengue viruses detected by co-localization magnetic and fluorescent particles at the detection module. This

method demonstrated to be 1000 times more sensitive than conventional immunoassay and 100 times than flow cytometry assay for UV-inactivated dengue viruses.

Another microfluidic approach was based on virus-modified MPs for dengue antibody identification in serum samples.[299] This chip consisted of different modules for the detection of IgG and IgM antiDengue antibodies-. Dengue virus was loaded on magnetic particles modified with and antiDengue antibody by incubation of the MPs with the virus culture. Sample purification, transporting, multiplex fluorescent labeling and optical detection was completely integrated in the microfluidic chip, being 30 min the total assay time. Finally, a miniaturized microfluidic flow cytometer integrated onto a single chip including a sample incubation module, a micro flow cytometry module and an optical detection module was designed.[300] The magnetic particles were conjugated with specific antibodies, which can specifically recognize and capture target viruses. Another dye-labeled anti-virus antibody was then used to mark the bead-bound virus for the subsequent optical detection. The micro flow cytometry and the optical detection module performed the virus counting and collection. Experimental results showed that virus samples could be detected successfully by the developed system.

1.8.2 Conclusions

The infectious diseases affecting global health (such as malaria, influenza, dengue, tuberculosis or HIV) are responsible for hundreds of thousands of deaths and an enormous burden of morbidity worldwide. Unfortunately, the areas mostly affected by these infection diseases are resource-limited countries. Although there are several methodologies for the early detection of these infection diseases including conventional culturing, ELISA, PCR based assays, among many others, few of them can be used at the community and primary care level in low-income countries.

The accurate identification of patients requiring treatment by affordable diagnostic tests is thus a major issue.

In this review the recent advances in infectious diseases diagnosis using magnetic particles based on novel biomarkers related with global infectious agents is discussed. The most prominent format is the integration of a magnetic capture step prior to detection, to achieve the preconcentration of the biomarker from the complex interferences present in the clinical

samples. Although in some instances the interaction of the MPs with the biomarker (virus capside, bacteria) is achieved by physical adsorption, in most of the cases, the immunomagnetic separation was used, by the tailored modification of the MPs with a specific antibody. This magnetic capture demonstrated to be compatible with different readout strategies, ranging from conventional methods such as culturing, microscopy, mass spectrometry, or emerging technologies such as lateral flow and biosensing devices, among others. In some instances, the biomarker is preconcentrated and then released for the further readout, although the detection of the biomarker is mostly performed when it is still attached on the MPs. In most of the formats, a label to achieve the readout is used, being a second antibody conjugated with enzymes, fluorophores, or nanomaterials (such as QDs or Au-NPs). Although the detection of biomarkers is in most of the instances performed by an immunological recognition, there are some examples of the integration of MP in devices for DNA determination. In this case, the MPs are used as a way for preconcentration of native DNA or RNA, or amplicons coming from PCR.

Although the MPs are mostly integrated in a preconcentration step prior to the readout, they can be also used as a carrier to achieve the movement of the biomarkers along a microfluidic devices through different reaction chambers, in order to achieve incubation and washing under magnetic actuation. Unfortunately, there are still few examples of total integration in a chip from sample introduction to readout, requiring in all cases bench-top equipments to achieve detection. Other limitations of these chips are the low sensitivity limited by the small sample volume, irreproducibility in microfabrication and high cost to scale down. One of the most promising approaches for rapid diagnostic in low resource settings are lateral flow with qualitative visual detection. Recently, the integration of magnetic particles in lateral flow design is demonstrated, improving the sensitivity and providing quantitative results when required. The equipment is inexpensive if compared with traditional ELISA readers. In here, the MPs are used not only for preconcentration, but also for the readout based on the magnetic moment of the superparamagnetic particles attached to the biomarker. Another approach based on the integration of MP is the magneto biosensor, mostly based on electrochemical detection. In this format, the MPs are used not only as a way to preconcentrate the sample, but also to immobilize the biomarker on the surface of the transducer, increasing thus the sensitivity of the assay, when compared with conventional surface modification of the biosensor.

In general, the integration of magnetic particles in different approaches demonstrated to improve the analytical performance in terms of specificity and sensitivity. Their use as solid

support in bioassays has shown to greatly improve the performance of the biological reactions, due to several factors: a) an increased surface area which improves the efficiency of the reactions, b) a faster assay kinetics achieved because the particles are in suspension and the analytical target does not have to migrate very far, and c) a minimized matrix effect due to the improved washing and separation steps.

The integration of magnetic particles can thus simplified the analytical procedure, avoiding the use of classical centrifugation or chromatography separation strategies, since no pre-enrichment, purification or pretreatment steps, which are normally used in standard analytical methods, are required. In here, the preconcentration and purification is achieved by simply applying an external magnet. The biomarkers can be specifically isolated and preconcentrated from complex biological matrixes by magnetic actuation, increasing the specificity of the assay. The MPs demonstrated to be a robust and versatile material for the detection of a whole range of biomarkers including mammalian cells, whole virus, bacteria, proteins, antibodies and DNA related with infectious diseases affecting global health such as malaria, influenza, dengue, tuberculosis or HIV. The integration of magnetic particles in emerging technologies shows very promising features, although there is still a long way to achieve point of care devices following the ASSURED recommendations given by WHO *(A*ffordable, *S*ensitive, *S*pecific, *U*ser-friendly, *R*apid and *R*obust, *E*quipment free, and *D*eliverable to those who need it).

1.9 References

[1] Davis, C.P., Normal Flora. (1996) In: Baron, S. (1996). Protozoa: Structure, Classification, Growth, and Development--Medical Microbiology. University of Texas Medical Branch at Galveston.

[2] Alters, S., Schiff, W. (2009). Essential concepts for healthy living. Jones & Bartlett Publishers.

[3] Dicker, R., Coronado, F., Koo, D., Parrish, R. G. (2006). Principles of epidemiology in public health practice. Atlanta GA: US Department of Health and Human Services.

[4] Centers for Disease Control and Prevention (CDC). (2006). Principles of epidemiology in public health practice: an introduction to applied epidemiology and biostatistics.

[5] Heller, M., Veach, L. M. (2008). Clinical Medical Assisting: A Professional, Field Smart Approach to the Workplace. Chapter 10. Cengage Learning. Chapter 10.

[6] Wilburta, L., Pooler, M., Tamparo, C. (2009). Delmar's comprehensive medical assisting: administrative and clinical competencies. Delmar Cenage Learning.

[7] National Institutes of Health. (2007). Understanding emerging and re-emerging infectious diseases. Biological sciences curriculum study. NIH Curriculum Supplement Series. National Institutes of Health, Bethesda, MD.

[8] Mabey, D., Peeling, R. W., Ustianowski, A., Perkins, M. D. (2004). Tropical infectious diseases: diagnostics for the developing world. Nature Reviews Microbiology, 2(3), 231.

[9] Hauck, T. S., Giri, S., Gao, Y., Chan, W. C. (2010). Nanotechnology diagnostics for infectious diseases prevalent in developing countries. Advanced drug delivery reviews, 62(4-5), 438-448.

[10] World Health Organization. (2018). Global health estimates 2016: Estimated deaths by age, sex, and cause. Geneva, WHO, 9. http://www.who.int/healthinfo/global_burden_disease/en/ Accessed 31 Aug 2018.

[11] Plasència, A. (2012). Global health challenges and personalised medicine. Contributions to science, 175-180.

[12] Macfarlane, S. B., Jacobs, M., Kaaya, E. E. (2008). In the name of global health: trends in academic institutions. Journal of public health policy, 29(4), 383-401.

[13] World Health Organization. (2009). Global health risks: mortality and burden of disease attributable to selected major risks. World Health Organization. http://www.who.int/healthinfo/global_burden_disease/GlobalHealthRisks_report_full.pdf. Accessed 31 Aug 2018.

[14] Caliendo, A. M., Gilbert, D. N., Ginocchio, C. C., Hanson, K. E., May, L., Quinn, T. C., Carroll, K. C. (2013). Better tests, better care: improved diagnostics for infectious diseases. Clinical Infectious Diseases, 57, S139-S170.

[15] Grijalva, C. G., Nuorti, J. P., Griffin, M. R. (2009). Antibiotic prescription rates for acute respiratory tract infections in US ambulatory settings. Jama, 302(7), 758-766.

[16] Hersh, A. L., Shapiro, D. J., Pavia, A. T., Shah, S. S. (2011). Antibiotic prescribing in ambulatory pediatrics in the United States. Pediatrics, 128(6), 1053-1061.

[17] Banoo, S., Bell, D., Bossuyt, P., Herring, A., Mabey, D., Poole, F., Smith, P. G., Sriram, N., Wongsrichanalai, C., Linke, R., O'Brien, R., Perkins, M., Cunningham, J., Matsoso, P., Nathanson, C. M., Olliaro, P., Peeling, R. W., Ramsay, A. (2008). Evaluation of diagnostic tests for infectious diseases: general principles. Nature Reviews Microbiology, 6, S16-S28.

[18] LaBarre, P., Hawkins, K. R., Gerlach, J., Wilmoth, J., Beddoe, A., Singleton, J., Boyle, D., Weigl, B. (2011). A simple, inexpensive device for nucleic acid amplification without electricity—toward instrument-free molecular diagnostics in low-resource settings. PloS one, 6(5), e19738.

[19] Goulart, L. R., Vieira, C. U., Freschi, A. P. P., Capparelli, F. E., Fujimura, P. T., Almeida, J. F., Ferreira, L. F., Goulart, I. M., Brito-Madurro, A. G., Madurro, J. M. (2010). Biomarkers for serum diagnosis of infectious diseases and their potential application in novel sensor platforms. Critical Reviews™ in Immunology, 30(2).

[20] Tallury, P., Malhotra, A., Byrne, L. M., Santra, S. (2010). Nanobioimaging and sensing of infectious diseases. Advanced drug delivery reviews, 62(4), 424-437.

[21] Thomas, E., Albritton, W. (1988). Office Microscopy in the Diagnosis of Infectious Diseases. Canadian Family Physician, 34, 379.

[22] Clerc, O., Greub, G. (2010). Routine use of point-of-care tests: usefulness and application in clinical microbiology. Clinical Microbiology and Infection, 16(8), 1054-1061.

[23] Houpikian, P., Raoult, D. (2002). Traditional and molecular techniques for the study of emerging bacterial diseases: one laboratory's perspective. Emerging infectious diseases, 8(2), 122.

[24] Alberts, B., Johnson, A., Lewis, J., Walter, P., Raff, M., Roberts, K. (2002). Molecular Biology of the Cell 4th Edition: International Student Edition.

[25] Kaye, D., Gorbach, S. L., Bartlett, J. G., Blacklow, N. R. (2004). Infectious disease.

[26] Engelkirk, P. G., Duben-Engelkirk, J. L. (2008). Laboratory diagnosis of infectious diseases: essentials of diagnostic microbiology. Lippincott Williams & Wilkins.

[27] Hnasko, R. (Ed.). (2015). ELISA. Springer New York.

[28] Lequin, R. M. (2005). Enzyme immunoassay (EIA)/enzyme-linked immunosorbent assay (ELISA). Clinical chemistry, 51(12), 2415-2418.

[29] Cox, K. L., Devanarayan, V., Kriauciunas, A., Manetta, J., Montrose, C., Sittampalam, S. (2014). Immunoassay methods. In: Sittampalam, G. S., Coussens, N. P., Brimacombe, K., Grossman, A., Arkin, M., Auld, D., Austin, C., Baell, J., Bejcek, B., Caaveiro, J. M. M., Chung, T. D. Y., Dahlin, J. L., Devanaryan, V., Foley, T. L., Glicksman, M., Hall, M. D., Haas, J. V., Inglese, J., Iversen, P. W., Kahl, S. D., Kales, S. C., Lal-Nag, M., Li, Z., McGee, J., McManus, O., Riss, T., Trask, O. J., Weidner, J. R., Wildey, M. J., Xia, M., Xu, X. (2004) editors. Assay Guidance Manual. Bethesda (MD): Eli Lilly & Company and the National Center for Advancing Translational Sciences.

[30] Lin, A. V. (2015). Direct ELISA. ELISA: Methods and Protocols, 61-67.

[31] Ademokun, A. A., Dunn-Walters, D. (2010). Immune responses: primary and secondary. eLS.

[32] Landry, M. L. (2016). Immunoglobulin M for acute infection: true or false? Clinical and Vaccine Immunology, 23(7), 540-545.

[33] Burnette, W. N. (1981). Western blotting: electrophoretic transfer of proteins from sodium dodecyl sulfate-polyacrylamide gels to unmodified nitrocellulose and radiographic detection with antibody and radioiodinated protein A. Analytical biochemistry, 112(2), 195-203.

[34] Mahmood, T., Yang, P. C. (2012). Western blot: technique, theory, and trouble shooting. North American journal of medical sciences, 4(9), 429.

[35] Hartl, D. L., Orel, V. (1992). What did Gregor Mendel think he discovered? Genetics, 131(2), 245.

[36] Sutton, W. S. (1902). On the morphology of the chromoso group in brachystola magna. The Biological Bulletin, 4(1), 24-39.

[37] Kossel, A. (1879). Ueber das Nucleïn der Hefe. Zeitschrift für physiologische Chemie, 3(4), 284-291.

[38] Kossel, A. (1880). Ueber das Nucleïn der Hefe II. Zeitschrift für physiologische Chemie, 4(4), 290-295.

[39] Levene, P. A. (1919). The structure of yeast nucleic acid. Studies from the Rockefeller Institute for Medical Research, 30, 221.

[40] Franklin, R. E., Gosling, R. G. (1953). Molecular configuration in sodium thymonucleate. Nature, 171, 740-741.

[41] Watson, J. D., Crick, F. H. (1953). Molecular structure of nucleic acids. Nature, 171(4356), 737-738.

[42] Centers for Disease Control and Prevention (CDC). (1996). Nucleic acid amplification tests for tuberculosis. MMWR. Morbidity and mortality weekly report, 45(43), 950.

[43] Dalovisio, J. R., Montenegro-James, S., Kemmerly, S. A., Genre, C. F., Chambers, R., Greer, D., Pankey, G. A., Failla, D. M., Haydel, K. G., Hutchinson, L., Lindley, M. F., Nunez, B. M., Praba, A., Eisenach, K. D., Cooper, E. S. (1996). Comparison of the amplified Mycobacterium tuberculosis (MTB) direct test, Amplicor MTB PCR, and IS6110-PCR for detection of MTB in respiratory specimens. Clinical infectious diseases, 23(5), 1099-1106.

[44] Tomaso, H., Kattar, M., Eickhoff, M., Wernery, U., Al Dahouk, S., Straube, E., Neubauer, H., Scholz, H. (2010). Comparison of commercial DNA preparation kits for the detection of Brucellae in tissue using quantitative real-time PCR. BMC infectious diseases, 10(1), 1.

[45] Erlich, H. A., Gelfand, D., Sninsky, J. J. (1991). Recent advances in the polymerase chain reaction. Science, 252(5013), 1643-1652.

[46] Vogelstein, B., Kinzler, K. W. (1999). Digital PCR. Proceedings of the National Academy of Sciences, 96(16), 9236-9241.

[47] Huckle, D. (2008). Point-of-care diagnostics: an advancing sector with nontechnical issues. Expert review of molecular diagnostics, 8(6), 679-688.

[48] Vincent, M., Xu, Y., Kong, H. (2004). Helicase-dependent isothermal DNA amplification. EMBO reports, 5(8), 795-800.

[49] Li, J., Macdonald, J. (2015). Advances in isothermal amplification: novel strategies inspired by biological processes. Biosensors and Bioelectronics, 64, 196-211.

[50] Jeong, Y. J., Park, K., Kim, D. E. (2009). Isothermal DNA amplification in vitro: the helicase-dependent amplification system. Cellular and molecular life sciences, 66(20), 3325-3336.

[51] Piepenburg, O., Williams, C. H., Stemple, D. L., Armes, N. A. (2006). DNA detection using recombination proteins. PLoS biology, 4(7), e204.

[52] Nagamine, K., Watanabe, K., Ohtsuka, K., Hase, T., Notomi, T. (2001). Loop-mediated isothermal amplification reaction using a nondenatured template. Clinical Chemistry, 47(9), 1742-1743.

[53] Notomi, T., Okayama, H., Masubuchi, H., Yonekawa, T., Watanabe, K., Amino, N., Hase, T. (2000). Loop-mediated isothermal amplification of DNA. Nucleic acids research, 28(12), e63-e63.

[54] Patterson, A. S., Hsieh, K., Soh, H. T., Plaxco, K. W. (2013). Electrochemical real-time nucleic acid amplification: towards point-of-care quantification of pathogens. Trends in biotechnology, 31(12), 704-712.

[55] Hartman, M. R., Ruiz, R. C., Hamada, S., Xu, C., Yancey, K. G., Yu, Y., Han, W., Luo, D. (2013). Point-of-care nucleic acid detection using nanotechnology. Nanoscale, 5(21), 10141-10154.

[56] Chen, Q., Bian, Z., Chen, M., Hua, X., Yao, C., Xia, H., Kuang, H., Zhang, X., Huang, J., Cai, G., Fu, W. (2009). Real-time monitoring of the strand displacement amplification (SDA) of human cytomegalovirus by a new SDA-piezoelectric DNA sensor system. Biosensors and Bioelectronics, 24(12), 3412-3418.

[57] Little, M. C., Andrews, J., Moore, R., Bustos, S., Jones, L., Embres, C., Durmowicz, G., Harris, J., Berger, D., Yanson, K., Rostkowski, C., Yursis, D., Price, J., Fort, T., Walters, A., Collis, M., Llorin, O., Wood, J., Failing, F., O'Keefe, C., Scrivens, B., Pope, B., Hansen, T., Marino, K., Williams, K., Boeisch, M. (1999). Strand displacement amplification and homogeneous real-time detection incorporated in a second-generation DNA probe system, BDProbeTecET. Clinical chemistry, 45(6), 777-784.

[58] Compton, J. (1991). Nucleic acid sequence-based amplification. Nature, 350(6313), 91.

[59] Guatelli, J. C., Whitfield, K. M., Kwoh, D. Y., Barringer, K. J., Richman, D. D., Gingeras, T. R. (1990). Isothermal, in vitro amplification of nucleic acids by a multienzyme reaction modeled after retroviral replication. Proceedings of the National Academy of Sciences, 87(5), 1874-1878.

[60] Gill, P., Ghaemi, A. (2008). Nucleic acid isothermal amplification technologies—a review. Nucleosides, Nucleotides, and Nucleic Acids, 27(3), 224-243.

[61] Ginocchio, C. C., Kemper, M., Stellrecht, K. A., Witt, D. J. (2003). Multicenter evaluation of the performance characteristics of the NucliSens HIV-1 QT assay used for quantitation of human immunodeficiency virus type 1 RNA. Journal of clinical microbiology, 41(1), 164-173.

[62] Fire, A., Xu, S. Q. (1995). Rolling replication of short DNA circles. Proceedings of the National Academy of Sciences, 92(10), 4641-4645.

[63] Liu, D., Daubendiek, S. L., Zillman, M. A., Ryan, K., Kool, E. T. (1996). Rolling circle DNA synthesis: small circular oligonucleotides as efficient templates for DNA polymerases. Journal of the American Chemical Society, 118(7), 1587-1594.

[64] Daubendiek, S. L., Ryan, K., Kool, E. T. (1995). Rolling-circle RNA synthesis: circular oligonucleotides as efficient substrates for T7 RNA polymerase. Journal of the American Chemical Society, 117(29), 7818-7819.

[65] Kornberg, A., Baker, T. A. (1992). DNA replication (Vol. 3). New York: Wh Freeman.

[66] Demidov, V. V. (2002). Rolling-circle amplification in DNA diagnostics: the power of simplicity. Expert review of molecular diagnostics, 2(6), 542-548.

[67] Banér, J., Nilsson, M., Mendel-Hartvig, M., Landegren, U. (1998). Signal amplification of padlock probes by rolling circle replication. Nucleic acids research, 26(22), 5073-5078.

[68] Christian, A. T., Pattee, M. S., Attix, C. M., Reed, B. E., Sorensen, K. J., Tucker, J. D. (2001). Detection of DNA point mutations and mRNA expression levels by rolling circle amplification in individual cells. Proceedings of the National Academy of Sciences, 98(25), 14238-14243.

[69] Melin, J., Jarvius, J., Göransson, J., Nilsson, M. (2007). Homogeneous amplified single-molecule detection: Characterization of key parameters. Analytical biochemistry, 368(2), 230-238

[70] Jarvius, J., Melin, J., Göransson, J., Stenberg, J., Fredriksson, S., Gonzalez-Rey, C., Bertilsson S., Nilsson, M. (2006). Digital quantification using amplified single-molecule detection. Nature methods, 3(9), 725.

[71] Clark, L. C., Lyons, C. (1962). Electrode systems for continuous monitoring in cardiovascular surgery. Annals of the New York Academy of sciences, 102(1), 29-45.

[72] Wang, J. (2001). Glucose biosensors: 40 years of advances and challenges. Electroanalysis, 13(12), 983-988.

[73] Newman, J. D., Turner, A. P. (2005). Home blood glucose biosensors: a commercial perspective. Biosensors and bioelectronics, 20(12), 2435-2453.

[74] Monošík, R., Streďanský, M., Šturdík, E. (2012). Biosensors-classification, characterization and new trends. Acta Chimica Slovaca, 5(1), 109-120.

[75] McNaught, A. D., McNaught, A. D. (1997). Compendium of chemical terminology (Vol. 1669). Oxford: Blackwell Science.

[76] Turner, A., Karube, I., Wilson, G. S. (1987). Biosensors: fundamentals and applications. Oxford University Press.

[77] Taylor, R. F.; Schultz, J. S. (Eds) (1996) Handbook of Chemical and Biological Sensors. CRC Press.

[78] Vo-Dinh, T., Cullum, B. (2000). Biosensors and biochips: advances in biological and medical diagnostics. Fresenius' journal of analytical chemistry, 366(6), 540-551.

[79] Borgmann, S., Schulte, A., Neugebauer, S., Schuhmann, W. (2011). Amperometric biosensors. Advances in Electrochemical Science and Engineering; WILEY-VCH Verlag GmbH & Co. KGaA: Weinheim, Germany.

[80] Haupt, K. (2004). Molecularly imprinted polymers as recognition elements in sensors. In Ultrathin Electrochemical Chemo-and Biosensors (pp. 23-39). Springer Berlin Heidelberg.

[81] Homola, J. (2003). Present and future of surface plasmon resonance biosensors. Analytical and bioanalytical chemistry, 377(3), 528-539.

[82] González, R. V., García, I. E., Ruiz, G. O., Gago, C. L. (2005). Aplicación de biosensores en la industria agroalimentaria. Informe de vigilancia tecnológica. Madrid.

[83] Pividori, M. I., Alegret, S. (2011). Electrochemical biosensors for food safety. Contributions to science, 6(2), 173-191.

[84] Pearson, J. E., Gill, A., Vadgama, P. (2000). Analytical aspects of biosensors. Annals of Clinical Biochemistry, 37(2), 119-145.

[85] Grieshaber, D., MacKenzie, R., Voeroes, J., Reimhult, E. (2008). Electrochemical biosensors-sensor principles and architectures. Sensors, 8(3), 1400-1458.

[86] Chaubey, A., Malhotra, B. (2002). Mediated biosensors. Biosensors and bioelectronics, 17(6), 441-456.

[87] Wang, J. (2006). Analytical electrochemistry. John Wiley & Sons

[88] Wang, J. (2002). Real-time electrochemical monitoring: toward green analytical chemistry. Accounts of chemical research, 35(9), 811-816.

[89] Hayat, A., Marty, J. L. (2014). Disposable screen printed electrochemical sensors: Tools for environmental monitoring. Sensors, 14(6), 10432-10453.

[90] Turner, A. P. (2000). Biosensors--sense and sensitivity. Science, 290(5495), 1315-1317.

[91] Bond, A. M. (1994). Past, present and future contributions of microelectrodes to analytical studies employing voltammetric detection. A review. Analyst, 119(11), 1R-21R.

[92] Stulík, K., Amatore, C., Holub, K., Marecek, V., Kutner, W. (2000). Microelectrodes. Definitions, characterization, and applications (Technical report). Pure and applied chemistry, 72(8), 1483-92.

[93] Li, M., Li, Y. T., Li, D. W., Long, Y. T. (2012). Recent developments and applications of screen-printed electrodes in environmental assays—a review. Analytica chimica acta, 734, 31-44.

[94] Šljukić, B. R., Kadara, R. O., Banks, C. E. (2011). Disposable manganese oxide screen printed electrodes for electroanalytical sensing. Analytical Methods, 3(1), 105-109.

[95] Kadara, R. O., Jenkinson, N., Banks, C. E. (2009). Disposable bismuth oxide screen printed electrodes for the high throughput screening of heavy metals. Electroanalysis, 21(22), 2410-2414.

[96] Pividori, M. I., Merkoçi, A., Alegret, S. (2003). Graphite-epoxy composites as a new transducing material for electrochemical genosensing. Biosensors and bioelectronics, 19(5), 473-484.

[97] Céspedes, F., Martinez-Fabregas, E., Alegret, S. (1996). New materials for electrochemical sensing I. Rigid conducting composites. TrAC Trends in Analytical Chemistry, 15(7), 296-304.

[98] Ocaña, C., Pacios, M., del Valle, M. (2012). A reusable impedimetric aptasensor for detection of thrombin employing a graphite-epoxy composite electrode. Sensors, 12(3), 3037-3048.

[99] Pividori, M. I., Alegret, S. (2005). DNA adsorption on carbonaceous materials. In Immobilisation of DNA on Chips I (pp. 1-36). Springer Berlin Heidelberg.

[100] Céspedes, F., Alegret, S. (2000). New materials for electrochemical sensing II. Rigid carbon–polymer biocomposites. TrAC Trends in Analytical Chemistry, 19(4), 276-285.

[101] Bonanni, A., Pividori, M. I., Del Valle, M. (2007). Application of the avidin–biotin interaction to immobilize DNA in the development of electrochemical impedance genosensors. Analytical and bioanalytical chemistry, 389(3), 851-861.

[102] Zacco, E., Pividori, M. I., Llopis, X., Del Valle, M., Alegret, S. (2004). Renewable Protein A modified graphite-epoxy composite for electrochemical immunosensing. Journal of immunological methods, 286(1), 35-46.

[103] Brasil de Oliveira Marques, P. R., Lermo, A., Campoy, S., Yamanaka, H., Barbe, J., Alegret, S., Pividori, M. I. (2009). Double-tagging polymerase chain reaction with a thiolated primer and electrochemical genosensing based on gold nanocomposite sensor for food safety. Analytical chemistry, 81(4), 1332-1339.

[104] Fenga, P. G., Stradiotto, N. R., Pividori, M. I. (2011). Silver nanocomposite electrode modified with hexacyanoferrate. Preparation, characterization and electrochemical behaviour towards substituted anilines. Electroanalysis, 23(5), 1100-1106.

[105] Merkoçi, A., Pumera, M., Llopis, X., Pérez, B., del Valle, M., Alegret, S. (2005). New materials for electrochemical sensing VI: carbon nanotubes. TrAC Trends in Analytical Chemistry, 24(9), 826-838.

[106] Philippova, O., Barabanova, A., Molchanov, V., Khokhlov, A. (2011). Magnetic polymer beads: recent trends and developments in synthetic design and applications. European Polymer Journal, 47(4), 542-559.

[107] Neamtu, M., Nadejde, C., Hodoroaba, V. D., Schneider, R. J., Verestiuc, L., Panne, U. (2018). Functionalized magnetic nanoparticles: Synthesis, characterization, catalytic application and assessment of toxicity. Scientific reports, 8(1), 6278.

[108] Schladt, T. D., Schneider, K., Schild, H., Tremel, W. (2011). Synthesis and bio-functionalization of magnetic nanoparticles for medical diagnosis and treatment. Dalton Transactions, 40(24), 6315-6343.

[109] Centers for Disease Control (CDC). (1981). Pneumocystis pneumonia--Los Angeles. MMWR. Morbidity and mortality weekly report, 30(21), 250.

[110] Friedman-Kien, A. E., Laubenstein, L., Marmor, M., Hymes, K., Green, J., Ragaz, A., Gottleib, J., Muggia, F., Demopoulos, R., Weintraub, M. (1981). Kaposis sarcoma and Pneumocystis pneumonia among homosexual men--New York City and California. MMWR. Morbidity and mortalityweeklyreport, 30(25), 305-8.

[111] Barre-Sinoussi, F., Chermann, J. C., Rey, F., Nugeyre, M. T., Chamaret, S., Gruest, J., Dauguet, C. (2004). Isolation of T-lymphotropic retrovirus from a patient at risk for acquired immune defficiency syndrome (AIDS). Revista de investigación clínica, 56(2), 126-129.

[112] Centers for Disease Control (CDC). (1985). Provisional Public Health Service inter-agency recommendations for screening donated blood and plasma for antibody to the virus causing acquired immunodeficiency syndrome. MMWR. 34(1), 1.

[113] Roberts, B.D. (1994) 'HIV Antibody Testing Methods' Journal of Insurance Medicine 26(1):13-14.

[114] Brook, I. (1987). Approval of zidovudine (AZT) for acquired immunodeficiency syndrome: a challenge to the medical and pharmaceutical communities. Jama, 258(11), 1517-1517.

[115] The Henry J. Kaiser Foundation (2014) 'HIV Testing in the United States'. Available in http://files.kff.org/attachment/Fact-Sheet-HIV-Testing-in-the-United%20States. Accessed 31 Aug 2018.

[116] Food and Drug Administration (FDA). HIV/AIDS Historical Time Line. Available in https://www.fda.gov/forpatients/illness/hivaids/history/ucm151081.htm. Accessed 31 Aug 2018.

[117] Parham, P. (2014). The immune system. Garland Science. 4th Edition.

[118] Roth, J. A. (1999). The immune system. Iowa State University

[119] Delves, P. J., Roitt, I. M. (2000). The immune system. New England Journal of Medicine, 343(1), 37-49.

[120] Streicher, H.Z., Reitz, M.S. Jr., Gallo, R.C. (2014) Human immunodeficiency viruses. in: G.L. Mandell, J.E. Bennett, R. Dolin (Eds.) Mandell, Douglas, and Bennett's Principles and Practice of Infectious Diseases. Elsevier Health Sciences.

[121] Montagnier, Luc. (1999) Human Immunodeficiency Viruses (Retroviridae). Encyclopedia of Virology (2nd Ed.) 763-774

[122] Rajarapu, G. (2013). Genes and Genome of HIV-1. Journal of Phylogenetics & Evolutionary Biology, 1-7.

[123] Chan, D. C., Kim, P. S. (1998). HIV entry and its inhibition. Cell, 93(5), 681-684.

[124] Lusso, P. (2006). HIV and the chemokine system: 10 years later. The EMBO journal, 25(3), 447-456.

[125] Cleghorn, F. R., Reitz, M. S., Popovic, M., Gallo, R. C. (2005). Human immunodeficiency viruses. Bennett's principles and practice of infectious diseases. 6th ed. Philadelphia USA: Churchill Caurehill Livingston, 2119-2125.

[126] Engelman, A., Cherepanov, P. (2012). The structural biology of HIV-1: mechanistic and therapeutic insights. Nature Reviews Microbiology, 10(4), 279-290.

[127] Pantaleo, G., Graziosi, C., Fauci, A. S. (1993). The immunopathogenesis of human immunodeficiency virus infection. New EnglandJournal of Medicine, 328(5), 327-335.

[128] Rosenberg, N. E., Pilcher, C. D., Busch, M. P., Cohen, M. S. (2015). How can we better identify early HIV infections? Current Opinion in HIV and AIDS, 10(1), 61-68.

[129] Ewings, F. M., Bhaskaran, K., McLean, K., Hawkins, D., Fisher, M., Fidler, S., Gilson, R., Nock, D., Brettle, R., Johnson, M., Phillips, A., Porter, K. (2008). Survival following HIV infection of a cohort followed up from seroconversion in the UK. Aids, 22(1), 89-95.

[130] Highleyman, L. (2009). Inflammation, immune activation, and HIV. BETA: bulletin of experimental treatments for AIDS: a publication of the San Francisco AIDS Foundation, 22(2), 12-26.

[131] Weiss, R. A., Dalgleish, A. G., Loveday, C., Pillay, D. (2004). Human immunodeficiency viruses. Principles and Practice of Clinical Virology, Fifth Edition, 721-757.

[132] Stedman, T. L. (2004). The American heritage Stedman's medical dictionary. Houghton Mifflin.

[133] Fiebig, E. W., Heldebrant, C. M., Smith, R. I., Conrad, A. J., Delwart, E. L., Busch, M. P. (2005). Intermittent low-level viremia in very early primary HIV-1 infection. JAIDS Journal of Acquired Immune Deficiency Syndromes, 39(2), 133-137.

[134] Lindbäck, S., Karlsson, A. C., Mittler, J., Blaxhult, A., Carlsson, M., Briheim, G., Karolinska Institutet Primary HIV Infection Study Group. (2000). Viral dynamics in primary HIV-1 infection. Aids, 14(15), 2283-2291.

[135] Vermeulen, M., Coleman, C., Mitchel, J., Reddy, R., Drimmelen, H., Fickett, T., Busch, M., Lelie, N. (2013). Comparison of human immunodeficiency virus assays in window phase and elite controller samples: viral load distribution and implications for transmission risk. Transfusion, 53(10pt2), 2384-2398.

[136] Fiebig, E. W., Wright, D. J., Rawal, B. D., Garrett, P. E., Schumacher, R. T., Peddada, L., Heldebrant, C., Smith, R., Conrad, A., Kleinman, S. H., Busch, M. P. (2003). Dynamics of HIV viremia and antibody seroconversion in plasma donors: implications for diagnosis and staging of primary HIV infection. Aids, 17(13), 1871-1879.

[137] McRae, B., Lange, J. A., Ascher, M. S., De Wolf, F., Sheppard, H. W., Goudsmit, J., Allain, J. P. (1991). Immune response to HIV p24 core protein during the early phases of human immunodeficiency virus infection. AIDS research and human retroviruses, 7(8), 637-643.

[138] Tomaras, G. D., Yates, N. L., Liu, P., Qin, L., Fouda, G. G., Chavez, L. L., Decamp, A. C., Parks, R. J., Ashley, V. C., Lucas, J. T., Cohen, M., Eron, J., Hicks, C. B., Liao, H. X., Self, S. G., Landucci, G., Forthal, D.

N., Weinhold, K. J., Keele, B. F., Hahn, B. H., Greenberg, M. L., Morris, L., Karim, S. S., Blattner, W. A., Montefiori, D. C., Shaw, G. M., Perelson, A. S., Haynes, B. F. (2008). Initial B-cell responses to transmitted human immunodeficiency virus type 1: virion-binding immunoglobulin M (IgM) and IgG antibodies followed by plasma anti-gp41 antibodies with ineffective control of initial viremia. Journal of virology, 82(24), 12449-12463.

[139] Delaney, K. P., Branson, B. M., Uniyal, A., Phillips, S., Candal, D., Owen, S. M., Kerndt, P. R. (2011). Evaluation of the performance characteristics of 6 rapid HIV antibody tests. Clinical infectious diseases, 52(2), 257-263.

[140] Branson, B. M., Owen, S. M., Wesolowski, L. G., Bennett, B., Werner, B. G., Wroblewski, K. E., Pentella, M. A. (2014). Laboratory testing for the diagnosis of HIV infection: updated recommendations.

[141] World Health Organization. (2013). Consolidated guidelines on the use of antiretroviral drugs for treating and preventing HIV infection: recommendations for a public health approach. Available: http://www.who.int/hiv/pub/guidelines/arv2013/. Accessed 31 Aug 2018.

[142] Altman, D. G., Bland, J. M. (1994). Diagnostic tests. 1: Sensitivity and specificity. BMJ: British Medical Journal, 308(6943), 1552.

[143] World Health Organization. (2004). HIV assays: operational characteristics (Phase 1): report 15 antigen/antibody ELISAs.

[144] Patel, P., Bennett, B., Sullivan, T., Parker, M. M., Heffelfinger, J. D., Sullivan, P. S., CDC AHI Study Group. (2012). Rapid HIV screening: missed opportunities for HIV diagnosis and prevention. Journal of ClinicalVirology, 54(1), 42-47.

[145] Ittiravivongs, A., Likanonsakul, S., Mastro, T. D., Tansuphasawadikul, S., Young, N., Naiwatanakul, T., Kitayaporn, D., Limpakarnjanarat, K. (1996). Evaluation of a confirmatory HIV testing strategy in Thailand not using Western blot. JAIDS Journal of Acquired Immune Deficiency Syndromes, 13(3), 296-297.

[146] Sato, P.A., Maskill, W. J., Tamashiro, H., Heymann, D. L. (1994). Strategies for laboratory HIV testing: an examination of alternative approaches not requiring Western blot. Bulletin of the World Health Organization, 72(1), 129-134.

[147] Martin, R. (2001). Guidelines for using HIV testing technologies in surveillance: selection, evaluation and implementation. S. Patel, & B. Divine (Eds.). UNAIDS.

[148] Fischer, A., Lejczak, C., Lambert, C., Servais, J., Makombe, N., Rusine, J., Staub, T., Hemmer, R., Schneider, F., Schmit, J. C., Arendt, V. (2004). Simple DNA extraction method for dried blood spots and comparison of two PCR assays for diagnosis of vertical human immunodeficiency virus type 1 transmission in Rwanda. Journal of clinical microbiology, 42(1), 16-20.

[149] Bremer, J.W., Lew, J.F., Cooper, E., Hillyer, G.V., Pitt, J., Handelsman, E., Brambilla, D., Moye, J., Hoff, R.Women and Infants' Transmission Study Group. (1996). Diagnosis of infection with human immunodeficiency virus type 1 by a DNA polymerase chain reaction assay among infants enrolled in the Women and Infants' Transmission Study. The Journal of pediatrics, 129(2), 198-207.

[150] Braun, J., Plantier, J.C., Hellot, M.F., Tuaillon, E., Gueudin, M., Damond, F., Malmsten, A., Corrigan, G. E., Simon, F. (2003). A new quantitative HIV load assay based on plasma virion reverse transcriptase activity for the different types, groups and subtypes. Aids, 17(3), 331-336.

[151] Rouet, F., Ekouevi, D.K., Chaix, M.L., Burgard, M., Inwoley, A., Tony, T.D.,Danel, C., Anglaret, X., Leroy, V., Msellati, P., Dabis, F., Rouzioux, C. (2005). Transfer and evaluation of an automated, low-cost real-time reverse transcription-PCR test for diagnosis and monitoring of human immunodeficiency virus type 1 infection in a West African resource-limited setting. Journal of clinical microbiology, 43(6), 2709-2717.

[152] Study, E.C. (1991). Children born to women with HIV-1 infection: natural history and risk of transmission. Thelancet, 337(8736), 253-260.

[153] Moodley, D., Coovadia, H.M., Bobat, R.A., Madurai, S., Sullivan, J.L. (1997) The relationship between maternal-infant antibody levels and vertical transmission of HIV-1 infection. Journal of tropical pediatrics, 43(2), 75-79.

[154] World Health Organization. (2010). WHO Recommendations on the Diagnosis of HIV Infection in Infants and Children.

[155] Berger, A., Preiser, W., Doerr, H.W. (2001). The role of viral load determination for the management of human immunodeficiency virus, hepatitis B virus and hepatitis C virus infection. Journal of clinicalvirology, 20(1), 23-30.

[156] Wittek, M., Stürmer, M., Doerr, H.W., Berger, A. (2007). Molecular assays for monitoring HIV infection and antiretroviral therapy. Expert review of molecular diagnostics, 7(3), 237-246.

[157] World Health Organization (WHO). (2014). HIV/AIDS Diagnostics Technology Landscape. 4th edtion. UNAIDS, Geneva.

[158] Brooks, J.T., Kaplan, J.E., Masur, H. (2009). What's new in the 2009 US guidelines for prevention and treatment of opportunistic infections among adults and adolescents with HIV. Top HIV Med, 17(3), 109-114.

[159] Panel on Antiretroviral Guidelines for Adults and Adolescents. Guidelines for the use of antiretroviral agents in HIV-1-infected adults and adolescents. Department of Health and Human Services.

[160] Givan, A. L. (2011). Flow cytometry: an introduction. Flow Cytometry Protocols, 1-29.

[161] Biosciences, B. D. (2000). Introduction to Flow Cytometry: A learning guide. Manual Part, 1.

[162] Hawley, T.S., Hawley, R. G. (Eds.). (2004). Flow cytometry protocols (Vol. 263, pp. 345-354). Totowa (NJ): Humana Press.

[163] Le Guenno, B., Formenty, P., Wyers, M., Gounon, P., Walker, F., Boesch, C. (1995). Isolation and partial characterisation of a new strain of Ebola virus. The Lancet, 345(8960), 1271-1274.

[164] Centers for Disease Control and Prevention (CDC). (2015). Outbreaks chronology: Ebola virus disease. Atlanta, GA: CDC.

[165] King, A. M., Lefkowitz, E., Adams, M. J., Carstens, E. B. (Eds.). (2011). Virus taxonomy: ninth report of the International Committee on Taxonomy of Viruses. Elsevier.

[166] Siegert, R., Shu, H. L., Slenczka, W., Peters, D., Müller, G. (1967). On the etiology of an unknown human infection originating from monkeys. Deutsche medizinische Wochenschrift (1946), 92(51), 2341.

[167] Breman, J. G., Piot, P., Johnson, K. M., White, M. K., Mbuyi, M., Sureau, P., Kintoki, V. (1978). The epidemiology of Ebola hemorrhagic fever in Zaire, 1976. Ebola virus haemorrhagic fever, 103-124.

[168] Feldmann, H., Geisbert, T. W. (2011). Ebola haemorrhagic fever. The Lancet, 377(9768), 849-862.

[169] Baron, S. (1996). Epidemiology-Medical Microbiology. University of Texas Medical Branch at Galveston. 4th edition. Chapter 72. Filovirus.

[170] Formenty, P., Hatz, C., Le Guenno, B., Stoll, A., Rogenmoser, P., Widmer, A. (1999). Human infection due to Ebola virus, subtype Cote d'Ivoire: clinical and biologic presentation. Journal of Infectious Diseases, 179(Supplement 1), S48-S53.

[171] Wamala, J. F., Lukwago, L., Malimbo, M., Nguku, P., Yoti, Z., Musenero, M., Amone, J., Mbabazi, W., Nanyunja, M., Zaramba, S., Opio, A., Lutwama, J. J., Talisuna, A. O., Okware, S. I. (2010). Ebola hemorrhagic fever associated with novel virus strain, Uganda, 2007–2008. Three ebola outbreaks in Uganda 2000-2011.

[172] Murphy, F. A., van der Groen, G., Whitfield, S. G., Lange, J. V. (1978). Ebola and Marburg virus morphology and taxonomy. Ebola Virus Haemorrhagic Fever, 61-82.

[173] Beer, B., Kurth, R., Bukreyev, A. (1999). Characteristics of filoviridae: Marburg and Ebola viruses. Naturwissenschaften, 86(1), 8-17.

[174] Martines, R. B., Ng, D. L., Greer, P. W., Rollin, P. E., Zaki, S. R. (2015). Tissue and cellular tropism, pathology and pathogenesis of Ebola and Marburg viruses. The Journal of pathology, 235(2), 153-174.

[175] Mylne, A., Brady, O. J., Huang, Z., Pigott, D. M., Golding, N., Kraemer, M. U., Hay, S. I. (2014). A comprehensive database of the geographic spread of past human Ebola outbreaks. Scientific Data, 1, 140042.

[176] Leroy, E. M., Kumulungui, B., Pourrut, X., Rouquet, P., Hassanin, A., Yaba, P., Délicat, A., Paweska, J. T., Gonzalez, J. P., Swanepoel, R. (2005). Fruit bats as reservoirs of Ebola virus. Nature, 438(7068), 575-576.

[177] Leroy, E. M., Epelboin, A., Mondonge, V., Pourrut, X., Gonzalez, J. P., Muyembe-Tamfum, J. J., Formenty, P. (2009). Human Ebola outbreak resulting from direct exposure to fruit bats in Luebo, Democratic Republic of Congo, 2007. Vector-borne and zoonotic diseases, 9(6), 723-728.

[178] Bermejo, M., Rodríguez-Teijeiro, J. D., Illera, G., Barroso, A., Vilà, C., Walsh, P. D. (2006). Ebola outbreak killed 5000 gorillas. Science, 314(5805), 1564-1564.

[179] Shoemaker, T., MacNeil, A., Balinandi, S., Campbell, S., Wamala, J. F., McMullan, L. K., Downing, R., Lutwana, J., Mbidde, E., Ströher, U., Rollin, P. E., Nichol, S. T. (2012). Reemerging Sudan ebola virus disease in Uganda, 2011. Emerging infectious diseases, 18(9), 1480.

[180] World Health Organization. (2014). Ebola and Marburg virus disease epidemics: preparedness, alert, control, and evaluation.

[181] Francesconi, P., Yoti, Z., Declich, S., Onek, P. A., Fabiani, M., Olango, J., Salmaso, S. (2003). Ebola hemorrhagic fever transmission and risk factors of contacts, Uganda. Emerging infectious diseases, 9(11), 1430.

[182] Hartman, A. L., Towner, J. S., Nichol, S. T. (2010). Ebola and marburg hemorrhagic fever. Clinics in laboratory medicine, 30(1), 161-177.

[183] Kadanali, A., Karagoz, G. (2015). An overview of Ebola virus disease. Northern clinics of Istanbul, 2(1), 81-86.

[184] Funk, D. J., Kumar, A. (2015). Ebola virus disease: an update for anesthesiologists and intensivists. Canadian Journal of Anesthesia/Journal canadien d'anesthésie, 62(1), 80-91.

[185] Baskerville, A., Fisher-Hoch, S. P., Neild, G. H., Dowsett, A. B. (1985). Ultrastructural pathology of experimental Ebola haemorrhagic fever virus infection. The Journal of pathology, 147(3), 199-209.

[186] Feldmann, H., Bugany, H., Mahner, F., Klenk, H. D., Drenckhahn, D., Schnittler, H. J. (1996). Filovirus-induced endothelial leakage triggered by infected monocytes/macrophages. Journal of virology, 70(4), 2208-2214.

[187] Li, J., Duan, H. J., Chen, H. Y., Ji, Y. J., Zhang, X., Rong, Y. H., Xu, Z., Sun, L. J., Zhang, J. Y., Liu, L. M., Jin, B., Zhang, J., Du, N., Su, H. B., Teng, G. J., Yuan, Y., Qin, E. Q., Jia, H. J., Wang, S., Guo, T. S., Wang, Y., Mu, J. S., Yan, T., Li, Z. W., Dong, Z., Nie, W. M., Jiang, T. J., Li, C., Gao, X. D., Ji, D., Zhuang, Y. J.., Li, L.., Wang, L. F., Li, W. G., Duan, X. Z., Lu, Y. Y., Sun, Z. Q., Kanu, A. B. J., Koroma, S. M., Zhao, M., Ji, J. S., Wang, F. S. (2016). Age and Ebola viral load correlate with mortality and survival time in 288 Ebola virus disease patients. International Journal of Infectious Diseases, 42, 34-39.

[188] Katz, L. M., Tobian, A. A. (2014). Ebola virus disease, transmission risk to laboratory personnel, and pretransfusion testing. Transfusion, 54(12), 3247-3251.

[189] Cotte, J., Janvier, F., Cordier, P. Y., Bordes, J., Kaiser, E. (2015). Organ support in Ebola virus disease: Utility of point-of-care blood tests. Anaesthesia, critical care & pain medicine, 34(6), 363-364.

[190] Martin, P., Laupland, K. B., Frost, E. H., Valiquette, L. (2015). Laboratory diagnosis of Ebola virus disease. Intensive care medicine, 41(5), 895-898.

[191] Broadhurst, M. J., Brooks, T. J., Pollock, N. R. (2016). Diagnosis of Ebola virus disease: past, present, and future. Clinical microbiology reviews, 29(4), 773-793.

[192] Ikegami, T., Niikura, M., Saijo, M., Miranda, M. E., Calaor, A. B., Hernandez, M., Acosta, L. P., Manalo, D. L., Kurane, I., Yoshikawa, Y., Morikawa, S. (2003). Antigen capture enzyme-linked immunosorbent assay for specific detection of Reston Ebola virus nucleoprotein. Clinical and diagnostic laboratory immunology, 10(4), 552-557.

[193] Lucht, A., Grunow, R., Möller, P., Feldmann, H., Becker, S. (2003). Development, characterization and use of monoclonal VP40-antibodies for the detection of Ebola virus. Journal of virological methods, 111(1), 21-28.

[194] Lucht, A., Grunow, R., Otterbein, C., Möller, P., Feldmann, H., Becker, S. (2004). Production of monoclonal antibodies and development of an antigen capture ELISA directed against the envelope glycoprotein GP of Ebola virus. Medical microbiology and immunology, 193(4), 181-187.

[195] Niikura, M., Ikegami, T., Saijo, M., Kurane, I., Miranda, M. E., Morikawa, S. (2001). Detection of Ebola viral antigen by enzyme-linked immunosorbent assay using a novel monoclonal antibody to nucleoprotein. Journal of clinical microbiology, 39(9), 3267-3271.

[196] Groen, J., van den Hoogen, B. G., Burghoorn-Maas, C. P., Fooks, A. R., Burton, J., Clegg, C. J., Zeller, H., Osterhaus, A. D. (2003). Serological reactivity of baculovirus-expressed Ebola virus VP35 and nucleoproteins. Microbes and infection, 5(5), 379-385.

[197] Prehaud, C., Hellebrand, E., Coudrier, D., Volchkov, V. E., Volchkova, V. A., Feldmann, H., Le Guenno, B., Bouloy, M. (1998). Recombinant Ebola virus nucleoprotein and glycoprotein (Gabon 94 strain) provide new tools for the detection of human infections. Journal of general virology, 79(11), 2565-2572.

[198] Saijo, M., Niikura, M., Morikawa, S., Ksiazek, T. G., Meyer, R. F., Peters, C. J., Kurane, I. (2001). Enzyme-linked immunosorbent assays for detection of antibodies to Ebola and Marburg viruses using recombinant nucleoproteins. Journal of clinical microbiology, 39(1), 1-7.

[199] Gibb, T. R., Norwood, D. A., Woollen, N., Henchal, E. A. (2001). Development and evaluation of a fluorogenic 5' nuclease assay to detect and differentiate between Ebola virus subtypes Zaire and Sudan. Journal of Clinical Microbiology, 39(11), 4125-4130.

[200] Sanchez, A., Ksiazek, T. G., Rollin, P. E., Miranda, M. E., Trappier, S. G., Khan, A. S., Peters, C. J., Nichol, S. T. (1999). Detection and molecular characterization of Ebola viruses causing disease in human and nonhuman primates. Journal of Infectious Diseases, 179(Supplement 1), S164-S169.

[201] Towner, J. S., Rollin, P. E., Bausch, D. G., Sanchez, A., Crary, S. M., Vincent, M., Spiropoulou, C. F., Ksiazek, T. G., Lukwiya, M., Kaducu, F., Downing, R., Nichol, S. T. (2004). Rapid diagnosis of Ebola hemorrhagic fever by reverse transcription-PCR in an outbreak setting and assessment of patient viral load as a predictor of outcome. Journal of virology, 78(8), 4330-4341.

[202] Weidmann, M., Mühlberger, E., Hufert, F. T. (2004). Rapid detection protocol for filoviruses. Journal of Clinical Virology, 30(1), 94-99.

[203] Centers for Disease Control and Prevention (CDC). (1996). Nucleic acid amplification tests for tuberculosis. MMWR. Morbidity and mortality weekly report, 45(43), 950-951.

[204] Gen-Probe. (1996) Amplified mycobacterium tuberculosis direct test for in-vitro diagnostic use: 50 test kit. San Diego, California: Gen-Probe.

[205] Posthuma-Trumpie, G. A., Korf, J., van Amerongen, A. (2009). Lateral flow (immuno) assay: its strengths, weaknesses, opportunities and threats. A literature survey. Analytical and bioanalytical chemistry, 393(2), 569-582.

[206] Singer, J. M., Plotz, C. M. (1956). The latex fixation test: I. Application to the serologic diagnosis of rheumatoid arthritis. The American journal of medicine, 21(6), 888-892.

[207] Ngom, B., Guo, Y., Wang, X., Bi, D. (2010). Development and application of lateral flow test strip technology for detection of infectious agents and chemical contaminants: a review. Analytical and bioanalytical chemistry, 397(3), 1113-1135.

[208] Marco, M. P., Gee, S., Hammock, B. D. (1995). Immunochemical techniques for environmental analysis I. Immunosensors. TrAC Trends in Analytical Chemistry, 14(7), 341-350.

[209] Banada, P. P., Bhunia, A. K. (2008). Antibodies and immunoassays for detection of bacterial pathogens. In Principles of bacterial detection: biosensors, recognition receptors and microsystems (pp. 567-602). Springer, New York, NY.

[210] Deshpande, A., White, P. S. (2012). Multiplexed nucleic acid-based assays for molecular diagnostics of human disease. Expert review of molecular diagnostics, 12(6), 645-659.

[211] Lee, H. H., Allain, J. P. (2004). Improving blood safety in resource-poor settings. Vox sanguinis, 87, 176-179.

[212] Reddy, L. H., Arias, J. L., Nicolas, J., Couvreur, P. (2012). Magnetic nanoparticles: design and characterization, toxicity and biocompatibility, pharmaceutical and biomedical applications. Chemical reviews, 112(11), 5818-5878.

[213] Hsing, I. M., Xu, Y., Zhao, W. (2007). Micro-and nano-magnetic particles for applications in biosensing. Electroanalysis: An International Journal Devoted to Fundamental and Practical Aspects of Electroanalysis, 19(7-8), 755-768.

[214] Berensmeier, S. (2006). Magnetic particles for the separation and purification of nucleic acids. Applied microbiology and biotechnology, 73(3), 495-504.

[215] Cao, M., Li, Z., Wang, J., Ge, W., Yue, T., Li, R., Colvin, V. L. William, W. Y. (2012). Food related applications of magnetic iron oxide nanoparticles: enzyme immobilization, protein purification, and food analysis. Trends in Food Science & Technology, 27(1), 47-56.

[216] Ademtech. Available in http://www.ademtech.com/. Consulted on 31 Aug 2018.

[217] Invitrogen, Life Technologies Corporation. Available in http://www.invitrogen.com/. Consulted on 31 Aug 2018.

[218] Bangs Laboratories, Inc. Available in http://www.bangslabs.com/. Consulted on 31 Aug 2018.

[219] Chemicell. Available in http://www.chemicell.com/. Consulted on 31 Aug 2018.

[220] Miltenyi Biotech. Available in http://www.miltenyibiotec.com/en. Consulted on 31 Aug 2018.

[221] Vikesland, P. J., Wigginton, K. R. (2010). Nanomaterial enabled biosensors for pathogen monitoring-a review. Environmental science & technology, 44(10), 3656-3669.

[222] World Health Organization (WHO). (1993). International Programme on Chemical Safety. Biomarkers and Risk Assessment: Concepts and Principles. Available in http://www.inchem.org/documents/ehc/ehc/ehc155.htm. Consulted on 31 Aug 2018.

[223] Van Ommering, K. (2010). Dynamics of individual magnetic particles near a biosensor surface. Doctoral dissertation, Technische Universiteit Eindhoven.

[224] Ward Jr, J. B., Henderson, R. E. (1996). Identification of needs in biomarker research. Environmental health perspectives, 104(Suppl 5), 895-900.

[225] Strimbu, K., Tavel, J. A. (2010). What are biomarkers? Current Opinion in HIV and AIDS, 5(6), 463-466.

[226] Wu, G., Zaman, M. H. (2012). Low-cost tools for diagnosing and monitoring HIV infection in low-resource settings. Bulletin of the World Health Organization, 90, 914-920.

[227] World Health Organization. (2005). Interim WHO clinical staging of HIV/AIDS and HIV/ AIDS case definitions for surveillance, Africa region. Geneva: WHO.

[228] Constantine, N. T., Kabat, W., Richard, Y. Z. (2005). Update on the laboratory diagnosis and monitoring of HIV infection. Cell research, 15(11-12), 870-876.

[229] World Health Organization. (2002). HIV simple/rapid assays: operational characteristics (Phase I). Report 12: Simple rapid tests, whole blood specimens (No. WHO/BCT/02.07). Geneva: WHO.

[230] Carrière, D., Vendrell, J. P., Fontaine, C., Jansen, A., Reynes, J., Pagès, I., Holzmann, C., Laprade, M., Pau, B. (1999). Whole blood Capcellia CD4/CD8 immunoassay for enumeration of CD4+ and CD8+ peripheral T lymphocytes. Clinical chemistry, 45(1), 92-97.

[231] Diaw, P. A., Daneau, G., Coly, A. A., Ndiaye, B. P., Wade, D., Camara, M., Mboup, S., Kestens, L., Dieye, T. N. (2011). Multisite evaluation of a point-of-care instrument for CD4+ T-cell enumeration using venous and finger-prick blood: The PIMA CD4. JAIDS Journal of Acquired Immune Deficiency Syndromes, 58(4), e103-e111.

[232] Volberding, P., Sande, M. A., Greene, W. C., Lange, J. M. (Eds.). (2008). Global hiv/aids medicine. Elsevier Health Sciences.

[233] Boyle, D. S., Hawkins, K. R., Steele, M. S., Singhal, M., Cheng, X. (2012). Emerging technologies for point-of-care CD4 T-lymphocyte counting. Trends in biotechnology, 30(1), 45-54.

[234] Lutwama, F., Serwadda, R., Mayanja-Kizza, H., Shihab, H. M., Ronald, A., Kamya, M. R., Thomas, D., Johnson, E., Quinn, T. C., Moore, R. D., Spacek, L. A. (2008). Evaluation of Dynabeads and Cytospheres compared with flow cytometry to enumerate CD4+ T cells in HIV-infected Ugandans on antiretroviral therapy. Journal of acquired immune deficiency syndromes (1999), 48(3), 297-303.

[235] World Health Organization. (2004). $CD4^+$ T-Cell enumeration technologies. Technical information. World Health Organization. Geneva: WHO.

[236] Larson, B. A., Brennan, A., McNamara, L., Long, L., Rosen, S., Sanne, I., Fox, M. P. (2010). Lost opportunities to complete CD4+ lymphocyte testing among patients who tested positive for HIV in South Africa. Bulletin of the World Health Organization, 88, 675-680. .

[237] World Health Organization. (2010). Antiretroviral therapy for HIV infection in adults and adolescents: recommendations for a public health approach. Geneva: WHO.

[238] HHS Panel on Antiretroviral Guidelines for Adults and Adolescents. (2012). Guidelines for the use of antiretroviral agents in HIV-1-infected adults and adolescents. 2012. Available in http://aidsinfo.nih.gov/contentfiles/AdultandAdolescentGL.pdf. Accessed 31 Aug 2018.

[239] Workman, S., Wells, S. K., Pau, C. P., Owen, S. M., Dong, X. F., LaBorde, R., Granade, T. C. (2009). Rapid detection of HIV-1 p24 antigen using magnetic immuno-chromatography (MICT). Journal of virological methods, 160(1-2), 14-21.

[240] Ning, G. A. N., Nai-Xing, L. U. O., Tian-Hua, L. I., Zheng, L., Min-Jun, N. I. (2010). A non-enzyme amperometric immunosensor for rapid determination of human immunodeficiency virus p24 based on magnetism controlled carbon nanotubes modified printed electrode. Chinese Journal of Analytical Chemistry, 38(11), 1556-1562.

[241] Albertoni, G. A., Arnoni, C. P., Araujo, P. R. B., Andrade, S. S., Carvalho, F. O., Girão, M. J. B. C., Schor, N., Barreto, J. A. (2011). Magnetic bead technology for viral RNA extraction from serum in blood bank screening. The Brazilian Journal of Infectious Diseases, 15(6), 547-552.

[242] Nam, J. M., Stoeva, S. I., Mirkin, C. A. (2004). Bio-bar-code-based DNA detection with PCR-like sensitivity. Journal of the American Chemical Society, 126(19), 5932-5933.

[243] Taton, T. A., Mirkin, C. A., Letsinger, R. L. (2000). Scanometric DNA array detection with nanoparticle probes. Science, 289(5485), 1757-1760.

[244] Stoeva, S. I., Lee, J. S., Thaxton, C. S., Mirkin, C. A. (2006). Multiplexed DNA detection with biobarcoded nanoparticle probes. Angewandte Chemie, 118(20), 3381-3384.

[245] Zitka, O., Skalickova, S., Merlos, M. A. R., Krejcova, L., Kopel, P., Adam, V., Kizek, R. (2013). Sequences of pandemic-causing viruses isolated and detected by paramagnetic particles coupled with microfluidic system and electrochemical detector. Int. J. Electrochem. Sci, 8, 12628-12642.

[246] Wang, S., Tasoglu, S., Chen, P. Z., Chen, M., Akbas, R., Wach, S., Ozdemir, C. I., Gurkan, U. A., Giguel, F. F., Kuritzkes, D. R., Demirci, U. (2014). Micro-a-fluidics ELISA for Rapid CD4 Cell Count at the Point-of-Care. Scientific reports, 4, 3796.

[247] Lyamuya, E. F., Kagoma, C., Mbena, E. C., Urassa, W. K., Pallangyo, K., Mhalu, F. S., Biberfeld, G. (1996). Evaluation of the FACScount, TRAx CD4 and Dynabeads methods for CD4 lymphocyte determination. Journal of immunological methods, 195(1-2), 103-112.

[248] Godreuil, S., Tazi, L., Bañuls, A. L. (2007). Pulmonary tuberculosis and Mycobacterium tuberculosis: modern molecular epidemiology and perspectives. Encyclopedia of infectious diseases: Modern methodologies. Hoboken, NJ: John Wiley & Sons, 1-30

[249] McNerney, R., Maeurer, M., Abubakar, I., Marais, B., Mchugh, T. D., Ford, N., , Weyer, K., Lawn, S., Grobusch, M. P., Memish, Z., Squire, S. B., Pantaleo, G., Chakaya, J., Casenghi, M., Migliori, G. B., Mwaba, P., Zijenah, L., Hoelscher, M., Cox, H., Swaminathan, S., Kim, P. S., Schito, M., Harari, A., Bates, M., Schwank, S., O'Grady, J., Pletschette, M., Ditui, L., Atun, R., Zumla, A.(2012). Tuberculosis diagnostics and biomarkers: needs, challenges, recent advances, and opportunities. Journal of Infectious Diseases, 205(suppl_2), S147-S158.

[250] Shingadia, D. (2012). The diagnosis of tuberculosis. The Pediatric infectious disease journal, 31(3), 302-305.

[251] Steingart, K. R., Ng, V., Henry, M., Hopewell, P. C., Ramsay, A., Cunningham, J., Urbanczik, R., Perkins, M. D., Aziz, M. A., Pai, M. (2006). Sputum processing methods to improve the sensitivity of smear microscopy for tuberculosis: a systematic review. The Lancet infectious diseases, 6(10), 664-674.

[252] Dinnes, J., Deeks, J., Kunst, H., Gibson, A., Cummins, E., Waugh, N., Drobniewski, F., Lalvani, A. (2007). A systematic review of rapid diagnostic tests for the detection of tuberculosis infection, 11:1–178.

[253] Dorman, S. E. (2010). New diagnostic tests for tuberculosis: bench, bedside, and beyond. Clinical Infectious Diseases, 50(Supplement_3), S173-S177.

[254] Wilson, D., Nachega, J., Morroni, C., Chaisson, R., Maartens, G. (2006). Diagnosing smear-negative tuberculosis using case definitions and treatment response in HIV-infected adults. The International Journal of Tuberculosis and Lung Disease, 10(1), 31-38.

[255] Al-Orainey, I. O. (2009). Diagnosis of latent tuberculosis: Can we do better? Annals of thoracic medicine, 4(1), 5.

[256] Konstantinos, A. (2010). Testing for tuberculosis. Australian prescriber, 33(1), 12-18.

[257] Aaron, L., Saadoun, D., Calatroni, I., Launay, O., Memain, N., Vincent, V., Marchal, G., Dupont, B., Bouchaud, O., Valeyre, D., Lortholary, O. (2004). Tuberculosis in HIV-infected patients: a comprehensive review. Clinical microbiology and infection, 10(5), 388-398.

[258] Galagan, J. E. (2014). Genomic insights into tuberculosis. Nature Reviews Genetics, 15(5), 307-320.

[259] World Health Organization. (2011). Global tuberculosis control: WHO report 2011, Geneva: WHO/HTM/TB/2010. Available in: http://apps.who.int/iris/handle/10665/44728. Accessed 31 Aug 2018.

[260] Ghodbane, R., Drancourt, M. (2013). A magnetic bead protocol for culturing Mycobacterium tuberculosis from sputum specimens. Journal of clinical microbiology, 51(5): 1578-1579.

[261] Microsens. Available in http://www.microsens.co.uk/tb-beads.html. Accessed 31 Aug 2018.

[262] Albert H, Ademun PJ, Lukyamuzi G, Nyesiga B, Manabe Y, Joloba M, et al. Feasibility of magnetic bead technology for concentration of mycobacteria in sputum prior to fluorescence microscopy. BMC Infect Dis 2011; 11:125.

[263] Wilson, S., Lane, A., Rosedale, R., Stanley, C. (2010). Concentration of Mycobacterium tuberculosis from sputum using ligand-coated magnetic beads. The International Journal of Tuberculosis and Lung Disease, 14(9), 1164-1168.

[264] Li, Z., Bai, G. H., von Reyn, C. F., Marino, P., Brennan, M. J., Gine, N., Morris, S. L. (1996). Rapid detection of Mycobacterium avium in stool samples from AIDS patients by immunomagnetic PCR. Journal of clinical microbiology, 34(8), 1903-1907.

[265] Rabe, O., Chanteau, S., Marchal, G., Rasolofo, V. R. (2001). Diagnosis of tuberculosis by immunocapture of the tuberculous bacillus (using magnetic beads). Archives de l'Institut Pasteur de Madagascar, 67(1-2), 37-40.

[266] Kim, J., Lee, J., Lee, K. I., Park, T. J., Kim, H. J., Lee, J. (2013). Rapid monitoring of CFP-10 during culture of Mycobacterium tuberculosis by using a magnetophoretic immunoassay. Sensors and Actuators B: Chemical, 177, 327-333.

[267] Lermo, A., Liébana, S., Campoy, S., Fabiano, S., García, M. I., Soutullo, A., Zumárraga, M. J., Alegret, S., Pividori, M. I. (2010). A novel strategy for screening-out raw milk contaminated with Mycobacterium bovis on dairy farms by double-tagging PCR and electrochemical genosensing. Int. Microbiol, 13, 91-97.

[268] Iwasaki, A., Pillai, P. S. (2014). Innate immunity to influenza virus infection. Nature Reviews Immunology, 14(5), 315.

[269] Global Report for Research on Infectious Diseases of Poverty. (2012) UNICEF/UNDP/World Bank/WHO Special Programme for Research and Training in Tropical Diseases. Geneva.

[270] Deng, M., Long, L., Xiao, X., Wu, Z., Zhang, F., Zhang, Y., Zheng, X., Xin, X., Wang, Q., Wu, D. (2011). Immuno-PCR for one step detection of H5N1 avian influenza virus and Newcastle disease virus using magnetic gold particles as carriers. Veterinary immunology and immunopathology, 141(3-4), 183-189.

[271] Zhou, C. H., Long, Y. M., Qi, B. P., Pang, D. W., Zhang, Z. L. (2013). A magnetic bead-based bienzymatic electrochemical immunosensor for determination of H9N2 avian influenza virus. Electrochemistry Communications, 31, 129-132.

[272] Lien, K. Y., Hung, L. Y., Huang, T. B., Tsai, Y. C., Lei, H. Y., Lee, G. B. (2011). Rapid detection of influenza A virus infection utilizing an immunomagnetic bead-based microfluidic system. Biosensors and Bioelectronics, 26(9), 3900-3907.

[273] Hung, L. Y., Huang, T. B., Tsai, Y. C., Yeh, C. S., Lei, H. Y., Lee, G. B. (2013). A microfluidic immunomagnetic bead-based system for the rapid detection of influenza infections: from purified virus particles to clinical specimens. Biomedical microdevices, 15(3), 539-551.

[274] Krejcova, L., Hynek, D., Kopel, P., Adam, V., Hubalek, J., Trnkova, L., Kizek, R. (2013). Paramagnetic particles isolation of influenza oligonucleotide labelled with CdS QDs. Chromatographia, 76(7-8), 355-362.

[275] Krejcova, L., Huska, D., Hynek, D., Kopel, P., Adam, V., Hubalek, J., Trnkova, L., Kizek, R. (2013). Using of paramagnetic microparticles and quantum dots for isolation and electrochemical detection of influenza viruses' specific nucleic acids. Int. J. Electrochem. Sci, 8(1), 689-702.

[276] Krejcova, L., Hynek, D., Kopel, P., Rodrigo, M. A. M., Adam, V., Hubalek, J., Babula, P., Trnkova, L., Kizek, R. (2013). Development of a magnetic electrochemical bar code array for point mutation detection in the H5N1 neuraminidase gene. Viruses, 5(7), 1719-1739.

[277] Chou, T. C., Hsu, W., Wang, C. H., Chen, Y. J., Fang, J. M. (2011). Rapid and specific influenza virus detection by functionalized magnetic nanoparticles and mass spectrometry. Journal of nanobiotechnology, 9(1), 52.

[278] Bell, D., Wongsrichanalai, C., Barnwell, J. W. (2006). Ensuring quality and access for malaria diagnosis: how can it be achieved? Nature Reviews Microbiology, 4(9), 682.

[279] Todd, C. W., Udhayakumar, V., Escalante, A. A., & Lal, A. A. (2007). Malaria Vaccines, in Tibayrenc, M. (Ed.). (2007). Encyclopedia of infectious diseases: modern methodologies. John Wiley & Sons.

[280] World Health Organization. (2014). World Malaria Report 2014. Joint United Nations Programme on HIV/AIDS (UNAIDS). Geneva: WHO.

[281] Sachs, J., Malaney, P. (2002). The economic and social burden of malaria. Nature, 415(6872), 680.

[282] Amexo, M., Tolhurst, R., Barnish, G., Bates, I. (2004). Malaria misdiagnosis: effects on the poor and vulnerable. The Lancet, 364(9448), 1896-1898.

[283] Hänscheid, T. (1999). Diagnosis of malaria: a review of alternatives to conventional microscopy. Clinical & Laboratory Haematology, 21(4), 235-245.

[284] Carnevale, E. P., Kouri, D., DaRe, J. T., McNamara, D. T., Mueller, I., Zimmerman, P. A. (2007). A multiplex ligase detection reaction-fluorescent microsphere assay for simultaneous detection of single nucleotide polymorphisms associated with Plasmodium falciparum drug resistance. Journal of clinical microbiology, 45(3), 752-761.

[285] LeClair, N. P., Conrad, M. D., Baliraine, F. N., Nsanzabana, C., Nsobya, S. L., Rosenthal, P. J. (2013). Optimization of a ligase detection reaction fluorescent microsphere assay for the characterization of resistance-mediating polymorphisms in African samples of Plasmodium falciparum. Journal of clinical microbiology, 51: 2564–70.

[286] de Souza Castilho, M., Laube, T., Yamanaka, H., Alegret, S., Pividori, M. I. (2011). Magneto immunoassays for Plasmodium falciparum histidine-rich protein 2 related to malaria based on magnetic nanoparticles. Analytical chemistry, 83(14), 5570-5577.

[287] Davis, K. M., Swartz, J. D., Haselton, F. R., Wright, D. W. (2012). Low-resource method for extracting the malarial biomarker histidine-rich protein II to enhance diagnostic test performance. Analytical chemistry, 84(14), 6136-6142.

[288] Lindenbach, B. D., Rice, C. M. Flaviviridae: The viruses and their replication, In: Knipe, D. M., Howley, P. M., Griffin, D. E., Lamb, R. A., Martin, M. A., Roizman, B. (2001). Fields virology, vol. 1. Philadelphia (EUA): Lippincott Williams & Wilkins.

[289] World Health Organization. (2000). Strengthening implementation of the global strategy for dengue fever/dengue haemorrhagic fever prevention and control. Report of the Informal Consultation, 18-20 October 1999. Geneva: WHO.

[290] World Health Organization. (2012). World Health Statistics. Fact sheet no. 117. Geneva: WHO. Available in: http://www.who.int/gho/publications/world health statistics/EN WHS2012 Full.pdf

[291] Lindegren, G., Vene, S., Lundkvist, Å., Falk, K. I. (2005). Optimized diagnosis of acute dengue fever in Swedish travelers by a combination of reverse transcription-PCR and immunoglobulin M detection. Journal of clinical microbiology, 43(6), 2850-2855.

[292] Cabezas, S., Rojas, G., Pavon, A., Alvarez, M., Pupo, M., Guillen, G., Guzman, M. G. (2008). Selection of phage-displayed human antibody fragments on Dengue virus particles captured by a monoclonal antibody: Application to the four serotypes. Journal of virological methods, 147(2), 235-243.

[293] Sakudo, A., Baba, K., Tsukamoto, M., Sugimoto, A., Okada, T., Kobayashi, T., Kawashita, N., Takagi, T., Ikuta, K. (2009). Anionic polymer, poly (methyl vinyl ether–maleic anhydride)-coated beads-based capture of human influenza A and B virus. Bioorganic & medicinal chemistry, 17(2), 752-757.

[294] Sakudo, A., Ikuta, K. (2008). Efficient capture of infectious H5 avian influenza virus utilizing magnetic beads coated with anionic polymer. Biochemical and biophysical research communications, 377(1), 85-88.

[295] Sakudo, A., Ikuta, K. (2012). A technique for capturing broad subtypes and circulating recombinant forms of HIV-1 based on anionic polymer-coated magnetic beads. International journal of molecular medicine, 30(2), 437-442.

[296] Patramool, S., Bernard, E., Hamel, R., Natthanej, L., Chazal, N., Surasombatpattana, P., Ekchariyawat, P., Daoust, S., Thongrungkiat, S., Thomas, F., Briant, L., Missé, D. (2013). Isolation of infectious chikungunya virus and dengue virus using anionic polymer-coated magnetic beads. Journal of virological methods, 193(1), 55-61.

[297] Chen, W. H., Hsu, I. H., Sun, Y. C., Wang, Y. K., Wu, T. K. (2013). Immunocapture couples with matrix-assisted laser desorption/ionization time-of-flight mass spectrometry for rapid detection of type 1 dengue virus. Journal of Chromatography A, 1288, 21-27.

[298] Chang, W. S., Shang, H., Perera, R. M., Lok, S. M., Sedlak, D., Kuhn, R. J., Lee, G. U. (2008). Rapid detection of dengue virus in serum using magnetic separation and fluorescence detection. Analyst, 133(2), 233-240.

[299] Lee, Y. F., Lien, K. Y., Lei, H. Y., Lee, G. B. (2009). An integrated microfluidic system for rapid diagnosis of dengue virus infection. Biosensors and Bioelectronics, 25(4), 745-752.

[300] Yang, S. Y., Lien, K. Y., Huang, K. J., Lei, H. Y., Lee, G. B. (2008). Micro flow cytometry utilizing a magnetic bead-based immunoassay for rapid virus detection. Biosensors and Bioelectronics, 24(4), 855-862.

Chapter 2

OBJECTIVES OF THE DISSERTATION

The aim of this dissertation is the design of novel diagnostic methods based on the integration of magnetic carriers for the detection of biomarkers related to communicable diseases. The development of these new approaches involves the integration of magnetic particles in bioassays and electrochemical biosensing devices since they greatly improve the performance of a diagnostic test. The diagnosis of clinical samples based on magnetic particles as carriers can easily be achieved without any purification or pretreatment steps, which are usually required for standard methods, simplifying the analytical procedure. Moreover, the targets can be specifically isolated and preconcentrated by magnetic actuation, increasing the specificity and the sensitivity of the assay. This dissertation addresses all these promising features of the magnetic particles and their integration in biosensing strategies and bioassays for the detection of biomarkers related to infectious diseases affecting global health such as the following up of HIV/AIDS infection, interferon gamma and Ebola virus detection. Different strategies involving the integration of magnetic particles were developed, and they are presented along four different Chapters of this dissertation.

To achieve the general goal, several specific objectives were proposed, as follows:

• Defining the needs of rapid diagnostic test in low-resource settings for global infection diseases.

• Setting the rapid diagnostic test specification accordingly to the needs in low-resource settings.

• Exploring novel solid-phase isolation methods for different targets, including cells, DNA and transcripts from clinical samples.

• Characterizing advanced materials, including biologically-modified magnetic particles functionalized with antibodies, oligonucleotides and affinity proteins.

• Designing novel strategies for nucleic-acid amplification.

• Studying and characterizing novel disease biomarkers.

• Interfacing solid-phase preconcentration strategies in rapid diagnostic test.

• Integrating isothermal amplification techniques of nucleic acid targets in rapid diagnostic test.

• Designing point-of-need, rapid methods for the early detection of communicable diseases based on novel biomarkers.

• Exploiting novel routes of analytical simplification to require minimal training for final users.

• Evaluating the analytical performance of the new methods taking as a reference of communicable emerging diseases.

In Chapter 1 the main features of magnetic particles for the diagnosis in low resource settings of many communicable conditions affecting global health (ranging from tuberculosis, influenza virus, malaria, dengue virus, among others) are reviewed and rationally discussed.

Chapter 3 describes a magneto-immunoassay for HIV infection monitoring based on the enumeration of CD4+ T lymphocytes. This CD4 counting magneto immunoassay is based on the magnetic separation of the lymphocytes, taking advantages of the magnetic particles to preconcentrate the target from complex specimens such as whole blood. The integration of magnetic particles provides improved analytical features regarding sensitivity and selectivity of the assay, and reducing the matrix effect.

Chapter 4 addresses on the design of a magneto-actuated biosensor for CD4 lymphocyte monitoring. The aim of this chapter is thus the development and evaluation of magneto-actuated rapid platforms appropriate for their use in low-resource settings for the following-up of patients under treatment.

Chapter 5 describes the development of a novel Interferon-γ release assay to evaluate the expression of interferon-γ transcripts as an intracellular infection biomarker, produced by isolated T cells. This approach combines the advantages of the integration of magnetic particles for the specific isolation of different targets for the assessment of interferon gamma expression by T cells. The transcript detection is based on a double-tagging amplification on magnetic particles followed by an electrochemical genosensing. The electrochemical genosensor has the advantage of combining high sensitivity/specificity and can be performed from only 100 μL of whole blood, which can be potentially obtained by fingerprick, demonstrating a further clear advantage to be considered as a promising strategy as an alarm for the quantification of this important biomarker in several clinical applications.

Chapter 6 addresses the design of a novel strategy for the sensitive, specific, and cost-effective a detection of RNA virus of emergency disease. An isothermal amplification, based on rolling circle amplification and circle-to-circle amplification on magnetic particles is combined with the electrochemical genosensing. Specific padlock probes are designed to *L-gene*

sequences present in Ebola virus. It is the first time that rolling circle/circle-to-circle amplification on magnetic particles is integrated in the same strategy with electrochemical readout.

Chapter 7 summarises the work, presenting also the final conclusions of this Dissertation with relevant considerations about the main features and drawbacks of the strategies presented.

Finally, Chapter 8 is related to dissemination of the results, in which publications in international journals, communication in scientific meetings, as well as the participation in workshops, organization of scientific events and teaching activities are detailed.

Chapter 3

CD4 QUANTIFICATION BASED ON MAGNETO ELISA FOR AIDS DIAGNOSIS IN LOW RESOURCE SETTINGS

Talanta 160 (2016) 36-45

3.1 Abstract

The Acquired Immune Deficiency Syndrome affects the life of millions of people around the world. Although rapid and low cost screening tests are widely available for the diagnosis of HIV infection, the count of CD4+ T lymphocytes remains a drawback in the areas mostly affected by the HIV, being this control imperative for assessing the deterioration of the immunological system and the progression towards AIDS, when the counting of cells falls down 200 cells μL^{-1}. This paper describes a high-throughput, simple and rapid method for CD4+ T lymphocytes quantification, directly in whole blood, based on a magneto ELISA. The CD4 cells are separated and preconcentrated from whole blood in magnetic particles, and labeled with an enzyme for the optical readout performed with a standard microplate reader. The magneto ELISA is able to reach the whole CD4 counting range of medical interest, being the limit of detection as low as 50 CD4+ cells per μL of whole blood, without any pretreatment. This method is a highly suitable alternative diagnostic tool for the expensive flow cytometry at the community and primary care level, providing a sensitive method but by using instrumentation widely available in low-resource settings laboratories and requiring low-maintenance, as is the case of a microplate reader operated by filters.

3.2 Introduction

The induction of progressive CD4+ T cell depletion is a hallmark of the Human Immunodeficiency Virus (HIV) infection.[1] Once the HIV enters the human body, the external envelope glycoprotein gp120 interacts with the CD4 receptor to initiate the infection,[2] being thus the CD4+ T lymphocytes and monocytes/macrophage lineage the predominant target cells of the virus.[3] The immune system starts producing anti-HIV antibodies (seroconversion stage) and the number of CD4+ lymphocytes in blood recovers the normal value (ranging from 500 to 1,200 cells μL^{-1}) due to proliferation of cells in lymph nodes. In the next stage (clinical latency) the count of CD4+ lymphocytes is progressively depleted by factors that include the direct effects of HIV on infected cells. The duration of this clinical latency stage varies considerably from person to person, from 2 to over 10 years. Progression to Acquired Immune Deficiency Syndrome (AIDS) occurs as a result of chronic depletion of CD4 cells falling below 200 cells μL^{-1}, at a functional level where opportunistic infections and malignancies cannot be controlled.[4] The CD4+ T lymphocyte count is one of the most important clinical biomarkers of HIV disease progression, especially during the clinical latency. The count is useful for assessing

the degree of immune deterioration and speed of progression towards AIDS, as well as for monitoring the efficacy of a treatment. This parameter is also used to decide the timing for starting the antiretroviral treatment (ART) and the prophylaxis against opportunistic infections. The gold standard method for CD4 count is the flow cytometry, performed in expensive instruments which are rather impractical and difficult to sustain in low-resource settings in the developing world. For instance, in Malawi in mid-2010, from a total of 396 ART delivery sites, as low as 1 in 10 sites had a functioning CD4 cytometer.[5] Moreover, in low-income countries, a health worker in a primary care centers who wish to perform a CD4 test faces not only the drawbacks in blood specimen transportation to a centralized laboratory, but also in returning back the CD4 result to the patient. Moreover, it was reported that nearly half of HIV-infected patients in South Africa, failed to have CD4 counts after HIV diagnosis,[6] highlighting the urgent need to develop new alternatives of CD4 count at point of care. Additional issues are the damage of blood specimens during transportation to the CD4 count central laboratory, machine malfunctions due to poor maintenance, and lack of reagents and funding limitations. The core of the problem is that current CD4 counting technology is too sophisticated and inappropriate in the context in which it is being used.

Currently, there are only few cheaper alternatives for CD4 counting commercially available,[7,8] for instance, PointCareNOW™ (PointCare Technologies, Inc., USA), CyFlows miniPOC (Sysmex Partec GmbH, Germany), Guava EasyCD4 (Merck Millipore, USA) and Alere Pima™ CD4 (Alere, USA). Their main features are summarized in §3.7.8. Although the accuracy and simplicity of most of these technologies are not under discussion, they required still costly equipment being thus not so suitable for resource-constrained small centers. On the other hand, the manual methods Coulter CD4 count kit (Beckman Coulter, Inc., USA) and Dynabeads® T4 Quant Kit (Thermo Fisher Scientific, Inc., USA) are limited to the number of samples analyzed per day, being inappropriate when a high sample throughput is an important requirement.

Since the introduction of the Enzyme-linked immunosorbent assays (ELISA) in 1971, [9,10] this methodology is widely used in clinical diagnosis in small centers due to its high sensitivity, specificity and accuracy. This methodology is recommended by the World Health Organization (WHO) for the detection of several infectious diseases affecting global heath in the developing world, including Influenza,[11] HIV,[12] Chagas,[13] Ebola,[14] among many others since it is a sensitive method but by using instrumentation available in low-resource settings laboratories and requiring low-maintenance, as is the case of a microplate reader operated by filters. Another important advantage of ELISA includes the high-throughput. As it is performed in 96-

wells microplaques, a technician can analyze over 230 samples per day. Moreover, the application to novel targets is not an issue since the instrumentation is widely available in small centers.

Novel development in clinical diagnosis that is also needed involves preconcentration procedures on solid supports which can be easily integrated with point-of-care devices. Biomarkers in complex clinical samples can be thus preconcentrated while the interfering matrix is removed at the same time, increasing the sensitivity and the specificity of the test. One of the most prominent materials to meet this challenge is magnetic particles (MPs).[15] MPs can be tailored to specifically bind the biomarkers and concentrate them from the complex specimen under magnetic actuation, avoiding interference before testing.[16] They are synthesized containing a magnetic element in their core such as iron, nickel, neodymium or magnetite. Nowadays several companies offer a wide range of products based on MPs, such as Adembeads, Dynabeads, BioMag, SiMAG, MACS, among many others. Recent advances have focused on their use in magneto-actuated rapid diagnostic tests (RDTs).[17] The integration of MPs can thus simplify the analytical procedure, avoiding the use of classical centrifugation or chromatography separation strategies, since no pre-enrichment, purification or pretreatment steps, which are normally used in standard analytical methods, are required. Moreover, their use as solid support in bioassays has been shown to greatly improve the performance of the biological reactions. In this paper, a high-throughput and sensitive magneto-actuated ELISA for CD4+ T cell quantification is presented for their implementation in decentralized small care centers as an alternative to the costly standard flow cytometry. In this approach, magnetic particles were integrated in a classical ELISA format. The integration of the magnetic particles allowed the preconcentration of CD4 cells from whole blood, without any pretreatment, by immunomagnetic separation. The captured CD4+ T cells were at the same time labeled with a biotinylated antiCD4 antibody, followed by the reaction with an enzyme for the optical readout using a standard microplate reader operated by filters. The CD4 magneto ELISA demonstrated to be a powerful tool for the screening of a large number of specimens at the community and primary care level, especially in the developing world, as well as in low-resource settings in the developed world.

3.3 Experimental section

3.3.1 Instrumentation

Optical measurements were performed on a TECAN Sunrise microplate reader with Magellan v4.0 software. The data were analyzed using the Graph Prism software (GraphPad Software, San Diego, CA). Polystyrene microtiter plates were purchased from Nunc (Maxisorb, Roskilde, DK). Cell count was obtained by counting in Neubauer chamber using Nikon Eclipse TS100 microscopy (Nikon Instrument, USA) and by flow cytometry using perfect count microspheres (Prod. No. CYT-PCM-100, from Cytognos SL, Spain) and analyzed in a FACSCanto cytometer (BD Bioscience, USA). The immunomagnetic separation was evaluated using Telaval 31 optical microscopy (Zeiss, Alemania). The SEM images were taken with the scanning electron microscope Zeiss Merlin (Resolution: 0.8 nm at 15 kV with EDS Detector Oxford LINCA X Max). E5000 Sputter Coater Polaron Equipment Limited metallizer and K850 Critical Point Drier Emitech (Ashford, UK) were used for sample treatment. The confocal fluorescence images were taken with the TCP-SP5 Leica Microscope, being the images processed with the Imaris X64 v.6.2.0 software (Bitplane, Switzerland).

3.3.2 Chemicals and Biochemicals

Magnetic particles modified with antiCD3 antibody (antiCD3-MPs) (Dynabeads® CD3 Prod. No. 111-51D) were purchased from Dynal Biotech ASA (Norway). Biotinylated antiCD4 antibody (antiCD4-biotin, Prod. No. 347321), antiCD4-FITC (Prod. No. 340422), antiCD3-Alexafluor 488 (Prod. No. 557694) and antiCD3-PerCP (Prod. No. 552851) were provided by BD Bioscience and the streptavidin–horseradish peroxidase conjugate (HRP 1.11.1.7) came from Roche Diagnostics. The streptavidin labeled with cyanine 5 (Strep-Cy5) dye used in confocal microscopy was purchased from Life Technologies (Prod No. SA-1011). ELISA Substrate kit (Prod. No. 34021) was purchased from Thermo Scientific.

The CD4+ T cell clone PB100.29 was obtained by cloning the infiltrating lymphocytes from a pancreatic donor organ. The expansion method is described in *§3.7.2*.[18]

All buffer solutions were prepared with milliQ water and all other reagents were in analytical reagent grade (supplied from Sigma and Merck). The composition of these solutions is described in *§3.7.1*.

3.3.3 SEM study of the immunomagnetic separation of CD4 cells

For the immunomagnetic separation (IMS), 1000 cells μL^{-1} were incubated with 8×10^6 beads mL^{-1} antiCD3-MPs at a 1:8 ratio for 30 min at 4 °C with shaking. A washing step with PBS 0.1% BSA was then performed. Samples were then filtered with a Nucleopore filter (0.2 μm) and fixed, as described in *§3.7.3*. CD4+ T lymphocytes attached to the antiCD3-MPs were examined by scanning electron microscope (SEM) operated at 15kV and by energy dispersive X-ray spectroscopy detector (EDS) for elemental analysis.

3.3.4 Evaluation of the CD4 cells/antiCD3-MPs optimal ratio by flow cytometry and optical microscopy

The optimal ratio of the CD4 cells/antiCD3-MPs in terms of binding efficiency was evaluated by flow cytometry and optical microscopy. Flow cytometry was performed with a solution of 1000 cells μL^{-1} captured with 2×10^6, 4×10^6 and 8×10^6 antiCD3-MPs mL^{-1} corresponding to CD4 cells/antiCD3-MPs ratios of 1:2, 1:4, 1:8, respectively. Cells were stained with propidium iodide during 10 min to assess cell viability. Besides measurement of fluorescence by excitation with the laser, cells itself scatters light at all angles, forward scatter (FSC) is roughly proportional to the cell size while the side scatter (SSC) is caused by cellular granularity and structural complexity. Cytometric analysis was performed by gating cells in size and complexity dot-plot (FSC vs. SSC). Additionally, CD4+ T lymphocytes were identified by double-color flow cytometry analysis using antiCD4-FITC and antiCD3-PerCP.

In order to quantify the percentage of CD4 cells captured, a standard tube containing 1000 cells μL^{-1} was also analyzed. The non-captured cells percentage was calculated as the number of free cells in each sample after IMS. Therefore, the binding efficiency was calculated as

100-[(non captured cells x 100)/total cells].

In order to study the binding pattern, optical microscopy was also performed at CD4 cells/antiCD3-MPs ratios of 1:40, 1:8, 1:4, 1:2.

3.3.5 Evaluation of the CD3 and CD4 expression by confocal microscopy

The confocal microscopy of the CD4+ cells by labeling the CD3 and CD4 receptor was performed as follows: a solution of 1000 cells μL^{-1} was incubated with Hoechst (45 $\mu g\ mL^{-1}$) for

15 min at room temperature (RT) in darkness, to stain DNA in living cells nuclei. The cells were labeled with the biotinylated antiCD4 antibody (36 ng mL^{-1}) and 3 μL antiCD3 AlexaFluor-488, respectively, in one step incubation. Washing steps with PBS 0.1% BSA were performed. Finally, cells were stained with Streptavidin-Cy5 fluorescent dye (2 μg mL^{-1}) for 30 min at RT.

3.3.6 CD4 magneto ELISA

The CD4 magneto ELISA (Figure 3.1) was performed in 96-well microtiter plates and involved the following steps: (A) Immunomagnetic separation of CD4+ T cells and labeling. In this step, antiCD3-MPs (8×10^5 MP per well) and the biotinylated antiCD4 antibody (36 ng mL^{-1}) were simultaneously incubated with 100 μL of sample for 30 min with shaking at 4 °C, followed by three washing steps with PBS 0.1% BSA. (B) Incubation with the optical reporter streptavidin-HRP (2 μg mL^{-1}) for 30 min while shaking at RT, followed by three washing steps with PBS 0.1% BSA as above. (C) Optical readout with 100 μL of substrate solution (0.004 % v/v H_2O_2 and 0.01 % w/v TMB in citrate buffer) incubated for 30 min at RT under dark conditions. The enzymatic reaction was stopped by adding 100 μL of H_2SO_4 (2 mol L^{-1}). The absorbance measurement of the supernatants was thus performed with the microplate reader using a 450 nm filter. After each incubation or washing step, a 96-well magnet plate separator was positioned under the microtiter plate until pellet formation on the bottom corner, followed by supernatant separation.

The calibration curve was achieved by spiking CD4+ lymphocytes (from 0 to 1200 cells μL^{-1} quantified by Neubauer Chamber Cell Counting) to an optimized leukocyte-depleted whole blood matrix, performed by Ficoll-Paque/IMS with Dynabeads® CD3, as detailed in *§3.7.5*. Serial concentrations of CD4 cells were chosen including the range of clinical interest for CD4+ lymphocytes in HIV diagnosis.

Two-dimensional (2D) serial dilution experiments were performed to select the optimal concentration for biotinylated antiCD4 antibody and streptavidin-HRP conjugate. Experimental parameters such as antiCD3-MPs concentration, blocking steps, incubation steps and sample pretreatment were also optimized. Experimental details for these procedures are extensively described in *§3.7.6*.

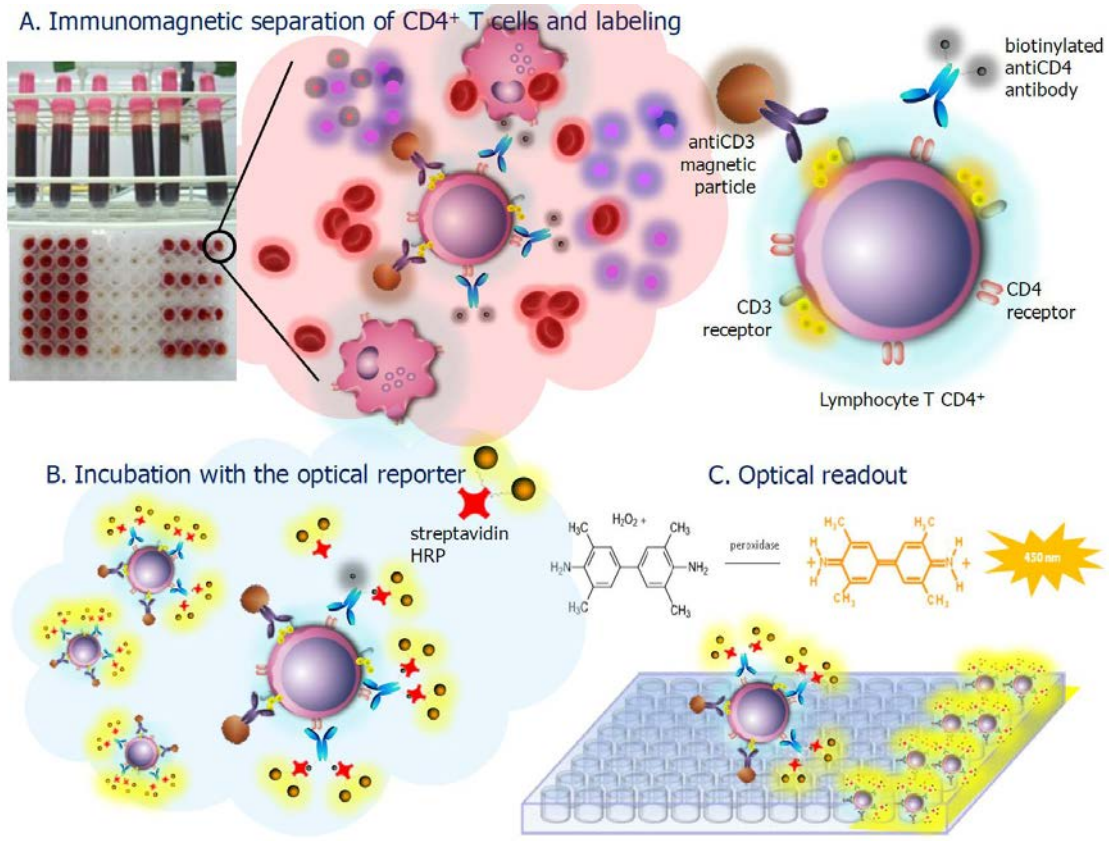

Figure 3.1. Schematic representation of the CD4 magneto ELISA. (A) The CD4+ T lymphocytes were captured from whole blood by the antiCD3-MPs and labeled in one step with antiCD4-biotin. (B) The incubation with the optical reporter streptavidin-HRP was then performed. (C) Finally, the optical readout was achieved with H_2O_2 and TMB. The enzymatic reaction was stopped by adding H_2SO_4 and the supernatant was measured at 450 nm.

3.3.7 Whole blood matrix effect study

CD4 count by standard method involves the incubation of anti-coagulated whole blood with monoclonal antibodies to various cellular antigens (CD3, CD4, and CD19) and then the lysis of blood to remove red blood cells. In order to verify if the CD4 magneto ELISA can be directly performed in whole blood without any sample pretreatment, the matrix effect was evaluated with the CD4 magneto ELISA by spiking CD4 cells (250, 500 and 1000 cells μL^{-1}) in a) leukocyte depleted whole blood (in the presence of red cells) and b) leukocyte depleted lysed blood, which is the sample treatment performed in flow cytometry. The experimental details of this procedure are shown in *§3.7.4*.

3.3.8 Recovery study

In order to evaluate the recovery of CD4 cells in whole blood a complete lymphocyte depleted whole blood matrix should be firstly achieved.

Prior to the recovery study, three different methods for the complete lymphocyte depletion from whole blood were tested with the CD4 magneto ELISA, namely a) Ficoll-Paque depletion; b) IMS with Dynabeads® CD3; and finally, c) a combination of both (Ficoll-Paque/IMS), as detailed in *§3.7.5*.

For the recovery study of the CD4 cells in whole blood, a standard curve was performed with different CD4+ T lymphocyte concentrations ranging from 0 to 1000 cells μl^{-1}. The samples were prepared by spiking a known number of CD4 cells in the optimized leukocyte-depleted whole blood matrix (Ficoll-Paque/IMS) and processed in triplicates. The recovery was calculated by spiking low (250 cells μL^{-1}), medium (400 cells μL^{-1}), and high (750 cells μL^{-1}) concentration levels of CD4 cells in blood, covering all the whole clinical interest range.

The recovery was calculated as

$$\% R = 100. (P1 / P0)$$

being P0 the real number of cells spiked to the sample and P1 the number of cells obtained by interpolating the signal in the standard curve.

3.3.9 Safety considerations

All the procedures involved the manipulation of human cells were handled using Biosafety Level 2 Laboratory and containment. All works were performed in a Biosafety cabinet, and all material decontaminated by autoclaving or disinfected before discarding in accordance with U.S. Department of Health and Human Services guidelines for level 2 laboratory Biosafety.[19]

3.4 Results and discussion

3.4.1 SEM study of the immunomagnetic separation of CD4 cells

Scanning electron microscopy was performed for the evaluation of the immunomagnetic separation. The CD4+ T cells were attached to the antiCD3-MPs in a 1:8 ratio throughout the immunological interaction with the CD3 receptors present in the cellular membrane. Figure 3.2

illustrates the microscopic characterization by SEM of CD4+ T lymphocytes bound to magnetic particles with a resolution of 1 and 2 μm. The images show T lymphocytes (7-15 μm of diameter) attached to 1, 2, 3 and 4 spherical magnetic particles (4.5 μm of diameter) (panels A to D, respectively). In most cases the binding was achieved with more than one specific binding site on the lymphocyte cellular surface to the magnetic particle, being the T lymphocytes surrounded by magnetic particles (panel D). Single-point attachment of cells to the magnetic particle was also observed (panel A). Finally, some aggregates were also observed due to multivalency of both antiCD3-MPs and CD4 cells (panels E and F). The X-ray spectrum is also shown, being the elemental analysis compatible with the MP (C, O and Fe in Panel G) and with the cells (Ca, C, N and O in Panel H), signaled by arrows.

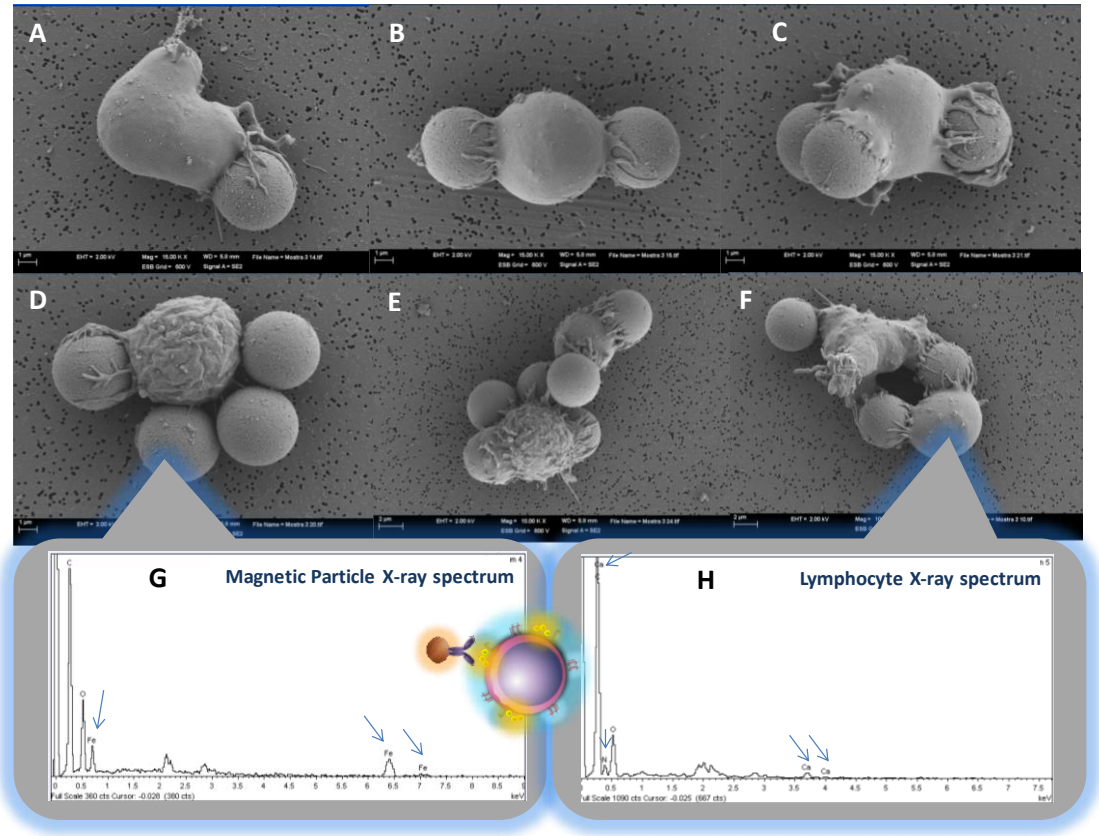

Figure 3.2. Evaluation of the CD4+ T lymphocytes immobilized on antiCD3 magnetic particles by SEM. The images show, at different resolution levels, the different patterns of lymphocyte binding to the magnetic particles, as well as the X-ray pattern. In all cases, identical acceleration voltage (15 KV) was used.

3.4.2 Evaluation of the CD4 cells/antiCD3-MPs optimal ratio by flow cytometry and optical microscopy

The binding efficiency of the immunomagnetic separation step under different ratios of CD4 cells/antiCD3-MPs was firstly studied by flow cytometry. This technique provides information about the relative size and granularity. Both FSC and SSC are representative parameters for every entity, and a combination of the two are used to differentiate cell types/entities in a heterogeneous sample. The Figure 3.3 shows a FSC-SSC dot plot where each entity in the sample is identified (gates P1, P2 and P3 as depicted in Figure 3.3). For instance, the antiCD3-MPs (gate P2) appear in the left corner because they are the entities in the sample with the smallest size.

The quantification was performed for CD4 cells/antiCD3-MPs ratios of 1:8, 1:4 and 1:2. The IMS was evaluated in terms of the binding efficiency, obtaining values of 96%, 91% and 75% respectively. Clearly, as the higher is the ratio of MPs, the higher the binding efficiency. In order to achieve a good performance for the IMS step (96 %), the CD4 cells/antiCD3-MPs ratio for further studies was optimized in 1:8. It is important to highlight that this amount is eight times higher than manufacturer recommendations.

For further studies, the amount of antiCD3-MPs was selected as 8 x 10^5 MP to keep the 1:8 in healthy donors (1x10^5 in 100 μL of whole blood), in order to ensure the efficient capturing of cells and to span the detection range for CD4 count not only to the AIDS medical interest range, but also to the whole clinical range.

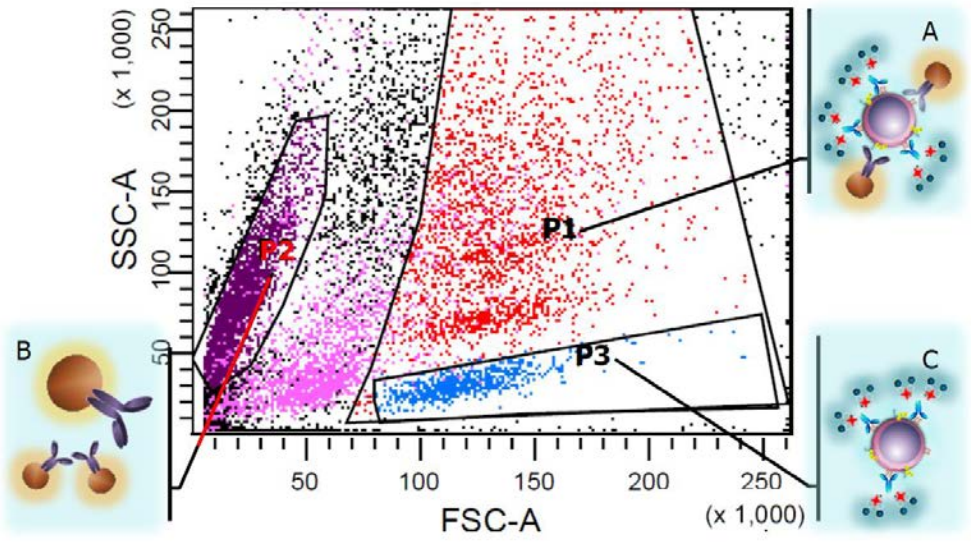

Figure 3.3. Representative dot plot graph in separated gates showing (A) the CD4 cells/antiCD3-MPs complexes (gate P1), (B) the antiCD3-MPs (gate P2) and, finally, (C) CD4 lymphocytes (gate P3).

In order to study the binding patterns under different CD4 cells/antiCD3-MPs ratios, (1:40, 1:8, 1:4 and 1:2), light microscopy was also performed. Figure 3.4 (panels A to D) shows the images corresponding to CD4 cells/antiCD3-MPs ratios of 1:40, 1:8, 1:4 and 1:2, respectively.

As shown in the Figure 3.4, high concentration of antiCD3-MPs favors the immunomagnetic capturing. On the contrary, the use of low antiCD3-MPs ratios results in a poor capture of lymphocytes. In some instances, the cells are not captured by the antiCD3-MPs when the ratio is near 1:1, as recommended by the manufacturer. Moreover, Figure 3.4 (E panels) shows the cells completely surrounded by the MPs when the amount of antiCD3-MPs is at the optimized binding ratio (1:8) in accordance with the results obtained by flow cytometry.

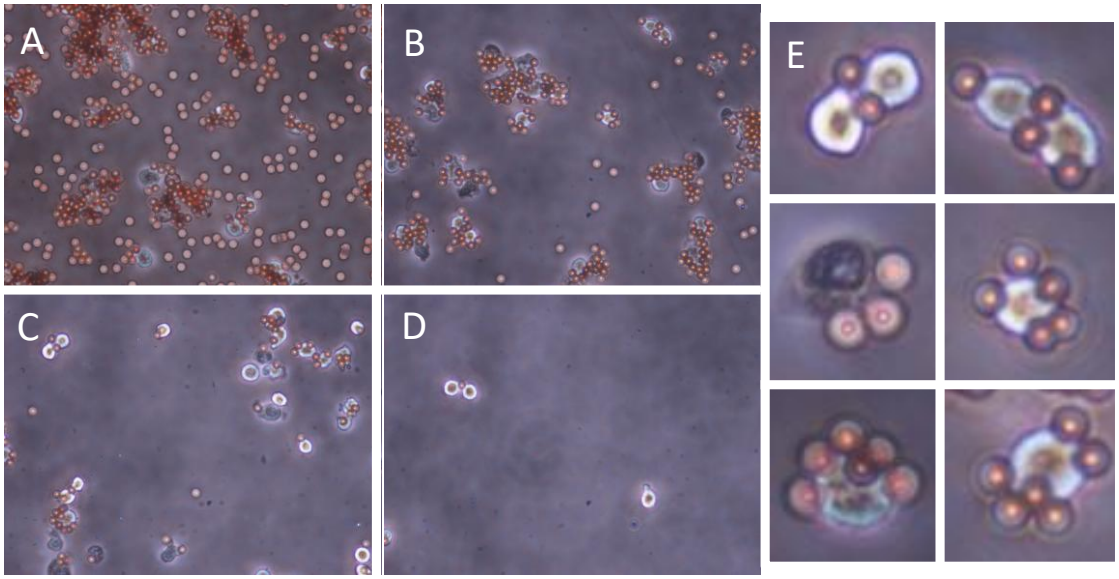

Figure 3.4. Optical microscopy of CD4 cells captured by antiCD3-MPs at A) 1:40; B) 1:8; C) 1:4; and D) 1:2 ratios. The resolution of the images was 40X in all cases. The E panels show details of the binding pattern at the optimum ratio (1:8).

3.4.3 Evaluation of the CD3 and CD4 expression by confocal microscopy

As the optical readout in the CD4 magneto ELISA is based on the immunological interaction with both the CD3 and the CD4 receptor, the study of the expression of these receptors on the CD4 cells by confocal microscopy was performed. The confocal microscopy was also used to characterize the distribution of the CD4 and CD3 receptors on the lymphocyte surface and their capability of being recognized by the antiCD3 and CD4 antibodies. The Figure 3.5, panel A shows the binding pattern of the CD4 cells (nucleus in blue) with the biotinylated antiCD4

antibody (red dots) while panel B shows the CD3 receptors after the interaction with antiCD3-PerCP antibody (in green). Both the CD3 and the CD4 receptors are distributed randomly on the cell surface (Figure 3.5, Panel C). The high expression of these receptors as well as the recognition with the specific antibodies ensures the good immunocapturing efficiency due to the CD3 molecule as well as a high sensitivity and a low limit of detection (LOD) due to the CD4 coreceptor.

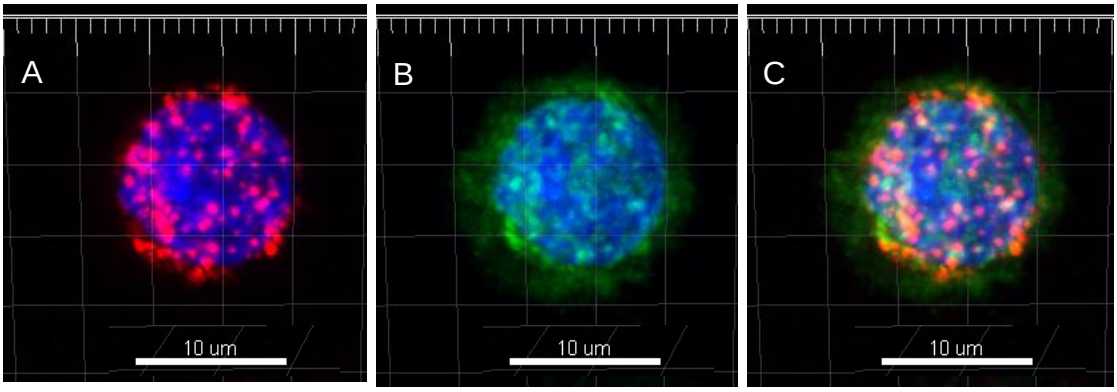

Figure 3.5. Confocal microscopy images of the CD4 T lymphocyte (1000 cells μL^{-1}) labeled with biotinylated antiCD4 antibody/streptavidin-Cy5 system (36 ng mL^{-1} and 2 μg mL^{-1}) (A) and antiCD3-AlexaFluor 488 (3 μL) (B). The nuclei were stained with the dye Hoechst in blue. Merged images (C) show the coincidence of the expression pattern of both molecules.

3.4.4 Whole blood matrix effect study

Many components in biological matrices influence the result of an analysis, affecting assay sensitivity and reproducibility.[20]

Although immunoassays are generally unaffected by sample haemolysis and icterus,[21] particulate matter including red blood cells can clearly affect the optical readout in an ELISA. In order to verify if the CD4 magneto ELISA can be directly performed in whole blood without any sample pretreatment, the matrix effect was evaluated by spiking CD4 cells (0, 250, 500 and 1000 cells μL^{-1}) in a) in leukocyte depleted whole blood by Ficoll-Paque/IMS depletion (in the presence of red cells) and b) leukocyte depleted lysed blood, which is the matrix treatment used in flow cytometry, since red blood cells interfere in this assay. As shown in Figure 3.6, no significant differences in all the concentration range were observed despite the matrix tested. In CD4 count by the gold standard flow cytometry, the incubation with the monoclonal antibodies was performed in anti-coagulated whole blood followed by the lysis of erythrocytes, which interfere in the analysis.[22] However, the CD4 magneto ELISA is not

affected by the presence of red blood cells, being a clear advantage in terms of the simplification of the analytical procedure by avoiding sample pretreatment. Moreover, the lysis procedure may result in cell loss and variability in the results.[23,24] This fact can be related with the integration of magnetic particles to the ELISA, which specifically bind the CD4 cells eliminating the interfering components which can affect the optical readout, including the red blood cells.

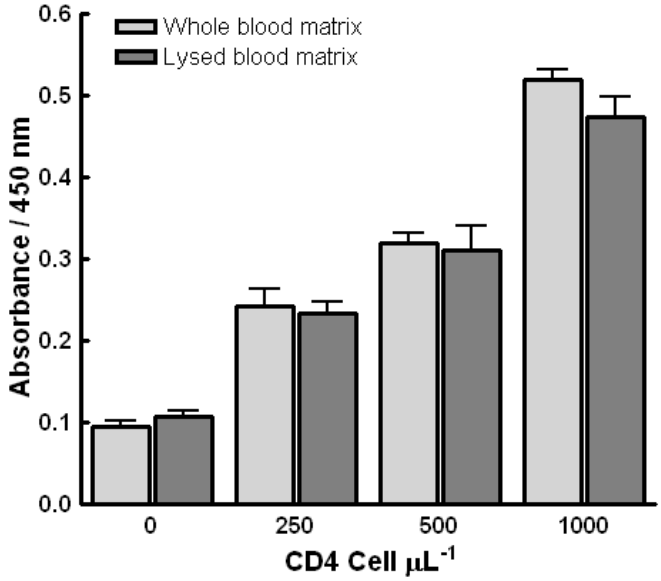

Figure 3.6. Evaluation of matrix effect in leukocyte depleted whole blood i) as it is (light grey bars) and ii) pretreated by lysis of the red blood cells the (dark grey line). Concentration of the reagents used was antiCD3-MPS 8 x 10^6 MPs mL^{-1}, biotinylated antiCD4 antibody 36 ng mL^{-1}, streptavidin-HRP 2 μg mL^{-1}. n=3.

3.4.5 CD4 magneto ELISA

The CD4 magneto ELISA in whole blood was optimized by changing the amount of biotinylated antiCD4 antibody and streptavidin-HRP conjugate, as shown in Figure S3.3 and S3.4 *(§3.7.6.1* and *§3.7.6.2*). Moreover, five different strategies were also performed for the incubation steps: (a) Immunomagnetic separation of CD4+ T cells by the antiCD3-MPs; (b) labeling with the biotinylated antiCD4 antibody, (c) Incubation with the optical reporter streptavidin-HRP) by changing the order or simplifying two incubations steps into one, and including preincubations to achieve analytical simplification, as schematically shown in Figure S3.5 (*§3.7.6.3*). The results are shown in Figure S3.6 and summarized in Table S3.2 (*§3.7.6.3*). Although all the strategies were able to clearly detect CD4 cells, improved analytical performance was achieved by one-step incubation with antiCD3-MPs and biotinylated antiCD4 reagents, followed by incubation with the optical reporter (streptavidin-HRP). The binding of

the biotinylated antiCD4 antibody seems to be hindered by the antiCD3-MP, competing both reagents for the binding their respective molecules. The fact of incubating antiCD3-MPs with the biotinylated antiCD4 antibody in one step allows both reagents to have the same opportunity for binding their receptors. A full discussion of the different procedures is presented in *§3.7.6.3*.

The optical response of the CD4 magneto ELISA towards the CD4 cells (from 0 to 1200 cells μL^{-1}) in whole blood is shown in Figure 3.7, panel A. Different amounts of CD4+ lymphocytes (quantified by flow cytometry) were spiked to the optimized leukocyte-depleted whole blood matrix, performed by Ficoll-Paque/IMS with Dynabeads® CD3, as detailed in *§3.7.5*. The CD4 cell range was chosen to include the concentration of clinical interest for CD4+ lymphocytes in HIV diagnosis.

The CD4 magneto ELISA was fitted (R^2=0.9752) using a nonlinear regression (Four Parameter logistic Equation– GraphPad Prism Software), as shown in Figure 3.7, panel B.

As the curve was performed in the optimized leukocyte-depleted whole blood matrix, the LOD was estimated by processing the negative control samples (n=8) in this matrix, containing all the components of whole blood except for the leukocytes obtaining a mean value of 0.107 AU with a SD of 0.042. The cut-off values were then determined with a one-tailed t test at a 95% confidence level, giving a value of 0.186 AU (shown in Figure 3.7, as the dotted lines). The LOD was found to be 50 CD4 cells μL^{-1}, being the logistic range from 63 to 979 CD4 cells μL^{-1}, including the whole range of clinical interest of CD4+ lymphocytes in HIV diagnosis.

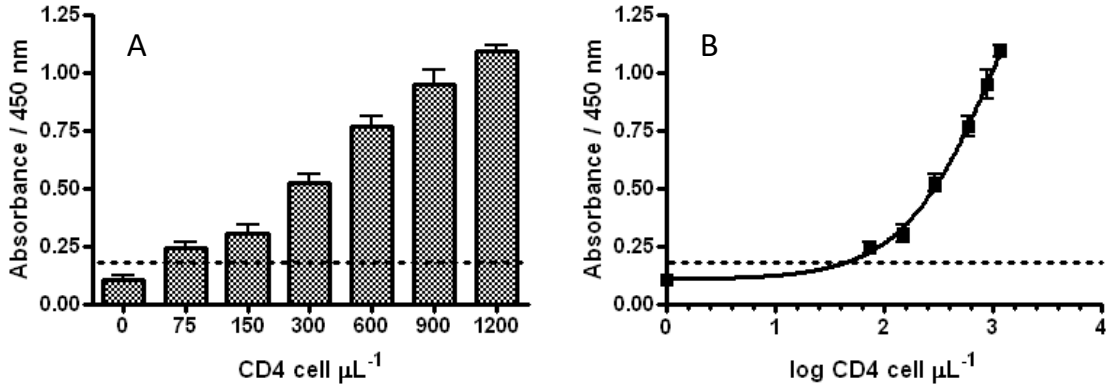

Figure 3.7. CD4 magneto ELISA for CD4 cells at a concentration covering the whole range of clinical interest (from 0 to 1200 CD4 cells μL^{-1}). The negative control in leukocyte-depleted whole blood is also shown (n=8). Other conditions as in Figure 3.6.

This value is suitable for application in CD4 determination in small care centers, since the clinically important range does not include CD4 counts smaller than 50 cells μL^{-1}.[25] For instance, a level of 500 cells μL^{-1} indicates that the CD4 cells monitoring has to be more frequent. The ART is initiated when CD4 count is 500, 350 or 200 cells μL^{-1}, depending on WHO´s disease stage. Moreover, a CD4 T lymphocyte count less than 200 cells μL^{-1} is recommended as a criterion of AIDS diagnosis for adults as well as for children. The CD4 count is also used in the diagnosis against opportunistic diseases. Candida infection or tuberculosis may become an issue when the CD4 lymphocyte level is 300 cells μL^{-1}. HIV-infected people, including pregnant women, should receive chemoprophylaxis against pneumonia with CD4+ count bellow 200 cells μL^{-1}. Toxoplasma-seropositive patients with CD4+ count bellow 100 cells μL^{-1} should be prophylactically treated against TE (toxoplasmic encephalitis).[26] These values are essentially the same for adults and for pediatric population. It is important to highlight the CD4 magneto ELISA provides no direct counting of the cells entities, since the CD4 quantification is obtained by extrapolation of the optical density to the number of CD4 T cells from a standard curve, being thus dependent on the expression of the CD4 receptor in the cells. However, it was extensively reported that the expression of the CD4 receptors in CD4+ T cells is comparable among individuals.[27,28] The double-marker strategy based on both CD3 (for the immunomagnetic separation) and CD4 receptors (for the labeling and the readout), as schematically shown in Figure 3.1, avoids overestimation due to interferences present in the sample such as soluble CD4 protein, as well as other cells sharing the CD4 receptor such as monocytes and macrophages. As the capture of the CD4 cells is performed using antiCD3-modified magnetic particles, soluble CD4 protein, monocytes and macrophages are not able to bind to the magnetic particles because of the absence of CD3 receptor. In that way, these interferences are removed after the first washing step. On the other hand, although cytotoxic T lymphocytes (CD8 T lymphocytes) express the CD3 receptor on their membrane and can be captured by the antiCD3-MPs, they lack of CD4 receptor, being thus not detected by the CD4 magneto ELISA procedure.

Currently, only few CD4+ T cell counting methods are commercially available, being their main features summarized in *§3.7.8*. The PointCareNOW™ (PointCare Technologies, Inc., USA), the Guava EasyCD4 (Merck Millipore, USA) and the CyFlows miniPOC (Sysmex Partec GmbH, Germany) are modified flow cytometers and measure absolute CD4+ T cell counts and the percentage of T cells expressing CD4+. Alere Pima™ CD4, (Alere, USA) is based on a dual-fluorescence image analysis to count CD3+/CD4+ cells.[29] These methods rely mostly on fluorescent labeling. Although the accuracy and simplicity (in terms of automation) of most of

these technologies are not under discussion, they required special equipment ranging from 6500 to 25000 $. Manual counting method such as Coulter CD4 count kit (Beckman Coulter, Inc., USA) and Dynabeads® T4 Quant Kit (Thermo Fisher Scientific, Inc., USA) are based on the use of beads for lymphocyte labeling and counting under light microscope.[30] Although rapid, they are also laborious and have a limited throughput (10 samples per day) in order to minimize reader error, technician fatigue and eyestrain.[31] Daktari is a direct cell counting using changes in impedance. The system uses a sensor that counts the captured CD4 cells by measuring their internal contents electrically. However, Daktari CD4 is still undergoing performance evaluation. Surprisingly, there are not commercially available ELISAs for CD4 counts.

The main features of other reports for CD4+ T cell counting are summarized in §3.7.9. In several reports, mostly based on counting by microscopy, the detection is limited to low[32] or high[33,34] levels of CD4 cells, being useful only for a specific stage of the disease. It is important to highlight that the CD4 magneto ELISA presented here showed a LOD of 50 cells μL^{-1} and a logistic range from 63 to 979 CD4 cells μL^{-1}, including the whole range of clinical interest of CD4+ lymphocytes in HIV diagnosis. Therefore, this method can be used for the diagnosis of HIV and monitoring of AIDS in any stage. Although an immunoassay for enumeration of CD4+ and CD8+ peripheral T lymphocytes was previously reported, the LOD was 230 cells μL^{-1}, being non useful for AIDS diagnosis and monitoring (CD4 count falling below 200 cells μL^{-1}) due to lack of sensitivity.[30] Our research group has recently reported an electrochemical magneto-actuated biosensor for CD4 quantification at point-of-care in low resource settings.[17] Despite the outstanding analytical performance (LOD of 44 cells μL^{-1}), this approach was designed for the detection of a single sample at point of care, being not suitable for the quantification of a large number of samples simultaneously. However, the high-throughput and sensitive magneto-actuated ELISA reported here represent a good alternative to the costly standard flow cytometry for the simultaneous detection of several samples in decentralized small health centers. The integration of magnetic particles in the magneto ELISA is the core of the strategy reported here, allowing a simple preconcentration of the sample by applying a magnet. In this way, the interfering compounds including red blood cells are eliminated at the same time the CD4 cells are concentrated, avoiding long tedious washing steps that are inherent of conventional ELISA methodology. A remarkable point to highlight is that although the CD4 magneto ELISA is not fully automated as most of the reported technologies in *§3.7.8*, it does not require special equipment since the readout can be performed with a widely available microplate reader operated by filters, being thus a good alternative, especially in resource-

constrained settings. Moreover, as ELISA is widely used in clinical laboratories, no special technician training is required. Despite the magneto ELISA is not an automatic technique, novel methods based on ELISA-technique, such as digital and microarray-based ELISA, are being developed due to their great features of reduction in background, amplification of signal, accuracy, precision and high sample throughput.[35]

3.4.6 Recovery study

First of all, the backcalculation of standards was performed, for assessing the quality of the curve fit by calculating the concentrations of the standards after the regression has been completed.[36,37] This procedure was performed by calculating the concentration of each standard and then comparing it to the actual concentration. Table S3.3 (*§3.7.7*) shows the values for the backcalculation of standards, yielding consistent values ranging from 86 % to 110 %. These values provide information about the relative error in the calculation of samples, due to the quality of the fit. In order to evaluate the recovery of CD4 cells spiked in whole blood, a lymphocyte depleted whole blood matrix was firstly performed, by combining Ficoll-Paque depletion and IMS with Dynabeads® CD3, achieving a whole blood matrix almost clean from lymphocytes (quantified by flow cytometry in 1 cells μL^{-1}). A detailed discussion of the procedure can be found in *§3.7.5*. Spiked recovery was also performed to assess the overall accuracy of the CD4 magneto immunoassay.[38] This method incorporates variables in assay preparation as well as the regression analysis.

In this case, the recovery was performed by spiking of low (257 cells μL^{-1}), medium (408 cells μL^{-1}), and high (744 cells μL^{-1}) concentration of CD4 cells (quantified by flow cytometry) to the optimized lymphocyte depleted whole blood matrix. Table 3.1 shows the spiked recovery values obtained for the three CD4 cell concentrations, ranging from 84 to 123%.

Table 3.1. Recovery study for the CD4 magneto ELISA.

Real concentration (cell μL^{-1})	Recovered concentration (cell μL^{-1}) / (SD)	% Recovery
744	627 / (52)	84
408	504 / (45)	123
257	245 / (12)	95

3.5 Conclusions

AIDS affects the life of millions of people around the world. Although screening tests for the diagnosis of HIV infection are commercially available, simple and affordable tests for CD4 counts are urgently required in low resource settings. Unfortunately, the areas mostly affected by the HIV epidemic are resource-limited countries, wherein the CD4 counting by flow cytometry is not available due to laboratory requirements and cost of the assay. Moreover, it would be very useful to have this technology at small health centers for getting the CD4 result back in a short period of time, to follow-up and prescribe the correct ART treatment without delay, avoiding high turnaround time. Currently, there are only few cheaper alternatives to the flow cytometer and they are mostly based on fluorescent labeling, requiring thus costly imaging equipment to achieve detection or, instead, on manual counting with light microscopes.

The suitability of the magneto ELISA reported here is based on its low-limit detection (50 CD4 cells μL^{-1}), covering the medical interest range from 63 to 979 CD4 cells μL^{-1}.

The integration of magnetic particles provides improved analytical features regarding sensitivity and selectivity of the assay, and reducing the matrix effect. The CD4 magneto ELISA is not affected by the presence of red blood cells, being a clear advantage in terms of the simplification of the analytical procedure in avoiding the sample pretreatment or the lysis of blood to remove red blood cells. Despite other reporter methods, the magneto ELISA was highly specific for CD4+ lymphocytes because of the use of two membrane biomarkers, CD4 and CD3 receptors. In this way, the monocytes (which have CD4 but lack CD3 receptor) are excluded of the count, avoiding overestimations.

To solve the urgent need for improving CD4 counting methods, the high-throughput and sensitive magneto-actuated ELISA reported here represent a good alternative to the costly standard flow cytometry for the simultaneous detection of several samples in decentralized small-care centers by using common microplate reader operated by filters. Since ELISA is a technique widely used in clinical laboratories, personnel training or special equipment are not required. Due to the promising results, further work will be focused on the clinical validation of the CD4 magneto ELISA.

3.6 Acknowledgements

Financial support from EC-Marie Curie actions and BioMaX (project number 264637), Ministerio de Economía y Competitividad (MINECO), Madrid (BIO2013-41242-R) and from Generalitat de Catalunya (Projects 2014 SGR 837) are acknowledged.

3.7 Supplementary Material

3.7.1 Composition of buffers and solutions

All buffer solutions were prepared with milliQ water and all other reagents were in analytical reagent grade (supplied from Sigma and Merck). The composition of these solutions was: PBS buffer: 0.01 mol L^{-1} Na_2HPO_4, 0.15 mol L^{-1} NaCl, 2 mmol L^{-1} EDTA, pH 7.4; fixation buffer: 0.1 mol L^{-1} cacodylate, 1% glutaraldehyde solution, pH 7.4.

3.7.2 Cell line

The CD4+ T cell clone PB100.29 was supplied by the Immunology Cellular Laboratory (Institute of Biotechnology and Biomedicine, UAB, Catalonia), and the cells were obtained by cloning the infiltrating lymphocytes from a pancreatic donor organ. Rapid expansion method was adapted as follows: 40,000 T-cell population were cultured in T25 flask containing 25 mL of IMDM media supplemented with 2 mmol L^{-1} L-Glutamine and 100 U mL^{-1} penicillin and 100 μg mL^{-1} streptomycin (all from Sigma-Aldrich), 10% human serum and 50 ng mL^{-1} OKT3 antibody with 25×10^6 γ-irradiated peripheral blood mononuclear cells and 5×10^6 γ-irradiated EBV-transformed lymphoblastoid cell line. Interleukin-2 was added at 45 U mL^{-1} on day +1. Cells remained untouched during the first 5 days of culture, and then cells were split every 3-4 days.[18] The cells were stained with Trypan Blue, and the viable cell concentration was determined by enumeration in a Neubauer counting chamber or by flow cytometry using absolute count microspheres.

3.7.3 SEM study of the immunomagnetic separation of CD4+ cells by antiCD3-MPs

For scanning electron microscopy, a solution of 1,000 CD4 cells μL^{-1} was incubated with magnetic particles modified with the antiCD3 antibody (8×10^6 beads mL^{-1}) at a 1:8 ratio for 30 min at 4 °C with shaking. A wash step with PBS 0.1% BSA was then performed. Samples were filtered with a Nucleopore filter (0.2 μm) and fixed, with freshly prepared fixation buffer for 2 hours at 4 °C rinsed in cacodylate buffer, and postfixed in 1% osmium tetroxide in PBS buffer for 2 h at 4 °C. Dehydration was carried out in a series of ethanol solutions from 30 to 90% for 30 min each and finally in two changes of 100% ethanol for 30 min. After critical point drying

with CO_2 the samples were coated with a thin layer of gold. Captured CD4+ T lymphocytes were examined by scanning electron microscope operated at 15kV.

3.7.4 Whole blood matrix effect study

The matrix effect was evaluated with the CD4 magneto immunoassay by spiking CD4 cells (250, 500 and 1,000 cells μL^{-1}) in a) leukocyte depleted whole blood (in the presence of red cells) and b) leukocyte depleted lysed blood. The experimental details of this procedure are as follows:

Leukocyte depleted whole blood. Lymphocytes were centrifuged and resuspended in an exact volume of leukocyte-depleted blood matrix by Ficoll-Paque/IMS depletion to reach the concentration of 250, 500 and 1,000 cells per μL. Because of this matrix had all the components of the blood except the leukocytes, it is called "whole blood matrix". The complete procedure to get the leukocyte-depleted blood matrix is described in the next section.

Leukocyte depleted lysed blood. Lymphocytes were centrifuged and resuspended in an exact volume of leukocyte-depleted blood matrix to reach the concentration of 250, 500 and 1,000 cells per μL. After that, erythrocytes were depleted by incubating for 10 min with FACS™ lysing solution, follow of two washing steps with PBS.

3.7.5 Lymphocyte depletion of whole blood

In order to obtain a complete lymphocyte depleted whole blood matrix, three different methods for the total leukocyte depletion from whole blood were tested, namely A) Ficoll-Paque depletion; B) IMS with Dynabeads® CD3; and finally, C) a combination of both (Ficoll-Paque/IMS), as follows:

Ficoll-Paque depletion. Leukocyte depleted whole blood matrix was prepared using Ficoll-Paque™ density gradient. Blood was diluted 1:1 with PBS, and layered onto Ficoll-Paque solution maintaining a 3:1 constant ratio of diluted blood: Ficoll. The blood was centrifuged at 600 g for 25 min at room temperature. Differential migration during centrifugation results in the formation of layers containing different cell types (from the bottom to the top): Red blood cells (erythrocytes); granulocytes; Ficoll-Paque; peripheral blood mononuclear cells –PBMC- (lymphocytes, platelets and monocytes); and plasma. The lymphocytes and the Ficoll layer

were removed, and the plasma and erythrocytes phases were then mixed to generate the leukocyte-depleted whole blood matrix (as shown in Figure S3.1).

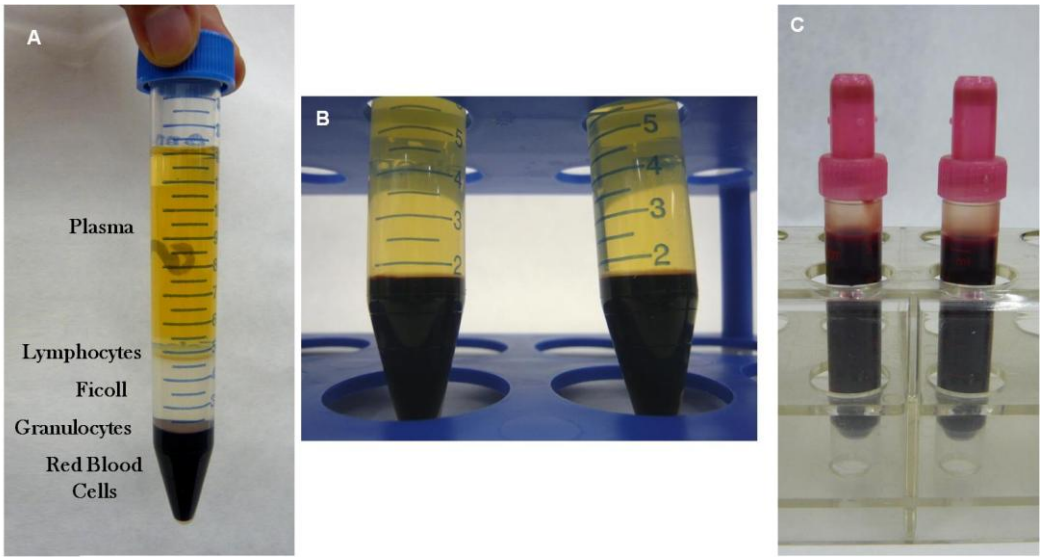

Figure S3.1. Leukocyte-depleted blood matrix by Ficoll-Paque™ depletion. The blood components were separated by density gradient centrifugation in Ficoll. After centrifugation, mononuclear cells remain at the plasma-Ficoll interface while granulocytes and erythrocytes in the sediment (A). Mononuclear cells and Ficoll layer were removed in order to obtain a free lymphocyte blood matrix (B).

IMS with Dynabeads® CD3 depletion. Dynabeads® CD3 are uniform, superparamagnetic beads (4.5 µm diameter) coated with a primary monoclonal antibody specific for the CD3 membrane antigen, mainly expressed on human mature T cells, for isolation or depletion cells from samples. Magnetic beads (4×10^8 beads mL^{-1}) were added to the sample under continuous mixing to favor the binding of the magnetic beads to the target cells. After 30 min of shaking at 4 °C, the sample was placed on a magnet. The supernatant was removed to a new tube and the bead-bound cells were eliminated.

Ficoll-Paque/IMS with Dynabeads® CD3. Leukocyte-depleted whole blood matrix was prepared by Ficoll-Paque method. After that, the remains lymphocytes present in the matrix were removed by the incubation with Dynabeads® CD3, as details above.

These three different strategies for the total depletion of lymphocyte from whole blood were tested with the CD4 magneto immunoassay, by evaluating nine replicates. The Figure S3.2 shows comparatively the optical readout obtained with the CD4 magneto immunoassay in the three leukocytes depleted whole blood matrixes: (A) Ficoll-Paque depletion; (B) IMS with Dynabeads® CD3; and finally, (C) a combination of both Ficoll-Paque/IMS with Dynabeads® CD3. According with the results, the combined method for leukocyte depletion (Ficoll-

Paque/IMS with Dynabeads® CD3) was found to be the best strategy to get a free-lymphocyte matrix. The CD4 count was also determined with the reference method by flow cytometry using microspheres for absolute counting. The absolute CD4 count for (A) Ficoll-Paque depletion; (B) IMS with Dynabeads® CD3; and finally, (C) a combination of both Ficoll-Paque/IMS, was found to be 295, 40 and 1 cells μL^{-1} respectively, in agreement with the results shown in Figure S3.2.

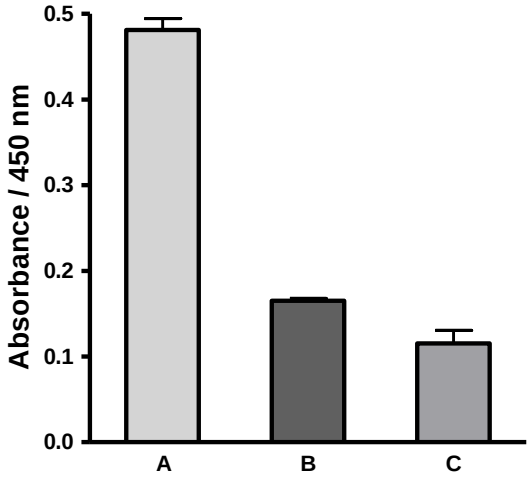

Figure S3.2. CD4 magneto immunoassay in leukocytes depleted whole blood matrixes (A) Ficoll-Paque depletion; (B) IMS with Dynabeads® CD3; and (C) a combination of both Ficoll-Paque/IMS with Dynabeads® CD3. antiCD3-MPS 8×10^6 MPs mL^{-1}, biotinylated antiCD4 antibody 36 ng mL^{-1}, Streptavidin-HRP 2 μg mL^{-1} n=9.

3.7.6 CD4 magneto ELISA. Optimization studies

The CD4 magneto immunoassay in whole blood was optimized by changing the amount of biotinylated antiCD4 antibody and streptavidin-HRP conjugate. Experimental parameters such as magnetic particle concentration, blocking steps, incubation steps and sample pretreatment were also optimized.

3.7.6.1 Biotinylated antiCD4 antibody

The effect of the concentration of the biotinylated antiCD4 antibody was studied ranging from 15 to 45 ng mL^{-1} at two optical reporter concentrations of streptavidin-HRP (1 and 2 μg mL^{-1}). This optimization was performed in presence (440 cells μL^{-1}) and absence the CD4 cells (0 cells μL^{-1}) as a negative control.

100 μL of sample (0 and 440 cells μL^{-1} in PBS) was added to 8×10^5 antiCD3-MPs in PBS 0.5% BSA as well as to biotinylated antiCD4 antibody (0; 15; 30; and 45 ng mL^{-1}) and were incubated for 30 min while shaking at 4 °C, followed by three washing steps with PBS 0.1% BSA. After that, 100 μL of streptavidin-HRP (1 and 2 μg mL^{-1}) were added and incubated for 30 min while shaking at room temperature. After incubation, three washing steps with PBS 0.1% BSA were done. Optical readout with 100 μL of substrate solution (0.004 % v/v H_2O_2 and 0.01 % w/v TMB in citrate buffer) incubated for 30 min at RT under dark conditions. The enzymatic reaction was stopped by adding 100 μL of H_2SO_4 (2 mol L^{-1}). The absorbance measurement of the supernatants was thus performed with the microplate reader using a 450 nm filter.

As can be seen in the Figure S3.3, by increasing the concentration of the biotinylated antiCD4 antibody increases the signal intensity, which reached a plateau after 30 ng mL^{-1}. No difference was further observed; hence a 36 ng mL^{-1} was selected as the most appropriate concentration and was used for all subsequent experiments performed. The streptavidin-HRP conjugate concentration was further optimized in the next section.

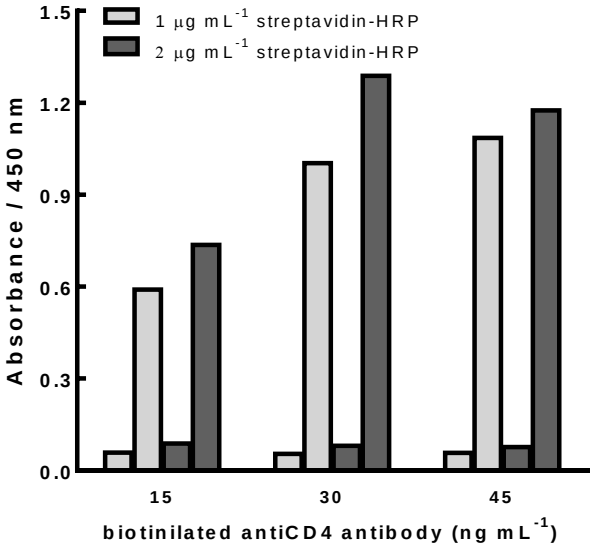

Figure S3.3. Optimization of the biotinylated antiCD4 antibody. 15; 30 and 45 ng mL^{-1} were evaluated for the detection of 440 cells μL^{-1}. The negative control is also plotted for each antibody concentration. In all cases the concentrations were fixed in 1×10^5 antiCD3-MPs per assay. The error bars show the standard deviation for n=3.

3.7.6.2 Streptavidin-HRP (optical reporter)

The effect of streptavidin-HRP concentration was studied in the range of 0.13 to 4.2 μg mL^{-1}. The assays were performed in presence (420 cells μL^{-1}) and absence the lymphocytes (0 cells μL^{-1}).

100 μL of a sample (420 cells μL^{-1} in PBS) was added to 1×10^5 antiCD3-MPs as well as to 36 ng mL^{-1}antiCD4-biotin and were incubated for 30 min while shaking at 4 °C, followed by three washing steps with PBS 0.1% BSA. After that, 100 μL of streptavidin-HRP (0.13, 0.26, 0.53, 1.10, 2.10 and 4.20 μg mL^{-1} respectively) were added and incubated for 30 min while shaking at room temperature. After incubations, three washing steps with PBS 0.1% BSA were done. Optical readout with 100 μL of substrate solution (0.004 % v/v H_2O_2 and 0.01 % w/v TMB in citrate buffer) incubated for 30 min at RT under dark conditions. The enzymatic reaction was stopped by adding 100 μL of H_2SO_4 (2 mol L^{-1}). The absorbance measurement of the supernatants was thus performed with the microplate reader using a 450 nm filter.

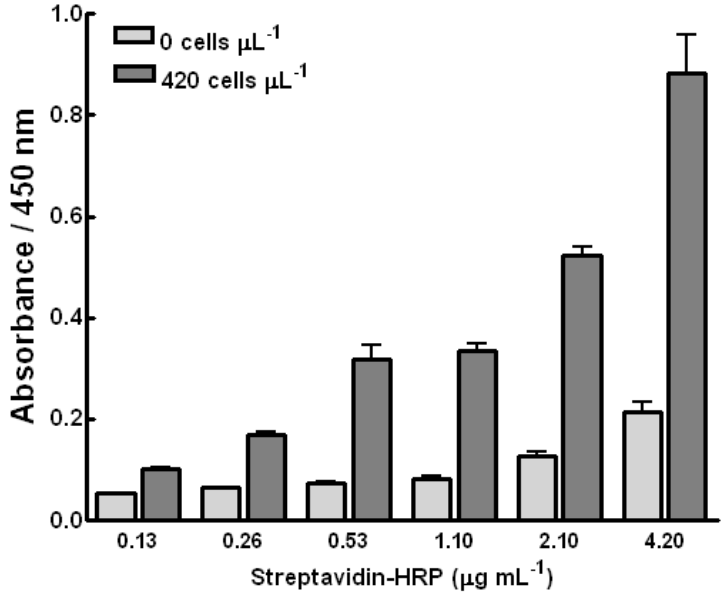

Figure S3.4. Optimization of the optical reporter (streptavidin-HRP). 0.13, 0.26, 0.53, 1.10, 2.10 and 4.20 μg mL^{-1} of streptavidin-HRP were evaluated for the detection of 420 cells μL^{-1}. The negative control is also plotted for each antibody concentration. In all cases the concentration was fixed in 1×10^5 antiCD3-MPs per assay and 36 ng mL^{-1} biotinylated antiCD4 antibody. The error bars show the standard deviation for n=3.

Table S3.1. Signal to background ratio for different concentrations of streptavidin-HRP.

Streptavidin-HRP (μg mL^{-1})	0.13	0.26	0.53	1.1	2.1
0 CD4 cell	0.054	0.065	0.075	0.083	0.126
420 CD4 cell	0.100	0.169	0.319	0.334	0.522
Signal to background ratio	**1.9**	**2.6**	**4.3**	**4.0**	**4.1**

The concentration of streptavidin-HRP was optimized in 2 μg mL^{-1} based on the signal to background ratio shown in Table S3.1. This concentration was used for all subsequent experiments performed. Although the specific signal was higher for higher enzyme conjugate concentration, the non-specific adsorption was also higher (Figure S3.4).

3.7.6.3 Optimization of incubation steps

For the optimization of the CD4 magneto immunoassay, five different immunological procedures were evaluated, which varied in the number and the order of the immunological steps (as detailed outlined in Figure S3.5).

The CD4 magneto immunoassay was performed in polystyrene microplates, and all quantities are referred as 'the amounts added per plate'. The exact concentration of the initial CD4+ lymphocyte solution was 500 cells per μL in PBS. 100 μL of this solution was used in the five procedures. After each incubation or washing step, a 96-well magnet plate separator was positioned under the microtiter plate until pellet formation on the bottom corner, followed by supernatant separation.

Procedure A. In this approach, three incubation steps were performed. The first step involved the immunocapture of 100 μL of sample with 8×10^5 antiCD3-MPs by incubation for 30 min while shaking at 4 °C. In the second step 36 ng mL^{-1} of biotinylated antiCD4 antibody were added and incubated for 30 min in slight agitation at room temperature. The last incubation step involved the enzymatic labeling by adding 2 μg mL^{-1} of streptavidin-HRP for 30 min in slight agitation at room temperature.

Procedure B. A preincubation step of 100 μL of sample with 36 ng mL^{-1} of biotinylated antiCD4 antibody for 15 min while shaking at room temperature was done. After that, 8×10^5 antiCD3-MPs were added to the initial solution and incubated for 30 min while shaking at 4 °C. The last step was incubation with 2 μg mL^{-1} of streptavidin-HRP for 30 min in slight agitation at room temperature.

Procedure C. Two incubation steps were performed. The first step involved the immunocapture of 100 μL of sample with 8×10^5 antiCD3-MPs and the labeled (at the same time) with 36 ng mL^{-1} of biotinylated antiCD4 antibody by incubation for 30 min while shaking at 4 °C. The second incubation step involved the enzymatic labeling by adding 2 μg mL^{-1} of streptavidin-HRP for 30 min in slight agitation at room temperature.

Procedure D. Two incubation steps were performed. The first step involved the immunocapture of 100 µL of sample with 8×10^5 antiCD3-MPs by incubation for 30 min while shaking at 4 °C. The last step was the simultaneous incubation of 36 ng mL^{-1} of biotinylated antiCD4 antibody and 2 µg mL^{-1} of streptavidin-HRP during 30 min in slight agitation at room temperature.

Procedure E. All the reagents were added at the same time. 100 µL of sample were incubated with 8×10^5 antiCD3-MPs, 36 ng mL^{-1} of biotinylated antiCD4 antibody and 2 µg mL^{-1} of streptavidin-HRP for 30 min in slight agitation at 4 °C.

In all cases (procedures A to E) the optical detection was performed with 100 µL of substrate solution (0.004%v/v H_2O_2 and 0.01% w/v TMB in citrate buffer) incubated for 30 min at room temperature under dark conditions. The enzymatic reaction was stopped by adding 100 µL of H_2SO_4 (2 mol L^{-1}). The absorbance measurement of the 140 µL of supernatants was thus performed with the microplate reader using the 450 nm filter.

The Figure S3.6 shows the signal obtained in each procedure under the same conditions of magnetic particles, biotinylated antiCD4 antibody and streptavidin-HRP concentration.

Although all the strategies are able to clearly detect CD4 cells, better results in terms of sensitivity were achieved with the Procedure C, when the labeling with the biotinylated antiCD4 antibody was performed during the magneto immunocapturing with antiCD3-MPs in one step, while the reaction with the optical reporter was performed in a separated step. It is important to highlight that in all cases consistent background adsorption is achieved, as shown in Table S3.2. It seems that these antibodies are hindered and compete for the union with the membrane receptors CD3 or CD4. These molecules are expressed on the surface of T lymphocytes. The CD3 complex is a group of cell surface molecules that associates with the T cell antigen receptor (TCR) and functions in the cell surface expression of TCR and in the signaling transduction cascade that originates when an antigen is recognized by the TCR. CD4 is a co-receptor that assists the TCR in communicating with an antigen-presenting cell. This effect is especially relevant in procedure D and E where the previous binding of the optical reporter (streptavidin-HRP) and the biotinylated antiCD4 antibody is achieved, resulting in a bigger macromolecular complex. The binding of the optical reporter is hindered due to the big size of the magnetic particles (4.5 µm diameter) by steric hindrance.

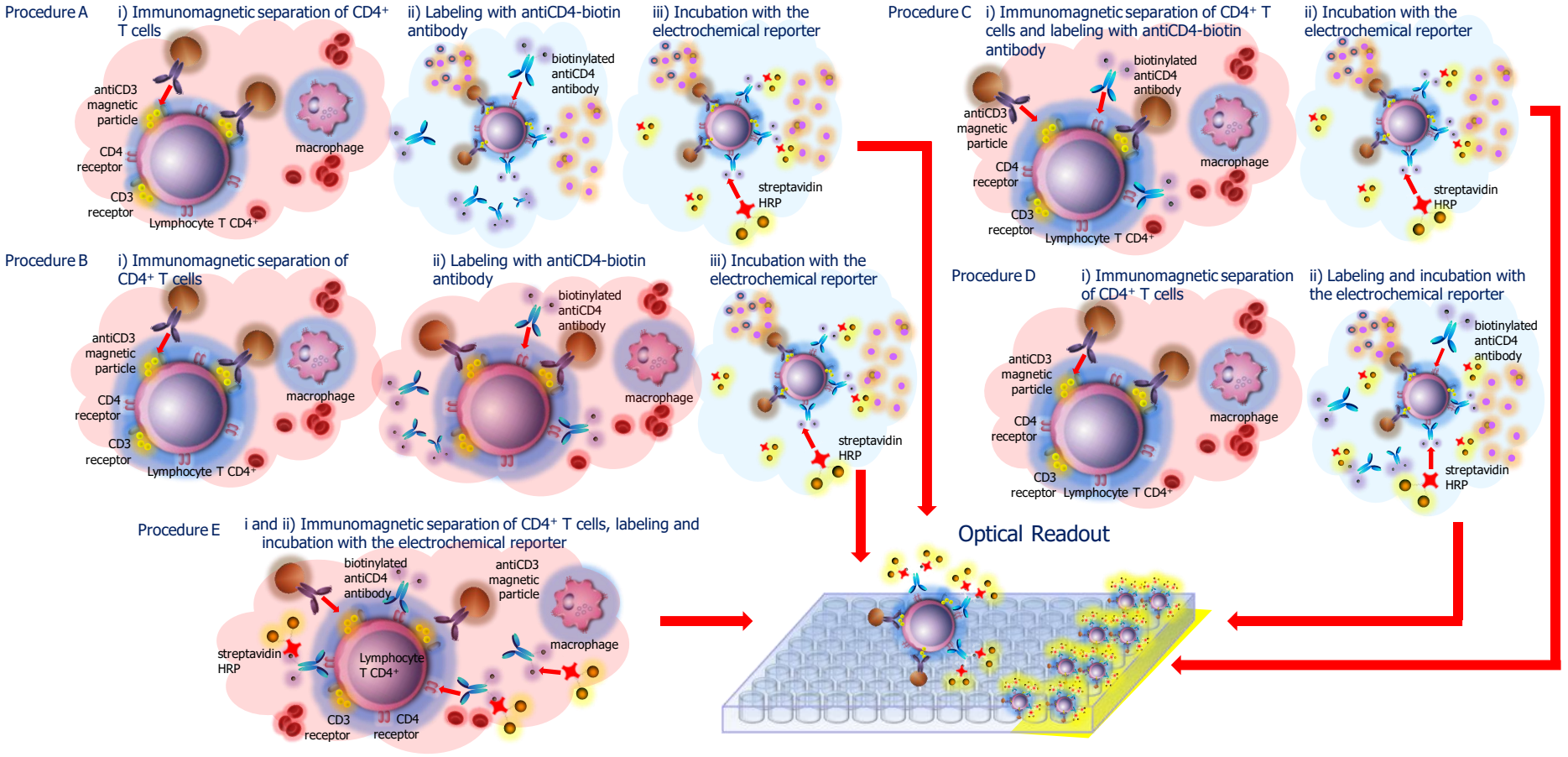

Figure S3.5. Schematic representation of the optimization of the incubation steps. Procedure A: Three incubation steps. Procedure B: A preincubation and two incubation steps. Procedure C and D: Two incubation steps. Procedure E: One incubation step, followed in all cases by the optical readout.

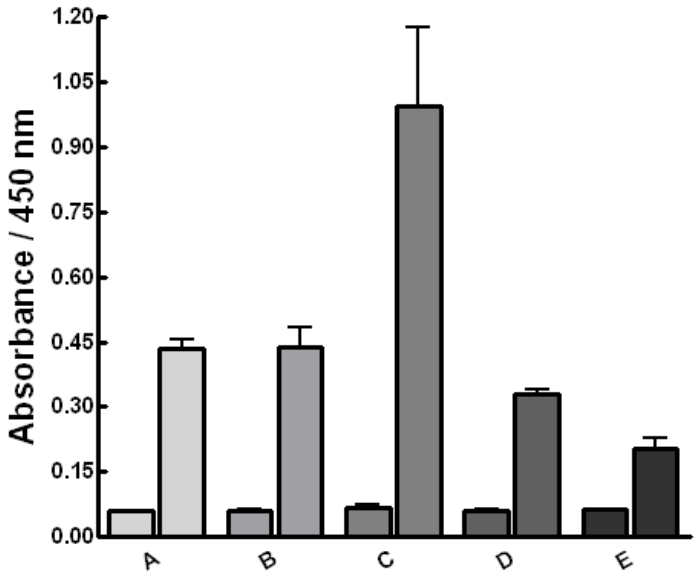

Figure S3.6. Strategies comparison for the optimization of the incubation steps, performed with 500 cells mL^{-1}. Procedure A: Three incubation steps. Procedure B: A preincubation and two incubation steps. Procedure C and D: two incubation steps. Procedure E: one incubation step, followed in all cases by the optical readout. The negative control is also shown. In all cases the concentration was fixed in 1×10^5 antiCD3-MPs per assay, 36 ng mL^{-1} biotinylated antiCD4 antibody and 2 μg mL^{-1} streptavidin-HRP. n=3.

In the case of procedures A and B, the binding by consecutive steps of one of the reagents impairs the subsequent binding, therefore the signal is lower. In the procedure A, the previous reaction with the antiCD3-MP hinders the binding of the biotinylated antiCD4 antibody, resulting in a lower signal. On the contrary, in the procedure B the binding of the antiCD3-MP to the CD4 cells is hindered by the previous reaction with the biotinylated antiCD4 antibody, decreasing the binding efficiency.

The best results were achieved with procedure C. In this case, the fact of incubating antiCD3-MPs with the biotinylated antiCD4 antibody at the same time allows both reagents to have the same opportunity for binding to their receptors, decreasing the steric hindrance. The Table S3.2 summarized all this effects, including the values of signal to background ratio. This procedure C was selected for further experiments due to the analytical performance.

Table S3.2. Comparison of the optical response obtained in each strategy.

	Procedure				
	A	B	C	D	E
Negative control	0.060	0.060	0.067	0.060	0.064
500 cells μL^{-1}	0.434	0.439	0.993	0.329	0.202
Signal to background ratio	7.2	7.3	14.9	5.5	3.2

3.7.7 Standards recovery

First of all, the backcalculation of standards was performed, for assessing the quality of a curve fit by calculating the concentrations of the standards after the regression has been completed.[36,37] This procedure is also known as standards recovery and is performed by calculating the concentration of each standard and then comparing it to the actual concentration using the formula:

Standards recovery = recovered concentration/ actual concentration x 100.

This method yields information about the relative error in the calculation of samples.

Table S3.3. Backcalculation of the standards.

Actual concentration CD4 cells μL^{-1}	Recovered concentration CD4 cells μL^{-1}	Standards Recovery (%)
75	81	108
150	142	95
300	289	96
450	493	110
600	515	86
900	904	100
1200	1222	102

3.7.8 Commercial approaches for CD4+ T lymphocytes count in AIDS diagnosis and following-up

Instrument/ Method	Features	Sample (μL)	Throughput/day	Remarks	Ref
PointCare NOW™	Modified flow cytometer. Single flow platform	Whole blood (4000 μL)	30-50 /day	FDA approved; 8 min per sample; Close system and fully automated Cost per assay: 10US$ Instrument cost: ~ US$ 25,000. Routine preventative maintenance for the optical instrument No sample preparation skilled personnel	WHO, 2014[39]
CyFlow miniPOC	Desktop single platform based on flow cytometry. Volumetric counting. Automatic data analysis and result display.	Whole blood (20 μL)	250/day	After 15 min incubation, 40-70 seconds per analysis Cost per assay: ~US$ 3.96 (€3) Instrument cost: ~US$ 11,748 (€ 8,390) without considering auto-preparation and auto-loading unit. Routine preventative maintenance required Moderate level of training required	WHO, 2014[39]
Guava EasyCD4	Microcapillary cytometry benchtop technology.	Whole blood (10 μL)	30-50 /day	30 min per sample Cost per assay: 4-5 € Instrument cost: ~20,000 €. Sample pretreatment is required Skilled laboratory worker	WHO, 2014[39]
Alere Pima™ CD4	Dual-fluorescence image analysis based on a disposable cartridge	Whole blood (25 μL)	20-25 /day	20 min per sample. No batching capabilities Cost per assay: US$ 6-12 Instrument cost: US$ 6,500-12,000. Maintenance free instrument Primary skill required	WHO, 2014[39]

3.7.8 Commercial approaches for CD4+ T lymphocytes count in AIDS diagnosis and following-up (continued).

Instrument/ Method	Features	Sample (μL)	Throughput/day	Remarks	Ref
Coulter CD4 count kit	Manual count of latex beads under light microscopy.	Whole blood (100 μL)	8 /day	Stained sample stable for 15 min after lysis limiting to 2 samples per batch Cost per assay: US$ 10 Subjective data interpretation. Eye fatigue Monocytes and lymphocytes can be difficult to differentiate. Minimum equipment requirement, suitable for small centers	Stevens, 2008; Lutwama, 2008[25,30]
Dynabeads® T4 Quant Kit	Manual count of stained CD4 nuclei under light or fluorescent microscopy. Works on haematology principle.	Whole blood (125 μL)	10-15 /day	FDA approved Sample stable for 1 h after nuclei staining limiting the batch samples Cost per assay: US$ 12-22 Monocytes removed using magnetic particles Subjective interpretation. Eye fatigue Minimum equipment requirement suitable for small centers	Stevens, 2008; Lutwama, 2008[25,30]
Daktari CD4 Counter	Cartridge microfluidic-based system with electrical sensing (impedance spectroscopy). Portable device.	Whole blood (16 μL)	30-35	Results in 10 min Cost per assay: US$ 9 Instrument cost: ~US$ 8,000. Maintenance free instrument High sensitivity (~90-100%) and medium specificity (~70-90%) Primary skill required	Stevens, 2008; Daktari[25,40]

3.7.9 Research approaches for CD4+ T lymphocytes count in AIDS diagnosis and following-up

Instrument/ Method	Features	Sample (μL)	Remarks	Ref
TRAx CD4 Test Kit	ELISA assay	Whole blood (200 μL)	LOD: NR Linear range: NR Application: point of care, for application in a single sample 40 samples in 6 h Assay based only in CD4 receptor Sample lysis required	Paxton, 1995[41]
Capcellia	Magnetic immunoassay with optical detection	Whole blood (100 μL)	LOD: 14-1,250 cells μL^{-1} Linear range: 230 cells μL^{-1} Application: high-throughput capability, for application in the simultaneous detection of several samples in small-care centers High T cell separation efficiency and high specificity	Carrière, 1999[42]
Quartz crystal microbalance	CD4 cells immobilized to the surface of gold coated quartz microbalance. Piezoelectric detection.	Lymphocyte cell culture	LOD: Not reported Linear range: 0-600 cells μL^{-1} Application: point of care, for application in a single sample Cost per sample: 15 dollars No real samples tested. Capture based only in CD4 receptor. Monocyte interference was not tested	Bachelder, 2005[43]
Bio-impedance-sensing device (BISD)	Electrical micro-biosensor chip with planar microelectrodes. Sample immobilization on micro-electrode	Lymphocyte cells culture	LOD: NR Linear range: NR Application: point of care, for application in a single sample Poor correlation with the number of captured cells Required lysed cells or PBMC for most consistent	Mishra, 2005[44]

LOD= Limit of detection; NR= Not reported

3.7.9 Research approaches for CD4+ T lymphocytes count in AIDS diagnosis and following-up (continued).

Instrument/ Method	Features	Sample (μL)	Remarks	Ref
CD4 Fluorescent fluidic microchip	Miniaturized flow cell combined with fluorescence imaging and digital image analysis	HIV-infected samples (33 μL)	LOD: NR Linear range: 0-200 cells μL^{-1} Application: point of care, for application in a single sample Poor accuracy at high CD4 concentration (up to 500 cells μL^{-1}). Cell capture on PMMA membrane (filtering of lymphocytes)	Rodriguez, 2005[45]
Lens-free cell platform coupled to an opto-electronic sensor array (LUCAS)	lens-free cell monitoring platform using an opto-electronic sensor array to record the cell shadow Image onto sensor plane. Automatic detection by software	Fibroblast as proof of concept	LOD: NR Linear range: NR Application: Point of care, high-throughput capability, for application in the simultaneous detection of several samples in small-care centers (4 chanels) Does not use optical components (lenses or microscope objectives) Can be integrated in different microfluidic devices	Ozcan & Demirci, 2008[46]
Portable and label free microchip CD4 count platform	Sample captured on microchip and detected using a portable CCD imaging platform (cell shadow detection)	HIV infected samples (10 μL-50 μL)	LOD: NR Linear range: NR Application: point of care, for application in a single sample Environmental and operator dependence under real world conditions Capture efficiency depends on cell concentration Samples cleanliness needed to avoid the identification of artifacts as cells	Moon, 2009 & 2011[47,48]
Magnetic particles based immunoassay on microfluidic device	PDMS chip on a fluidic platform with optical detection. CD4 cells magnetic captured on chip.	Mouse lymphocyte cells (1 μL)	LOD: NR Linear range: NR Application: point of care, for application in a single sample Capture efficiency depend of the chamber length 20 min per assay on chip follow by a manual count under microscope	Gao, 2010[49]

LOD= Limit of detection; NR= Not reported

3.7.9 Research approaches for CD4+ T lymphocytes count in AIDS diagnosis and following-up (continued).

Instrument/ Method	Features	Sample (μL)	Remarks	Ref
Label free optofluidic ring resonator (OFRR) biosensor	CD4 label free detection in a microfluidic sensing platform	Lymphocyte cells	LOD: NR Linear range: 180-320 cells μL^{-1} Application: point of care, for application in a single sample Cellular lysis is required for reducing error bars. Need of regeneration of immobilization surface after each measurement Non linear relationship due to the saturation of the detector	Gohring & Fan, 2010[32]
Quantitative microchip based on electrochemical impedance biosensor with electrode pixels.	Cells captured on electrode pixels, and detected individually by monitoring the interfacial impedance changes on each independent pixel (system "on-off").	Lymphocyte cell culture (1 μL)	LOD: NR Linear range: NR Application: point of care, for application in a single sample Tested with very low amount of cells, limited to the pixel numbers (200 pixels) High fabrication cost	Jiang & Spencer, 2010[50]
Chemiluminescent microfluidic CD4 counting	Semiquantitative microfluidic platform with chemiluminescent readout. Cell capture based on an immunoaffinity microchannel	HIV-infected samples (3 μL)	LOD: NR Linear range: 100-800 cells μL^{-1} Application: point of care, for application in a single sample Good sensitivity, high standard deviation High Non specific binding of cells by nonspecific interaction to the surface	Wang, 2010[51]

LOD= Limit of detection; NR= Not reported

3.7.9 Research approaches for CD4+ T lymphocytes count in AIDS diagnosis and following-up (continued).

Instrument/ Method	Features	Sample (μL)	Remarks	Ref
Microfabricated electrical differential CD4 counter	Electrical impedance sensor coupled with immunoaffinity chromotography to differentiate betweenCD4+ cells and other leukocytes	Whole blood (5 μL)	LOD: NR Linear range: 100-700 cells μL^{-1} Application: point of care, for application in a single sample Moderate specificity (~80%) and low capture efficiency Overestimation of CD4 count below 200 cells due to monocyte interferences Erythrocytes lysis off-chip is required. Low capture efficiency (60%)	Watkins, 2011[52]
MBio Diagnostics	Disposable cartridge for CD4 enumeration based on static imaging cytometry with fluorescent immunostaining	HIV infected samples (15 μL)	LOD: NR Linear range: NR Application: point of care, high-throughput capability, for application in the simultaneous detection of several samples in small-care centers (60-80 samples/day, 15 cartridge/hour x operator) ~23 minutes(20 min incubation, 3-minute analysis) US$ 6 per test (estimated), Less than US$ 5000 per system No routine maintenance or service	Logan, 2013[53]
Disposable microfluidic, dual force device	Chip using fluidic and magnetic force for CD4 isolation. CD4 cell detected in capture chamber by visual or fluorescence readout.	Lymphocyte cell culture(less than 10 μL)	LOD: NR Linear range: 0-1,600 cells μL^{-1} Application: point of care, for application in a single sample Results affected by a subjective degree depending on the observer. High efficiency capture	Glynn, 2014[54]

LOD= Limit of detection; NR= Not reported

3.7.9 Research approaches for CD4+ T lymphocytes count in AIDS diagnosis and following-up (continued).

Instrument/ Method	Features	Sample (μL)	Remarks	Ref
Magneto-actuated electrochemical biosensor	Magnetic sample isolation with amperometric detection	Whole blood (100 μL)	LOD: 44 cells μL^{-1} Linear range: 89-912 cells μL^{-1} Application: point of care, for application in a single sample Cost per sample: ~ 3€ High specificity and sensitivity, without matrix effect Not interference from monocytes Sample pretreatment not required	Carinelli, 2015[17]
CD4 magneto ELISA	Magneto ELISA	Whole blood (100 μL)	LOD: 50 cells μL^{-1} Linear range: 63-979 cells μL^{-1} Application: Point of care, high-throughput capability (more than 40 sample per batch) Cost per sample: Less than 1€. Basic laboratory skill required	This study

LOD= Limit of detection; NR= Not reported

3.8 References

[1] Lelievre, J. D., Mammano, F., Arnoult, D., Petit, F., Grodet, A., Estaquier, J., Ameisen, J. C. (2004). A novel mechanism for HIV1-mediated bystander CD4+ T-cell death: neighboring dying cells drive the capacity of HIV1 to kill noncycling primary CD4+ T cells. Cell death and differentiation, 11(9), 1017-1027.

[2] Lusso, P. (2006). HIV and the chemokine system: 10 years later. The EMBO journal, 25(3), 447-456.

[3] Pan, X., Baldauf, H. M., Keppler, O. T., Fackler, O. T. (2013). Restrictions to HIV-1 replication in resting CD4+ T lymphocytes. Cell research, 23(7), 876-875.

[4] Wu, G., Zaman, M. H. (2012). Low-cost tools for diagnosing and monitoring HIV infection in low-resource settings. Bulletin of the World Health Organization, 90, 914-920.

[5] Zachariah, R., Reid, S. D., Chaillet, P., Massaquoi, M., Schouten, E. J., Harries, A. D. (2011). Why do we need a point-of-care CD4 test for low-income countries? Tropical Medicine & International Health, 16(1), 37-41.

[6] Losina, E., Bassett, I. V., Giddy, J., Chetty, S., Regan, S., Walensky, R. P., Scott, C. A., Uhler, L. M., Katz, J. N., Holst, H., Freedberg, K. A. (2010). The "ART" of linkage: pre-treatment loss to care after HIV diagnosis at two PEPFAR sites in Durban, South Africa. PloS one, 5(3), e9538.

[7] Boyle, D. S., Hawkins, K. R., Steele, M. S., Singhal, M., Cheng, X. (2012). Emerging technologies for point-of-care CD4 T-lymphocyte counting. Trends in biotechnology, 30(1), 45-54.

[8] Carinelli, S., Martí, M., Alegret, S., Pividori, M. I. (2015). Biomarker detection of global infectious diseases based on magnetic particles. New biotechnology, 32(5), 521-532.

[9] Engvall, E., Perlmann, P. (1971). Enzyme-linked immunosorbent assay (ELISA) quantitative assay of immunoglobulin G. Immunochemistry, 8(9), 871-874.

[10] Van Weemen, B. K., Schuurs, A. H. W. M. (1971). Immunoassay using antigen—enzyme conjugates. FEBS letters, 15(3), 232-236.

[11] World Health Organization. (2007). Recommendations for laboratory procedures to detect avian influenza A H5N1 virus in specimens from suspected human cases. Geneva: WHO. Available online at http://www.who.int/influenza/resources/documents/RecAIlabtestsAug07.pdf

[12] World Health Organization/ Joint United Nations Programme on HIV/AIDS (UNAIDS). (1998). Operational Characteristics of commercially available assays to determine antibodies to HIV-1 and/or HIV-2 in human sera: report 9/10.

[13] Voller, A., Draper, C., Bidwell, D., Bartlett, A. (1975). Microplate enzyme-linked immunosorbent assay for Chagas disease. The Lancet, 305(7904), 426-428.

[14] Centers for Disease Control and Prevention (CDC). Available online at http://www.cdc.gov/vhf/ebola/diagnosis/.

[15] Reddy, L. H., Arias, J. L., Nicolas, J., Couvreur, P. (2012). Magnetic nanoparticles: design and characterization, toxicity and biocompat., Draper, C., Bidwell, D., Bartlett, A. (1975). Microplate enzyme-linked immunosorbent assay for Chagas disease. The Lancet, 305(7904), 426-428.

[16] Berensmeier, S. (2006). Magnetic particles for the separation and purification of nucleic acids. Applied microbiology and biotechnology, 73(3), 495-504.

[17] Carinelli, S., Ballesteros, C. X., Martí, M., Alegret, S., Pividori, M. I. (2015). Electrochemical magneto-actuated biosensor for CD4 count in AIDS diagnosis and monitoring. Biosensors and Bioelectronics, 74, 974-980.

[18] Xufré, C., Costa, M., Roura-Mir, C., Codina-Busqueta, E., Usero, L., Pizarro, E., Obiols, D., Jaraquemada, D., Martí, M. (2013). Low frequency of GITR+ T cells in ex vivo and in vitro expanded Treg cells from type 1 diabetic patients. International immunology, 25(10), 563-574.

[19] Chosewood, L. C., Wilson, D. E. (1999). Biosafety in microbiological and biomedical laboratories, 5th ed.

[20] Chiu, M. L., Lawi, W., Snyder, S. T., Wong, P. K., Liao, J. C., Gau, V. (2010). Matrix effects—a challenge toward automation of molecular analysis. JALA: Journal of the Association for Laboratory Automation, 15(3), 233-242.

[21] Jones, G. (2002). Handling common laboratory interferences. Clinical Biochemist Reviews, 23(4), 105-111.

[22] World Health Organization. (2009). Laboratory guidelines for enumeration CD4 T lymphocytes in the context of HIV. Geneva: WHO.

[23] Pacifici, R., Zuccaro, P., Cozzi-Lepre, A., Di Carlo, S., Bacosi, A., Fattorossi, A. (1998). Quantification of the variation due to lysing technique in immunophenotyping of healthy and HIV-infected individuals. Clinical biochemistry, 31(3), 165-172.

[24] Crowe, S., Turnbull, S., Oelrichs, R., Dunne, A. (2003). Monitoring of human immunodeficiency virus infection in resource-constrained countries. Clinical Infectious Diseases, 37(Supplement_1), S25-S35.

[25] Stevens, W., Gelman, R., Glencross, D. K., Scott, L. E., Crowe, S. M., Spira, T. (2008). Evaluating new CD4 enumeration technologies for resource-constrained countries. Nature reviews Microbiology, 6, S29-S38.

[26] Benson, C. A., Brooks, J. T., Holmes, K. K., Kaplan, J. E., Masur, H., Pau, A. (2009). Guidelines for prevention and treatment opportunistic infections in HIV-infected adults and adolescents; recommendations from CDC, the National Institutes of Health, and the HIV Medicine Association/Infectious Diseases Society of America. MMWR 58, 1-207.

[27] Lee, B., Sharron, M., Montaner, L. J., Weissman, D., Doms, R. W. (1999). Quantification of CD4, CCR5, and CXCR4 levels on lymphocyte subsets, dendritic cells, and differentially conditioned monocyte-derived macrophages. Proceedings of the National Academy of Sciences, 96(9), 5215-5220.

[28] Ginaldi, L., Farahat, N., Matutes, E., De Martinis, M., Morilla, R., Catovsky, D. (1996). Differential expression of T cell antigens in normal peripheral blood lymphocytes: a quantitative analysis by flow cytometry. Journal of clinical pathology, 49(7), 539-544.

[29] Diaw, P. A., Daneau, G., Coly, A. A., Ndiaye, B. P., Wade, D., Camara, M., Dieye, T. N. (2011). Multisite evaluation of a point-of-care instrument for CD4+ T-cell enumeration using venous and finger-prick blood: the PIMA CD4. JAIDS Journal of Acquired Immune Deficiency Syndromes, 58(4), e103-e111.

[30] Lutwama, F., Serwadda, R., Mayanja-Kizza, H., Shihab, H. M., Ronald, A., Kamya, M. R., Thomas, D., Johnson, E., Quinn, T. C., Moore, R. D., Spacek, L. A. (2008). Evaluation of Dynabeads and Cytospheres compared with flow cytometry to enumerate CD4+ T cells in HIV-infected Ugandans on antiretroviral therapy. Journal of acquired immune deficiency syndromes, 48(3), 297-303.

[31] Volberding, P., Sande, M. A., Greene, W. C., Lange, J., Gallant, J. (2007) Global HIV/AIDS Medicine, Elsevier: New York.

[32] Gohring, J. T., Fan, X. (2010). Label free detection of CD4+ and CD8+ T cells using the optofluidic ring resonator. Sensors, 10(6), 5798-5808.

[33] Moon, S., Gurkan, U. A., Blander, J., Fawzi, W. W., Aboud, S., Mugusi, F., Kuritzkes, D. R., Demirci, U. (2011). Enumeration of CD4+ T-cells using a portable microchip count platform in Tanzanian HIV-infected patients. PloS one, 6(7), e21409.

[34] Thorslund, S., Larsson, R., Bergquist, J., Nikolajeff, F., Sanchez, J. (2008). A PDMS-based disposable microfluidic sensor for CD4+ lymphocyte counting. Biomedical microdevices, 10(6), 851-857.

[35] Chin, C. D., Laksanasopin, T., Cheung, Y. K., Steinmiller, D., Linder, V., Parsa, H., Wang, J., Moore, H., Rouse, R., Umviligihozo, G., Karita, E., Mwambarangwe, L., Braunstein, S.L., van de Wijgert, J., Sahabo, R., Justman, J.E., El-Sadr, W., Sia, S.K. (2011). Microfluidics-based diagnostics of infectious diseases in the developing world. Nature medicine, 17(8), 1015-1020.

[36] Nix, B., Wild, D. (2001). The immunoassay handbook. New York: Nature, 198-210.

[37] Baud, M. (1993). Data analysis, mathematical modeling. Methods of immunological analysis, 1, 656-671.

[38] Davies, C., Wild, D. (2001). The immunoassay handbook, 2nd ed.

[39] World Health Organization. (2014). HIV/AIDS Diagnostics Technology Landscape. 4th edition. Geneve: WHO.

[40] www.daktaridx.com/

[41] Paxton, H., Pins, M., Denton, G., McGonigle, A. D., Meisner, P. S., Phair, J. P. (1995). Comparison of CD4 cell count by a simple enzyme-linked immunosorbent assay using the TRAx CD4 test kit and by flow cytometry and hematology. Clinical and diagnostic laboratory immunology, 2(1), 104-114.

[42] Carrière, D., Vendrell, J. P., Fontaine, C., Jansen, A., Reynes, J., Pagès, I., Holzmann, C., Laprade, B., Pau, B. (1999). Whole blood Capcellia CD4/CD8 immunoassay for enumeration of CD4+ and CD8+ peripheral T lymphocytes. Clinical chemistry, 45(1), 92-97.

[43] Bachelder, E. M., Ainslie, K. M., Pishko, M. V. (2005). Utilizing a quartz crystal microbalance for quantifying CD4+ T cell counts. Sensor Letters, 3(3), 211-215.

[44] Mishra, N. N., Retterer, S., Zieziulewicz, T. J., Isaacson, M., Szarowski, D., Mousseau, D. E., Lawrence, D. A., Turner, J. N. T (2005). On-chip micro-biosensor for the detection of human CD4+ cells based on AC impedance and optical analysis. Biosensors and Bioelectronics, 21(5), 696-704.

[45] Rodriguez, W. R., Christodoulides, N., Floriano, P. N., Graham, S., Mohanty, S., Dixon, M., Hsiang, M., Peter, T., Zavahir, S., Thior, I., Romanovicz, D., Bernard, B., Goodey A.P., Walker, B.D., McDevitt, J.T., (2005). A microchip CD4 counting method for HIV monitoring in resource-poor settings. PLoS medicine, 2(7), e182.

[46] Ozcan, A., Demirci, U. (2008). Ultra wide-field lens-free monitoring of cells on-chip. Lab on a Chip, 8(1), 98-106.

[47] Moon, S., Keles, H. O., Ozcan, A., Khademhosseini, A., Hæggstrom, E., Kuritzkes, D., Demirci, U. (2009). Integrating microfluidics and lensless imaging for point-of-care testing. Biosensors and Bioelectronics, 24(11), 3208-3214.

[48] Moon, S., Gurkan, U. A., Blander, J., Fawzi, W. W., Aboud, S., Mugusi, F., Kuritzkes, D. R. Demirci, U. (2011). Enumeration of CD4+ T-cells using a portable microchip count platform in Tanzanian HIV-infected patients. PloS one, 6(7), e21409.

[49] Gao, D., Li, H. F., Guo, G. S., Lin, J. M. (2010). Magnetic bead based immunoassay for enumeration of CD4+ T lymphocytes on a microfluidic device. Talanta, 82(2), 528-533.

[50] Jiang, X., Spencer, M. G. (2010). Electrochemical impedance biosensor with electrode pixels for precise counting of CD4+ cells: A microchip for quantitative diagnosis of HIV infection status of AIDS patients. Biosensors and Bioelectronics, 25(7), 1622-1628.

[51] Wang, Z., Chin, S. Y., Chin, C. D., Sarik, J., Harper, M., Justman, J., Sia, S. K. (2009). Microfluidic CD4+ T-cell counting device using chemiluminescence-based detection. Analytical chemistry, 82(1), 36-40.

[52] Watkins, N. N., Sridhar, S., Cheng, X., Chen, G. D., Toner, M., Rodriguez, W., Bashir, R. (2011). A microfabricated electrical differential counter for the selective enumeration of CD4+ T lymphocytes. Lab on a Chip, 11(8), 1437-1447.

[53] Logan, C., Givens, M., Ives, J. T., Delaney, M., Lochhead, M. J., Schooley, R. T., Benson, C. A. (2013). Performance evaluation of the MBio Diagnostics point-of-care CD4 counter. Journal of immunological methods, 387(1-2), 107-113.

[54] Glynn, M. T., Kinahan, D. J., Ducrée, J. (2014). Rapid, low-cost and instrument-free CD4+ cell counting for HIV diagnostics in resource-poor settings. Lab on a Chip, 14(15), 2844-2851.

Chapter 4

ELECTROCHEMICAL MAGNETO-ACTUATED BIOSENSOR FOR CD4 COUNT IN AIDS DIAGNOSIS AND MONITORING

Biosensors and Bioelectronics 74 (2015) 974-980

4.1 Abstract

The counting of CD4+ T lymphocytes is a clinical parameter used for acquired immune deficiency syndrome (AIDS) diagnosis and follow-up. As this disease is particularly prevalent in developing countries, simple and affordable CD4 cell counting methods is urgently needed in resource-limited settings. This paper describes a magneto-actuated electrochemical biosensor for CD4 count in whole blood. The CD4+ T lymphocytes were isolated, preconcentrated and labeled from 100 μL of whole blood by immunomagnetic separation with magnetic particles modified with antiCD3 antibodies. The captured cells were labeled with a biotinylated antiCD4 antibody, followed by the reaction with the electrochemical reporter streptavidin-peroxidase conjugate. The limit of detection for the CD4 counting magneto biosensor in whole blood was as low as 44 cells μL^{-1} while the logistic range was found to be from 89 to 912 cells μL^{-1}, which spans the whole medical interest range for CD4 counts in AIDS patients.

The electrochemical detection together with the immunomagnetic separation confers high sensitivity, resulting in a rapid, inexpensive, robust, user-friendly method for CD4 counting. This approach is a promising alternative for costly standard flow cytometry and suitable as diagnostic tool at decentralized practitioner sites in low resource settings, especially in less developed countries.

4.2 Introduction

The Human Immunodeficiency Virus (HIV) and the AIDS affect the life of millions of people around the world, mainly in low- and middle-income countries. According to the World Health Organization (WHO), globally 35 million people were living with HIV in 2013. An estimated 0.8 % of adults aged between 15-49 years are living with HIV worldwide. However, sub-Saharan Africa remains most severely affected, with nearly 1 in every 20 adults (4.7 %) living with HIV and accounting for 68 % of the people living with HIV worldwide.[1] The HIV virus infects the cells of the immune system, primarily CD4+ T lymphocytes decreasing CD4 levels from the normal values (ranging from 500 to 1,200 cells μL^{-1}), which weakens the immune system and causes the progression to AIDS and death from cancer or opportunistic infections.[2] When the number of the CD4 cells falls below 200 cells μL^{-1} of blood, it is considered to have progressed to AIDS.[2] AIDS it is also diagnosed with the emergence of one or more opportunistic illnesses regardless the CD4 count. Without treatment, people who progress to AIDS typically survive about 3 years. However, life-expectancy without treatment falls to about 1 year with the presence of opportunistic illness. Under antiretroviral treatment (ART) while

maintaining a low viral load, a patient may enjoy a near normal life span without progression to AIDS. The CD4+ T cell count is thus a critical parameter in monitoring HIV disease, since lower numbers of circulating CD4+ T cells imply a more advanced stage of HIV disease and less competent defense mechanisms. In HIV infected patients, the CD4+ T cell count is useful not only for assessing the degree of immune deterioration and speed of progression towards AIDS, but also for initiating ART, for deciding the timing for prophylaxis of opportunistic infections and, finally, for monitoring the efficacy of the treatment.[3] The new recommendations encourage all countries to initiate the treatment in HIV infected adults with CD4 cell count down to 500 cells μL^{-1} when their immune systems are still strong, regardless of the presence or absence of clinical symptoms.[4] Unfortunately, the areas mostly affected by the HIV epidemic are resource-limited countries, wherein the CD4 count is not available due to laboratory requirements and cost of the assay.[5]

Flow cytometry is the gold standard technology for CD4+ T cell count because of its accuracy, precision and reproducibility. This technology is also capable of high sample throughput. However, flow cytometry based CD4 counting is relatively complex, and therefore technically demanding and costly, requiring regular maintenance, reliable electric supply and skilled personnel. Moreover, the instruments commercially available are significantly expensive (US$ 20-95 000).[3] These instruments are thus rather impractical and difficult to sustain in resource-scarce settings. Currently, there are only few cheaper alternatives to flow cytometer and they are based mostly on fluorescent labeling, requiring thus costly imaging equipment to achieve detection or, instead, based on manual counting with light microscopes.[5,6] For instance, the PointCare NOW™ and the CyFlow® miniPOC are modified flow cytometers. PIMA™ is based on a dual-fluorescence image analysis to count CD3+/CD4+ cells.[7] The Coulter® CD4Count Kit and the Dynal T4 Quant Kit are manual CD4 tests based on the use of beads for lymphocyte capturing, labeling and counting under light microscope.[8] These manual counting methods are rapid but laborious and have a limited throughput. In order to minimize reader error, they are restricted to 10 samples per day to prevent technician fatigue and eyestrain.[9] An enzyme immunoassay was also developed, showing a limit of detection (LOD) for CD4 cells of 230 cells μL^{-1}, being thus rather impractical for AIDS and opportunistic diseases diagnosis due to lack of sensitivity.[10] Finally, microfluidic devices based mostly on optical,[11-13] fluorescence[14] or impedance [15-17] detection were reported. However, the cost of production of some microfabricated devices still constitute a bottleneck and may put them out of range for end users in the developing world.[13]

To solve the urgent need for improving the diagnostic tools of AIDS, electrochemical biosensors offer an exciting alternative, especially in resource-scarce settings, as rapid, cost-effective devices that can be handled for unskilled personnel at the community and primary care level.

This paper addresses a magneto actuated electrochemical biosensor for CD4+ T lymphocytes count in whole blood. In this work, CD4 cells are preconcentrated from whole blood by immunomagnetic separation based on the CD3 receptor and using magnetic particles (MPs) modified with an antiCD3 antibody. The captured cells are at the same time labeled with a biotinylated antiCD4 antibody, followed by the reaction with an electrochemical reporter. As monocytes and macrophages also express the CD4+ molecule, they are excluded from the absolute count: although a number of blood cell types may express either CD4 or CD3 antigens (for instance, monocytes, and thymocytes, respectively), only CD4+ T lymphocytes express both CD4 and CD3 simultaneously. Due to the high sensitivity, the CD4 counting electrochemical magneto biosensor offers outstanding analytical performances and advantages compared with the gold standard flow cytometry method.

4.3 Experimental section

4.3.1 Instrumentation

Amperometric measurements were performed with a LC-4C amperometric controller (BAS Bioanalytical Systems Inc, USA). Voltammetric characterization was carried out using an Autolab PGSTAT Eco-chemie. A three-electrode setup was used comprising a platinum auxiliary electrode (Crison 52-67 1), a double junction Ag/AgCl reference electrode (Orion 900200) with 0.1 mol L^{-1} KCl as external reference solution and a working electrode (the magneto graphite-epoxy composite electrode, m-GEC).[18] The data were analyzed using the Graph Prism software (GraphPad Software, San Diego, CA).

Cell count was performed in Neubauer counting chamber using Nikon Eclipse TS100 microscope (Nikon Instrument, USA) or by flow cytometry using FACSCanto cytometer (BD Bioscience, USA).

The confocal images were taken with the TCS-SP5 Leica Microscope. The software used for the image process was Imaris X64 v.6.2.0 (Bitplane, Zurich, Switzerland).

The SEM images were taken with the scanning electron microscope Hitachi LTD S-570 (Hitachi LTD, Tokyo, Japan). For the sample treatment an E5000 Sputter Coater Polaron Equipment Limited metallizer and K850 Critical Point Drier Emitech (Ashford, UK) was used.

4.3.2 Chemicals and Biochemicals

Magnetic particles modified with antiCD3 antibody (antiCD3-MPs, Dynabeads® CD3 Prod. No. 111-51D) were purchased from Dynal Biotech ASA. Biotinylated antiCD4 antibody (Prod. No. 347321) was provided by BD Bioscience and the streptavidin–horseradish peroxidase conjugate (streptavidin-HRP) (HRP, 1.11.1.7) came from Roche Diagnostics. Perfect count microspheres (Prod. No. CYT-PCM-100) used for absolute cell count by flow cytometry were purchased from Cytognos SL, Spain. The streptavidin labeled with cyanine 5 (Strep-Cy5) dye used in confocal microscopy was purchased from Life Technologies (Prod No. SA-1011).

All buffer solutions were prepared with milliQ water and all other reagents were in analytical reagent grade (supplied from Sigma and Merck). The composition of these solutions is described in *§4.7.1*.

4.3.3 Cell culture

The CD4+ T cell clone PB100.29 was obtained by cloning the infiltrating lymphocytes from a pancreatic donor organ.[19] The expansion method is described in detail in *§4.7.2*.

4.3.4 Confocal microscopy study of the immunomagnetic separation and labeling

Confocal microscopy was performed to characterize not only the distribution of CD4 and CD3 receptors on the lymphocyte surface but also their capability of being recognized by the antiCD3 antibody immobilized on the magnetic particles and the biotinylated antiCD4 antibody.

A solution of 1000 cells μL^{-1} was incubated with Hoechst (45 $\mu g\ mL^{-1}$) for 15 min at room temperature in darkness, to stain DNA of the living cells nuclei. The cells were then captured with the antiCD3-MPs (8×10^5 CD3-MPs per well) and labeled with biotinylated antiCD4 antibody (36 $ng\ mL^{-1}$), respectively, in one step procedure. Washing steps with PBS 0.1% BSA were performed. Finally, cells were incubated with strep-Cy5 (2 $\mu g\ mL^{-1}$) for 30 min at room temperature (RT) to achieve the fluorescence readout.

4.3.5 SEM study of the immunocaptured CD4 cells- on the electrode surface

The distribution of the antiCD3-MPs after the binding of the CD4 cells on the magneto electrode surface was evaluated by scanning electron microscopy (SEM). 500 cells μL^{-1} of CD4+ T lymphocytes were captured with 8×10^5 antiCD3-MPs.

The CD4 cells were incubated with magnetic particles for 30 minutes while shaking at 4 °C followed by a washing step. The modified magnetic particles were then resuspended in 140 μL of PBS 0.5% BSA and captured by the m-GEC. The CD4 cells/antiCD3-MPs complexes captured on the magneto electrode surface were then fixed with fixation buffer (0.1 mol L^{-1} cacodylate, 1% glutaraldehyde, pH 7.4) for 1 hour at room temperature and rinsed in cacodylate buffer. Dehydration was carried out in ethanol solution from 50 to 95% for 5 min each at room temperature and finally twice at 100% ethanol for 10 min. The treated electrodes were coated with a thin layer of gold.

4.3.6 CD4 counting magneto biosensor in whole blood

The CD4 counting electrochemical magneto biosensor is based on the following four steps, as depicted in Figure 4.1: (A) Immunomagnetic separation of CD4+ T cells and labeling. In this step, the antiCD3-MPs (8×10^5 MP per well) and the biotinylated anti-CD4 antibody (36 ng mL^{-1}) were simultaneously incubated with 100 μL of sample for 30 min with shaking at 4 °C, followed by three washing steps with PBS 0.1% BSA, (B) Incubation with the optical reporter streptavidin-HRP (30 μg mL^{-1}) for 30 min while shaking at RT, followed by two washing steps with PBS 0.1% BSA, (C) Magnetic actuation of the modified magnetic particles on the m-GEC electrode surface, and (D) Amperometric detection using the m-GEC electrodes polarised at –0.150 V (vs. Ag/AgCl), under enzyme saturation conditions with the substrate. The explanation of the amperometric detection using m-GEC electrodes as working electrodes, as well as the selection of the potential applied for the measurements is fully detailed in *§4.7.3* and *§4.7.4*. A steady-state current was obtained normally after 1 min upon the addition of hydroquinone (HQ) (1.8×10^{-3} mol L^{-1}) and hydrogen peroxide (H_2O_2) (1.1×10^{-3} mol L^{-1}) in phosphate buffer (ePBS), as mediator and substrate for the enzyme HRP, respectively. This steady-state current was used for the electrochemical signal plotted in further results shown in Figure 4.1.

After each incubation (steps A and B) or washing step, a magnetic separator was positioned under the tubes until pellet formation on the tube side wall, followed by supernatant separation. After the amperometric detection (step D), the surface of the m-GEC electrodes were renewed for

further uses by the elimination of the modified magnetic particles with a simple polishing procedure, as detailed in *§4.7.4*.

Three different methods for the total depletion of lymphocyte from whole blood were tested with the CD4 counting magneto immunoassay, namely A) Ficoll-Paque depletion; B) Immunomagnetic separation (IMS) with Dynabeads® CD3; and finally, C) a combination of both (Ficoll-Paque/IMS), as detailed in *§4.7.5*. The matrixes were evaluated by the CD4 counting magneto biosensor. By the combination of Ficoll-Paque/IMS, a whole blood matrix almost clean from lymphocytes (quantified by flow cytometry in 4 cells μL^{-1}) was achieved. This lymphocyte depleted whole blood matrix was used in further studies for diluting the whole blood.

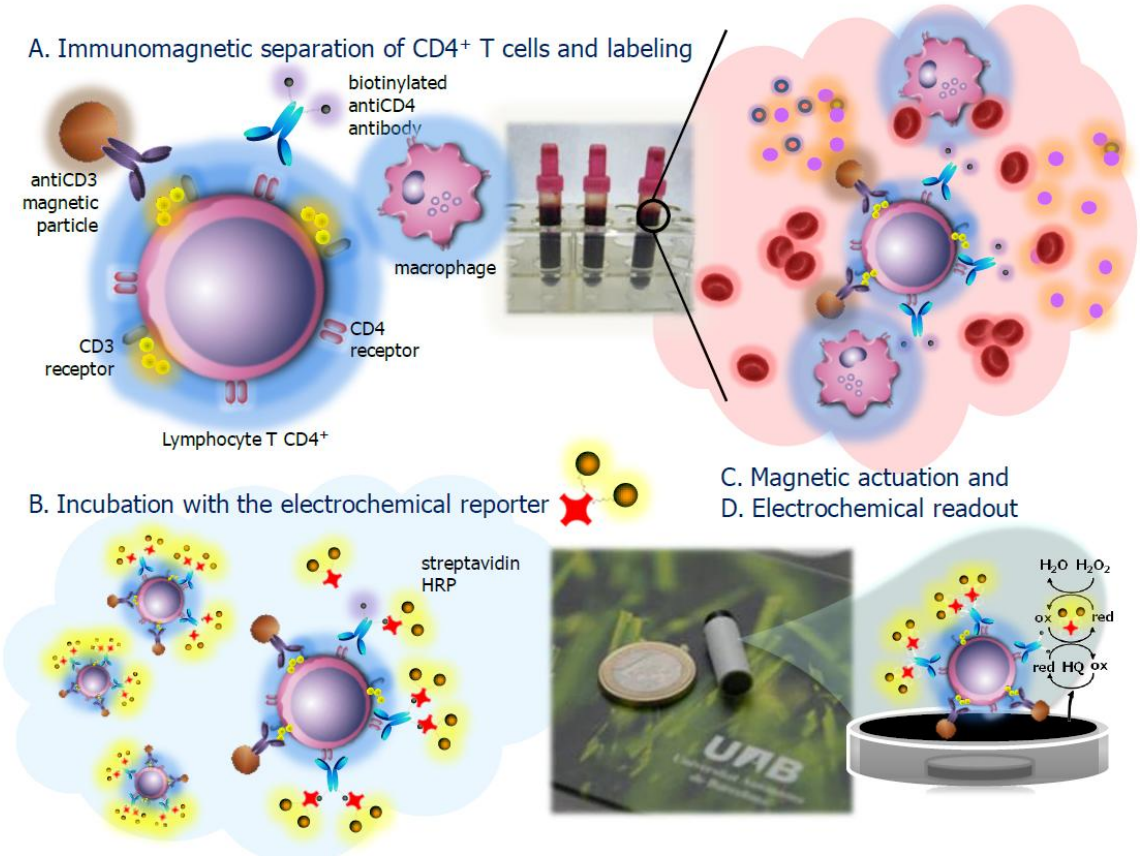

Figure 4.1. Schematic representation of the CD4 counting magneto biosensor (A) The CD4+ T lymphocytes are captured from whole blood by the CD3-MPs (8×10^5 MPs per assay) and labeled in one step with antiCD4-biotin (36 ng mL^{-1}); (B) The incubation with the electrochemical reporter streptavidin-HRP (30 μg mL^{-1}) is then performed. (C) Finally, the electrochemical readout is achieved with H_2O_2 and HQ as mediator.

The calibration curve was prepared as follow: the exact concentration of the initial whole blood sample was firstly determined by flow cytometry. Serial dilutions of whole blood were performed using the optimized leukocyte-depleted whole blood matrix (Ficoll-Paque/IMS), to achieve the

concentration range from 0 to 1200 cells μL^{-1}. The CD4 cell range was chosen to include the concentration of clinical interest for CD4+ lymphocytes in AIDS diagnosis.

The recovery was determined by spiking low (200 cells μL^{-1}), medium (350 cells μL^{-1}), and high (500 cells μL^{-1}) concentration level of CD4 cells in the lymphocyte-depleted whole blood, covering all the whole clinical interest range.

The recovery was calculated as % R = 100. (P_1 / P_0), being P_0 the real number of cells spiked to the sample and P_1 the number of cells obtained by interpolating the signal in the standard curve.

4.3.7 Safety considerations

All the procedures involving the manipulation of human cells were handled using Biosafety Level 2 Laboratory and containment. All works were performed in a Biosafety cabinet, and all material decontaminated by autoclaving or disinfected before discarding in accordance with U.S. Department of Health and Human Services guidelines for level 2 laboratory Biosafety.[20]

4.4 Results and discussion

4.4.1 Confocal microscopy study of the immunomagnetic separation and labeling

The distribution of CD4 and CD3 receptors on lymphocyte membrane was evaluated by confocal microscopy, as shown in Figure 4.2.

The typical dense nucleus of the lymphocytes is shown in blue due to Hoescht dye, a cell permeable DNA stain which is excited by ultraviolet light and emits blue fluorescence at 460 to 490 nm. The lymphocytes were immunocaptured by the antiCD3-MPs. As the particles are coated with polystyrene, they show green autofluorescence.[21] The CD4 receptors of the cells were labeled with the biotinylated antiCD4 antibody and Strep-Cy5 to achieve the fluorescence readout in red wavelength. Figure 4.2, panel A, shows the effectiveness of the selected system to achieve the CD4 counting, based on the magnetic immunoseparation and the CD4 labeling. Single binding of CD4 cells to the antiCD3-MPs is shown in Figure 4.2, panel B. Figure 4.2, panel C shows the 3D binding pattern achieved by treating the confocal images with the Imaris X64 v.6.2.0 software. CD4 cells are captured

by one or more magnetic particles. Some aggregates are also observed, due to multivalency of both antiCD3-MPs and CD4 cells.

Figure 4.2, panels D and F, shows single planes for the confocal images. The CD4 receptors (red dots) are distributed throughout the CD4 cell surface. The high expression of these receptors guarantees a high sensitivity and low limit of detection. Moreover, the binding of the CD4 receptor is not hindered by the antiCD3-MPs.

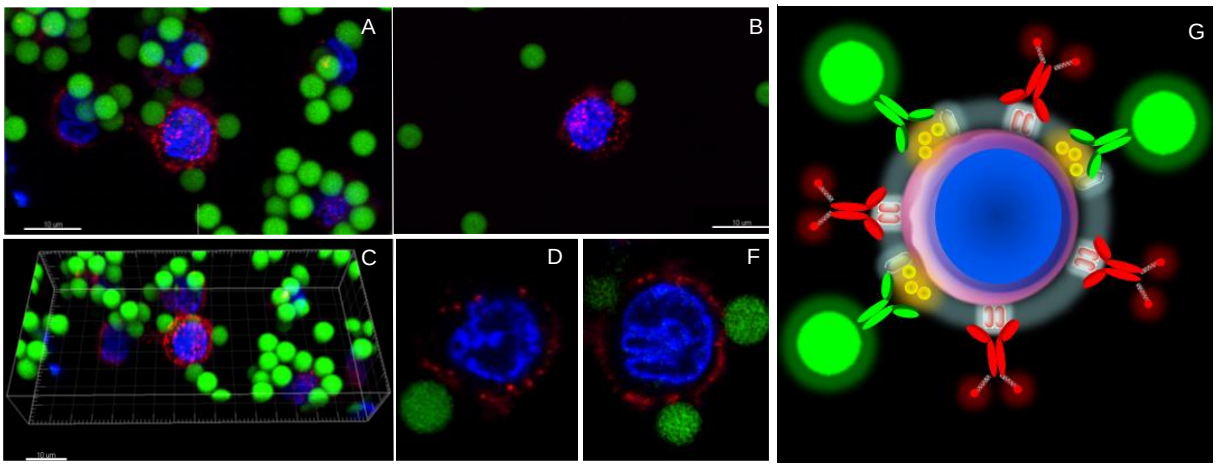

Figure 4.2. Confocal microscopy images of the CD4+ T lymphocyte (1×10^5) captured by antiCD3-MPs (8×10^5 magnetic particles) and labeled with biotinylated antiCD4 antibody/Strep-Cy5 system (36 ng mL^{-1} and 2 μg mL^{-1}). The nuclei of the CD4 cells were stained with the dye Hoechst in blue. Streptavidin conjugated to the fluorescent dye cyanine was used to visualize the biotinylated antiCD4 antibody attached to the CD4 receptor, as red dots. Magnetic particles are shown in green due to autofluorescent.

4.4.2 SEM study of the immunocaptured CD4 cells on the electrode surface

Scanning electron microscopy was used to evaluate the distribution on the magneto electrode surface of the magnetic particle bind to the CD4 cells after the magnetic actuation. 500 cells μL^{-1} of CD4+ T lymphocytes were captured with 8×10^5 antiCD3-MPs.

The Figure 4.3, panel A shows, at a resolution of 20 μm, the distribution of the MPs on the electrode surface, following the pattern of magnetic fields. In some areas including the center, agglomerates of MPs are shown, while in others the bare surface of the electrode can be clearly identified. The bare areas of the m-GEC electrode allow the mediator to reach the surface, granting the electrochemical readout. Figure 4.2 also shows the SEM images at a resolution of 2 (panels B to D), and 1 μm (panels E and F). The pictures illustrate the T lymphocytes (7-15 μm of diameter) attached to the spherical magnetic particles (4.5 μm of diameter). Some aggregates were observed due to the binding of two or more different magnetic particles with many lymphocyte cells (panels B

to D) as a result of multivalency. In most of the cases, the binding to the magnetic particles was achieved with more than one specific binding site on the lymphocyte, being the T lymphocytes surrounded by magnetic particles (panel E).

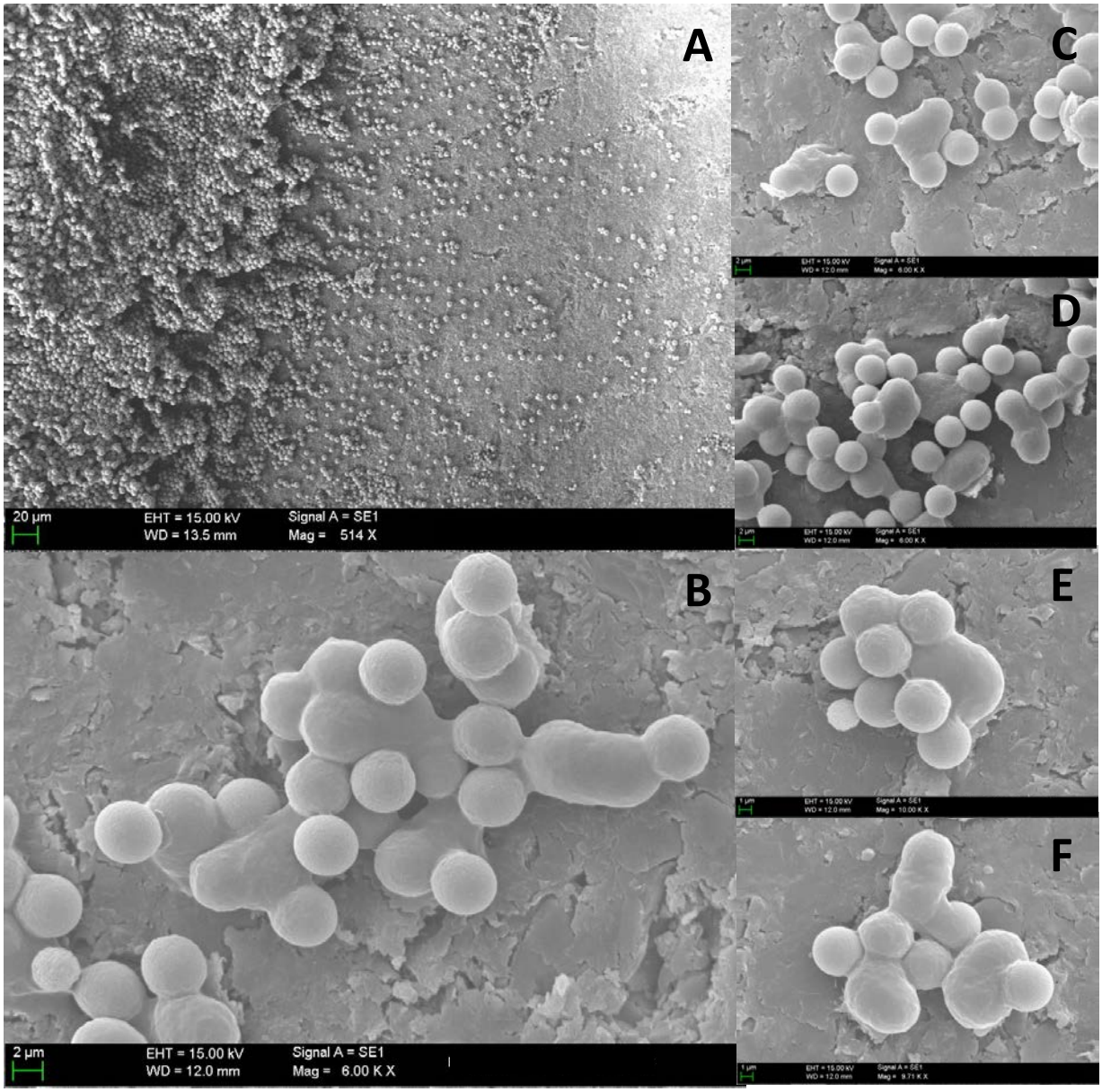

Figure 4.3. Scanning electron microphotographs of CD4 cells/antiCD3-MPs captured on the surface of m-GEC electrodes at different resolution levels. (A) 20 µm; (B) to (D), 2 µm; (E) and (F), 1 µm. In all cases, identical acceleration voltage (15 kV) was used.

4.4.3 CD4 counting magneto biosensor in whole blood

The CD4 counting magneto biosensor in whole blood was firstly optimized by changing the amount of the electrochemical reporter (streptavidin-HRP conjugate) and the antiCD3-MPs and, as

shown in Figure S4.6 and S4.7 (*§4.7.7*). Moreover, two different strategies were also performed by simplifying the labeling step into one to achieve analytical simplification, as schematically shown in Figure S4.8 (*§4.7.8*). Improved analytical performance was achieved by the simultaneous incubation of the CD4 cells with the antiCD3-MPs and the biotinylated antiCD4 antibody in one step, and doing in a consecutive step the incubation with the optical reporter (streptavidin-HRP). The results are presented in Figure S4.9. It seems that the binding of the biotinylated antiCD4 antibody to the CD4 cells is hindered by the electrochemical reporter, achieving thus better results when the incubation of the electrochemical reporter is performed in a separate step. A full discussion of the different procedures is presented in *§4.7.8*.

The electrochemical response of the CD4 counting magneto biosensor towards the CD4 cells (from 0 to 1150 cells μL^{-1}) in whole blood is shown in Figure 4.4, panel A. The CD4 cell range was chosen to include the concentration of clinical interest for CD4+ lymphocytes in AIDS diagnosis. The CD4 counting magneto biosensor was fitted using a nonlinear regression (Four Parameter logistic Equation– GraphPad Prism Software) (R^2=0.9862), as shown in Figure 4.4, panel B. The LOD was estimated by processing the negative control samples (n=16) (optimized leukocyte-depleted whole blood matrix by Ficoll-Paque/IMS) obtaining a mean value of 0.191 μA with a standard deviation (SD) of 0.060. The cut-off value was then determined with a one-tailed t test at a 95% confidence level, giving a value of 0.297 μA (shown in Figure 4.4, as the dotted lines). The LOD was found to be 44 CD4 cells μL^{-1}, being the logistic range from 89 to 912 CD4 cells μL^{-1}, including the whole range of clinical interest of CD4+ lymphocytes in AIDS diagnosis.

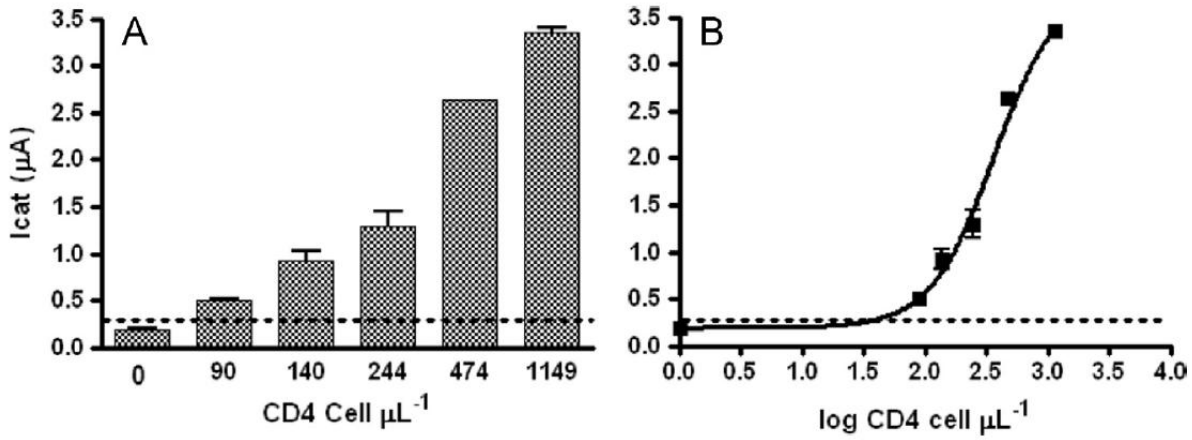

Figure 4.4. Calibration curve for detection of CD4 cells with the CD4 counting magneto biosensor in whole blood. The reagent concentrations were: 8×10^5 antiCD3-MPs, 36 ng mL^{-1} biotinylated antiCD4 antibody, 30 μg mL^{-1} streptavidin-HRP conjugate. In all cases, n=3, except for the negative control (n=16).

Spiked recovery was performed to assess the overall accuracy of the CD4 counting magneto immunoassay.[22] This method incorporates variables in assay preparation as well as the regression analysis. In this case, the recovery was performed by spiking to the leukocyte-depleted whole blood, low (200 cells μL^{-1}), medium (350 cells μL^{-1}), and high (500 cells μL^{-1}) concentration of CD4+ lymphocytes (quantified by flow cytometry) in the range of clinical interest for AIDS diagnosis and follow up. Table 4.1 shows the spiked recovery values obtained for the CD4 cell concentrations, ranging from 89 to 109 %.

Table 4.1. Recovery study for the CD4 counting magneto biosensor.

Actual concentration (cell μL^{-1}) by flow cytometry	Recovered concentration (cell μL^{-1}) / (SD)	% Recovery
500	457 / (57)	**91**
350	311 / (41)	**89**
200	218 / (10)	**109**

The CD4 counting magneto biosensor in whole blood showed also an outstanding reproducibility and reusability, as shown in Figure S4.10 (*§4.7.9*). No matrix effect was observed when comparing phosphate buffer and whole blood as matrixes (Figure S4.11 in the *§4.7.10*), confirming thus that the immunomagnetic separation completely removed the red cells (Figure S4.12) as well as other interfering molecules, which are not able to bind the antiCD3-MPs. Although there are only few examples of emerging technologies for CD4 cell count,[5] mostly of them based on cell counting by microscopy, the detection range was very narrow or only limited to few discrete values of CD4 cells [8,11-14] being thus these methods only useful for a specific stage of the disease. It is important to highlight the wider logistic range of detection for the CD4 counting magneto biosensor (from 89 to 912 CD4 cells μL^{-1}). This range ensures that this device can be used for the diagnosis of AIDS and the monitoring of the disease in any stage. For instance, 500 cells μL^{-1} is used not only for increasing the CD4 monitoring but also for initiating ART. Moreover, CD4 count thresholds are related to common HIV-associated-diseases, for instance pneumonia (<200 cells μL^{-1}), encephalitis (<100 cells μL^{-1}) or Mycobacterium (<50 cells μL^{-1}) coinfections, and should be taken into account for prophylaxis and treatment of associated-AIDS infection diseases.[23]

Although good correlation with the gold standard flow cytometry was obtained with some emerging technologies previously reported,[11,17] the CD4 counting magneto biosensor showed a lower LOD value (44 CD4 cells μL^{-1}), wider range of detection (from 89 to 912 CD4 cells μL^{-1}), higher specificity (because two receptors, CD4 and CD3, are used for the accurate identification of CD4 cells) and the advantage of being able to quantify CD4 cells. Moreover, the use of magnetic particles allows

the detection in whole blood without any sample pretreatment. The analytical performance of other CD4 counting sensors platforms, in terms of a) Assay format, b) Detection technique, c) Test matrix, d) Limit of detection (LOD), linear range are summarized in the Table S4.2 (*§4.7.11*).

4.5 Conclusions

Recent guidelines published by WHO recommend that diagnostic devices for developing countries to be ASSURED being this acronym defined by (A) *A*ffordable, (SS) *S*ensitive, *S*pecific, (U) *U*ser-friendly, (R) *R*apid and *R*obust, (E) *E*quipment free, and (D) *D*eliverable to those who need it. Although there are many commercially available methods for point of care HIV diagnosis, there is still the need for novel affordable alternatives to flow cytometry for CD4 count in order to monitor the AIDS disease and the treatment in low resource settings. In order to meet these demands, a CD4 counting electrochemical magneto biosensor for whole blood, based on the magnetic separation of the CD4 lymphocytes is presented for the first time. The integration of the antiCD3 magnetic particles provides specificity to the biosensor. As not only CD4 T lymphocytes express CD4 receptor but also other immunological cells (for instance monocytes, macrophages, and dendritic cells), the immunomagnetic separation of the CD4 lymphocytes by the CD3 receptor avoids interferences of other expressing CD4 receptor cells. Moreover, the magnetic particles also enhance the performance of the immunological reaction. Due to the improved washing and separation steps, the matrix effect of whole blood was eliminated. Therefore, the analysis of samples performed on magnetic particles is easily achieved in whole blood without any purification or pretreatment steps such as lysis or centrifugation, which is normally necessary for the gold standard flow cytometry, being an analytical simplification.

As the CD4 count must be quantitative, associated instrumentation is required. The electrochemical readout can be achieved with instrumentation designed to be low maintenance, battery/solar energy operated, and low cost, to meet the demands for ASSURED diagnosis recommended by WHO.

The CD4 counting electrochemical biosensor shows a LOD as low as 44 cells μL^{-1}, being the logistic range from 89 to 912 CD4 cells μL^{-1}, including the whole range of clinical interest of CD4+ lymphocytes in AIDS diagnosis and follow up.

The CD4 counting electrochemical biosensors presented in this work offers an exciting alternative, especially in countries with limited resources, as a rapid, cost-effective, analytical strategy that can be handled for unskilled personnel at the community and primary care level.

4.6 Acknowledgments

Financial support from BioMaX ‘‘Novel diagnostic bioassays based on magnetic particles’’, Marie Curie Initial Training Networks (FP7-PEOPLE-2010-ITN), the Ministry of Economy and Competitiveness (MINECO), Madrid (Project BIO2013-41242-R) and the Generalitat de Catalunya (Projects 2014 SGR 837) are gratefully acknowledged.

4.7 Supplementary Material

4.7.1 Composition of buffers and solutions

All buffer solutions were prepared with milliQ water and all other reagents were in analytical reagent grade (supplied from Sigma and Merck). The composition of these solutions was: phosphate buffer for electrochemical measurement (ePBS): 0.1 mol L^{-1} Na_2HPO_4, 0.1 mol L^{-1} KCl; PBS: 0.01 mol L^{-1} Na_2HPO_4, 0.15 mol L^{-1} NaCl, 2 mmol L^{-1} EDTA, pH 7.4; fixation buffer: 0.1 mol L^{-1} cacodylate, 1% glutaraldehyde solution, pH 7.4.

4.7.2 Cell culture

The CD4+ T cell clone PB100.29 was supplied by the Immunology Cellular Laboratory (Institute of Biotechnology and Biomedicine, UAB, Catalonia), and the cells were obtained by cloning the infiltrating lymphocytes from a pancreatic donor organ.[19] Rapid expansion method was adapted as follows: 40000 T-cell population were cultured in T25 flask containing 25 mL of IMDM media supplemented with 2 mmol L^{-1} L-Glutamine and 100 U mL^{-1} penicillin and 100 μg mL^{-1} streptomycin (all from Sigma-Aldrich), 10% human serum and 50 ng mL^{-1} OKT3 antibody with 25×10^6 γ-irradiated peripheral blood mononuclear cells and 5×10^6 γ-irradiated EBV-transformed lymphoblastoid cell line. Interleukin-2 was added at day 1 at 45 U mL^{-1} on day +1. Cells remained untouched during the first 5 days of culture, and then cells were split every 3-4 days. The cells were stained with Trypan Blue, and the viable cell concentration was determined by enumeration in a Neubauer counting chamber or by flow cytometry using absolute count microspheres.

4.7.3 Amperometric detection using the m-GEC electrodes

The electrochemical magneto-actuated biosensing strategy is based on amperometry, in the presence of hydrogen peroxide as a substrate of the enzyme and HQ as mediator to shuttle electrons between the m-GEC electrode and the horseradish peroxidase enzyme. The enzyme streptavidin-HRP conjugate is used as electrochemical reporter, since it is coupled to the CD4 cells by the reaction with the biotinylated anti-CD4 antibody. The mediator was regenerated by applying a reduction potential on the surface of the electrode being the current measured directly proportional to the concentration of HRP, when saturated substrate (H_2O_2) conditions were used, as shown in Figure S4.1 and, in detail, in Figure 4.1, panel C.

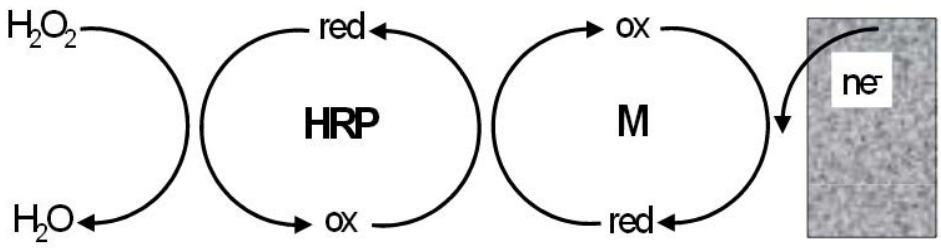

Figure S4.1. Enzymatic mechanism of the HRP enzyme in the surface of the m-GEC electrode, using H_2O_2 as a substrate of the enzyme and hydroquinone as a mediator.

In each measurement a steady-state current was obtained normally after 1 min of hydroquinone (1.8×10^{-3} mol L^{-1}) and hydrogen peroxide (1.1×10^{-3} mol L^{-1}) addition in phosphate buffer (ePBS), as mediator and substrate for the enzyme HRP respectively. After each use, the surface of the m-GEC electrodes were renewed by a simple polishing procedure, wetted with double-distilled water, and then thoroughly smoothed with abrasive paper and then with alumina paper (polishing strips 301044-001, Orion).[24]

4.7.4 Characterization of the m-GEC electrodes and selection of the applied potential for the amperometric measurements

The characterization of a batch of 5 electrodes (prepared as detailed in Ref.[24] as well as the selection of the applied potential for the amperometric readout was performed by cyclic voltammetry. The three-electrode setup (Ag/AgCl as reference electrode, the platinum as auxiliary electrode and m-GEC electrodes as working electrode) was immersed into the electrochemical cell containing 20 mL of phosphate buffer (ePBS) and the cyclic voltammetry were recorded from -1.00 V to +1.00 V, at a scan rate of 100 mV/s. Figure S4.2 shows the typical cyclic voltammograms obtained with the batch of 5 m-GEC electrodes, upon the addition of hydroquinone (1.8×10^{-3} mol L^{-1}) in phosphate buffer solution (ePBS). Outstanding reproducibility in the preparation of the m-GEC electrodes was achieved. Accordingly to Figure S4.2, a potential of -0.150 V corresponding to the reduction of the mediator was chosen for the amperometric readout in further experiments.

Renewal of the m-GEC electrodes. After each use, the surface of the m-GEC electrodes were renewed by a simple polishing procedure, wetted with double-distilled water, and then thoroughly smoothed with abrasive paper and then with alumina paper (polishing strips 301044-001, Orion).[24] Figure S4.3 shows the cyclic voltammograms obtained before and after the renewal of an m-GEC

electrode, upon the addition of hydroquinone (1.8×10^{-3} mol L^{-1}) in phosphate buffer solution (ePBS). No significant differences were observed with the same electrode submitted to the renewal processes of the surface by polishing.

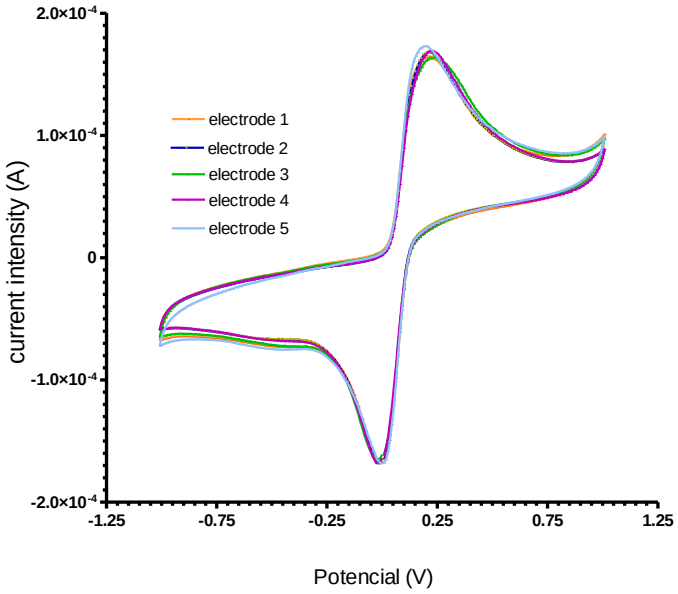

Figure S4.2. Typical cyclic voltammograms of a batch of 5 m-GEC electrodes upon the addition of 1.8 10^{-3} mol L^{-1} of hydroquinone in phosphate buffer pH= 7.0 vs. Ag/AgCl reference electrode.

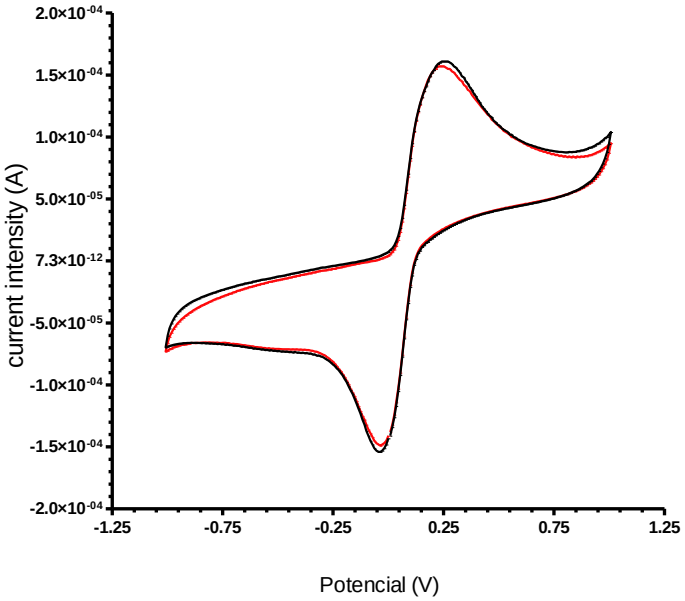

Figure S4.3. Cyclic voltammograms obtained before (red) and after (black) the renewal of an m-GEC electrode upon the addition of 1.8 10^{-3} mol L^{-1} of hydroquinone in phosphate buffer pH= 7.0 vs. Ag/AgCl reference electrode.

4.7.5 Ficoll-Paque depletion

Leukocyte-depleted whole blood matrix was prepared using Ficoll-Paque™ density gradient. Blood was diluted 1:1 with PBS, and layered onto Ficoll-Paque solution maintaining a 3:1 constant ratio of diluted blood: Ficoll. The blood was centrifuged at 1700 rpm for 25 min at room temperature. Differential migration during centrifugation results in the formation of layers, from the bottom to the top, containing the different cell types: red blood cells (erythrocytes); granulocytes; Ficoll-Paque; peripheral blood mononuclear cell –PBMC- (lymphocytes, platelets and monocytes); and plasma. The lymphocytes and the Ficoll layer were removed, and the plasma and erythrocytes phases were then mixed to generate the leukocyte-depleted whole blood matrix (As shown in Figure S4.4).

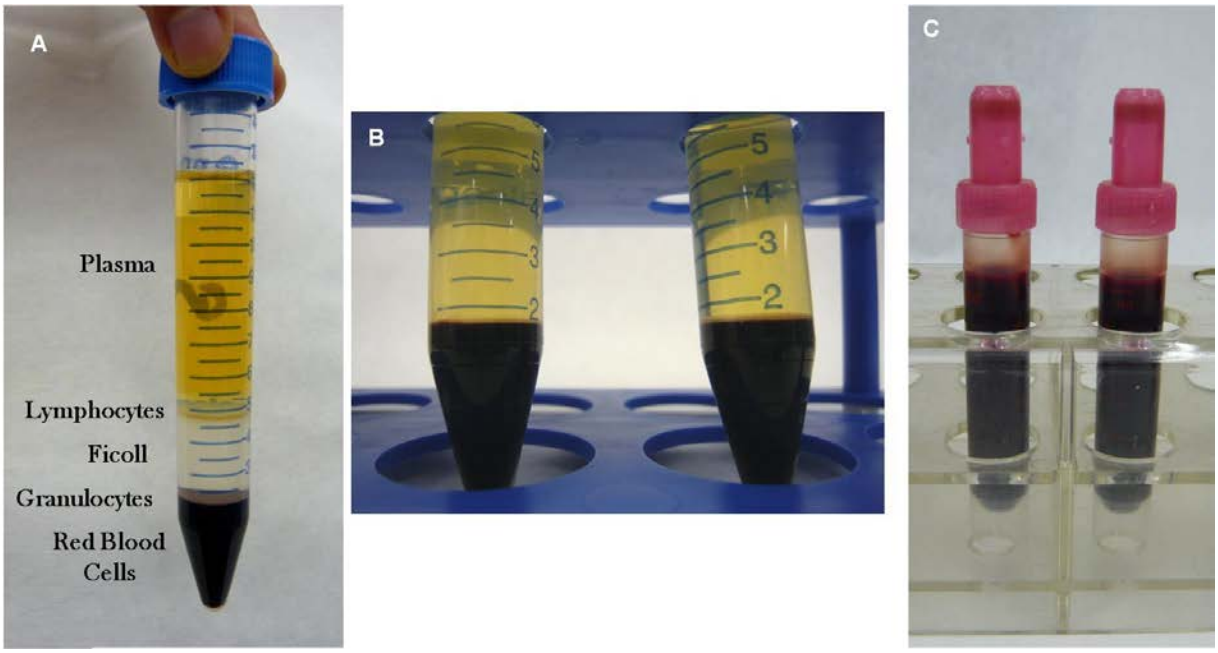

Figure S4.4. Leukocyte-depleted blood matrix by Ficoll-Paque™ depletion. The blood components were separated by density gradient centrifugation in Ficoll. After centrifugation, mononuclear cells remain at the plasma-Ficoll interface while granulocytes and erythrocytes in the sediment (A). Mononuclear cells and Ficoll layer were removed (B) in order to obtain a free lymphocyte blood matrix (C).

4.7.6 Lymphocyte depletion of whole blood

In order to obtain a complete lymphocyte depleted whole blood matrix, three different methods for the total leukocyte depletion from whole blood were tested, namely A) Ficoll-Paque depletion; B) Immunomagnetic separation with Dynabeads® CD3; and finally, C) a combination of both (Ficoll-Paque/IMS), as follows:

Ficoll-Paque depletion. Leukocyte-depleted whole blood matrix was prepared using Ficoll-Paque™ density gradient. Blood was diluted 1:1 with PBS, and layered onto Ficoll-Paque solution

maintaining a 3:1 constant ratio of diluted blood: Ficoll. The blood was centrifuged at 1700 rpm for 25 min at room temperature. Differential migration during centrifugation results in the formation of layers, from the bottom to the top, containing the different cell types: red blood cells (erythrocytes); granulocytes; Ficoll-Paque; PBMC (lymphocytes, platelets and monocytes); and plasma. The lymphocytes and the Ficoll layer were removed, and the plasma and erythrocytes phases were then mixed to generate the leukocyte-depleted whole blood matrix (As shown in Figure S4.4, *§4.7.5*).

IMS with Dynabeads® CD3 depletion. Dynabeads® CD3 are uniform, superparamagnetic beads (4.5 µm diameter) coated with a primary monoclonal antibody specific for the CD3 membrane receptor, mainly expressed on human mature T cells, for isolation or depletion cells from samples. Magnetic beads ($8x10^6$ beads per mL of blood) were added to the sample under continuous mixing to favor the binding of the magnetic beads to the target cells. After 30 min of shaking at 4 °C, the sample was placed on a magnet. The supernatant was removed to a new tube and the bead-bound cells were eliminated.

Ficoll-Paque/IMS with Dynabeads® CD3 depletion. Leukocyte-depleted whole blood matrix was prepared by Ficoll-Paque method. After that, the remains lymphocytes present in the matrix were removed by the incubation with Dynabeads CD3, as details above.

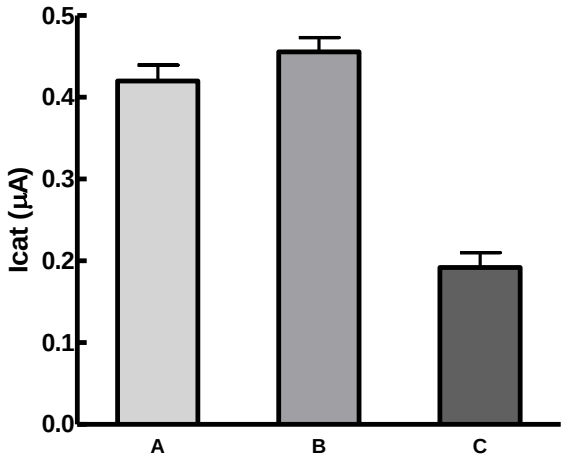

Figure S4.5. CD4 counting magneto-actuated biosensor in leukocytes depleted whole blood matrixes A) Ficoll-Paque depletion; B) IMS with Dynabeads® CD3; and finally, C) a combination of both Ficoll-Paque/IMS with Dynabeads® CD3. AntiCD3-MPs $8x10^6$ MPs mL^{-1}, biotinylated antiCD4 antibody 36 ng mL^{-1}, streptavidin-HRP 30 µg, n=16.

The Figure S4.5 shows comparatively the electrochemical readout obtained with the CD4 counting magneto-actuated biosensor in the three leukocytes depleted whole blood matrixes: A) Ficoll-Paque depletion; B) IMS with Dynabeads® CD3; and finally, C) a combination of both Ficoll-Paque/IMS with Dynabeads® CD3. According to the results, the combined method for leukocyte

depletion (Ficoll-Paque/IMS with Dynabeads® CD3) provided an almost complete lymphocyte depleted whole blood matrix. These results are in agreement with the flow cytometry results. The absolute CD4 count for A) Ficoll-Paque depletion; B) IMS with Dynabeads® CD3; and finally, C) a combination of both Ficoll-Paque/IMS, was found to be 88, 81 and 4 cells μL^{-1} respectively.

For further studies, the lymphocyte depleted whole blood matrix was used, by combining Ficoll-Paque depletion and IMS with Dynabeads® CD3, to achieve a whole blood matrix almost clean from lymphocytes (quantified by flow cytometry in 4 cells μL^{-1}).

4.7.7 CD4 counting magneto-actuated biosensor in whole blood. Optimization studies

The CD4 counting magneto-actuated biosensor in whole blood was optimized by changing the amount of antiCD3-MPs and streptavidin-HRP conjugate, as shown in Figure S4.6 and S4.7.

4.7.7.1 Streptavidin-HRP (electrochemical reporter)

100 µL of a sample (560 cells μL^{-1} in PBS) were added to 25 µL of antiCD3-MP3 ($8x10^5$ MPs) as well as 25 µL of biotinylated antiCD4 antibody (36 ng mL^{-1}) and were incubated for 30 min while shaking at 4 °C, followed by three washing step with PBS 0.1% BSA. After that, 100 µL of streptavidin-HRP conjugate (30, 60, 100 and 120 µg mL^{-1}) was added and incubated for 30 min while shaking at room temperature. After incubations, two washing step with PBS 0.1% BSA was done. Finally, the sample was resuspended in 140 µL of incubation solution and captured by dipping the magneto-electrode (m-GEC) inside the reaction tube. The modified m-GEC electrode was immersed into the electrochemical cell containing 20 mL of ePBS buffer and the amperometric determination was performed adding 1.8 $\times 10^{-3}$ mol L^{-1} hydroquinone (as mediator) and 1.11×10^{-3} mol L^{-1} hydrogen peroxide as enzymatic substrate. A potential of -0.150 V vs Ag/AgCl was applied.

As shown in Figure S4.6, the specific signal increased by increasing the electrochemical reporter concentration. However, the non-specific adsorption was also higher.

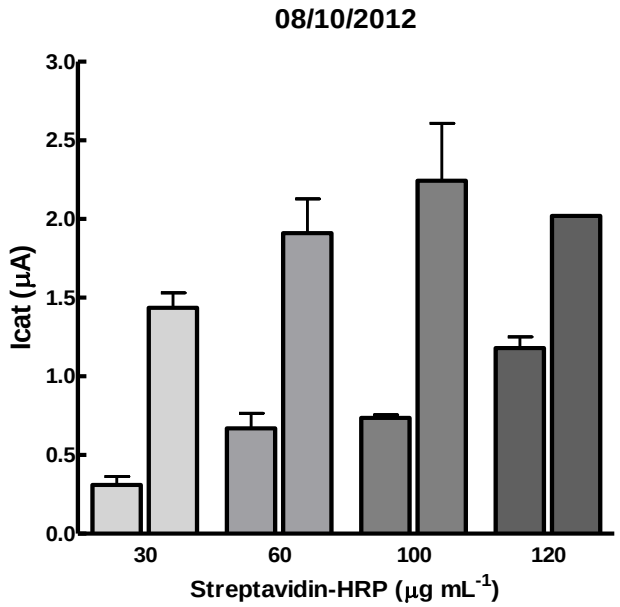

Figure S4.6. Optimization of the electrochemical reporter (streptavidin-HRP) by the evaluation of the signal-to-background ratio. 30, 60, 100 and 120 μg mL^{-1} of streptavidin-HRP were tested. In all cases the CD4 cell concentration was 560 cells μL^{-1}. 36 ng mL^{-1} biotinylated antiCD4 antibody and 8x 10^5 antiCD3-MPs were used per assay. The error bars show the standard deviation for n=3.

The concentration of streptavidin-HRP conjugate was optimized thus in 30 μg mL^{-1} based on the higher signal to background ratio, as shown in Table S4.1. This concentration was used for all subsequent experiments performed.

Table S4.1. Signal to background ratio for different of streptavidin-peroxidase concentration conjugate.

	Streptavidin-HRP (μg mL^{-1})			
CD4 (cells μL^{-1})	**30**	**60**	**100**	**120**
0	0.31	0.67	0.74	1.18
560	1.44	1.91	2.24	2.02
Signal-to-background ratio	4.6	2.9	3.1	1.7

4.7.7.2. antiCD3-MP concentration

100 μL of a sample (0, 160 y 720 cells μL^{-1} in PBS) were added to antiCD3-MPs (8x10^5; 1.33x10^5; 8x10^4) and 25 μL of biotinylated antiCD4 antibody (36 ng mL^{-1}) and were incubated for 30 min while shaking at 4 °C, followed by three washing steps with PBS 0.1% BSA. After that, streptavidin-HRP conjugate (30 μg mL^{-1}) was added and incubated for 30 min while shaking at room temperature. After incubations, two washing steps with PBS 0.1% BSA was done. Finally, the sample was resuspended in

140 µL of PBS 0.1% BSA and captured by dipping the m-GEC inside the reaction tube. The modified m-GEC electrode was immersed into the electrochemical cell containing 20 mL of ePBS buffer and the amperometric determination was performed adding 1.81 mmol L^{-1} hydroquinone (as mediator) and 1.11 mmol L^{-1} hydrogen peroxide as enzymatic substrate. A potential of -0.150 V vs Ag/AgCl was applied.

The amount of magnetic particles was optimized in 8×10^5 MP per assay. The signal obtained with this amount of MPs was the highest at both cell concentration levels (Figure S4.7). In addition, flow cytometry studies also confirmed that the higher is the magnetic particle concentration, the higher is the capture efficiency of the CD4 cells.

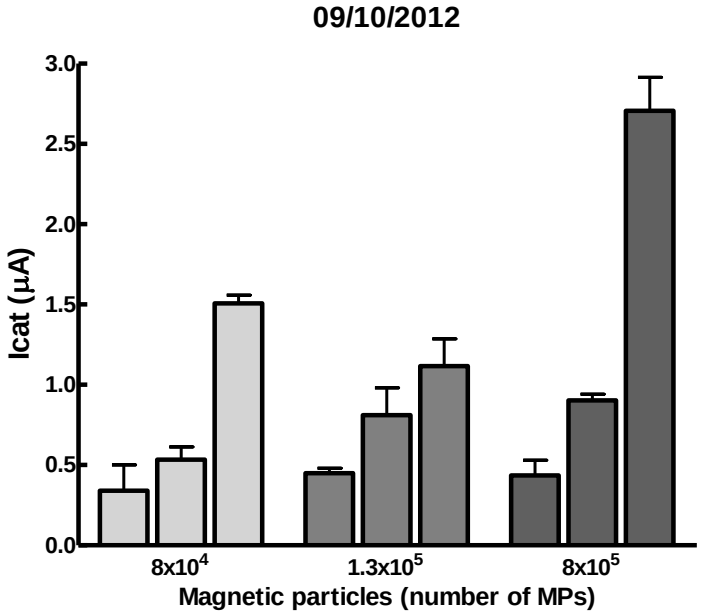

Figure S4.7. Optimization of antiCD3-MPs (8×10^4, 1.3×10^5, and 8×10^5). In all cases the CD4 cell concentrations were 0, 160 and 720 cells μL^{-1} (bars from left to right), 36 ng mL^{-1} of antiCD4-biotin and 30 µg mL^{-1} of streptavidin-HRP. The error bars show the standard deviation for n=3.

4.7.8 Optimization of the incubation steps

For the optimization of the CD4 counting electrochemical magneto-actuated biosensor, two different procedures were evaluated, which varied in the number of the immunological steps, as shown in Figure S4.8.

The CD4 counting electrochemical magneto-actuated biosensor was performed in whole blood. The exact concentration of the initial sample was determined by flow cytometry. Serial dilutions of whole blood at low concentration of CD4 cells were performed using an optimized leukocyte-depleted matrix. After each incubation or washing step, a magnetic separator was positioned under the tubes until pellet formation on the tube side wall, followed by supernatant separation.

Procedure A. Two incubation steps were performed. The first step involved the immunomagnetic separation of 100 µL of sample with 8×10^5 antiCD3-MPs and the labeling (in one step) with 36 ng mL^{-1} of biotinylated antiCD4 antibody by incubation for 30 min while shaking at 4 °C. The second incubation step involved the enzymatic labeling by adding 30 µg mL^{-1} of streptavidin-HRP for 30 min in slight agitation at room temperature.

Procedure B. All the reagent were added at the same time. 100 µL of sample were incubated with 8×10^5 antiCD3-MPs, 36 ng mL^{-1} of biotinylated antiCD4 antibody and 30 µg mL^{-1} of streptavidin-HRP for 30 min in slight agitation at 4 °C.

In all cases (procedures A and B) the electrochemical detection was performed by immersing the magneto-electrode into the electrochemical cell containing 20 mL of ePBS buffer and the amperometric determination was performed adding 1.8×10^{-3} mol L^{-1} hydroquinone (as mediator) and 1.11×10^{-3} mol L^{-1} hydrogen peroxide as enzymatic substrate. A potential of -0.150 V vs Ag/AgCl was applied.

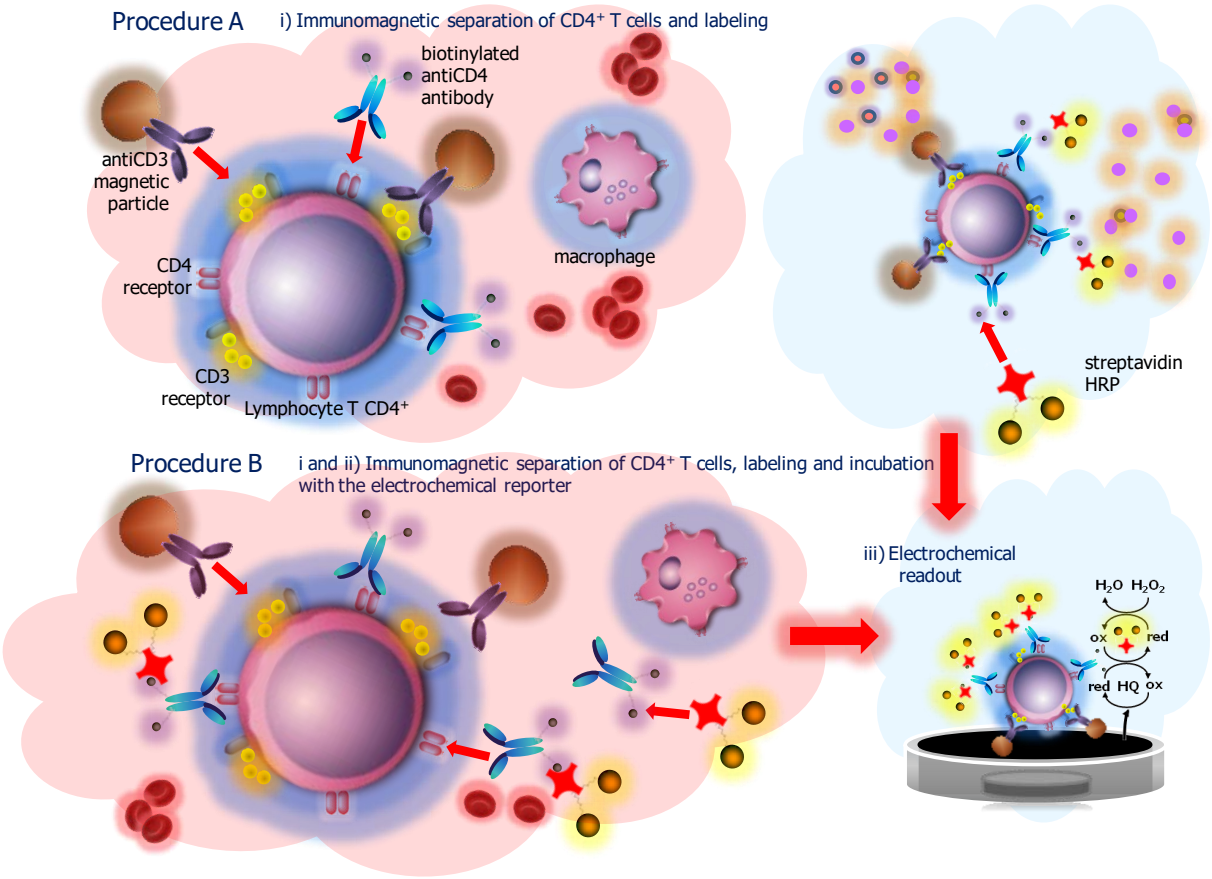

Figure S4.8. Schematic representation of the optimization of the incubation steps. Procedure A: two incubation steps. Procedure B: one incubation step, followed in both cases by the electrochemical readout.

The Figure S4.9 shows the signal obtained in each procedure under the same conditions of antiCD3-MPs, biotinylated antiCD4 antibody and streptavidin-HRP concentration.

As can be seen in the Figure S4.9, the procedure A is able to clearly distinguish the positive signal from the matrix at low concentration level, while the procedure B is not able to give a clear positive signal. From these results, it seems that the binding of the antiCD3-MPs and the biotinylated antiCD4 antibody are hindered and compete for the union with the membrane receptors CD3 or CD4, respectively. These molecules are expressed on the surface of T lymphocytes. The CD3 complex is a group of cell surface molecules that associates with the T-cell antigen receptor (TCR) and functions in the cell surface expression of TCR and in the signaling transduction cascade that originates when an antigen is recognized by the TCR. CD4 is a co-receptor that assists the TCR in communicating with an antigen-presenting cell. As shown in Figure S4.9, this effect is especially relevant in procedure B where the previous binding of the optical reporter (streptavidin-HRP) and the biotinylated antiCD4 antibody is achieved, resulting in a bigger macromolecular complex. The binding of the optical reporter seems to be hindered due to the big size of the magnetic particles (4.5 μm diameter) by steric hindrance.

Better results were achieved with procedure A. In this case, the fact of incubating antiCD3-MPs with the biotinylated antiCD4 antibody at the same time allows both reagents to have the same opportunity for binding their receptors, decreasing the steric hindrance. This procedure A was selected for further experiments due to the analytical performance.

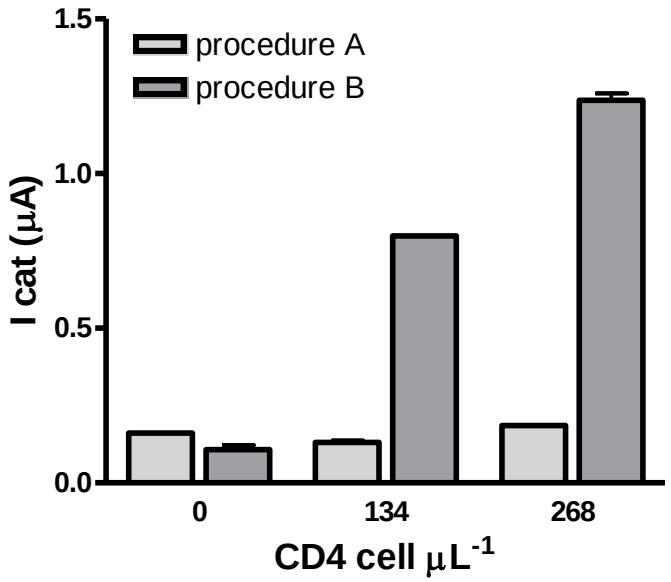

Figure S4.9. Optimization of the incubation steps. Procedure A: two incubation steps. Procedure B: one incubation step. In all cases, 8×10^5 antiCD3-MPs, 36 ng mL^{-1} of antiCD4-biotin and 30 μg mL^{-1} of streptavidin-HRP were used.

4.7.9 Reproducibility and reusability studies

The reproducibility of the procedure as well as the reusability of the m-GEC electrodes were evaluated with the set of 5 m-GEC electrodes of the same batch that were used for this study, by processing the same whole blood sample containing 250 CD4 cells μL^{-1}. The sample was prepared as follow: the exact concentration of the initial whole blood sample was firstly determined by flow cytometry. A dilution of whole blood was performed using the optimized leukocyte-depleted whole blood matrix (Ficoll-Paque/IMS), to achieve the concentration of 250 cells μL^{-1}. The same sample was evaluated with the set of 5 m-GEC electrodes. Moreover, for each electrode, three replicates were performed to evaluate the reusability of each electrode after the renewal of the surface by the polishing procedure. Figure S4.10 shows the results as vertical bar charts, where each bar shows the mean value for each of the five electrodes. The error bars represent the standard deviation of the mean value, by processing three replicates after the renewal of the surface of each electrode by the polishing procedure.

An outstanding reproducibility in the procedure, as well as in the construction of the set of the 5 m-GEC electrodes was observed, since similar mean values were achieved despite of the electrode used. Moreover, each electrode shows an excellent reusability upon renewal of the surface, since very low standard deviation values were observed.

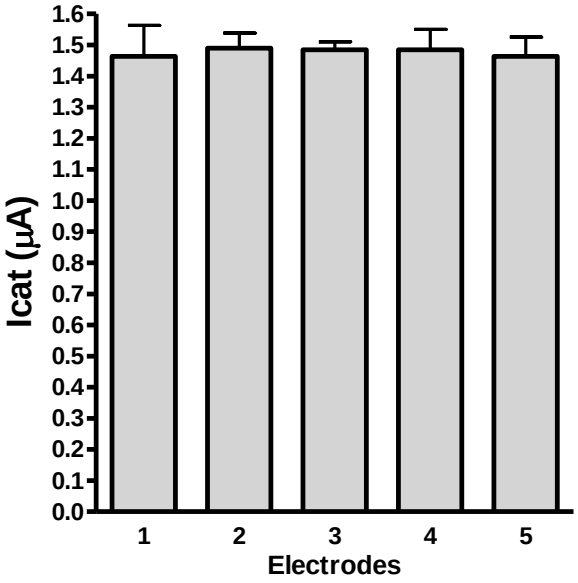

Figure S4.10. Reproducibility and reusability study performed on a set of 5 m-GEC electrodes for detection of CD4 cells with the CD4 counting magneto-actuated biosensor in whole blood containing 250 cells μL^{-1}. In all cases, 8×10^5 antiCD3-MPs, 36 ng mL^{-1} of antiCD4-biotin and 30 μg mL^{-1} of streptavidin-HRP were used. The replicates (n=3) were performed with the same electrode under three renewal processes of the surface by polishing.

4.7.10 Matrix effect study

The matrix effect is defined as the combined effect of all components of the sample other than the analyte on the measurement of the quantity and consists of a bias in the analyte determination performed in different matrixes. The electrochemical response of three different concentrations of CD4+ T lymphocytes spiked in two different matrixes (whole blood and PBS) was thus compared. A number of cultured CD4+ lymphocytes were centrifuged, quantified by flow cytometry and resuspended in an exact volume of matrix (leukocyte-depleted whole blood matrix by Ficoll-Paque/IMS and PBS) in order to reach 450 cells μL^{-1}. Subsequently two serial dilutions of 1:1 sample:matrix were performed reaching concentrations of 225 and 112 cells μL^{-1}. The results in the Figure S4.11 shows the electrochemical response obtained with PBS buffer and whole blood matrix at CD4+ lymphocyte concentration of 112, 225 and 500 cells μL^{-1}, performed by three replicates.

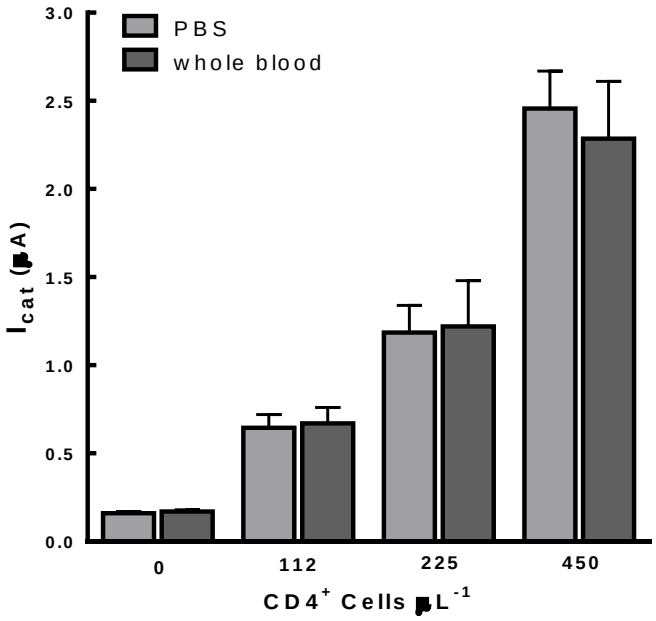

Figure S4.11. Matrix effect study for detection of CD4 cells spiked in PBS and whole blood from 0 to 450 cells μL^{-1}, with the CD4 counting magneto-actuated biosensor. In all cases, 8×10^5 antiCD3-MPs, 36 ng mL^{-1} of antiCD4-biotin and 30 μg mL^{-1} of streptavidin-HRP were used. n=3.

As shown in the Figure S4.11, the electrochemical response is quite similar for both PBS buffer and whole blood. Nevertheless, the standard deviations in whole blood is a slightly higher than in PBS buffer. As the selectivity of a method refers to the extent to which it can determine particular analyte(s) in a complex mixture without interference from other components in the mixture, from these results can be concluded that the combination of the immunomagnetic separation performed with magnetic particles for capturing the cells from the complex samples, together with the

electrochemical readout performed with an specific antibody, confirmed that this is an specific method for the determination of CD4 cells in whole blood without any sample pretreatment. The Figure S4.12 shows the aspect of the whole blood matrix before (left panel) and after (right panel) the IMS and washing steps. The red cells as well as other interfering molecules which are not able to bind the antiCD3-MPs are completely removed due to the magnetic actuation.

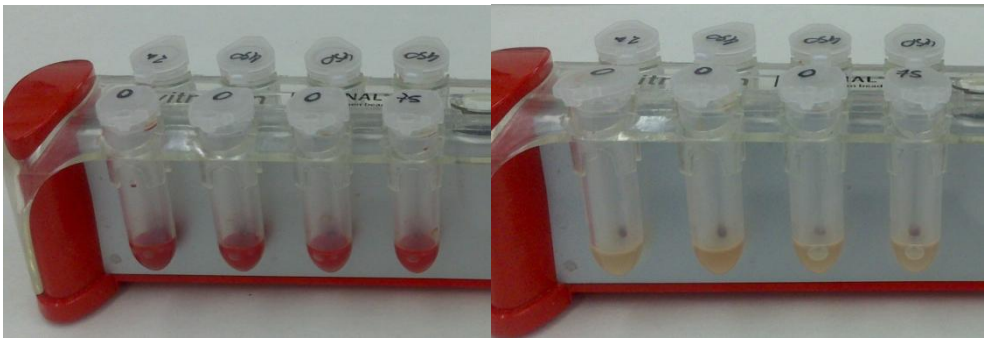

Figure S4.12. Aspect of the whole blood matrix before (left panel) and after (right panel) the IMS and the first washing step. The red cells as well as other interfering molecules which are not able to bind the antiCD3-MPs are completely removed due to the magnetic actuation.

4.7.11 Main features of methodologies for the CD4 counting.

Assay format	Detection	Test matrix	LOD/linear range	Description	Ref
Quartz crystal microbalance	Piezoelectric detection	Jurkat cells (CD4+ lymphocytes)	NR / from 0 to 600 μL^{-1} (exponential response)	-No real samples tested. -CD4 cells immobilized to the surface of gold coated quartz microbalance -Monocyte interference on the detection was not tested.	Bachelder, 2005[25]
Microfluidic cell chromatography	Impedance spectroscopy	HIV infected samples	Not specified	- Portable device (less than 3 kg) with test results in 10 min -High sensitivity (~90-100%) and medium specificity (~70-90%) -Good correlation with FC - Under evaluation studies (stability studies)	Daktari[26]
MP based immunoassay on microfluidic device	Optical detection (manual count based on microscopy)	Lymphocyte solution in phosphate buffer (100 μL)	NR/NR	-PDMS chip on a fluidic platform -Capture efficiency depend of the chamber length -Monocyte differentiation by controlling the shear stress	Gao, 2010[27]
Disposable microfluidic, dual force device (fluidic and magnetic)	Optical detection (bright-field)	HL60 cells spiked to depleted blood (less than 10 μL)	NR / linear response from 0 to 1600 cell μL^{-1} (few points determined: 0-500-1000 and 1600 cells μL^{-1})	-Magnetophoretic isolation of CD4 cells from whole blood using magnetic beads. - High efficiency capture (93.0 ± 3.3%)	Glynn, 2014[28]
Label free optofluidic ring resonator (OFRR) biosensor	Optical detection	Human lymphocyte in phosphate buffer	Tested at 160, 200, 250 and 300 cells μL^{-1}	- Regeneration of the immobilization surface after each measurement -Non linear relationship due to the saturation of the detector.	Gohring, 2010 [**¡Error! Marcador no definido.**]

LOD= Limit of detection; NR= Not reported; FC= Flow cytometry; LOA= Limit of agreement; SD= Standard deviation.

4.7.11 Main features of methodologies for the CD4 counting (continued).

Assay format	Detection	Test matrix	LOD/linear range	Description	Ref
Quantitative microchip based on electrochemical impedance biosensor with electrode pixels.	Impedance spectroscopy (working electrode pixels)	J45.01 cells as mimic of human CD4+ T Lymphocyes	NR /NR	-Cells captured on electrode pixels, and detected individually by monitoring the interfacial impedance changes on each independent pixel (system "on-off"). -Tested with very low amount of cells, limited to the pixel numbers (200 pixels). -High fabrication cost	Jiang & Spencer, 2010[15]
MBio SnapCount System based on static imaging cytometry	Optical detection (laser-based illumination approach combined with planar waveguide technology)	HIV infected samples (10μL)	NR/NR	-60-80 samples in a day -Disposable cartridge for CD4 enumeration -LOA= -132 to 112 cells μL^{-1} and -92 to 96 for clinically relevant samples	Logan, 2013[29]
Electrical Micro-biosensor chip with planar microelectrodes	Impedance	Peripheral blood mononuclear cells (PBMC) from human blood resuspended in phosphate buffer	NR/NR	-Poor correlation with the number of captured cells -Required lysed cells or PBMC for most consistent results. -Results highly dependent on the specimen preparation method used	Mishra, 2005[¡Error! Marcador no definido.]
Portable and label free microchip CD4 count platform	CCD sensor (shadow detection)	HIV infected samples (10μL-50μL)	NR/NR	- Environmental and operator dependence under real world conditions of resource limited settings -Capture efficiency depends on cell concentration -Samples cleanliness to avoid the identification of artifacts as cells -Good correlation with FC in top lab but poor in African lab	Moon, 2009 & 2011[¡Error! Marcador no definido.,30]

LOD= Limit of detection; NR= Not reported; FC= Flow cytometry; LOA= Limit of agreement; SD= Standard deviation.

4.7.11 Main features of methodologies for the CD4 counting (continued).

Assay format	Detection	Test matrix	LOD/linear range	Description	Ref
Lens-free cell platform coupled to and opto-electronic sensor array (LUCAS)	opto-electronic sensor	Proof-of-concept. Tested in fibroblasts, red blood cells, white blood cells and murine stem cells	NR/NR	-Does not use optical components (lenses or microscope objectives) -LUCAS can be chosen to be a top-of-shelf 'charged-coupled device' (CCD) or a 'complementary metal-oxide semiconductor' (CMOS). -LUCAS can be integrated in different microfluidic devices.	Ozcan & Demirci 2008 [31]
Fluorescent fluidic microchip	Optical detection (fluorescence)	HIV-infected samples (33 μL)	NR/ 0-200 cell μL^{-1}	-Cell capture on PMMA membrane (Filtering of lymphocytes) -Miniaturized flow cell with digital image analysis - Good correlation with FC (r=0.95)	Rodriguez, 2005 [32]
Chemiluminescent microfluidic device	Chemiluminescence	HIV-infected samples (3μL)	NR/ 100-800 cell μL^{-1}	- Semiquantitative microfluidic platform -Cell capture based on an immunoaffinity microchannel - Good sensitivity, high SD -Nonspecific binding of blood cells via nonspecific adsorption on the surface.	Wang, 2009 [33]
Differential cell counter device using the reverse-flow technique and cell immunoaffinity chromatography.	Electrical impedance sensor and immunoaffinity chromatography	Purified leukocyte from healthy donors (5μL)	NR / from approximately 100 to 700 cells per μL	-Monocytes removed by a controlled shear stress, however, it causes a positive bias for counts below 200 cells μL^{-1} (20% of the captured cells are monocytes). -Erythrocytes lysis off-chip is required. -Low capture efficiency (60%) due to a short time of interaction with the antibody.	Watkins, 2011 [¡Error! Marcador no definido.]
Magneto-actuated electrochemical biosensor	Amperometry	Leukocytes from healthy donors (whole blood)	44 cells μL^{-1}, linear range from 89 to 912 cells μL^{-1}	-The integration of MP provides specificity to the biosensor and avoids the matrix effect. -High specificity and sensitivity due to the use of two receptors. -Not interference from monocyte - Sample pretreatment not required	This study

LOD= Limit of detection; NR= Not reported; FC= Flow cytometry; LOA= Limit of agreement; SD= Standard deviation.

4.8 References

[1] Joint United Nations Programme on HIV/AIDS (UNAIDS). (2013). Global report: UNAIDS report on the global AIDS epidemic 2013. Geneva: UNAIDS.

[2] World Health Organization. (2005). Interim WHO: clinical staging of HIV/Aids and HIV/Aids case definitions for surveillance: African region. Geneva: WHO.

[3] World Health Organization. (2004). CD4+ T-Cell enumeration technologies. Technical information. Geneva: WHO.

[4] World Health Organization. (2013). Consolidated guidelines on the use of antiretroviral drugs for treating and preventing HIV infection: Recommendations for a public health approach.

[5] Carinelli, S., Martí, M., Alegret, S., Pividori, M. I. (2015). Biomarker detection of global infectious diseases based on magnetic particles. New biotechnology, 32(5), 521-532.

[6] Boyle, D. S., Hawkins, K. R., Steele, M. S., Singhal, M., Cheng, X. (2012). Emerging technologies for point-of-care CD4 T-lymphocyte counting. Trends in biotechnology, 30(1), 45-54.

[7] Diaw, P. A., Daneau, G., Coly, A. A., Ndiaye, B. P., Wade, D., Camara, M., Mboup, S., Kestens, L., Dieye, T. N. (2011). Multisite evaluation of a point-of-care instrument for CD4+ T-cell enumeration using venous and finger-prick blood: the PIMA CD4. JAIDS Journal of Acquired Immune Deficiency Syndromes, 58(4), e103-e111.

[8] Lutwama, F., Serwadda, R., Mayanja-Kizza, H., Shihab, H. M., Ronald, A., Kamya, M. R., Thomas, D., Johnson, E., Quinn, T. C, Moore, R. D., Spacek, L. A. (2008). Evaluation of Dynabeads and Cytospheres compared with flow cytometry to enumerate CD4+ T cells in HIV-infected Ugandans on antiretroviral therapy. Journal of acquired immune deficiency syndromes (1999), 48(3), 297-303.

[9] de Wit, T. F. R. (2008). Affordable CD4 T-cell Enumeration and HIV/AIDS Viral Load Monitoring in Resource-poor Settings. In Global HIV/AIDS Medicine (pp. 649-660). Rinke de Wit, T.F., (2007). Affordable CD4 T-cell enumeration and HIV/AIDS Viral Load monitoring in resource-poor settings, in: Volberding, P. A.; Sande, M.A.; Greene, W. C.; Lange J., Gallant J. (Eds.), Global HIV/AIDS Medicine, Elsevier: New York, pp. 649-660

[10] Carrière, D., Vendrell, J. P., Fontaine, C., Jansen, A., Reynes, J., Pagès, I., Holzmann, C., Laprade, M., Pau, B. (1999). Whole blood Capcellia CD4/CD8 immunoassay for enumeration of CD4+ and CD8+ peripheral T lymphocytes. Clinical chemistry, 45(1), 92-97.

[11] Cheng, X., Irimia, D., Dixon, M., Ziperstein, J. C., Demirci, U., Zamir, L., Tompkins, G. T., Toner, M., Rodriguez, W. R. (2007). A microchip approach for practical label-free CD4+ T-cell counting of HIV-infected subjects in resource-poor settings. JAIDS Journal of Acquired Immune Deficiency Syndromes, 45(3), 257-261.

[12] Gohring, J. T., Fan, X. (2010). Label free detection of CD4+ and CD8+ T cells using the optofluidic ring resonator. Sensors, 10(6), 5798-5808.

[13] Moon, S., Gurkan, U. A., Blander, J., Fawzi, W. W., Aboud, S., Mugusi, F., Kuritzkes, D.R., Demirci, U. (2011). Enumeration of CD4+ T-cells using a portable microchip count platform in Tanzanian HIV-infected patients. PloS one, 6(7), e21409.

[14] Thorslund, S., Larsson, R., Bergquist, J., Nikolajeff, F., Sanchez, J. (2008). A PDMS-based disposable microfluidic sensor for CD4+ lymphocyte counting. Biomedical microdevices, 10(6), 851-857.

[15] Jiang, X., Spencer, M. G. (2010). Electrochemical impedance biosensor with electrode pixels for precise counting of CD4+ cells: A microchip for quantitative diagnosis of HIV infection status of AIDS patients. Biosensors and Bioelectronics, 25(7), 1622-1628.

[16] Mishra, N. N., Retterer, S., Zieziulewicz, T. J., Isaacson, M., Szarowski, D., Mousseau, D. E., Lawrence, D.A., Turner, J. N. (2005). On-chip micro-biosensor for the detection of human CD4+ cells based on AC impedance and optical analysis. Biosensors and Bioelectronics, 21(5), 696-704.

[17] Watkins, N. N., Sridhar, S., Cheng, X., Chen, G. D., Toner, M., Rodriguez, W.,Bashir, R. (2011). A microfabricated electrical differential counter for the selective enumeration of CD4+ T lymphocytes. Lab on a Chip, 11(8), 1437-1447.

[18] Pividori, M. I., Alegret, S. (2005). Electrochemical genosensing based on rigid carbon composites. A review. Analytical letters, 38(15), 2541-2565.

[19] Xufré, C., Costa, M., Roura-Mir, C., Codina-Busqueta, E., Usero, L., Pizarro, E., Obiols, G., Jaraquemada, D., Martí, M. (2013). Low frequency of GITR+ T cells in ex vivo and in vitro expanded Treg cells from type 1 diabetic patients. International immunology, 25(10), 563-574.

[20] Chosewood, L.C., Wilson, D.E. (2009). Biosafety in Microbiological and Biomedical Laboratories. 5th ed. US Health and Human Services Publication No. (CDC) 21-1112.

[21] Nurmukhametov, R. N., Volkova, L. V., Kabanov, S. P. (2006). Fluorescence and absorption of polystyrene exposed to UV laser radiation. Journal of Applied Spectroscopy, 73(1), 55-60.

[22] Wild, D. (2001). The Immunoassay Handbook. 2nd. Ed. Nature Publishing Group, pp 78–110.

[23] Panel on Opportunistic Infections in HIV-Infected Adults and Adolescents. Guidelines for the prevention and treatment of opportunistic infections in HIV-infected adults and adolescents: recommendations from the Centers for Disease Control and Prevention, the National Institutes of Health, and the HIV Medicine Association of the Infectious Diseases Society of America. Available in https://aidsinfo.nih.gov/contentfiles/lvguidelines/adult_oi.pdf

[24] Zacco, E., Pividori, M. I., Alegret, S., Galve, R., Marco, M. P. (2006). Electrochemical magnetoimmunosensing strategy for the detection of pesticides residues. Analytical chemistry, 78(6), 1780-1788.

[25] Bachelder, E. M., Ainslie, K. M., Pishko, M. V. (2005). Utilizing a quartz crystal microbalance for quantifying CD4+ T cell counts. Sensor Letters, 3(3), 211-215.

[26] www.daktaridx.com/

[27] Gao, D., Li, H. F., Guo, G. S., Lin, J. M. (2010). Magnetic bead based immunoassay for enumeration of CD4+ T lymphocytes on a microfluidic device. Talanta, 82(2), 528-533.

[28] Glynn, M. T., Kinahan, D. J., Ducrée, J. (2014). Rapid, low-cost and instrument-free CD4+ cell counting for HIV diagnostics in resource-poor settings. Lab on a Chip, 14(15), 2844-2851.

[29] Logan, C., Givens, M., Ives, J. T., Delaney, M., Lochhead, M. J., Schooley, R. T., Benson, C. A. (2013). Performance evaluation of the MBio Diagnostics point-of-care CD4 counter. Journal of immunological methods, 387(1-2), 107-113.

[30] Moon, S., Keles, H. O., Ozcan, A., Khademhosseini, A., Hæggstrom, E., Kuritzkes, D., Demirci, U. (2009). Integrating microfluidics and lensless imaging for point-of-care testing. Biosensors and Bioelectronics, 24(11), 3208-3214.

[31] Ozcan, A., Demirci, U. (2008). Ultra wide-field lens-free monitoring of cells on-chip. Lab on a Chip, 8(1), 98-106.

[32] Rodriguez, W. R., Christodoulides, N., Floriano, P. N., Graham, S., Mohanty, S., Dixon, M., Hsiang, M., Peter, T., Zavahir, S., Thior, I., Romanovicz, D., Bernard, B., Goodey, A.P., Walker, B.D., McDevitt, J.T. (2005). A microchip CD4 counting method for HIV monitoring in resource-poor settings. PLoS medicine, 2(7), e182.

[33] Wang, Z., Chin, S. Y., Chin, C. D., Sarik, J., Harper, M., Justman, J., Sia, S. K. (2009). Microfluidic CD4+ T-cell counting device using chemiluminescence-based detection. Analytical chemistry, 82(1), 36-40.

Chapter 5

INTERFERON GAMMA TRANSCRIPT DETECTION ON T CELLS BASED ON MAGNETIC ACTUATION AND MULTIPLEX DOUBLE-TAGGING ELECTROCHEMICAL GENOSENSING

Biosensors and Bioelectronics 117 (2018) 183-190

5.1 Abstract

Interferon-γ is a proinflammatory cytokine, and its production is related with effective host defense against intracellular pathogens. Therefore, the level of interferon-γ is considered a good biomarker for intracellular infections. It is also useful for the assessment, treatment progression and follow-up of non-communicable diseases, including cancer and autoimmune disorders, among others. This work addresses the development of a novel interferon-γ release assay to evaluate the expression of interferon-γ transcripts as biomarker produced by isolated T cells, as a main advantage. The method sequentially combined three different types of magnetic separation, including the immunomagnetic separation of the T cells performed on antiCD3 modified magnetic particles, the retrotranscription and multiplex double-tagging PCR on polydT-modified magnetic particles and, finally, the electrochemical genosensing on streptavidin magnetic particles as a support. This approach is able to quantify the levels of cellular interferon-γ produced by as low as 150 T cells with outstanding analytical features. The detection of interferon-γ transcripts is performed from only 100 µL of whole blood which can be potentially obtained by fingerprick, demonstrating a further clear advantage to be considered as a promising strategy for the quantification of this important biomarker in several clinical applications.

5.2 Introduction

Interferon gamma (IFN-γ) is a proinflammatory cytokine produced by activated natural killer cells, NKT cells, effector T CD4+ cells (T helper 1 cells, Th1) and CD8+ T cells (cytotoxic T cells) during the immune response against intracellular pathogens, such as virus and bacteria.[1] Individuals with deficiency in either IFN-γ production, receptor expression or the signaling pathway (IL-2/IL-23/IFN-γ) show high incidence of infections due to Salmonella or intracellular bacteria as Mycobacterium [2,3] and viruses.[4] On the contrary, the increased production of IFN-γ is associated to an improved anti-tumor response,[5] and plays also an important role in autoimmune disorders,[6,7] for instance in Systemic Lupus Erythematosus [8] and psoriasis,[9] among others. Interferon-γ release assay (IGRA) is based on the production and quantification of IFN-γ upon in vitro stimulation of the T lymphocytes with specific antigens. In detail, the assay is performed by 24 h incubation of 1 mL whole blood from the patients, containing the T lymphocytes, with the antigen, followed by centrifugation and the

quantification on the supernatant of the released IFN-γ by ELISA. This test can be potentially used in the diagnosis of all the diseases based on cell-mediated immunity, and the specificity is provided by the stimulation of the T lymphocytes with the antigens driving the immune response. However, it is especially useful in routine clinical practice for the diagnosis of latent tuberculosis (TB).[10] Latent TB infection is a non-communicable asymptomatic condition which can turn into active TB in people who have a weak immune system. Lately, TB incidence is increased due to HIV coinfection,[11] and anti-TNF alpha immunotherapy in rheumatic diseases.[12] The diagnosis of latent TB is usually performed by the Tuberculin skin test based on the intradermic injection of a purified protein from Mycobacterium. However, this test can provide false positives due to exposure to non-tuberculous *Mycobacteria* as well as the previous vaccination with BCG (Bacillus Calmett-Guérin). Besides, this test is time consuming (up to 48–72 h). Identification and treatment of latent TB can substantially reduce the risk of developing active TB and is a worldwide major focus of TB control. However, identification of all persons with latent TB would require screening large numbers of low-risk individuals that would not be cost-effective with the current IGRA test.[10] There are two IGRA kits currently in the market for the diagnosis of Latent TB: QuantiFERON-TB Gold (Qiagen, The Netherlands) and T-SPOT.TB (Oxford Immunotec, UK). Several studies compare the efficiency of both methods [13-15] and their principles are detailed discussed in *§5.7.1.1* and Table S5.1. Individuals infected with Mycobacterium tuberculosis usually have lymphocytes in their blood that recognize the mycobacterial antigens, generating and secreting IFN-γ. Another commercial application of IGRA test is the QuantiFERON-CMV (Qiagen), which was developed for the detection of human cytomegalovirus (CMV) reactivation after transplantation.[16] The transplanted patients at risk to developed CMV disease produced a minimal IFN-γ response. In this paper, a novel IGRA test based on electrochemical for the detection of IFN-γ transcripts produced by isolated T lymphocytes is described. To the extent of our knowledge, this is the first time that a biosensor for the detection of IFN-γ transcripts produced by isolated T cells is reported. This approach combines the advantages of the integration of magnetic particles (MPs) for the preconcentration and isolation of different targets (including whole T cells, mRNA transcripts and double-tagged DNA) for the assessment of IFN-γ expression by T cells. Firstly, the method involves the preconcentration of T lymphocytes from whole blood by immunomagnetic separation on magnetic particles modified with the antiCD3 antibody.[17] The messenger RNA is then released and isolated on polydT-MPs, followed by retrotranscription to obtain cDNA (complementary DNA). The cDNA is amplified on beads by a multiplex double-tagging PCR using a double-tagging set of primers specific for IFN-γ and glyceraldehyde-3-

phosphate dehydrogenase (GAPDH) as housekeeping gene control. Finally, the simultaneous electrochemical magneto-genosensing of the two transcripts is performed on streptavidin-magnetic particles as a support.[18,19] As summarized in Table S5.1 (*§5.7.1.1*) the main advantages of this method compared with the commercial available IGRA test is that the T cells producing IFN-γ are specifically separated from whole blood by immunomagnetic separation, thus increasing the sensitivity of the assay and removing potentially interfering substances that can affect test results. Moreover, the electrochemical genosensor detects the IFN-γ mRNA while other methods are based on the determination of IFN-γ (protein). Furthermore, the electrochemical genosensor has the advantage of combining high sensitivity/specificity as well as simplicity of instrumentation, and can be easily expanded into multiplex detection platform. Finally, the detection of IFN-γ transcripts is performed from only 100 µL of blood which can be potentially obtained by fingerprick, demonstrating a further clear advantage over commercial IGRA test requiring up to 4–5 mL of blood obtained by extraction (Table S5.1, *§5.7.1.1*). Therefore, the development of the electrochemical sensing platform is a significant step towards a low cost, sensitive, and specific transcript detection of IFN-γ.

5.3 Experimental section

5.3.1 Chemicals and Biochemicals

Magnetic particles modified with antiCD3 antibody (antiCD3-MPs) (Dynabeads™ CD3 Prod. No. 111-51D, 4.5 µm diameter), MPs modified with polydT (polydT-MPs) (Dynabeads® Oligo $(dT)_{25}$ Prod. No. 610.02, 2.8 µm diameter) and MPs modified with streptavidin, (streptAv-MPs) (Dynabeads™ M-280 streptavidin Prod. No. 112.05, 2.8 µm diameter), SuperScript™ III Reverse Transcriptase (Prod. No. 18080-044) and RNaseOUT recombinant Ribonuclease Inhibitor (Prod No. 10777-019) were purchased from Thermo Fisher. Taq polymerase 1U μL^{-1} (Prod. No. 10002-4100) was purchased from Biotools. Anti-digoxigenin-peroxidase Fab fragments (antiDIG-HRP) (Prod. No. 1214667) and anti-fluorescein-peroxidase Fab fragments (antiFLU-HRP) (Prod. No. 11426346910) were purchased from Roche Diagnostics GmbH (Mannheim, Germany).

The primers for the multiplex double-tagging RT-PCR amplification were obtained from Sigma-Aldrich, and are detailed in Table S5.2, *§5.7.2.1*. These primers were selected for the

specific amplification of GAPDH (glyceraldehyde 3-phosphate dehydrogenase) and IFN-γ genes (Genbank reference NM_002046.4 and NM_000619.2, respectively, described in *§5.7.2.2*.

The T cell clone PB100.2i was obtained by cloning the infiltrating T lymphocytes from a pancreatic donor organ. The expansion method is detailed described in *§5.7.2.4*.[20]

All buffer solutions were prepared with milliQ water and all other reagents were in analytical reagent grade (supplied from Sigma and Merck). Any solution used in RNA preparation was RNase-free by treatment with diethylpyrocarbonate (DEPC). The composition of these solutions is described in *§5.7.2.3*.

5.3.2 Instrumentation

Amperometric measurements were performed with a LC-4C amperometric controller (BAS Bioanalytical Systems Inc, USA). A three-electrode setup was used comprising a platinum auxiliary electrode (Crison Instruments 52-67), a double junction Ag/AgCl reference electrode (Orion 900200) with 0.1 mol L^{-1} KCl as external reference solution and a magneto electrode (m-GEC) as working electrode.[21] Cell concentration was determined by Neubauer chamber using Nikon Eclipse TS100 microscopy (Nikon Instrument, USA). Retrotranscription and polymerase chain reaction were carried out in MyCycler Thermal Cycler (Bio-Rad). After extraction, RNA was quantified with a Nanodrop 1000 spectrophotometer (Thermo Scientific, USA).

5.3.3 Immunomagnetic separation, multiplex double-tagging reverse transcription PCR of IFN-γ transcripts on magnetic beads and electrochemical genosensing

This approach sequentially combines three different types of magnetic separations, as depicted in Figure 5.1. Firstly, the method involves the preconcentration of T lymphocytes from whole blood based on the CD3 receptor by immunomagnetic separation on magnetic particles modified with the antiCD3 antibody[17] (Figure 5.1, panel a1). The messenger RNA was released (Figure 5.1, panel a2) and isolated on polydT-MPs based on the poly(A) tail present in the transcript, followed by retrotranscription to obtain cDNA (Figure 1, panel b1). After that, the cDNA was amplified by multiplex double-tagging PCR on beads (Figure 5.1, panel b2), using a double-tagging set of primers specific for IFN-γ and GAPDH as housekeeping gene control. During PCR, the cDNA is not only amplified but also labeled at the same time with

biotin/fluorescein (BIO/FLU) or biotin/digoxigenin (BIO/DIG) tags for IFN-γ and GAPDH transcript, respectively. Finally, the electrochemical magneto-genosensing was performed on streptavidin-magnetic particles as a support, based on the BIO tags on both amplicon through biotin-streptavidin interaction. The FLU and DIG-tags, carried by the other primer, were used for the labeling with the specific antibodies, antiFLU-HRP and antiDIG-HRP, coding for interferon-γ and GAPDH, respectively, and performed in two separated reaction chambers (Figure 5.1, panel c1). The simultaneous electrochemical readout of the two transcripts was based on peroxidase (HRP) enzyme as electrochemical reporter and performed in the same electrochemical cell on m-GEC electrodes, as previously reported [18,19] (Figure 5.1, panel c2). The experimental details are described in the next sections.

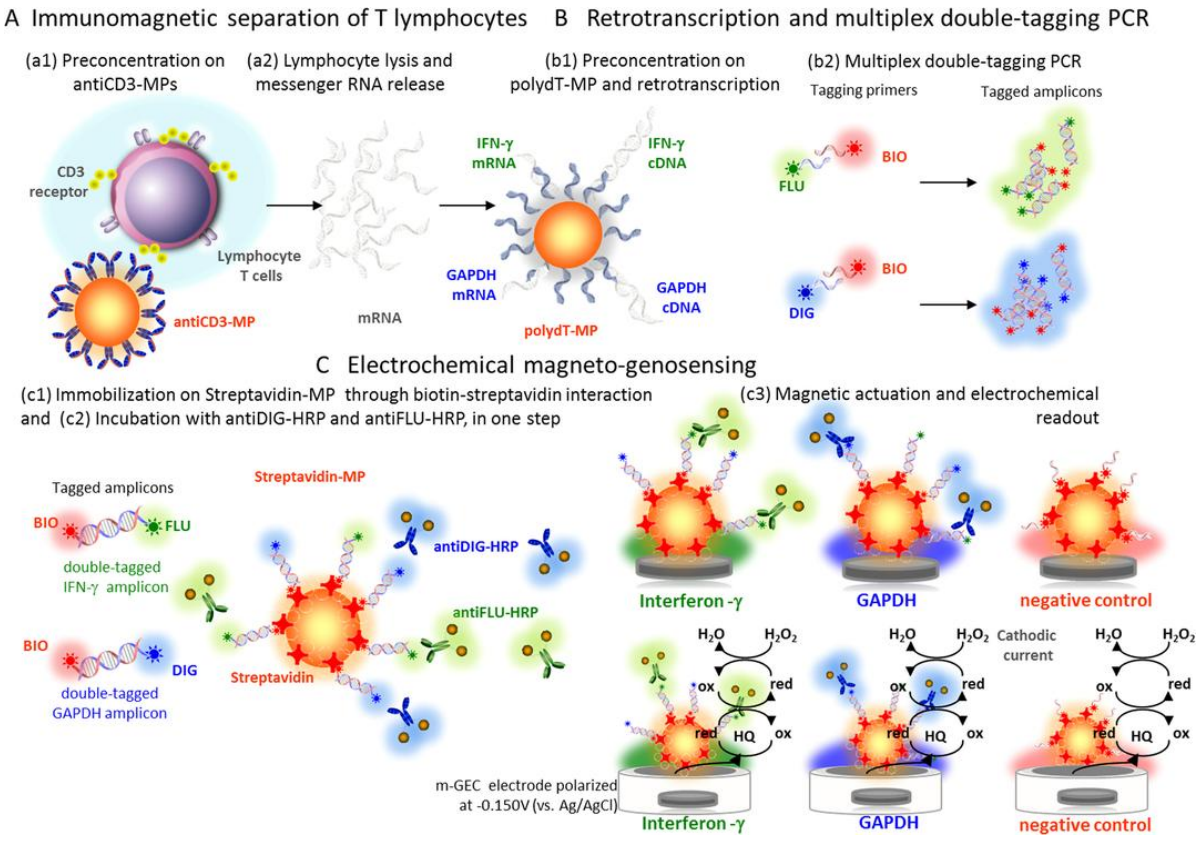

Figure 5.1. Schematic representation for the assessment of IFN-γ expression by immunomagnetic separation, retrotranscription and multiplex double-tagging PCR on magnetic beads and electrochemical genosensing.

5.3.4 Immunomagnetic separation of T lymphocytes

100 µL of T cells (at different concentration ranging from 0.1 to 1000 cells μL^{-1}) were incubated with 8×10^5 antiCD3-MPs for 30 min at 4 °C while shaking, followed by a washing steps with PBS 0.1% BSA. The content of the preconcentrated cells on antiCD3-MPs was released by resuspending them on 1 mL of Lysis/Binding buffer, and disrupted using a syringe.

5.3.5 Retrotranscription and multiplex double-tagging PCR on magnetic beads

First of all, the mRNA extraction and purification on polydT-MPs based on the polyA tail of the transcripts was performed, followed by cDNA retrotranscription on polydT-MPs, (further experimental details are described in *§5.7.2.5*. The multiplex double-tagging PCR was performed in 15 µL of reaction mixture containing the cDNA as sample. Each reaction tube contained 0.25 mmol L^{-1} of each deoxynucleotide triphosphate (dATP, dGTP, dCTP, and dTTP), 0.5 µmol L^{-1} of each tagging primers for GAPDH and IFN-γ transcripts and 3U of Taq polymerase. The reaction was carried out in buffer containing 75 mmol L^{-1} Tris-HCl (pH 9.0), 50 mmol L^{-1} KCl, 20 mmol L^{-1} $(NH_4)_2SO_4$, and 2 mmol L^{-1} $MgCl_2$. The amplification mixture was exposed to an initial step at 95 °C for 3 min followed by 28 cycles of 95 °C for 30 s, 61 °C for 30 s, and 72 °C for 30 s, and a last step of 7 min at 72 °C. The annealing temperature was optimized by performing PCR at different annealing temperature range from 60 °C to 70 °C in the same reaction. In all instances, the negative controls for the retrotranscription and the PCR, which contained all reagents in the mixture except the mRNA and cDNA template respectively, were tested. The performance of the multiplex double-tagging PCR was analyzed with conventional agarose gel electrophoresis on 2% agarose gel in TAE buffer containing 0.5 mg mL^{-1} ethidium bromide or 1 × GelRed dye. A molecular weight (MW) marker consisting of DNA fragments ranged from 100 to 1000 base pair (bp) was used as size amplicon control. The DNA bands were visualized by UV transillumination.

5.3.6 Electrochemical magneto-genosensing

Briefly, after the multiplex double-tagging PCR, the product was divided in two separated reaction chambers. The common BIO-tag was used for the immobilization of the amplicons on streptavidin-magnetic particles through the high affinity biotin-streptavidin interaction, while the FLU and DIG tags allowed the labeling by the specific antibodies, antiFLU-HRP and antiDIG-

HRP, coding for IFN-γ and GAPDH, respectively, in one 15 min step. The procedure comprised: (a) the immobilization and preconcentration of the tagged amplicons on 6×10^6 streptAv-MPs and (b) the incubation with the electrochemical reporters in one step for 15 min at 42 °C, in details antiFLU-HRP and antiDIG–HRP (60 µg each) coding for IFN-γ (FLU-tag), and GAPDH (DIG-tag), respectively. Two washing steps with 500 µL of Tris buffer for 2 min at 42 °C were performed. After incubation or washing step, a magnetic separator was positioned under the tubes until pellet formation on the tube side wall, followed by supernatant separation; (c) magnetic actuation by an array of two working electrodes (one coding for IFN-γ, while the other for GAPDH), which contain a small magnet (m-GEC); (d) electrochemical readout based on amperometry on m-GEC electrodes polarized at − 0.150 V (vs. Ag/AgCl), under enzyme saturation conditions (typically after 1 min) in ePBS buffer, upon the addition of hydroquinone (1.8×10^{-3} mol L^{-1}) and hydrogen peroxide (1.1×10^{-3} mol L^{-1}). The steady-state cathodic amperometric current (I*cat*, in µA) was used for the electrochemical signal plotted in all the figures. Before each use, the electrode surface of m-GEC was renewed by a simple polishing procedure to eliminate the magnetic particles for further reusability. In order to determine the limit of detection (LOD), a calibration curve was performed with increasing amount of cells, ranging from 0.1 up to 1000 cells μL^{-1}. The specificity of the assay was studied by performing the multiplex double-tagging RT-PCR with all possible combinations, including a) the binary combinations (IFN-γ/GAPDH), and b) individual measurements for each gene, as well as the negative controls for each individual gene and its combinations.

The stability of the magneto-genosensing approach is determined by the stability of the reagents (antiCD3-MPs, polydT-MPs, strepAv-MP, retrotranscription and PCR mix), that were kept at 4 °C as recommended by the manufacturers. The m-GEC electrodes were storaged at RT since they are not biologically-modified. Further details about reproducibility of the construction, renewal and reusability, and stability of the m-GEC electrodes have been extensively reported by our group.[17,19]

5.3.7 IFN-γ transcript detection in T lymphocytes from whole blood samples

The performance of this approach was evaluated in whole blood by stimulation of the lymphocytes as a model for intracellular infection in real samples. For this model, the lymphocytes were isolated from whole blood anonymized samples by Ficoll-Paque density gradient centrifugation (*§5.7.2.7*) and then stimulated with phytohemagglutinin (PHA). PHA is

a mitogen that stimulates cell division of lymphocytes and induces de novo synthesis of cytokines as IFN-γ, simulating the events which occur during intracellular infections. [22, 23] This procedure is similar to the in vitro stimulation with specific antigen of whole blood samples that is performed to measure IFN-γ by IGRAs. The cells were split in a positive control (stimulated with PHA at 1 mg mL^{-1}), and the reference sample (no stimulation), and processed at $t = 0$ and $t = 48$ h, by culturing in Iscove's Modified Dulbecco's Medium (IMDM) supplemented with heat inactivated human serum at 10% and penicillin and streptomycin at 1%. In parallel, IFN-γ released to the supernatant by activated T cell cultures was measured by BD™ Cytometric Bead Array (CBA) (Becton Dickinson Bioscienes, USA) (*§5.7.2.10*).

5.4 Results and discussion

5.4.1 Optimization of the immunomagnetic separation, multiplex double-tagging reverse transcription PCR on magnetic beads and electrochemical genosensing

First of all, the performance of polydT-MPs for the RNA purification and retrotranscription was evaluated using GAPDH transcript as a model. To achieve that, total RNA obtained by lysis of 3×10^6 cells were processed either by a) classical mRNA extraction and purification procedure (RNeasy kit, Qiagen), followed by classical cDNA retrotranscription, and b) mRNA extraction and purification on polydT-MPs, followed by cDNA retrotranscription on polydT-MPs. The experimental details of each purification and retrotrancription procedures are described in *§5.7.2.5* and *§5.7.2.8*. In both cases, double-tagging PCR was performed with the single set of specific primers for GAPDH amplification, labeled with DIG/BIO tags. The double-tagged amplicons were submitted to both gel electrophoresis and electrochemical genosensing for quantification. The results are comparatively depicted in Figure 5.2, showing that both RNA extraction and retrotranscription can be performed on the polydT-MPs with a comparable analytical performance than the classical procedure. However, the use of polydT-MPs and the magnetic actuation simplifies the analytical procedure, avoiding the use of separation columns and further centrifugation.

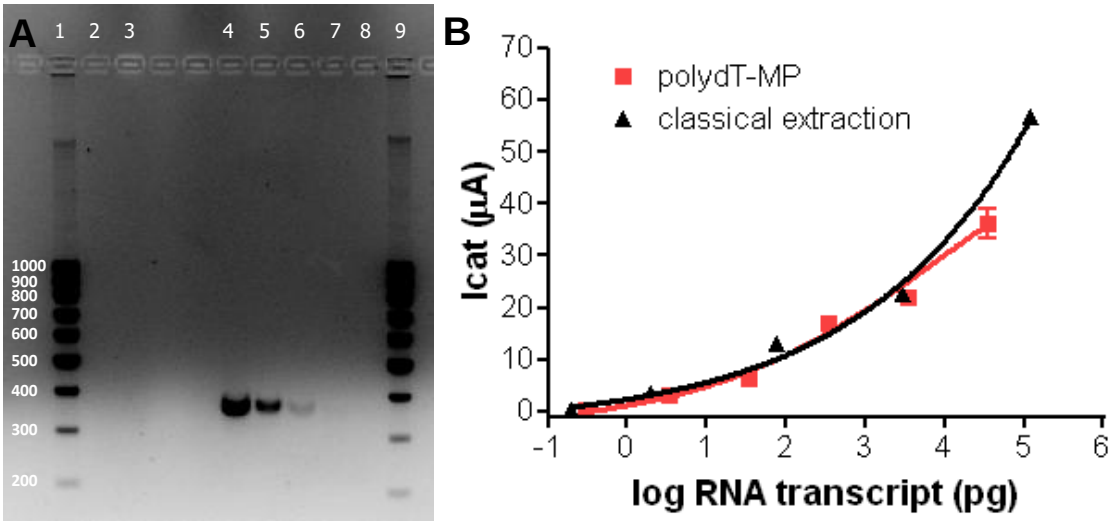

Figure 5.2. Study of the performance for the mRNA extraction and cDNA retrotranscription on the polydT-MPs. Panel A shows the gel electrophoresis: Lanes 1 and 9, molecular weight marker; Lane 2, retrotranscription negative control; Lane 3, PCR negative control; Lane 4–8, transcript concentration 34.3×10^3; 3.4×10^3; 340; 34 and 3.43.4 pg, respectively. Panel B, shows comparatively the electrochemical signals, for the RNA extraction performed on polydT-MPs (from 3.4 to 34.3×10^3 pg) and classical extraction (2; 75; 3×10^3; 120×10^3 pg), fitted by a Four Parameter logistic Equation (R2 = 0.9703 and 0.9959, respectively) followed by retrotranscription and electrochemical genosensing.(n = 3). RSD % ranging from 2.6 to 13.6 for all the concentration range.

Different parameters were evaluated, including the efficiency study of the immunomagnetic separation, as well as the main factors affecting the performance of the electrochemical genosensing, such as the washing step time, the incubation time with the electrochemical reporter, the concentration of streptAv-MPs and the electrochemical reporter, and finally the procedure in one or two steps for the electrochemical genosensing. The experimental details and the corresponding results in order to set the main analytical parameters are discussed in *§5.7.3.1* to *§5.7.3.6* (Figures S5.2 to S5.7 therein). Furthermore, Figure S5.8 shows the results for the detection of GAPDH transcripts, performed with lymphocytes T in a range from 0.1 to 1000 cells μL^{-1}. The LOD was found to be as low as 0.017 cells μL^{-1} (which corresponds to 2 cells) much lower than the gel electrophoresis, which is able to detect 10 cells μL^{-1} (corresponding to 1000 cells, as shown in lane 6, Figure S5.8, panel A). As the number of copies for GAPDH transcripts is approximately 1000/2000 copies per cell,[24,25] the LOD corresponds to a detection of as low as 2×10^4 transcript copies mL^{-1} by this strategy.

5.4.2 Immunomagnetic separation, multiplex double-tagging reverse transcription PCR on magnetic beads of IFN-γ/GAPDH transcripts and electrochemical genosensing

In order to evaluate the overall performance of the procedure for the multiplex detection of IFN-γ and GAPDH transcripts, a calibration curve was performed using IFN-γ positive T cells. T cell clone, PB100.2i, produces high titers of IFN-γ after activation through its T cell receptor (TCR). Thus, different concentrations of lymphocytes were evaluated, ranging from 0.1 to 1000 cells μL^{-1}, involving the IMS with antiCD3-MPs, the transcript extraction and retrotranscription on polydT-MPs, the multiplex double-tagging PCR with the double-tagging set of primer specific for the amplification of IFN-γ/GAPDH and labeled with FLU/BIO and DIG/BIO tags, respectively; and finally, the electrochemical genosensing following the procedure described in Figure 5.1. These results are comparatively presented in Figure 5.3.

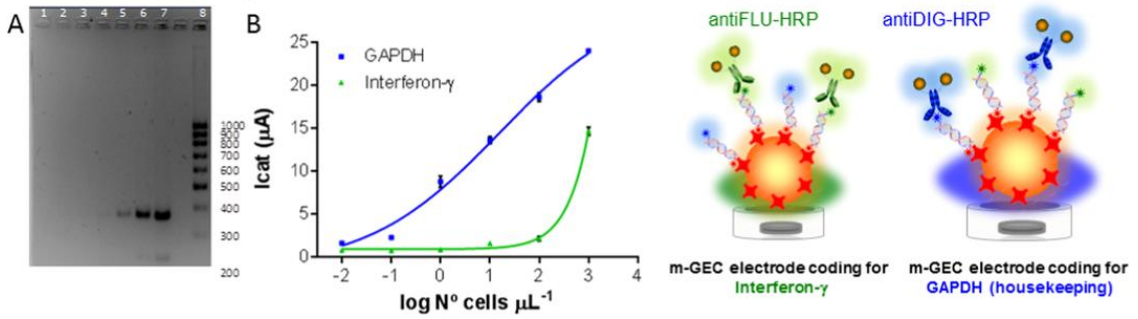

Figure 5.3. Multiplex detection of IFN-γ and GAPDH transcripts by IMS of T cells, ranging from 0.1 to 1000 cells μL^{-1}, double-tagging RT-PCR on magnetic beads and electrochemical genosensing. Panel A, Electrophoresis gel, lane 1 retrotranscription negative control, lane 2, PCR negative control, lane 3–7, cell concentration 0.1, 1, 10, 100 and 1000 cell μL^{-1} respectively, and lane 8 molecular weight marker. Panel B, electrochemical signals for GAPDH/IFN-γ transcript detection by immunomagnetic separation of T cells ranged from 0.1 to 1000 cells μL^{-1}. n = 3. RSD % ranging from 3.9 to 10.5 for all the concentration range.

The LODs for each transcript in the multiplex approach were estimated by fitting the raw data using a nonlinear regression (Four Parameter logistic Equation) (R2 = 0.9937 and 0.9895, for IFN-γ and GAPDH) as shown in Figure 5.3, panel B, by processing the negative control samples (n = 4), obtaining a mean value of 0.850 μA with a standard deviation (SD) of 0.046 μA (for IFN-γ) and 1.687 μA/SD 0.140 μA (for GAPDH). The cut-off value was then determined in both cases with a one-tailed t-test at a 95% confidence level, giving values of 0.967 and 2.018 μA, respectively, for IFN-γ and GAPDH. These values were interpolated in each plot and the

LODs were found to be as low as 1.5 cells μL^{-1} (which corresponds to 150 cells) for IFN-γ and 0.022 cells μL^{-1} (which corresponds to 3 cells) for the housekeeping transcript.

The specificity of the magneto-genosensor coding for each transcripts, IFN-γ and GADPH, was further studied by performing the double-tagging RT-PCR from 1000 cells μL^{-1}, with all possible combinations, including a) the binary combination (GAPDH/IFN-γ), b) the single combination (GAPDH and IFN-γ), as well as the negative control towards the two electrochemical reporters (antiDIG–HRP and antiFLU-HRP, respectively). Negative controls were performed with all reagents (IFN-γ and/or GAPDH primers), but omitting the template. As observed in Figure 5.4, panels A and B, each of the electrodes only detected one of the two transcripts, even in the presence/absence of the other one.

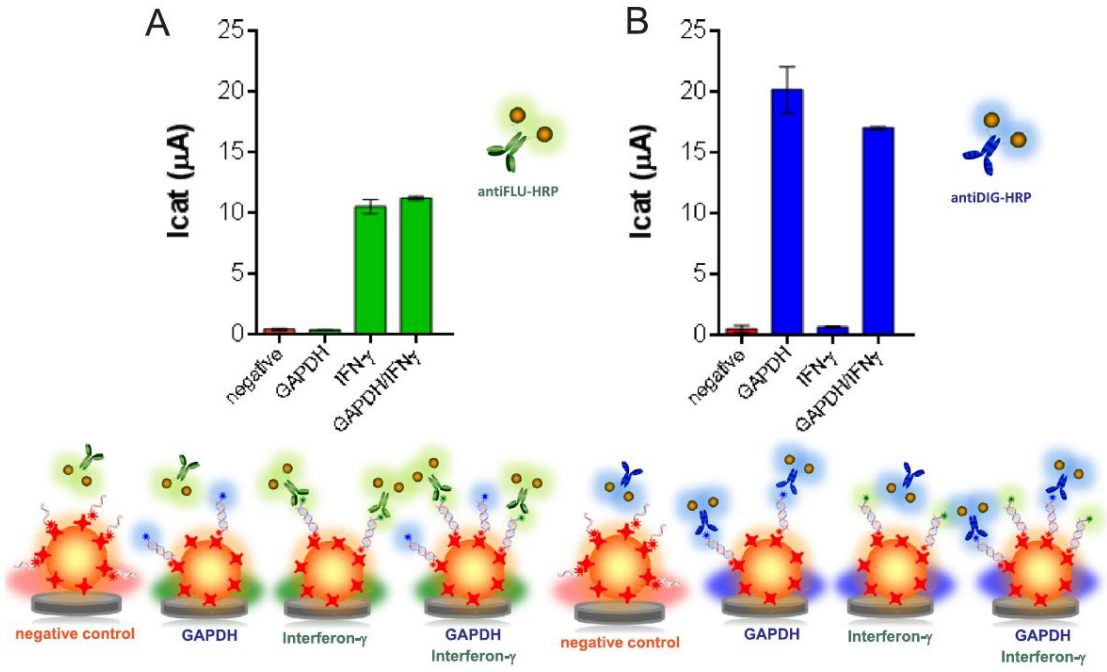

Figure 5.4. Specificity study for the transcript detection by the multiplex double-tagging RT-PCR and electrochemical genosensing performed with a) the binary combinations (GAPDH/IFN-γ), and b) the single transcript (GAPDH or IFN-γ), challenged towards (A) 60 μg antiFLU–HRP coding for IFN-γ and (B) 60 μg antiDIG-HRP coding for GAPDH as a housekeeping gene. In all cases, the transcripts were obtained from 1000 cells μL^{-1}. The negative controls are also shown. RSD % ranging from 0.8 to 10.2 for all instances.

For instance, in the electrode coding for IFN-γ (Figure 5.4, panel A), the electrochemical signal obtained for IFN-γ (10.90 μA) was almost the same when the housekeeping transcript was also present (GAPDH/IFN-γ) (11.30 μA). In contrast, when IFN-γ was absent (negative control) (0.40 μA), the signal was equal even in the presence of GAPDH at high concentration

level (0.35 µA). Similar results were obtained in the case of GAPDH (Figure 5.4, panel B). This data highlight the specificity of both, the double-tagging RT-PCR, as well as the electrochemical detection. Hence, the results show that this approach was able to clearly distinguish among the two different transcripts and their single and binary combinations.

5.4.3 IFN-γ transcript detection in T lymphocytes from whole blood samples

The performance of this approach was evaluated in lymphocytes isolated from whole blood anonymized samples in healthy donors by the Ficoll-Paque method and then stimulated with phytohemagglutinin as a model for intracellular infection. First of all, BD™ Cytometric Beads Analysis was performed to demonstrate the release of IFN-γ protein upon stimulation with PHA. The CBA analysis for IFN-γ secretion was accordingly performed as described in *§5.7.2.10*, with two samples at t = 0 and t = 48 h under PHA stimulation and their corresponding negative controls (Figure 5.5).

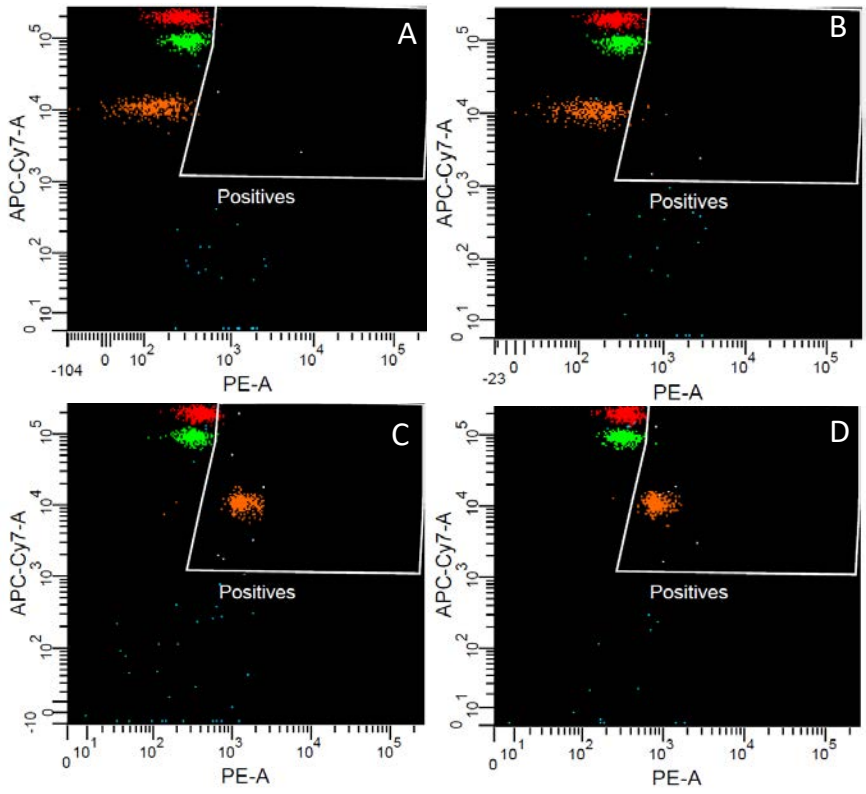

Figure 5.5. Cytometric Beads Analysis (CBA) for cytokines secretion of two anonymized samples from healthy donors. Panels A and B show the non-stimulated samples S1 and S2 (t=0). Panels C and D show the stimulated samples S1 and S2 with PHA (t = 48 h). IL-4 (in red), IL-17A (in green) and IFN-γ (in orange) were analyzed by CBA. Dot shift for PE-A fluorescence indicates the presence of the cytokines in the culture supernatant.

The CBA analysis also included the detection of other cytokines such as IL4 and IL17A as protein secretion control for the T helper 2 (Th2) and 17 (Th17) lymphocytes, respectively. The induction of lymphocyte by PHA not only stimulate the expression of IFN-γ (orange), but also the release of the protein out of the cell in the real samples, as can be confirmed by the results shown in Figure 5.5 (panels C and D), when compared with the non-stimulated samples (Figure 5.5, panels A and B). Moreover, the quantification of the IFN-γ by this method is also shown in Table S5.3 (*§5.7.3.7*).

Finally, the procedure for the detection of IFN-γ and GAPDH as housekeeping transcript on non-stimulated (t=0) and stimulated (t = 48 h) real samples was performed, involving the immunomagnetic separation of 1000 cell μL^{-1}, multiplex double-tagging RT-PCR on magnetic beads, and the electrochemical genosensing. A negative control of lymphocytes cultured for 48 h without stimulation was processed in parallel.

Figure 5.6 shows the results performed by gel electrophoresis (panel A) and the multiplex electrochemical genosensors (panel B) for each sample before and after stimulation with PHA as well as the negative controls, for the electrode coding for IFN-γ (using as electrochemical reporter antiFLU-HRP, shown in green) and GAPDH (using as electrochemical reporter antiDIG-HRP shown in blue).

GADPH is a constitutive gene, which codified for an enzyme of ~37 kDa that catalyzes the sixth step of glycolysis and thus serves to break down glucose for energy and carbon molecules in all cells. As GAPDH is involved in this long established metabolic function, its expression is detected in both stimulated (t = 48 h) and non-stimulated samples (t = 0). On the other hand, IFN-γ is a cytokine produced during intracellular infections, and its expression in this model was stimulated with PHA. The values for the IFN-γ shown in Figure 5.6 were accordingly normalized against GAPDH as housekeeping gene. As it is shown in Figure 5.6, there was a minimal expression of this transcript in the non-stimulated samples (t = 0) in which the signal obtained for both samples were similar to the negative control. In detail, the expression for the IFN-γ in non-stimulated samples was found to be 4.9% and 5.7% compared to the housekeeping gene expression. However, upon stimulation of the cells, the expression of IFN-γ was found to be 66.5 and 78.6% compared to the housekeeping gene expression. Thus, the electrochemical genosensor developed in this work can be potentially used for many applications involving the detection of IFN-γ transcript upon activation of the T cells with specific antigens, as a biomarker for intracellular infections, among other medical conditions based on cell-mediated immunity.

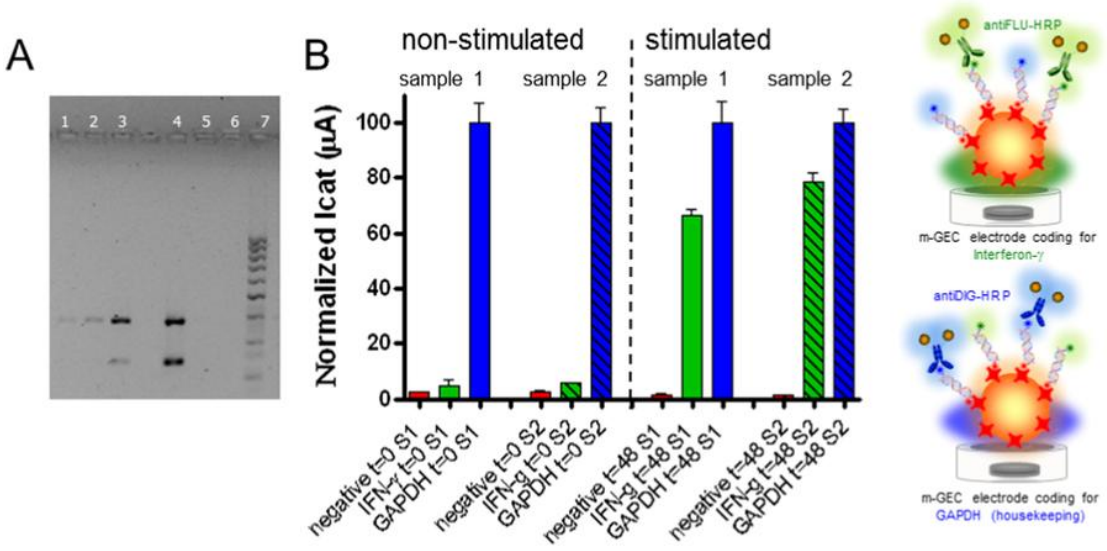

Figure 5.6. Evaluation of the transcript expression by immunomagnetic separation of 1000 cells μL^{-1} and the multiplex double-tagging RT-PCR by gel electrophoresis (panel A) and multiplex electrochemical genosensing (panel B) performed in stimulated and non-stimulated real samples. Panel A shows the gel electrophoresis: Lane 1 and 2, non-stimulated samples (t=0) for sample 1 and 2, respectively. Lane 3 and 4, stimulated samples (t = 48 h) for sample 1 and 2. Lanes 5 and 6, negative controls. Lane 7, MW marker. The normalized corresponding signals for the multiplex electrochemical genosensing are shown in panel B. n = 3. RSD % ranging from 1.9 to 12.7 for all instances.

Electrochemical immunosensors for cytokine detection such as IL1, IL6, tumor necrosis factor, among others, were previously reported.[26,27] These approaches showed similar analytical performance than the ELISA kits currently in the market (IFN gamma Human ELISA Kit, Thermo Fisher, among many others). Moreover, both the immunosensors and the ELISA kits rely on the determination of the total protein in the clinical specimen, while the genosensor presented here determines the expression of IFN-γ (mRNA). Moreover, no information of the functional release of the biomarker by the cells upon exposure to specific antigens is provided by these immunological tests.

As previously discussed, in some medical conditions it is required the information of the increased/decreased release of IFN-γ specifically produced by T lymphocytes upon the exposure to an antigen, as it is provided by the genosensor presented in this work, by the specific isolation of T cells and comparison of the expression with a constitutive gene as positive control.

5.5 Conclusions

The work addressed the design of a genosensor to detect the expression of genes on T cells, by sequentially combining three different types of magnetic separation, including the immunomagnetic separation of the T cells performed on antiCD3-MPs, the multiplex double-tagging reverse transcription PCR, for the isolation, preconcentration, amplification and tagging of the IFN-γ (and GAPDH as housekeeping control) on polydT-MPs magnetic particles and, finally, the electrochemical genosensing on magneto electrodes using streptAv-MPs as a support. This approach shows a high sensitivity and specificity for gene expression, being able to detect the transcripts produced by as low as 150 cells for IFN-γ and only 3 cells for the housekeeping transcript used as positive control. Moreover, this approach is able to determine the functional production of cytokines by the lymphocytes upon stimulation. The genosensor presented in this work can be potentially relevant in the routine clinical practice for the diagnosis of all the diseases based on cell-mediated immunity, being the specificity provided by the antigen used in the stimulation of isolated T lymphocytes. The genosensor presented here is promising as an alternative to IGRA test currently in the market for being used to screen-out population at primary health care in low-resource settings. Future work will be focused on challenging the test in samples at risk to develop tuberculosis, among other applications.

5.6 Acknowledgments

Financial support from Ministry of Economy and Competitiveness (MINECO) Madrid (Grants BIO2016–75751-R) are gratefully acknowledged.

5.7 Supplementary Material

5.7.1 Introduction

5.7.1.1 Interferon gamma release assays

Interferon gamma release assays are blood-tests which can be potentially used for the diagnosis of all the diseases based on cell-mediated immunity. However, it is especially useful in routine clinical practice for the diagnosis of latent tuberculosis. These tests are based on immune reactivity of a person. White blood cells from an *M. tuberculosis*-infected person release interferon-gamma (IFN-γ) when they are exposed to *Mycobacterium* antigens. However, it is not possible to differentiate latent tuberculosis infection from tuberculosis disease with these kinds of tests. The main advantages of IGRAs tests are that prior BCG vaccination does not cause false positive results and the results are available within 24 hours. However, they are not recommended in children under 5 years old, in person with low risk of infection and low risk of disease due to *M. tuberculosis*. Currently, there are two commercial test based on IGRAs approved by FDA: QuantiFERON®-TB Gold In-Tube test (QFT-GIT) and T-SPOT®.*TB* test (T-Spot).

QuantiFERON-TB Gold test (QFT-G) (Qiagen, The Netherlands) is based on the quantification of interferon-gamma released from sensitized lymphocytes in whole blood incubated with purified protein derivative from *M. tuberculosis* and control antigens. This test assesses antigen-specific T cell activation against TB antigens such as ESAT-6, CFP-10 and TB 7.7 after the exposure of viable blood to them (coated on the inner surface of the tubes). The kit provides three tubes containing TB antigens, a negative and a positive control containing phytohemagglutinin. Thus, whole blood is dispensed directly on the tubes, incubated for 16 – 24h at 37 °C and centrifuged to obtain the plasma. Next, the secreted IFN-γ is determined by ELISA and a computer program performs the calculations and the interpretation of the results.[28] QFT-G results are based on the proportion of IFN-γ released in response to tuberculin as compared with the mitogen, or tuberculin response.

T-SPOT.TB (Oxford Immunotec, UK) is based on an enzyme-linked immunospot (ELISPOT) that determines the quantity of effector T cells responding to antigen stimulation. For the T-SPOT.TB test, PBMCs are separated from the blood and washed. The PBMCs are then added into microtiter wells at a fix concentration. Each test uses 4 wells: control, PHA, and 2 separate wells for ESAT-6 and CFP-10 antigens. Since the plates are covered with antibodies antiIFN-γ, the IFN-γ released from stimulated T cells is captured on the plate. After that, they are incubated with a secondary antibody and finally, a substrate is added which produces dark

blue spots where interferon gamma is secreted by T cells. The spots can be counted and the results are interpreted according to the number of spots (number of IFN-γ producing cells). The result can be positive, negative, indeterminate and borderline.

Table S5.1. Comparison of the analytical performance and main characteristics of commercially available IGRA test and the IFN-γ transcript detection on T cells based on electrochemical genosensing (this work).

	QuantiFERON-TB Gold (Qiagen, The Netherlands)	T-SPOT.TB (Oxford Immunotech, UK)	IFN-γ transcript detection on T cells based on electrochemical genosensing (this work)
Target	IFN-γ (protein)	IFN-γ (protein) released by isolated Peripheral blood mononuclear cells (PBMCs)	IFN-γ transcripts (mRNA) released by isolated T-cells
Isolation of IFN-γ producing cells	Not performed	Non-specific isolation: PBMCs containing T cells by Ficoll-Paque or alternative PBMC separation Centrifugation required	Specific isolation of T-cells: Immunomagnetic isolation by antiCD3 magnetic particles No centrifugation required
Readout technology	ELISA	ELISPOT	Electrochemical magneto-genosensor
Readout time	ELISA: Approx. 3 h	ELISPOT: Approx. 3 h	Approx. 3 h
Sample	Whole blood Up to 4 mL (1 mL per tube) Draw required	Whole blood 2-8 mL depending of the age Draw required	Whole blood 100 μL per tube can be potentially obtained by fingerprick
Incubation of the sample for stimulation	required	required	required
Cost	107$	60-85$	20$
Information provided by the test	Concentration of IFN-γ (protein)	Number of IFN- γ (protein) producing cells	Concentration of IFN- γ (transcript) produced by T-cells
FDA approved	×	✓	×

5.7.2 Materials and methods

5.7.2.1 Oligonucleotide sequences

Table S5.2. Sequence of the set of primers for the multiplex double-tagging PCR amplification of GAPDH and IFN-γ.

Gene	Primer sequence (5´-3´)	Type	5´-Labels	Size (bp)
GAPDH	AGCCCCAGCCTTCTCCA	Forward	Biotin	371
	CTTCTTTTGCGTCGCCAG	Reverse	Digoxigenin	
IFN-γ	TGACCAGAGCATCCAAAAGA	Forward	Fluorescein	236
	CTCTTCGACCTCGAAACAGC	Reverse	Biotin	

5.7.2.2. mRNA sequence of GAPDH and IFN-γ

Glyceraldehyde-3-phosphate dehydrogenase mRNA sequence. The position of the set of primers are highlighted in red (Forward BIO-primer) and blue (Reverse DIG-primer).

>gi|378404906|ref|NM_002046.4|Homo sapiens glyceraldehyde-3-phosphate dehydrogenase (GAPDH), transcript variant 1, mRNA

GGCTGGGACTGGCTGAGCCTGGCGGGAGGCGGGGTCCGAGTCACCGCCTGCCGCCGCGCCCCCGGTTTCTATAA
ATTGAGCCCGCAGCCTCCCGCTTCGCTCTCTGCTCCTCCTGTTCGACAGTCAGCCGCATCTTCTTTTGCGTCGCCAGC
CGAGCCACATCGCTCAGACACCATGGGGAAGGTGAAGGTCGGAGTCAACGGATTTGGTCGTATTGGGCGCCTGG
TCACCAGGGCTGCTTTTAACTCTGGTAAAGTGGATATTGTTGCCATCAATGACCCCTTCATTGACCTCAACTACATG
GTTTACATGTTCCAATATGATTCCACCCATGGCAAATTCCATGGCACCGTCAAGGCTGAGAACGGGAAGCTTGTCA
TCAATGGAAATCCCATCACCATCTTCCAGGAGCGAGATCCCTCCAAAATCAAGTGGGGCGATGCTGGCGCTGAGT
ACGTCGTGGAGTCCACTGGCGTCTTCACCACCATGGAGAAGGCTGGGGCTCATTTGCAGGGGGGAGCCAAAAGG
GTCATCATCTCTGCCCCCTCTGCTGATGCCCCCATGTTCGTCATGGGTGTGAACCATGAGAAGTATGACAACAGCC
TCAAGATCATCAGCAATGCCTCCTGCACCACCAACTGCTTAGCACCCCTGGCCAAGGTCATCCATGACAACTTTGGT
ATCGTGGAAGGACTCATGACCACAGTCCATGCCATCACTGCCACCCAGAAGACTGTGGATGGCCCCTCCGGGAAA
CTGTGGCGTGATGGCCGCGGGGCTCTCCAGAACATCATCCCTGCCTCTACTGGCGCTGCCAAGGCTGTGGGCAAG
GTCATCCCTGAGCTGAACGGGAAGCTCACTGGCATGGCCTTCCGTGTCCCCACTGCCAACGTGTCAGTGGTGGAC
CTGACCTGCCGTCTAGAAAAACCTGCCAAATATGATGACATCAAGAAGGTGGTGAAGCAGGCGTCGGAGGGCCC
CCTCAAGGGCATCCTGGGCTACACTGAGCACCAGGTGGTCTCCTCTGACTTCAACAGCGACACCCACTCCTCCACC
TTTGACGCTGGGGCTGGCATTGCCCTCAACGACCACTTTGTCAAGCTCATTTCCTGGTATGACAACGAATTTGGCTA
CAGCAACAGGGTGGTGGACCTCATGGCCCACATGGCCTCCAAGGAGTAAGACCCCTGGACCACCAGCCCCAGCAA
GAGCACAAGAGGAAGAGAGAGACCCTCACTGCTGGGGAGTCCCTGCCACACTCAGTCCCCCACCACACTGAATCT
CCCCTCCTCACAGTTGCCATGTAGACCCCTTGAAGAGGGGAGGGGCCTAGGGAGCCGCACCTTGTCATGTACCAT
CAATAAAGTACCCTGTGCTCAACCAAAAAAAAAAAAAAAAAA

Interferon gamma mRNA sequence. The position of the set of primers are highlighted in green (Forward FAM-primer) and red (Reverse BIO-primer).

>gi|56786137|ref|NM_000619.2|Homo sapiens interferon, gamma (IFNG), mRNA

CACATTGTTCTGATCATCTGAAGATCAGCTATTAGAAGAGAAAGATCAGTTAAGTCCTTTGGACCTGATCAGCTTG
ATACAAGAACTACTGATTTCAACTTCTTTGGCTTAATTCTCTCGGAAACGATGAAATATACAAGTTATATCTTGGCTT
TTCAGCTCTGCATCGTTTTGGGTTCTCTTGGCTGTTACTGCCAGGACCCATATGTAAAAGAAGCAGAAAACCTTAA
GAAATATTTTAATGCAGGTCATTCAGATGTAGCGGATAATGGAACTCTTTTCTTAGGCATTTTGAAGAATTGGAAA
GAGGAGAGTGACAGAAAAATAATGCAGAGCCAAATTGTCTCCTTTTACTTCAAACTTTTTAAAAACTTTAAAGATG
ACCAGAGCATCCAAAAGAGTGTGGAGACCATCAAGGAAGACATGAATGTCAAGTTTTTCAATAGCAACAAAAAGA
AACGAGATGACTTCGAAAAGCTGACTAATTATTCGGTAACTGACTTGAATGTCCAACGCAAAGCAATACATGAACT
CATCCAAGTGATGGCTGAACTGTCGCCAGCAGCTAAAACAGGGAAGCGAAAAAGGAGTCAGATGCTGTTTCGAG
GTCGAAGAGCATCCCAGTAATGGTTGTCCTGCCTGCAATATTTGAATTTTAAATCTAAATCTATTTATTAATATTTAA

CATTATTTATATGGGGAATATATTTTTAGACTCATCAATCAAATAAGTATTTATAATAGCAACTTTTGTGTAATGAAA
ATGAATATCTATTAATATATGTATTATTTATAATTCCTATATCCTGTGACTGTCTCACTTAATCCTTTGTTTTCTGACT
AATTAGGCAAGGCTATGTGATTACAAGGCTTTATCTCAGGGGCCAACTAGGCAGCCAACCTAAGCAAGATCCCAT
GGGTTGTGTGTTTATTTCACTTGATGATACAATGAACACTTATAAGTGAAGTGATACTATCCAGTTACTGCCGGTTT
GAAAATATGCCTGCAATCTGAGCCAGTGCTTTAATGGCATGTCAGACAGAACTTGAATGTGTCAGGTGACCCTGAT
GAAAACATAGCATCTCAGGAGATTTCATGCCTGGTGCTTCCAAATATTGTTGACAACTGTGACTGTACCCAAATGG
AAAGTAACTCATTTGTTAAAATTATCAATATCTAATATATATGAATAAAGTGTAAGTTCACAACAAAAAAAAAAAA
AAAAAAAAAAAAAAAAAA

5.7.2.3 Composition of buffers and solutions

All buffer solutions were prepared with milliQ water and all other reagents were in analytical reagent grade (supplied from Sigma and Merck). The composition of these solutions is listed below:

- Binding Buffer. 20 mmol L^{-1} Tris-HCl, pH 7.5, 1.0 mol L^{-1} lithium chloride (LiCl), 2 mmol L^{-1} ethylenediaminetetraacetic acid (EDTA)

- Lysis/Binding Buffer. 100 mmol L^{-1} Tris-HCl, 500 mmol L^{-1} LiCl, 10 mmol L^{-1} EDTA, 1% lithium dodecyl sulfate (LiDS), 5 mmol L^{-1} dithiothreitol (DTT). Note: LiDS is a strong inhibitor of enzymatic reaction.

- RLT Buffer (QiaGen). The composition of Buffer RLT is confidential. This buffer is a proprietary component of RNeasy Kits. Buffer RLT contains a high concentration of guanidine isothiocycanate, which supports the binding of RNA to the silica membrane.

- RW1 Buffer (QiaGen). The composition of Buffer RW1 is confidential. Buffer RW1 is a proprietary component of RNeasy Kits. Buffer RW1 contains a guanidine salt, as well as ethanol, and is used as a stringent washing buffer that efficiently removes biomolecules such as carbohydrates, proteins, fatty acids etc., that are non-specifically bound to the silica membrane. At the same time, RNA molecules larger than 200 bases remain bound to the column. Note: Buffer RW1 should not be used for isolation of small RNAs, for example microRNAs or fragmented RNA from formalin-fixed tissues, as these smaller fragments will be washed away. Buffer RWT should be used instead.

- RPE Buffer (QiaGen). The composition of Buffer RPE is confidential. This buffer is a proprietary component of RNeasy Kits. Its main function is to remove traces of salts.

- Washing Buffer A. 10 mmol L^{-1} Tris-HCl, pH: 7.5, 0.15 mol L^{-1} LiCl, 1 mmol L^{-1} EDTA, 0.1% LiDS
- Washing Buffer B. 10 mmol L^{-1} Tris-HCl, pH: 7.5, 0.15 mol L^{-1}, LiCl, 1 mmol L^{-1} EDTA
- Tris buffer. 0.1 mol L^{-1} Tris, 0.15 mol L^{-1} NaCl, pH 7.5
- Tris Blocking buffer. 2% w/v BSA, 0.1% w/v Tween 20, 5 mmol L^{-1} EDTA, in Tris buffer
- PBS buffer. 0.01 mol L^{-1} Na_2HPO_4, 0.15 mol L^{-1} NaCl, 2 mmol L^{-1} EDTA, pH 7.4
- ePBS buffer. 0.1 mol L^{-1} Na_2HPO_4, 0.1 mol L^{-1} KCl pH:7.

5.7.2.4 Cell line

The T lymphocyte cell clone PB100.2i was supplied by the Immunology Cellular Laboratory (Institute of Biotechnology and Biomedicine). The cells were obtained by cloning the infiltrating lymphocytes from a pancreatic donor organ.[20] Rapid expansion method (REM) was adapted as follows: 40000 T cell population were cultured in T25 flask containing 25 mL of Iscove's Modified Dulbecco's Media (IMDM) supplemented with 2 mmol L^{-1} L-Glutamine and 100 U mL^{-1} penicillin and 100 μg mL^{-1} streptomycin, 10% human serum and 50 ng mL^{-1} OKT3 antibody with 25×10^6 γ-irradiated peripheral blood mononuclear cells and 5×10^6 γ-irradiated EBV-transformed lymphoblastoid cell line. Interleukin-2 was added at 45 U mL^{-1} on day +1. Cells remained untouched during the first 5 days of culture, and then cells were split every 3-4 days. The cells were stained with Trypan Blue, and the viable cell concentration was determined by enumeration in a Neubauer counting chamber.

5.7.2.5 mRNA extraction and purification on polydT-MPs

RNA purification using oligo$(dT)_{25}$ magnetic particles was performed from a cell culture lysate. In detail, 100 μL of T lymphocytes (at different concentration ranging from 0.1 to 1000 cells μL^{-1}) were resuspended in 1 mL of Lysis/Binding buffer. The cells were disrupted by pipetting up and down a couple of times to ensure a complete lysis. In order to reduce the viscosity and for sample homogenization, the lysate was passed through a 21 gauge needle using a 2 mL syringe. (NOTE: In the case of T lymphocytes preconcentrated with antiCD3-MP, after disrupting the cells, the tube was placed in a magnet and the supernatant was used for further analysis). After that, 30 μL of polydT-MPs was added for incubation 10 min under rotation at RT. In this step, the polyadenylated tail of mRNA hybridized the polydT of the

magnetic particles. Finally, the mRNA/MP was washed with 500 μL of washing buffer A, followed by a second washing with 500 μL of washing buffer B and finally with 100 μL of DEPC-treated water.

5.7.2.6 cDNA synthesis on polydT-MPs

The retrotranscription was performed on magnetic particles. The cDNA was thus obtained by retrotranscription on the beads by incubation with 0.15 mg mL^{-1} of Dynabeads® Oligo $(dT)_{25}$ and 10 mmol L^{-1} of deoxynucleotide (dNTP) mix (10 mmol L^{-1} each dATP, dGTP, dCTP and dTTP at neutral pH) for 5 min at 65 °C and cooled on ice for 1 min. After that, a mix containing 0.1 mmol L^{-1} DTT, 40 U μL^{-1} RNAseOUT, 200 U μL^{-1} SuperScript III and 1X First-Strand buffer (50 mmol L^{-1} Tris-HCl pH 8.3, 75 mmol L^{-1} KCl, 3 mmol L^{-1} $MgCl_2$) was added and incubated for 60 min at 55 °C, and 15 min at 70 °C for inactivating the reaction. If necessary, the cDNA was stored at 20 °C until use.

5.7.2.7 Lymphocyte purification by Ficoll-Paque

Lymphocyte purification from human blood was obtained using Ficoll-Paque method. Blood was diluted 1:1 with PBS, and layered onto Ficoll-Paque™ solution maintaining a 3:1 constant ratio of diluted blood:Ficoll. The blood was centrifuged at 600 g for 25 min at room temperature. The lymphocytes layer was separated by using a glass Pasteur pipette and the lymphocytes were washed with PBS buffer. Finally, the supernatant was eliminated after centrifugation at 400 g for 5 minutes and the cells were resuspended in IMDM medium for the culturing.

5.7.2.8 Classical mRNA extraction and purification procedure

The RNA was extracted and purified by using RNeasy Mini kit (Qiagen) according to the instructions provided by the manufacturer. This procedure allows an enrichment for RNA species >200 nucleotide while small RNAs such as 5.8S RNA; 5S RNA, and tRNA are selectively excluded. For the mRNA enrichment, 3×10^6 T lymphocytes were resuspended in 600 μL of RLT buffer containing β-mercaptoethanol. The cells were disrupted to release all the RNA and homogenized using a 2 mL syringe and a 21 gauge needle. The homogenization process sheared genomic DNAs as well as other high molecular weight cellular components to create a homogeneous lysate. After that, the lysate was transferred to a gDNA Eliminator spin column

placed into a 2 mL collection tube, and centrifuged for 30 s at ≥ 8000 g in order to eliminate the genomic DNA. The supernatant was transferred to a new tube and 600 µL of 70% ethanol was added. The sample was transferred to an RNeasy spin column placed in a 2 mL collection tube and centrifuged for 30 s at ≥ 8000 g, discarding the flow-through. Then, the sample was washed adding 700 µL of RW1 buffer and centrifuged for 30 s at ≥ 8000 g, discarding the flow-through. After that, two additional washing steps were performed with 500 µL of RPE buffer. Finally, RNeasy spin column was placed in a new 1.5 mL collection tube and 30-50 µL of RNase-free water was directly added to the membrane to elute the RNA by centrifuging 1 min at ≥ 8000 g. The purified RNA suspensions were spectrophotometrically quantified using Nanodrop 1000 and used immediately or stored at -80 °C until use. The integrity of mRNA was assessed by using LabChip 2100 BioAnalyzer (Agilent technologies). This analyser provides sizing, quantification, and purity assessment for RNA based on electrophoretic separation. The ribosomal RNAs appear as sharp bands or peaks. The apparent ratio of 28S rRNA to 18S rRNA should be approximately 2:1. Agilent biolanalyzer also provides an RNA Integrity number (RIN) as a useful measure of RNA integrity. Ideally the RIN should be close to 10. Figure S5.1 shows the results for a RNA integrity analysis.

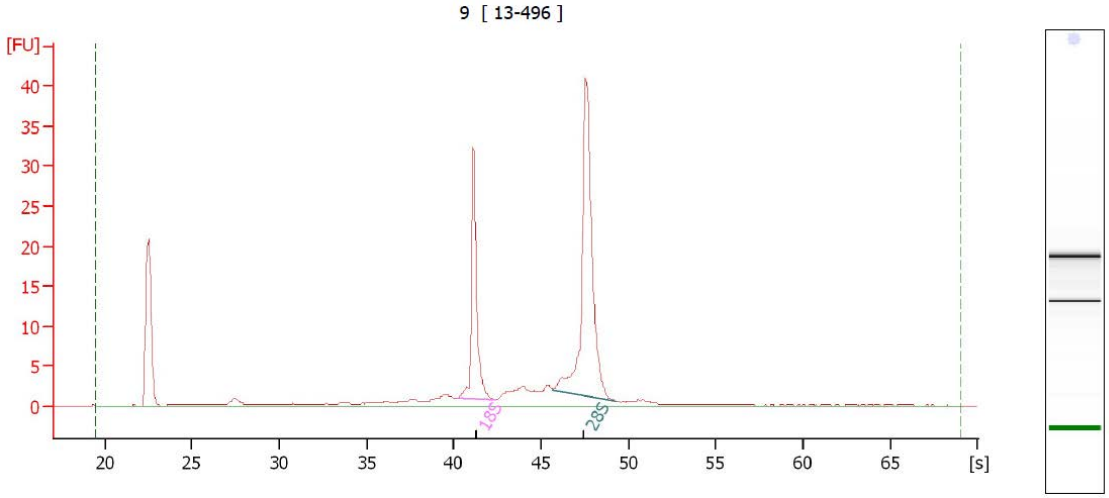

Overall Results for sample 9 : 9

RNA Area:	132,7	RNA Integrity Number (RIN):	9.8 (B.02.07)
RNA Concentration:	57 ng/µl	Result Flagging Color:	
rRNA Ratio [28s / 18s]:	2,0	Result Flagging Label:	RIN: 9.80

Fragment table for sample 9 : 9

Name	Start Time [s]	End Time [s]	Area	% of total Area
18S	40,20	42,35	27,7	20,9
28S	45,65	49,30	55,5	41,8

Figure S5.1. Results obtained for the RNA integrity analysis. 18S and 28S band appears in a ratio of 20.9:41.8 ≈ 1:2, with a high RNA integrity number (RIN = 9.8)

5.7.2.9 Classical cDNA synthesis by retrotranscription

For the cDNA synthesis, mRNA was incubated with 1 mg mL^{-1} of oligo$(dT)_{20}$ primer and 10 mmol L^{-1} of dNTP mix (10 mmol L^{-1} each dATP, dGTP, dCTP and dTTP at neutral pH) for 5 min at 65 °C and cooled on ice for at least 1 min. After that, a mix containing 0.1 mmol L^{-1} DTT, 40 U μL^{-1} RNAseOUT and 200 U μL^{-1} SuperScript III and 1X First-Strand buffer (50 mmol L^{-1} Tris-HCl pH 8.3, 75 mmol L^{-1} KCl, 3 mmol L^{-1} $MgCl_2$) was added and incubated for 60 min at 55 °C, and 15 min at 70 °C for inactivating the reaction. The cDNA was stored at 20 °C until use.

5.7.2.10 Cytometric Bead Array

Cytokine secretion from lymphocytes was analysed by Cytometric Bead Array on culture supernatants. Cytometric bead array provides the simultaneous measure of different proteins in a single reaction by flow cytometry. The assay is based on the use of antibody-coated beads to efficiently capture a specific protein that serve as the solid support for a sandwich-type immunoassay and fluorescence-conjugated antibody for the detection.

For the IL-4, IL-17 and IFN-γ protein detection, 25 μL of cell culture supernatant was mixed with 25 μL of IL-4, IL-17 and IFN-γ capture beads, and incubated for 1 hour at room temperature. After that, 25 μL of a mix containing phycoerythrin detection reagent was added and incubated for 2 hours at room temperature. Afterwards, the sample was washed with 500 μL of washing buffer, followed by a centrifugation at 200 g for 5 min to eliminate the reagent excess by discarding the supernatant. Finally, the sample was resuspended in 150 μL of washing buffer and analyzed by flow cytometry.

5.7.3 Results and discussion

5.7.3.1 Efficiency study of the immunomagnetic separation (IMS)

In order to determine the IMS efficiency, 100 μL of 500 cells μL^{-1} were firstly counted in a Neubauer chamber (Nº of total cells), and incubated with antiCD3-MPs (8×10^5) for 30 minutes under gentle shaking. After that, the supernatant was removed by placing the tube on the magnet and the non-bound cells were counted in a Neubauer chamber (Nº non-bound cells). The IMS efficiency was calculated as follows.

$$\textit{IMS efficiency (\%)} = \frac{\textit{No. total cells - No. nonbound cells}}{\textit{No. total cells}}$$

The IMS efficiency (%) was found to be 96 ±3 % (n=3).

5.7.3.2 Optimization of the washing step time for the electrochemical genosensing

In order to simplify the analytical procedure and reduce the experimental time, the washing step during the electrochemical genosensing was optimized, taking GAPDH transcript, obtained from 1000 cells μL^{-1}, as a model. After the double-tagging RT-PCR amplification of GAPDH transcript with the double-tagging set of primers (BIO/DIG), the amplicons were incubated for 15 min at 42 °C with 6 $\times 10^6$ of streptAv-MPs in 140 μL of Tris blocking buffer. Then, two washing steps were performed with 500 μL of Tris-HCl buffer for 2, 5, and 10 min at 42 °C. After that, the incubation with the electrochemical reporter was performed with 60 μg antiDIG-HRP in Tris-HCl blocking buffer at a final volume of 140 μL for 30 min at 42 °C. After that, two washing steps with 500 μL of Tris buffer for 2, 5 and 10 min at 42 °C, followed by electrochemical detection were performed. In all instances, a negative control, which contained all reagents except the double-tagged amplicons, was processed.

As shown in Figure S5.2, three different washing times were tested (2, 5 and 10 min) and the signal obtained was comparable in all cases.

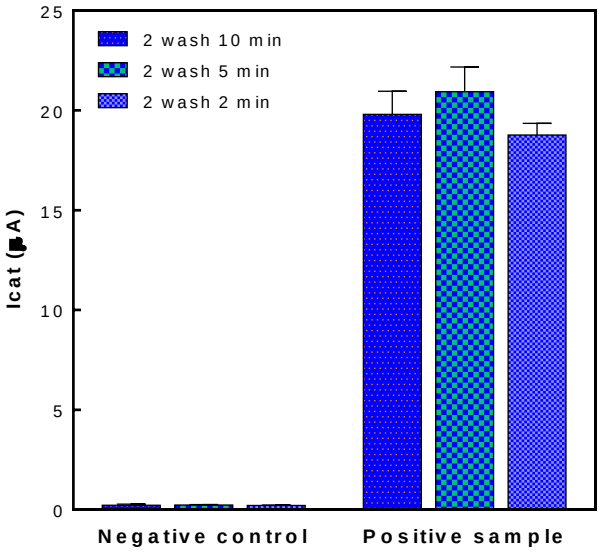

Figure S5.2. Optimization of the washing step time for the electrochemical genosensing. n=3.

In order to confirm if the washing time has an effect on the analytical performance, statistical t-test for mean comparison was performed,[29] resulting in no significant differences

among the mean values (t=1.58208, p=0.1888 for 5 and 2 min comparison; t=0.80095, p=0.46804 for 10 and 2 min comparison; t=0.66886, p=0.54021 for 10 and 5 min comparison). ANOVA analysis was performed to compare if the signal obtained with the different washing times differ significantly among them (F=1.099; P_{value}=0.392). In both cases, no significant differences were found. Thus, in order to minimize the assay time, 2 min was used for all washing steps for the electrochemical genosensing in further experiments.

5.7.3.3 Optimization of the incubation time with the electrochemical reporter for the electrochemical genosensing

In order to further minimize the assay time and simplify the analytical procedure, the incubation time with the electrochemical reporter during the electrochemical genosensing was optimized. For this study, GAPDH transcript, obtained from 1000 cells μL^{-1}, was used as a model. After the double-tagging RT-PCR amplification of GAPDH transcript with the double-tagging set of primers (BIO/DIG), the amplicon was incubated for 15 min at 42 °C with 6 $\times 10^6$ of streptAv-MPs in 140 μL of Tris blocking buffer. Then, two washing steps were performed with 500 μL of Tris buffer for 2 min at 42 °C. After that, the incubation with the electrochemical reporter was performed with 60 μg antiDIG-HRP in Tris blocking buffer at a final volume of 140 μL for 10 and 30 min at 42 °C, followed by two washing steps with 500 μL of Tris buffer for 2 min at 42 °C. Finally, the electrochemical detection was performed. In all instances, a negative control, which contained all reagents except the double-tagged amplicons, was processed. The results are shown in the Figure S5.3.

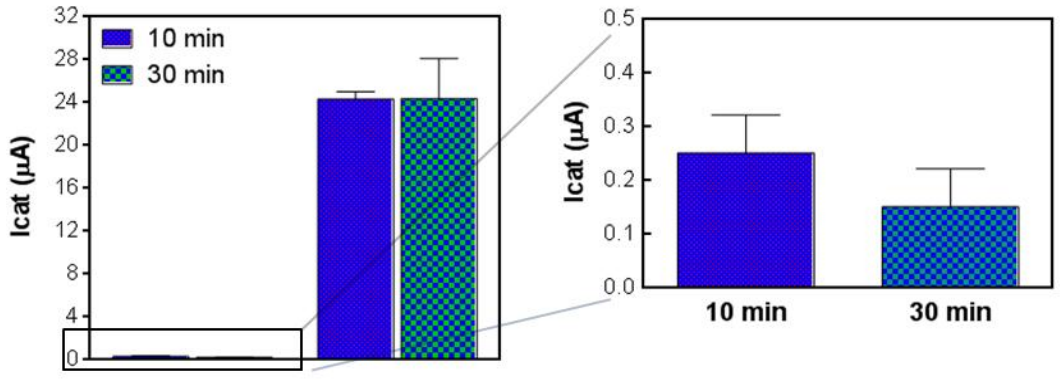

Figure S5.3. Optimization of the incubation time of the electrochemical reporter for the detection of GAPDH transcripts by electrochemical genosensing. n=3.

The ANOVA analysis (F=1.7179 10-4, p=0.99073) and t-test (t=0.01311, p= 0.99073) were performed for both conditions, showing that no significant differences were observed. Thus, in order to minimize the assay time; 10 min was used in all cases for the incubation with the electrochemical reporter during the electrochemical genosensing in further experiments.

5.7.3.4 Optimization of the concentration of streptAv-MPs for the electrochemical genosensing

The concentration of streptAv-MPs was optimized in order to obtain the higher signal-to-background ratio in the electrochemical genosensing, For this study, GAPDH transcript, obtained from 1000 cells μL^{-1}, was used as a model. After the double-tagging RT-PCR amplification of GAPDH transcript with the double-tagging set of primers (BIO/DIG), the amplicon was incubated for 15 min at 42 °C with different concentration of streptAv-MPs ranging from 2.4×10^5 , 6×10^5 , 1.2×10^6, and 6×10^6 in 140 μL of Tris blocking buffer, and proceed as above. The electrochemical signal obtained with each concentrations of streptAv-MP was compared, and the results are shown in Figure S5.4.

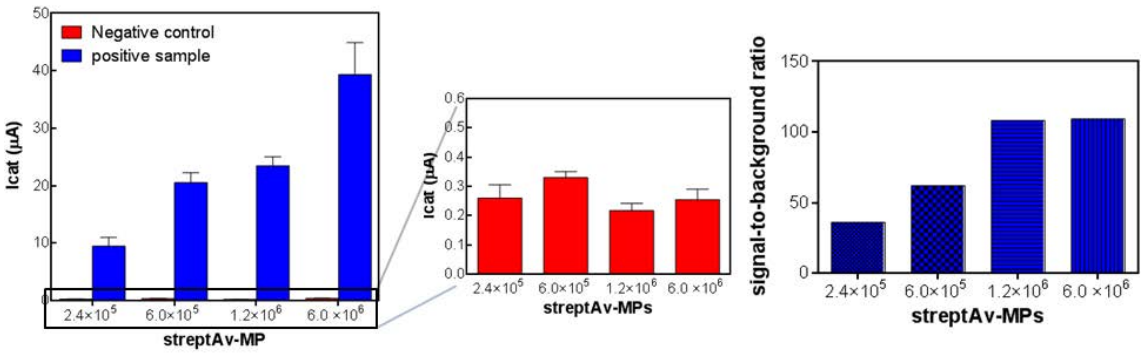

Figure S5.4. Optimization of the concentration of streptAv-MPs for the electrochemical genosensing for the detection of GAPDH transcripts. The inset shows in detail the values for the negative controls for 2.4×10^5 , 6×10^5, 1.2×10^6, 6×10^6 streptAv-MP. n=3.

As shown in Figure S4, the higher signal-to-background ratio was obtained at a concentration of 1.2×10^6 and 6×10^6 streptAv-MPs. In order to achieve maximal binding, the optimal concentration of streptAv-MPs particles was selected as 6×10^6 streptAv-MP (0.7 mg mL^{-1} of streptAv-MP).

5.7.3.5 Optimization of the concentration of the electrochemical reporter for the electrochemical genosensing

The concentration of the electrochemical reporter was optimized in order to obtain the higher signal-to-background ratio with the electrochemical genosensing. For this study, GAPDH transcript, obtained from 1000 cells μL^{-1}, was used as a model. After the double-tagging RT-PCR amplification of GAPDH transcript with the double-tagging set of primers (BIO/DIG), the amplicons were diluted in distilled water and incubated for 15 min at 42 °C with 6×10^6 of streptAv-MPs and different amount of antiDIG-HRP (ranging from 7, 15, 30 and 60 μg) coding for GAPDH transcript as a housekeeping gene, in Tris blocking buffer at a final volume of 140 μL. Then, two washing steps were performed with 500 μL of Tris buffer for 2 min at 42 °C. Finally, the electrochemical detection was performed. In all instances, a negative control, which contained all reagents except the double-tagged amplicons, was processed. Figure S5.5 shows raw data for all the concentration range, as well as the signal-to-background ratio.

The optimal amount of electrochemical reporter was determined in 60 μg of antiDIG-HRP. Although an increased non-specific signal is observed at this concentration, the highest electrochemical signal was also obtained.

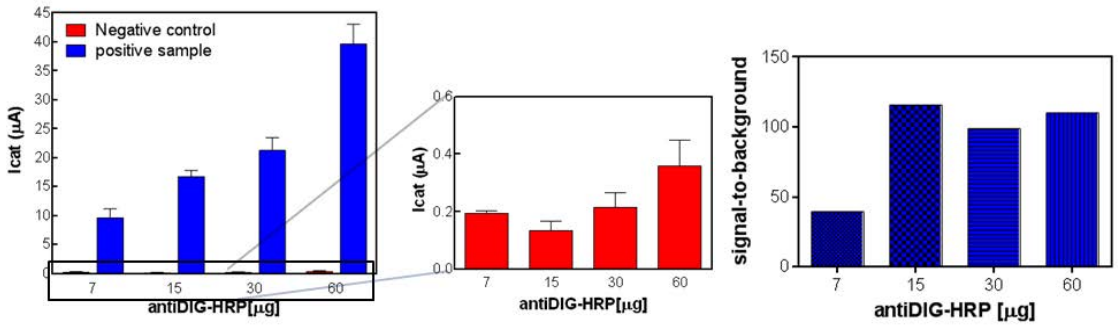

Figure S5.5. Optimization of the electrochemical reporter (antiDIG-HRP). Amounts of 7, 15, 30 and 60 μg were tested. In all cases negative and positive samples were processed. The error bars show the standard deviation for n=3.

5.7.3.6 Optimization of the incubation steps for the electrochemical genosensing

In order to simplify the analytical procedure, two different strategies were evaluated in terms of the analytical performance, as schematized in the Figure S5.6. The optimal protocol was evaluated by following the different procedures and comparing the responses of a

negative and a positive control using the double-tagging PCR with the electrochemical detection taking GAPDH transcript as a model.

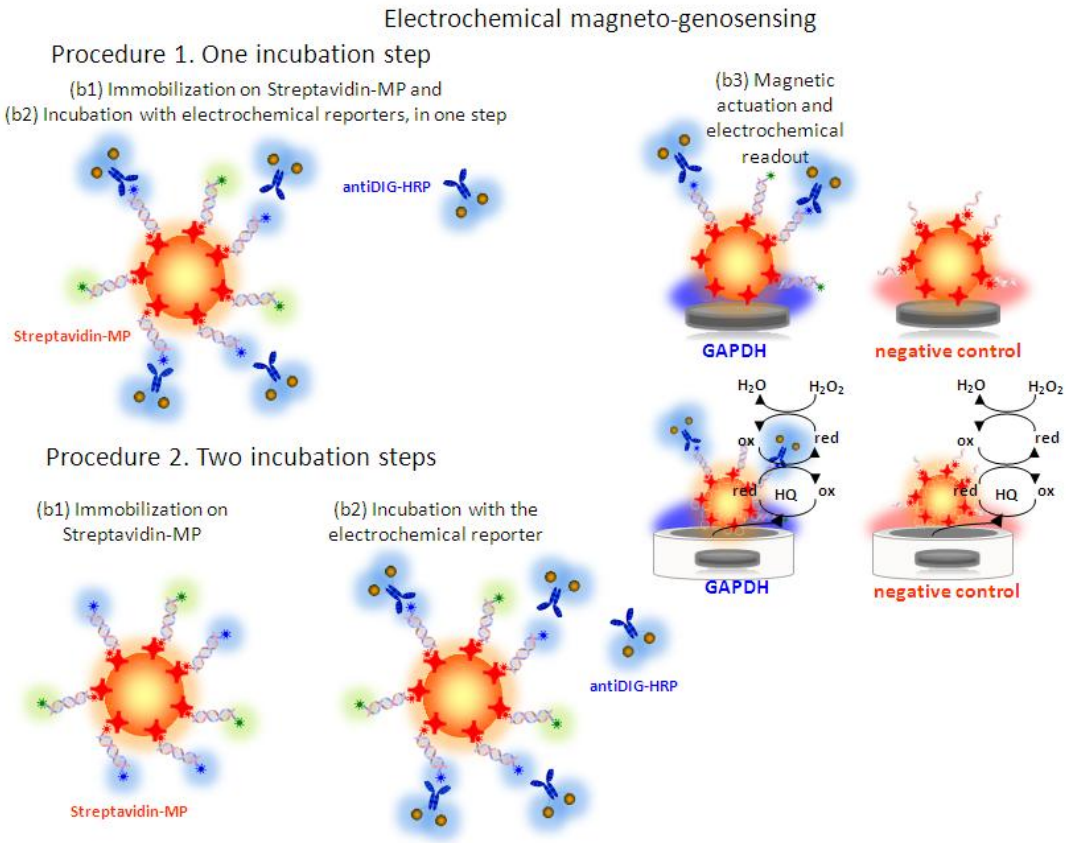

Figure S5.6. Schematic representation of the optimization of the incubation steps for the electrochemical genosensing.

Figure S5.7 shows the electrochemical signal obtained in both cases, under the same conditions including concentration of streptAv-MPs, and antiDIG-HRP, among others.

Procedure 1. One incubation step. The double-tagged amplicons for GAPDH were incubated with 6×10^6 streptAv-MP and 60 μg of antiDIG-HRP in Tris blocking buffer for 15 min at 42 °C, in one step. After that, two washing steps with 500 μL of Tris-HCl buffer for 2 min at 42 °C were performed.

Procedure 2. Two incubation steps. The double-tagged amplicons were firstly incubated with 6×10^6 of streptAv-MP in Tris blocking buffer for 15 min at 42 °C. After that, two washing steps with 500 μL of Tris buffer for 2 min at 42 °C were performed. The incubation with the electrochemical reporter was performed with 60 μg of antiDIG-HRP in Tris blocking buffer for 15 min at 42 °C. Finally, two washing steps with 500 μL of Tris-HCl buffer for 2 min at 42 °C were performed.

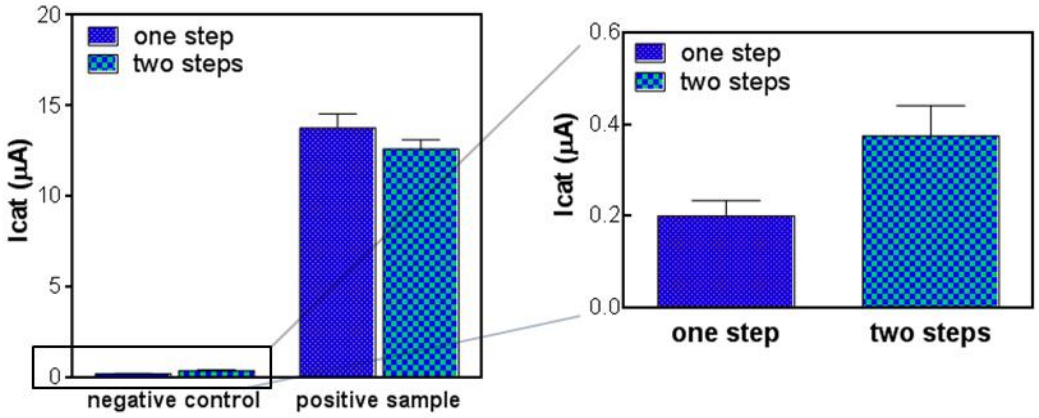

Figure S5.7. Optimization of the incubation steps for the electrochemical genosensing of GAPDH transcript. Comparison between one and two steps procedures. The two strategies were evaluated by comparing the response of a negative and a positive control. StreptAv-HRP 6×10^6, antiDIG-HRP 60 μg. n=3.

As shown in Figure S5.7, no significant differences were observed. Since the procedure 1 involves only one incubation step, being a clear advantage in terms of the simplification of the analytical procedure, it was selected for the final procedure.

Finally, The Figure S5.8 shows the results for the detection of GAPDH transcripts, performed with lymphocytes in a range from 0.1 to 1000 cells μL^{-1}, which involves the IMS with antiCD3-MPs, the transcript extraction and retrotranscription on polydT-MPs, double-tagging PCR with the single set of specific primers for the amplification of GAPDH and labeled with DIG/BIO tags and, finally, electrochemical genosensing.

The LOD value (dotted line) shown in Figure S5.8, panel B, was estimated by fitting the raw data using a nonlinear regression (R^2= 0.9494), as shown in Figure S5.8, panel C, by processing the negative control samples (n=3) obtaining a mean value of 0.837 μA with a standard deviation of 0.172 μA. The cut-off value was then determined with a one-tailed t-test at a 95% confidence level, giving a value of 1.338 μA (indicated as a dotted-line in Figure S5.8, panel B). The LOD was found to be as low as 0.017 cells μL^{-1} (which corresponds to 2 cells) much lower than the gel electrophoresis, which is able to detect 10 cells μL^{-1} (corresponding to 1000 cells, as shown in lane 6, Figure S5.8, panel A). As the number of copies for GAPDH transcripts is approximately 1000/2000 copies per cell, [24,25] this LOD corresponds to the detection of as low as 2×10^4 transcript copies mL^{-1}.

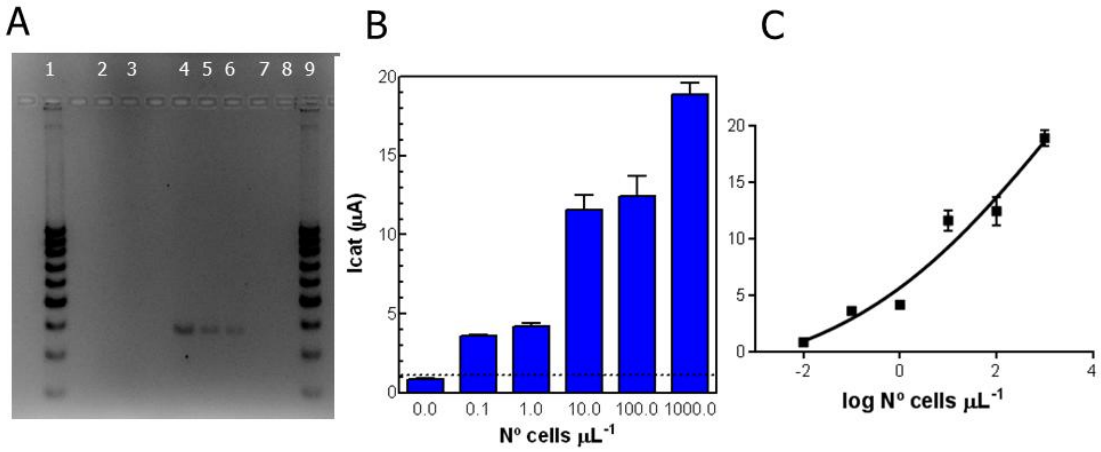

Figure S5.8. GAPDH transcript detection by immunomagnetic separation of cells, double-tagging RT-PCR on magnetic beads and electrochemical genosensing. Panel A shows the gel electrophoresis: Lanes 1 and 9, molecular weight marker; Lane 2, RT negative control; Lane 3, PCR negative control; Lanes 4 to 8, correspond to 1000; 100; 10; 1 and 0.1 cells μL^{-1}, respectively. Panel B, shows the electrochemical signals for the GAPDH detection on cells. n=3, while Panel C shows the Four Parameter logistic Equation fitted data.

5.7.3.7 Quantification of IFN-γ by Cytometric Bead Array

Table S5.2. Quantification of IFN-γ in the cell culture supernatant by Cytometric Bead Array

Sample	Day 0 (pg/ml)	48 h (pg/ml)
S1	18.69	3430.08
S2	113.4	13106

5.8 References

[1] Van de Vosse, E., Hoeve, M. A., Ottenhoff, T. H. (2004). Human genetics of intracellular infectious diseases: molecular and cellular immunity against mycobacteria and salmonellae. The Lancet infectious diseases, 4(12), 739-749.

[2] Lamhamedi, S., Jouanguy, E., Altare, F., Roesler, J., Casanova, J. L. (1998). Interferon-gamma receptor deficiency: relationship between genotype, environment, and phenotype. International journal of molecular medicine, 1(2), 415-423.

[3] Noordzij, J. G., Hartwig, N. G., Verreck, F. A., De Bruin-Versteeg, S., De Boer, T., Van Dissel, J. T., De Groot R, Ottenhoff T.H., Van Dongen, J. J., (2007). Two patients with complete defects in interferon gamma receptor-dependent signaling. Journal of clinical immunology, 27(5), 490-496.

[4] Dammermann, W., Bentzien, F., Stiel, E. M., Kühne, C., Ullrich, S., zur Wiesch, J. S., Lüth, S. (2015). Development of a novel IGRA assay to test T cell responsiveness to HBV antigens in whole blood of chronic Hepatitis B patients. Journal of translational medicine, 13(1), 157.

[5] Dunn, G. P., Koebel, C. M., Schreiber, R. D. (2006). Interferons, immunity and cancer immunoediting. Nature Reviews Immunology, 6(11), 836.

[6] Baccala, R., Kono, D. H., Theofilopoulos, A. N. (2005). Interferons as pathogenic effectors in autoimmunity. Immunological reviews, 204(1), 9-26.

[7] Pollard, K. M., Cauvi, D. M., Toomey, C. B., Morris, K. V., Kono, D. H. (2013). Interferon-γ and systemic autoimmunity. Discovery medicine, 16(87), 123.

[8] Welcher A. A., Boedigheimer M., Kivitz A. J., Amoura Z., Buyon J., Rudinskaya A., Latinis K., Chiu K., Oliner K. S., Damore M. A., Arnold G. E., Sohn W., Chirmule N., Goyal L., Banfield C. and Chung J. B., (2015). Blockade of interferon-γ normalizes interferon-regulated gene expression and serum CXCL10 levels in patients with systemic lupus erythematosus. Arthritis & Rheumatology, 67(10), 2713-2722.

[9] Latorre, I., Carrascosa, J. M., Vilavella, M., Díaz, J., Prat, C., Domínguez, J., Ferrándiz, C. (2014). Diagnosis of tuberculosis infection by interferon-gamma release assays in patients with psoriasis. Journal of Infection, 69(6), 600-606.

[10] Horsburgh C.R., Jr and Rubin E.J., N. Engl. J. Med. 364 (15), 2011, 1441–1448. Horsburgh Jr, C. R., & Rubin, E. J. (2011). Latent tuberculosis infection in the United States. New England Journal of Medicine, 364(15), 1441-1448.

[11] Chiacchio T., Delogu G., Vanini V., Cuzzi G., De Maio F., Pinnetti C., Sampaolesi A., Antinori A. and Goletti D. (2017). Immune characterization of the HBHA-specific response in Mycobacterium tuberculosis-infected patients with or without HIV infection. PloS one, 12(8), e0183846.

[12] Vassilopoulos D., Tsikrika S., Hatzara C., Podia V., Kandili A., Stamoulis N. and Hadziyannis E. (2011). Comparison of two gamma interferon release assays and tuberculin skin testing for tuberculosis screening in a cohort of patients with rheumatic diseases starting anti-tumor necrosis factor therapy. Clinical and Vaccine Immunology, 18(12), 2102-2108.

[13] Domínguez J., Ruiz-Manzano J., De Souza-Galvão M., Latorre I., Milà C., Blanco S., Jiménez M. A., Prat C., Lacoma A., Altet N., Ausina V. (2008). Comparison of two commercially available gamma interferon blood tests for immunodiagnosis of tuberculosis. Clinical and Vaccine Immunology, 15(1), 168-171.

[14] Ayubi E., Doosti-Irani A., Moghaddam A. S., Khazaei S., Mansori K., Safiri S., Sani M. Mostafavi E. (2017). Comparison of QuantiFERON-TB Gold In-Tube (QFT-GIT) and tuberculin skin test (TST) for diagnosis of latent tuberculosis in haemodialysis (HD) patients: a meta-analysis of κ estimates. Epidemiology & Infection, 145(9), 1824-1833.

[15] Sharma S. K., Vashishtha R., Chauhan L. S., Sreenivas V. Seth D. (2017). Comparison of TST and IGRA in diagnosis of latent tuberculosis infection in a high TB-burden setting. PloS one, 12(1), e0169539.

[16] Nesher L., Shah D. P., Ariza-Heredia E. J., Azzi J. M., Siddiqui H. K., Ghantoji S. S., Marsh L. Y., Michailidis L., Makedonas G., Rezvani K., Shpall E. J. Chemaly R. F., (2016). Utility of the Enzyme-Linked Immunospot Interferon-γ–Release Assay to Predict the Risk of Cytomegalovirus Infection in Hematopoietic Cell Transplant Recipients. The Journal of infectious diseases, 213(11), 1701-1707.

[17] Carinelli, S., Ballesteros, C. X., Martí, M., Alegret, S., Pividori, M. I. (2015). Electrochemical magneto-actuated biosensor for CD4 count in AIDS diagnosis and monitoring. Biosensors and Bioelectronics, 74, 974-980.

[18] Brandão, D., Liébana, S., Campoy, S., Cortés, M. P., Alegret, S., Pividori, M. I. (2015). Simultaneous electrochemical magneto genosensing of foodborne bacteria based on triple-tagging multiplex amplification. Biosensors and Bioelectronics, 74, 652-659.

[19] Ben Aissa A., Jara J. J., Sebastián R. M., Vallribera A., Campoy S. Pividori M. I. (2017). Comparing nucleic acid lateral flow and electrochemical genosensing for the simultaneous detection of foodborne pathogens. Biosensors and Bioelectronics, 88, 265-272.

[20] Xufré C., Costa M., Roura-Mir C., Codina-Busqueta E., Usero L., Pizarro E., Obiols G., Jaraquemada D. and Martí M. (2013). Low frequency of GITR+ T cells in ex vivo and in vitro expanded Treg cells from type 1 diabetic patients. International immunology, 25(10), 563-574.

[21] Pividori M. I., Alegret S. (2005). Electrochemical genosensing based on rigid carbon composites. A review. Analytical letters, 38(15), 2541-2565.

[22] O'Flynn K., Russul-Saib M., Ando I., Wallace D. L., Beverley P. C., Boylston A. W., Linch D. C. (1986). Different pathways of human T-cell activation revealed by PHA-P and PHA-M. Immunology, 57(1), 55.

[23] Tiefenthaler, G., Hünig, T. (1989). The role of CD2/LFA-3 interaction in antigen-and mitogen-induced activation of human T cells. International immunology, 1(2), 169-175.

[24] Barber, R. D., Harmer, D. W., Coleman, R. A., Clark, B. J. (2005). GAPDH as a housekeeping gene: analysis of GAPDH mRNA expression in a panel of 72 human tissues. Physiological genomics, 21(3), 389-395.

[25] White A. K., VanInsberghe M., Petriv I., Hamidi M., Sikorski D., Marra M. A., Piret J., Aparicio S. Hansen C. L. (2011). High-throughput microfluidic single-cell RT-qPCR. Proceedings of the National Academy of Sciences, 108(34), 13999-14004.

[26] Krause C. E., Otieno B. A., Bishop G. W., Phadke G., Choquette L., Lalla R. V., Peterson D. E., Rusling J. F. (2015). Ultrasensitive microfluidic array for serum pro-inflammatory cytokines and C-reactive protein to assess oral mucositis risk in cancer patients. Analytical and bioanalytical chemistry, 407(23), 7239-7243.

[27] Sánchez-Tirado E., Martínez-García G., González-Cortés A., Yáñez-Sedeño P. and Pingarrón J. M. (2017). Electrochemical immunosensor for sensitive determination of transforming growth factor (tgf)-β1 in urine. Biosensors and Bioelectronics, 88, 9-14.

[28] Mazurek, G. H., Jereb, J., Vernon, A., LoBue, P., Goldberg, S., Castro, K. (2010). Updated Guidelines for Using Interferon Gamma Release Assays to Detect Mycobacterium tuberculosis Infection, United States. Centers for Disease Control and Prevention. MMWR 2010; 59(No. RR-55):1-25.

[29] Whitley, E., Ball, J. (2002). Statistics review 5: Comparison of means. Critical Care, 6(5), 424.

Chapter 6

YOCTOMOLE ELECTROCHEMICAL GENOSENSING OF EBOLA VIRUS cDNA BY ROLLING CIRCLE AND CIRCLE TO CIRCLE AMPLIFICATION

Biosensors and Bioelectronics 93 (2016) 65-71

6.1 Abstract

This work addresses the design of an Ebola diagnostic test involving a simple, rapid, specific and highly sensitive procedure based on isothermal amplification on magnetic particles with electrochemical readout. Ebola padlock probes were designed to detect a specific *L-gene* sequence present in the five most common Ebola species. Ebola cDNA was amplified by rolling circle amplification (RCA) on magnetic particles. Further re-amplification was performed by circle-to-circle amplification (C2CA) and the products were detected in a double-tagging approach using a biotinylated capture probe for immobilization on magnetic particles and a readout probe for electrochemical detection by square-wave voltammetry on commercial screen-printed electrodes. The electrochemical genosensor was able to detect as low as 200 ymol, corresponding to 120 cDNA molecules of *L-gene* Ebola virus with a limit of detection of 33 cDNA molecules. The isothermal double-amplification procedure by C2CA combined with the electrochemical readout and the magnetic actuation enables the high sensitivity, resulting in a rapid, inexpensive, robust and user-friendly sensing strategy that offers a promising approach for the primary care in low resource settings, especially in less developed countries.

6.2 Introduction

Since the early reports on amplification of nucleic-acid sequences by the polymerase chain reaction (PCR),[1] this technique has found widespread application in many areas of genetic analysis, ranging from forensics to diagnostics of genetic and infectious diseases, among many others. PCR generates billions of DNA copies from a single target molecule within an hour.[2] As main advantage, PCR can improve detection sensitivities up to 100-fold over antigen detection tests with faster turnaround times. The detection of PCR products can be easily achieved by electrochemical genosensing.[3] Since this early report, novel routes based on PCR for the amplification of the analytical signal to increase the sensitivity of the electrochemical readout were explored. For instance, a double-tagging PCR amplification strategy with electrochemical readout was reported.[4,5] During PCR, not only the amplification of the DNA was achieved, but also the double-tagging of the amplicon to enhance the electrochemical detection. The integration of magnetic particles (MPs) provides additional advantages: (a) Sensitivity is increased by combining this approach with immunomagnetic [6] or phagomagnetic [7] separation, and (b) the use of MPs greatly improves the performance of the biological reaction by increasing the surface area, improving the washing steps and, importantly, minimizing the

matrix effect. (c) MPs allow reduction of reaction times and reagent volumes. In addition, (d) MPs can be easily magneto-actuated using permanent magnets.[8]

The first generation of nucleic-acid amplification technologies based on PCR requires thermocycling platforms, trained personnel, and infrastructure. However, many infectious diseases are endemic in low resource settings where the lack of reliable power supply is a critical barrier for PCR.[9] Recently, there have been significant developments in a class of amplification techniques that do not require temperature cycling [10,11] such as helicase-dependent amplification [12] loop-mediated isothermal amplification [13] and rolling circle amplification,[14,15] among others. These methods use a variety of reaction principles to specifically amplify nucleic acid targets through isothermal conditions, and the amplicons can be detected in some instances directly without the need for an instrument.[10,16] RCA is based on the continuing replication of circles.[17] The phi29 (ϕ29) DNA polymerase, initiated by a primer or the detected target sequence itself synthesizes a long linear concatenated replica of the circular DNA template until the process is terminated. The long DNA repeats can readily and sensitively be detected upon hybridization with a label probe. Importantly, RCA has no requirement of special instrumentation to cycle the temperature, contrary to PCR-based DNA diagnostics. More than billion-fold amplification can be achieved with hyperbranched RCA [14] or circle-to-circle amplification [18] in less than 3 h, thus ensuring ultrasensitive detection. The target recognition can be achieved with padlock probes, linear oligonucleotides that contain a unique target recognition sequence in each probe arm and a target-independent sequence as a linker.[19] The target recognition sequences are designed to bind head to tail on a genomic target DNA. Upon hybridization to target DNA, the probes are circularized by enzymatic ligation, while if there is no DNA target present, the padlock probes remain linear. Only the circularized padlock probe can then be amplified by RCA. The ligation reaction is highly sequence specific and allows even for discrimination of single nucleotide variations.[19,20] Variations in target sequences in rapidly mutating viruses can be compensated for by using padlock probe cocktails that assure detection of viruses with high specificity and efficiency.[21] Progress in isothermal amplification techniques will without doubt be critically relevant for the monitoring of infectious disease outbreaks in low-resource settings, such as the recent Ebola virus outbreak.

Ebola virus is the causative agent of hemorrhagic fever with a very high case fatality.[22] However, while Ebola outbreaks may be geographically localized in West Africa, migration and international travel lead to its rapid spread around the world. The most widespread epidemic of Ebola virus disease began in Guinea in December 2013, with minor outbreaks in other

developed countries including UK, USA and Spain.[23] The diagnosis during this outbreak was based on quantitative reverse transcription polymerase chain reaction (qRT-PCR). In 2014 the World Health Organization (WHO) launched an urgent and major initiative to stimulate diagnostic innovation and expedite the delivery of better and faster tests for Ebola virus in low resource settings.[24] Improvements in isothermal amplification procedures that can be adapted to a point-of-care format can overcome this issue. The simplicity and efficiency of RCA technology, along with the accuracy in quantification, makes it amenable for miniaturization and automation in high-throughput analysis in resource-constrained small centres. Moreover, electrochemical-based detection offers a promising alternative with inherent features including low cost, low power requirements, high sensitivity and compatibility with portable technology.

This work addresses the design of a novel strategy for the sensitive, specific, cost-effective and portable detection of Ebola virus as a model for emerging infectious diseases by combining isothermal DNA amplification, based on RCA and C2CA on magnetic particles, with electrochemical genosensing. Ebola padlock probes were designed to specifically detect the *L-gene* sequence present in the five most common Ebola species and the utility of the electrochemical genosensing approach for highly sensitive rapid detection of Ebola virus sequences is demonstrated. To the best of our knowledge, it is the first time that integration of the rolling circle/circle-to-circle amplification is combined in the same strategy using magnetic particles with electrochemical readout and disposable screen-printed electrodes.

6.3 Experimental section

6.3.1 Instrumentation

The electrochemical measurements on carbon screen-printed electrodes (ref. DRP-110) were performed on a portable bipotentiostat DRP-STAT200 using DropView 2.2 for instrument control and data acquisition from Dropsens, Spain. Fluorescently labelled rolling circle products were detected using Aquila 400 (Q-linea AB, Sweden).

6.3.2 Chemicals and biochemicals

Streptavidin magnetic particles (streptavidin-MPs) (Dynabeads® MyOne Streptavidin T1 Prod. No. 65601) were purchased from Life Technologies. For the magnetic actuation of the

streptavidin-MPs, the magnetic separator DynaMag 96 side (Ref No. 12331D, Life Technologies) was used. T4 ligase and ϕ29 DNA polymerase came from Thermo Fisher Scientific. Probes modified with peroxidase (HRP) were purchased from Biomers, Germany. Synthetic cDNA, padlock probes, and Cy3 labelled detection probes were purchased from Integrated DNA technologies, USA. The composition of buffer solutions is detailed in *§6.7.1*.

6.3.3 Padlock probe design and oligonucleotides

The Ebola virion contains one molecule of linear, single-stranded, negative-sense RNA, and approximately 18,900 nucleotides in length (GenBank accession Nº KJ660346.2). Due to the limitations of Biosafety level 4 facilities for handing Ebola virus, this work was performed with a synthetic biotinylated cDNA as a target, mimicking the product obtained after retrotranscription with a biotinylated primer of the *L-gene* in Ebola virus. Three padlock probes, 85 base pairs long, were designed for targeting different regions of the specific *L-gene* for the Ebola virus, present in the five known Ebola species (including Zaire ebolavirus, Sudan ebolavirus, Taï Forest ebolavirus, Bundibugyo ebolavirus and Reston ebolavirus), based on Ebola virus sequencing data released after the 2014 outbreak. Padlock probes are long synthetic single-stranded oligonucleotides, whose ends are complementary to adjacent target sequences (Figure 6.1, panel A). Upon hybridization with the target (as shown in detail in Figure 6.1, panel B), the two ends of the padlock probe are put into close contact, allowing the circularization by enzymatic ligation (Figure 6.1, panel C and D), while if there is no DNA target present, the padlock probes remain linear. Padlock probe thus provides an extremely specific target recognition, which is followed by isothermal amplification by using ϕ29 DNA polymerase.

Among the *L-gene* hybridization sites, a restriction site for the *Alu*I restriction enzyme was included in the linker sequence of the padlock probes, as well as the hybridization sequences for the detection of the amplified RCA and C2CA products by either Cy3-labelled or peroxidase-modified detection probes to achieve fluorescence or electrochemical readouts, respectively (Figure 6.1, panel A). Additionally, for the magnetic actuation on streptavidin-MPs of the amplified products, a hybridization sequence complementary to a biotinylated capture probe was included in the padlock sequence. Table S6.1 (*§6.7.2*) summarizes the oligonucleotide sequences used in this study.

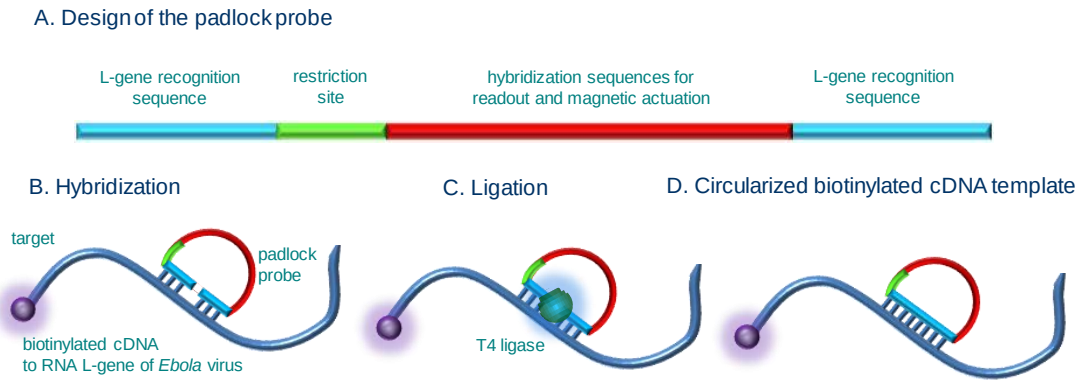

Figure 6.1. (A) Design of the *L-gene* specific padlock probe for the detection of Ebola virus and further amplification by RCA; B) Head-to-tail hybridization of padlock probe with biotinylated cDNA used as a target and mimicking the product obtained after retrotranscription with a biotinylated primer of the Ebola virus *L-gene*; C) Ligation with the enzyme T4 ligase for 15 min at 37 °C; D) Circularized cDNA templates.

6.3.4 Generation of circularized DNA templates

In order to test and optimize the electrochemical detection of rolling circle amplification products, circular templates for RCA were generated, as schematically shown in Figure 6.1. Upon hybridization of the padlock probes, phosphorylated at 5´end, with the cDNA target (Figure 6.1, panel B), the probes were ligated with T4 ligase (Figure 6.1, panel C) to obtain the circularized biotinylated cDNA template (Figure 6.1, panel D). The ligation reaction was performed by incubation of 10 nM of the biotinylated cDNA target (mimicking the product obtained after reverse transcription with a biotinylated primer of the *L-gene* in Ebola virus) with 30 nM of the phosphorylated padlock probe in a T4 ligation reaction mix containing 40 mM Tris-HCl, 10 mM $MgCl_2$, 10 mM DTT, 1.5 mM ATP, 0.2 μg μL^{-1} BSA and 5 U T4 DNA ligase in a 100 μL reaction volume. The incubation was performed at 37 °C for 15 min and 65 °C for 2 min to inactivate T4 ligase enzyme. The resulting biotinylated DNA circle concentration was then 10 nM. Circles were diluted in log-dilution series and were used for further experiments (Figure 6.1, panel D).

6.3.5 Rolling circle amplification and electrochemical genosensing

Rolling circle amplification was performed with 5 μL of Ebola biotinylated cDNA ranging from 200 zmol up to 20 amol. Briefly, 4 μL of streptavidin-MPs were added and incubated for 5 min at room temperature (RT) under rotation, to achieve the coupling of the circularized

biotinylated cDNA template to the MPs thought the high affinity biotin-streptavidin bond (as schematically shown in Figure 6.2, panel A1). The remaining reagents were removed and the sample-particles were washed once in washing buffer. After each incubation and washing steps, the magnetic separator was positioned under the tubes until pellet formation on the tube side wall, followed by supernatant separation. After that, the RCA mix was added, containing 1x ϕ29 DNA polymerase buffer, 125 μM dNTPs, 0.2 mg ml^{-1} BSA, and 4 U ϕ29 DNA polymerase. The RCA was performed at 37 °C for 60 min, followed by a short incubation at 65 °C for 1 min to inactivate the ϕ29 DNA polymerase (Figure 6.2, panel A2). After that, the hybridization with the readout probe 2 (labelled with HRP, 5 nM) was performed for 15 min at 37 °C in hybridization buffer, followed by two washing steps under magnetic actuation, to eliminate the excess of labelled probe (Figure 6.2, panel A3). Finally, the electrochemical readout (Figure 6.2, panel A4) was performed. A full description of this procedure is provided in *§6.7.3* (outlined in S6.1 and S6.2). Briefly, each sample was resuspended in 60 μL of 0.25 mmol L^{-1} hydrogen peroxide (H_2O_2) and 1 mmol L^{-1} hydroquinone (HQ), acting as substrate and mediator of the HRP enzyme conjugated on the readout probe (Figure S6.2, *§6.7.3*). After 2 min of reaction, the solution was added to the screen-printed electrode surface and measured by square wave voltammetry (SWV). The applied potential was ranged from 0 to -0.7 V with potential step and amplitude of 10 mV and frequency of 1 Hz. The cathodic signals corresponding to the peaks were used for the calibration plots. As the screen-printed electrodes are disposable, after each use, the electrodes were discarded. The reproducibility of the electrodes was studied by cyclic voltammetry, and the results are shown in Figure S6.3 (*§6.7.3*).

As a gold standard method for the detection of the RCA products, the Aquila amplified single molecule counter (Q-linea) based on fluorescence readout was used to count the RCA products.[25] To achieve that, the RCA procedure was performed as above but omitting the coupling with streptavidin-MPs, as shown in Figure 6.2, panel B1, since in this instance, the excess of fluorescent readout probes does not interfere in the detection, in which only big blobs labelled with thousands of probes are detected due to the resolution of the confocal microscopy. In detail, the RCA amplified product was incubated for 15 min at 55 °C with the readout probe 1 labelled with Cy3 (5 nM) in hybridization buffer (Figure 6.2, panel B2). Each amplified entity was then counted with Aquila amplified single molecule counter (Q-linea) (Figure 6.2, panel B3).

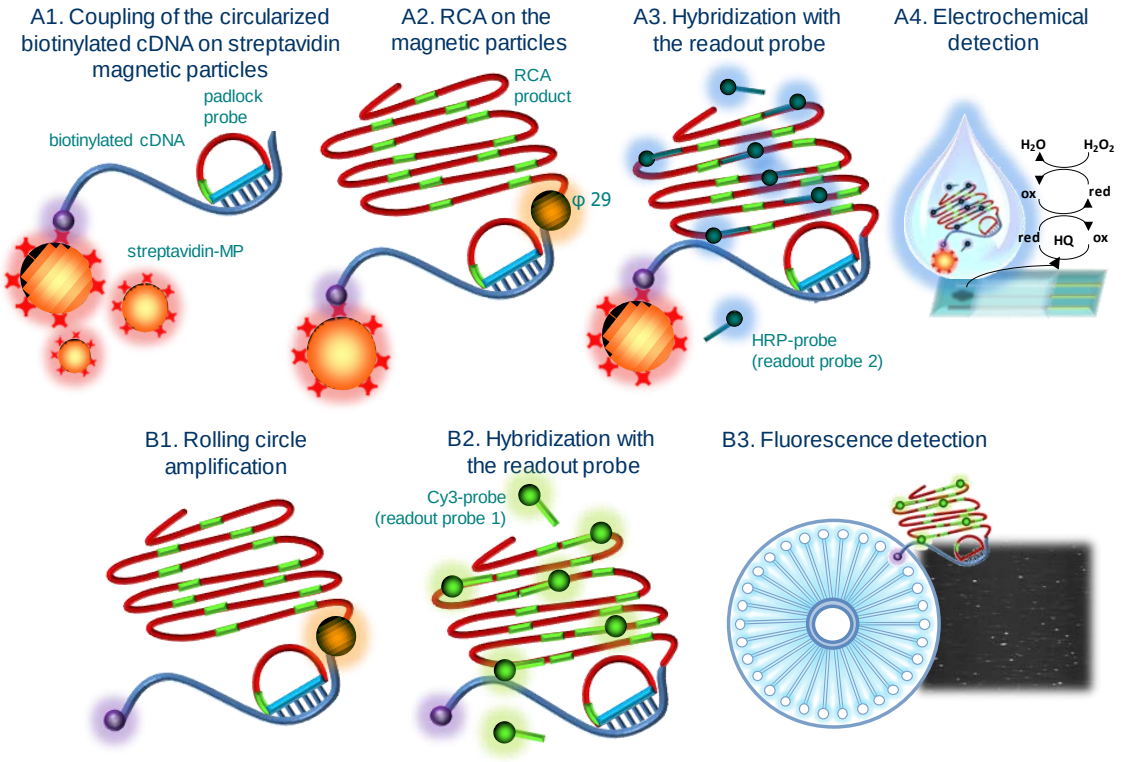

Figure 6.2. Schematic representation of the electrochemical genosensing of Ebola virus cDNA by rolling circle amplification. A1) Coupling of the circularized biotinylated cDNA (from 200 zmol up to 20 amol) on streptavidin magnetic particles for 5 min at RT; A2) RCA on the streptavidin-MPs using ϕ29 DNA polymerase for 60 min at 37 °C; A3) Hybridization with readout probe 2 labelled with HRP for 15 min at 37 °C; A4) Enzymatic reaction (with H_2O_2 as substrate and HQ as mediator) and electrochemical determination on screen-printed electrodes by square wave voltammetry at a potential ranging from 0 to -0.7 V. Schematic representation of the Aquila amplified single molecule counter procedure. B1) RCA using ϕ29 DNA polymerase for 60 min at 37 °C; B2) Hybridization with the readout probe 1 labelled with Cy3; D3) Counting of each amplified entity with Aquila amplified single molecule counter (Q-linea).

6.3.6 Ultra-sensitive Ebola detection by circle-to-circle amplification and electrochemical genosensing

A strategy to achieve higher sensitivity based on further amplification by C2CA was tested, as shown in Figure 6.3. A first round of RCA was performed with circular cDNA templates ranging from 200 ymol to 200 zmol in 20 µl RCA mix (containing ϕ29 DNA polymerase buffer, 125 µM dNTPs, 0.2 mg ml^{-1} BSA, and 4 U ϕ29 DNA polymerase) and incubated at 37 °C for 60 min. The reaction mixture was then submitted to 65 °C for 1 min to inactivate the ϕ29 DNA polymerase (Figure 6.3, panel A). The amplified RCA products were then reamplified by a second round of RCA, as shown in Figure 6.3, panel B. To achieve that, the RCA products were monomerized by addition of 5 µL digestion mix containing 40 mU $µl^{-1}$ *Alu*I restriction enzyme, ϕ29 DNA polymerase buffer, 120 nM restriction probe, and 0.2 mg ml^{-1} BSA and 2 min

incubation at 37 °C and 1 min at 65 °C to inactivate the *Alu*I enzyme. The monomers were then recircularized and reamplified in a second RCA round by addition of 25 µL ligation and RCA mix containing 1x ϕ29 DNA polymerase buffer, 0.2 mg ml^{-1} BSA, 0.7 mM ATP, 100 µM dNTP, 20 mU $µL^{-1}$ T4 DNA ligase, and 6U of ϕ29 DNA polymerase. This reaction was incubated for 30 min at 37 °C and briefly at 65 °C for 1 min to stop the reaction. After that, the hybridization and double-tagging with the readout probe 4 (labelled with HRP, 5 nM) and the capture probe (labelled with biotin, 0.5 nM) was performed in hybridization buffer for 15 min at 37 °C, as schematically shown in Figure 6.3, panel C. The double-tagged hybrids were then captured on 4 µL of streptavidin-MPs for 5 min at room temperature (Figure 6.3, panel D).

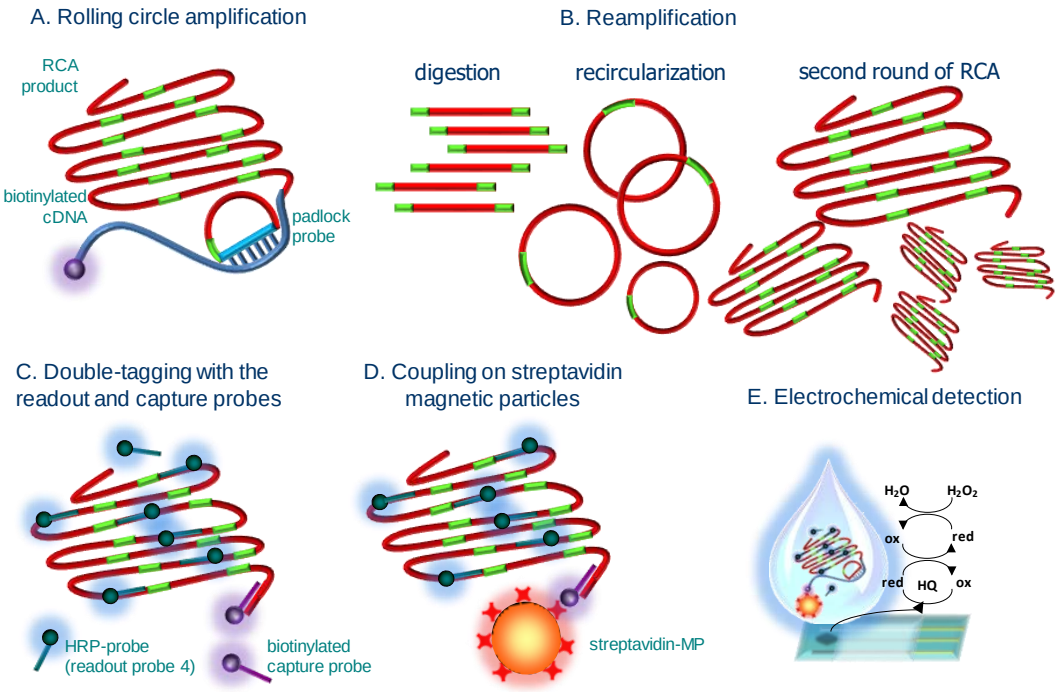

Figure 6.3. Schematic representation of the electrochemical genosensing of Ebola virus cDNA by C2CA. A) First round of RCA of circular cDNA (from 200 ymol to 200 zmol) using ϕ29 DNA polymerase for 60 min at 37 °C; B) Reamplification by a second round of RCA (60 min at 37 °C) after digestion with *Alu*I restriction enzyme and recirculation of the RCA products using T4 DNA ligase; C) Double-tagging of the C2CA products with 5 nM readout probe (labelled with HRP) and 0.5 nM capture probe (labelled with biotin) for 15 min at 37 °C; D) Coupling of the biotinylated product on streptavidin magnetic particles for 5 min at RT; E) Enzymatic reaction (with H_2O_2 as enzymatic substrate and HQ as mediator) and electrochemical determination on screen-printed electrodes by square wave voltammetry at a potential ranging from 0 to -0.7 V.

The use of the streptavidin-MPs allowed the preconcentration of the C2CA product through the biotin tag of the capture probe, as well as the elimination of the excess readout probe by means of two washing steps. For washing, a magnetic separator was positioned under the

tubes until pellet formation on the tube side wall, followed by supernatant. The electrochemical readout (shown in Figure 6.3, panel E) was performed as described in §6.3.5 for RCA, and as fully described in *§6.7.3* (outlined in Figure S6.1 and S6.2).

As a gold standard and benchmark against the state-of-the-art fluorescent RCA detection method, the Aquila amplified single molecule counter (Q-linea) was used to count the C2CA products. For that purpose C2CA products were fluorescently labelled by incubation for 15 min at 55 °C with 5 nM of the readout probe 3 labelled with Cy3 in hybridization buffer. The labelled C2CA products were then counted with Aquila amplified single molecule counter (Q-linea).

6.4 Results and Discussion

6.4.1 Selection of the padlock probe

Three different padlock probes (Table S6.1, *§6.7.2*) were designed for targeting different regions of the Ebola virus *L-gene*, one of the most conserved gene of the Ebola genome,[23] in order to firstly select which one produces higher RCA product yield. The three different padlock probes were accordingly circularized, as described in §6.3.4, at a biotinylated cDNA target concentration of 1 nmol L^{-1}. The circularized cDNA template was preconcentrated on streptavidin magnetic particles and further amplified by RCA. Negative controls for each padlock probe were also processed without cDNA target. As no cDNA target was present, the padlock probes remain linear, and cannot be further amplified by RCA in the negative controls. The RCA products were then labelled with the same readout probe 2, tagged with HRP, followed by the electrochemical readout, as shown in Figure 6.2. It is important to highlight that as the three padlock probe were designed for targeting different regions of the Ebola virus, the *L-gene* recognition sequence is unique for each padlock probe, while the hybridization sequence was designed to be the same (Figure 6.1 and Table S6.1). As such, the RCA products obtained for each padlock probe were recognized by hybridization with the same readout probe 2. The raw square wave voltammograms are shown in Figure 6.4, panel A, while the mean value for three replicates of the maximal cathodic signals are shown in Figure 6.4, panel B. Mean values of 11.0 μA with a standard deviation (SD) of 0.45 μA (for padlock probe 1), 9.8 μA (SD 1.79 μA) (for padlock probe 2) and 8.3 μA (SD 1.66 μA) (for padlock probe 3) were obtained. The mean values for the background signals from the negative controls were 0.45 μA (SD 0.23 μA) (for padlock probe 1), 2.5 μA (SD 0.11 μA) (for padlock probe 2) and 2.80

μA (SD 0.69 μA) (for padlock probe 3), with a signal-to-background ratio of 24.49, 3.94 and 2.98 for padlocks probes 1, 2 and 3, respectively, confirming an increased yield of the rolling circle amplification performed with the padlock probe 1. This padlock probe was used for further experiments.

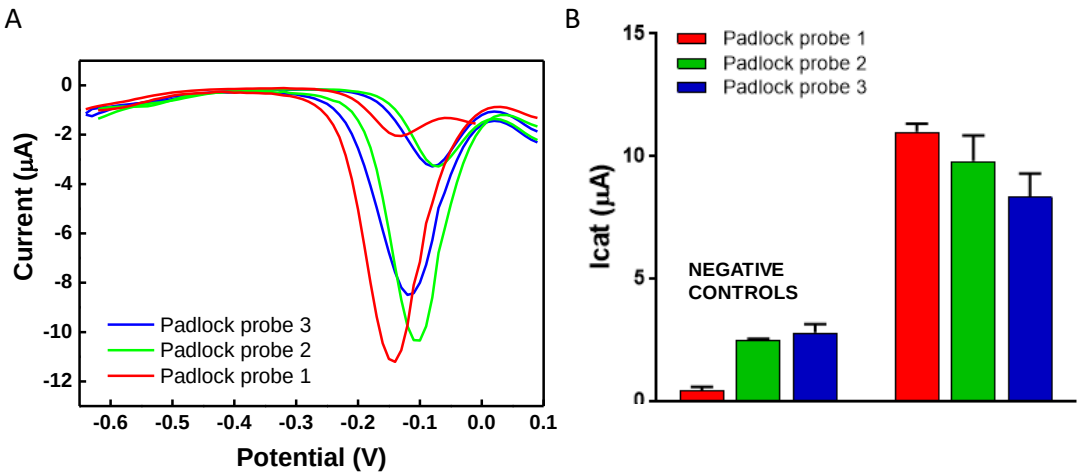

Figure 6.4. Performance study of the rolling circle amplification and electrochemical genosensing by using three different padlock probe. A) Square wave voltamograms. B) Graph bars of the voltamograms maximal signal. The bars represent the mean value of the maximal signal and the error bars, the standard deviation for n=3. In all cases, cDNA target concentration of 1 nmol L^{-1} was used, except for the negative controls. Medium: phosphate-buffered saline. Mediator: HQ 1.0 mmol L^{-1}. Substrate: H_2O_2 0.25 mmol L^{-1}. The SWV conditions were: potential range from 0 to -0.7 V, potential step and amplitude of 10 mV and frequency of 1 Hz.

6.4.2 Rolling circle amplification and electrochemical genosensing

To determine the performance and limit of detection (LOD) of electrochemical genosensing of RCA products, RCA was performed on a serial dilution of Ebola biotinylated cDNA (ranging from 200 zmol to 20 amol), as schematically shown in Figure 6.2. The raw square wave voltammograms are shown in Figure 6.5, panel A, while the mean value for three replicates of the maximal cathodic signals are shown in Figure 6.5, panel B and C. In Figure 6.5, panel B, the electrochemical signal was fitted using a nonlinear regression (One-site binding, Hyperbola– GraphPad Prism Software) (R^2=0.9096). The LOD was estimated by fitting the raw data using a nonlinear regression (Four Parameter logistic Equation– GraphPad Prism Software) (R^2=0.9799), as shown in Figure 6.5, panel C, by processing the negative control samples (n=3) obtaining a mean value of 0.840 μA with a standard deviation of 0.261. The cut-off value was then determined with a one-tailed t test at a 95% confidence level (t=2.920), resulting in a value of 1.601 μA (shown in Figure 6.5, panels B and C, as the dotted lines). The LOD was found to be 966 zmol. The electrochemical genosensor combined with RCA was thus able to detect as

low as 5.8 × 10^5molecules of cDNA targets (1.2 × 10^8 cDNA target mL^{-1}) with a single RCA amplification, offering a comparable sensitivity to recently proposed nanopore detection of RCA products on magnetic particles.[26] This performance may be suitable for the application in Ebola virus detection, as this disease usually presents a high level of viremia, especially in the early-stage of the disease, ranging from 10^6 to 10^{10} RNA copies per mL.[23, 27] However, it should be highlighted that a further improvement of the LOD can be achieved by the magnetic actuation on a higher volume of sample (100 μL of sample instead of 5 μL), theoretically increasing the LOD two order of magnitude. In order to achieve a lower limit of detection to assure the detection of minute amounts of Ebola virus at clinically relevant levels, a further improvement in the LOD can be achieved by re-amplification of the RCA products by C2CA.

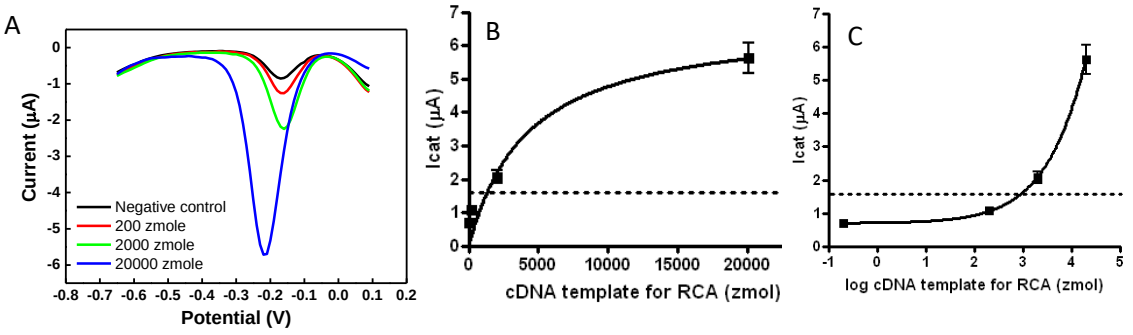

Figure 6.5. Electrochemical signals for the rolling circle amplification and electrochemical genosensing. cDNA target amount ranging from 200 zmol to 20 amol was used, except for the negative controls. A) Raw square wave voltammograms; B) One-site binding fitting; C) Four Parameter logistic fitting. Medium: phosphate buffer. Mediator: HQ 1.0 mmol L^{-1}. Substrate: H_2O_2 0.25 mmol L^{-1}. All other conditions as in Figure 6.4. n=3.

6.4.3 Ultra-sensitive Ebola detection by circle-to-circle amplification and electrochemical genosensing

In order to improve the LOD, a second strategy based on a further reamplification of RCA products by C2CA was performed, as shown in Figure 6.3. Preformed circles at a concentration ranging from 200 ymol to 200 zmol were subjected to C2CA, as outlined in Figure 6.3. The raw square wave voltammograms are shown in Figure 6.6, panel A, while the mean value for two replicates of the maximal cathodic signals are shown in Figure 6.6, panel B and C. In Figure 6.5, panel B, the electrochemical signal was fitted using a nonlinear regression (One-site binding, Hyperbola– GraphPad Prism Software) (R^2= 0.9475). The LOD was estimated by fitting the raw data using a nonlinear regression (Four Parameter logistic Equation– GraphPad Prism Software) (R^2= 0.9930), as shown in Figure 6.6, panel C, by processing the negative control

samples (n=2) obtaining a mean value of 0.103 μA with a standard deviation of 0.012. The cut-off value was then determined with a one-tailed t test at a 95% confidence level (t=6.314), giving a value of 0.178 μA (shown in Figure 6.6, panels B and C, as the dotted lines). The LOD was found to be 53 ymol in 2 μL of reaction volume. The electrochemical genosensor combined with C2CA was thus able to reach a LOD of as low as 33 molecules of cDNA target (1.65×10^4 molecules of cDNA target mL^{-1}). The system was able to effectively detect 200 ymol of cDNA target (corresponding to 120 cDNA molecules, 6×10^4 molecules of cDNA target mL^{-1}) with a mean value of 0.271 μA (SD 0.097 μA) (above the cut-off value) and a signal-to-background ratio of 2.0.

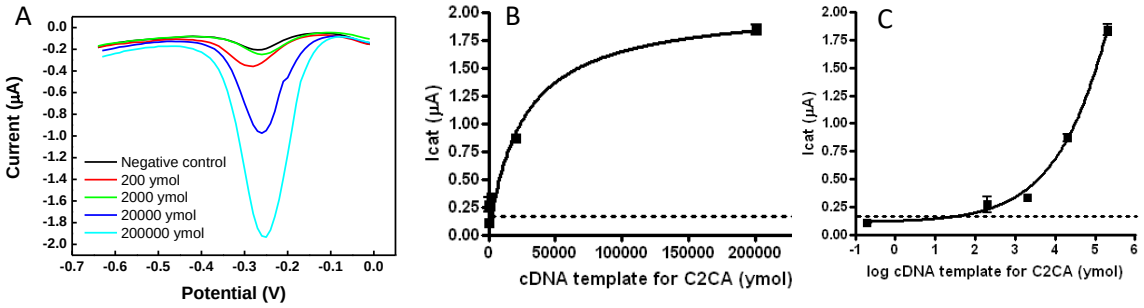

Figure 6.6. Electrochemical signals for the circle-to-circle amplification and electrochemical genosensing. cDNA target amount ranging from 200 ymol to 200 zmol was used, except for the negative controls A) Raw square wave voltammograms; B) One-site binding fitting; C) Four Parameter logistic fitting. Medium: phosphate buffer. Mediator: HQ 1.0 mmol L^{-1}. Substrate: H_2O_2 0.25 mmol L^{-1}. All other conditions as in Figure 6.4. n=2.

In order to compare the sensitivity of this electrochemical C2CA method with state-of-the-art fluorescent RCA quantification, a fraction of C2CA products were fluorescently labelled and analyzed by a commercially available amplified single molecule counting device (Q-linea, Sweden). The results are discussed in Supp Material. Similar LOD was achieved (171 cDNA molecules) (Figure S6.4, *§6.7.4*), demonstrating that the herein proposed electrochemical C2CA-based genosensing strategy achieves even better sensitivity than sophisticated and costly bench top fluorescent detectors. It is important to highlight that the RCA strategy is able to generate up to one thousand copies for each molecule of the original target, due to the processivity of the ϕ29 polymerase, resulting in RCA products which can contain up to 1,000 concatemeric repeats for each padlock probe. Since C2CA involves two consecutive RCA cycles, this isothermal strategy is able to amplify up to one million each DNA target molecule. The low LOD achieved by this strategy meets the requirements for Ebola detection and may indeed be suitable for its application in Ebola virus detection at early-stage of the disease, ranging from

10^6 to 10^{10} RNA copies per mL.[23,27] The isothermal nature of RCA based assays in combination with the portable and low cost magneto-electrochemical read out presents a promising approach for point-of-care infectious disease monitoring in the field.

6.5 Conclusions

Recent guidelines published by WHO recommend that diagnostic devices for developing countries to be ASSURED being this acronym defined by (A) Affordable, (SS) Sensitive, Specific, (U) User-friendly, (R) Rapid and Robust, (E) Equipment free, and (D) Deliverable to those who need it. In 2014, WHO launched an urgent and major initiative to stimulate diagnostic innovation and expedite the delivery of simpler and faster tests for Ebola virus in low resource settings. As a consequence, rapid diagnostic tests based on a lateral flow assay were conceived. Although these tests are extremely useful in some settings, it shows low sensitivity and specificity, highlighting that nucleic acid tests are more accurate for the diagnosis. In this manuscript we present a very promising test based on isothermal amplification and electrochemical genosensing which can easily be adapted to a point-of-care. The integration of RCA and further reamplification by C2CA, the magnetic actuation and the electrochemical detection provides an ultra-sensitive test able to detect as low as 33 molecules of cDNA target in a total assay time of below 2.5 hours. Although this work was performed with a synthetic biotinylated cDNA as a target due to the limitations of BSL-4 facilities for handing real Ebola patient samples, the successful detection of viruses through C2CA in true clinical samples has previously been demonstrated.[28] The herein proposed genosensing method has very low LOD that is highly promising for the detection of RNA Ebola virus in real samples. As the viral load must be quantitative, associated instrumentation is required. The electrochemical readout can be achieved with instrumentation designed to be low maintenance, battery/solar energy operated, and low cost, to meet the demands for ASSURED diagnosis recommended by WHO, while the isothermal amplification can be adapted to be performed at room temperature. The electrochemical genosensor presented in this work offers a promising alternative to the gold standard qRT-PCR, especially in resource-constrained West African settings, as a rapid, cost-effective, analytical strategy that can be handled for unskilled personnel at the community and primary care level.

6.6 Acknowledgments

Financial support from BioMaX ‘‘Novel diagnostic bioassays based on magnetic particles’’, Marie Curie Initial Training Networks (FP7-PEOPLE-2010-ITN), the Ministry of Economy and Competitiveness (MINECO), Madrid (Project BIO2013-41242-R) and the project EbolaMoDRAD, receiving funding from the Innovative Medicines Initiative 2 Joint Undertaking under grant agreement No. 115843, are gratefully acknowledged.

6.7 Supplementary material

6.7.1 Buffers and solutions

All buffer solutions were prepared with milli-Q water and all other reagents were in analytical reagent grade (supplied from Sigma and Merck). The composition of these solutions were: phosphate buffer for electrochemical measurement (ePBS): 0.1 mol L^{-1} Na_2HPO_4, 0.1 mol L^{-1} KCl; ϕ29 DNA polymerase buffer: 33 mM Tris-acetate pH 7.9, 10 mM magnesium acetate, 66 mM potassium acetate, 0.1% Tween-20, 1 mmol L^{-1} DTT; hybridization buffer: 20 mmol L^{-1} EDTA, 20 mmol L^{-1} Tris-HCl, 1.4 mol L^{-1} NaCl, and 0.1% Tween-20; and washing buffer: 10 mmol L^{-1} Tris-HCl pH 7.5, 5 mmol L^{-1} EDTA, 0.1% Tween-20 and 0.1 mol L^{-1} NaCl.

6.7.2 Padlock probe design and oligonucleotides

Table S6.1. Oligonucleotide sequences used in this study.

Name	Sequence	Modifications
cDNA to RNA *L-gene* of Ebola virus (synthetic cDNA target)	TTGCGAGTCGGATAAGGCAATTTTCCGAAAGTTCTACCTACATTCAA CTCTTTCTCTTTCAATGAGAAAGAAAAATTCCGATATTGTGGTAGTAG ATAC	5’ Biotin
Padlock Probe 1	CTTTCTCATTGAAAGAGAAGTGTATGCAGCTCCTCAGTAAGTAGCCG TGACTATCGACTTCAAAGGCCACAATATCGGAATTTTT	5’ Phos
Padlock Probe 2	CGGAATTTTTCTTTCTCATGTGTATGCAGCTCCTCAGTAAGTAGCCGT GACTATCGACTTCAAAGGGTATCTACTACCACAATAT	5’ Phos
Padlock Probe 3	AGAACTTTCGGAAAATTGCGTGTATGCAGCTCCTCAGTAAGTAGCCG TGACTATCGACTTCAAAGGGAAAGAGTTGAATGTAGGT	5’ Phos
Restriction probe	GTGTATGCAGCTCCTCAGTA	
Readout probe 1 (RCA)	AGTAGCCGTGACTATCGACT	3’ Cy3
Readout probe 2 (RCA)	TTTTTTTTTTGTGTATGCAGCTCCTCAGTA	5’ HRP
Readout probe 3 (C2CA)	TACTGAGGAGCTGCATACAC	3’ Cy3
Readout probe 4 (C2CA)	TTTTTTACTGAGGAGCTGCATACAC	5’ HRP
capture probe	CCTTTGAAGTCG	5’ Biotin

6.7.3 Electrochemical readout

The Figure S6.1 shows the whole set-up for the electrochemical readout. Carbon screen-printed electrodes were purchased from Dropsens, Spain (ref. DRP-110). These electrodes consist in a ceramic substrate (L 34 x W 10 x H 0.5 mm) with a carbon working electrode, a graphite counter electrode and a silver pseudo-reference electrode printed on it (Figure S6.1,

panel A). The circular working electrode is only 4 mm diameter, allowing to drop only small volume of samples such as those used in this work (60 µL) (Figure S6.1, panel B). The electrodes were connected to the portable bipotentiostat (DRP-STAT200, DropSens, Spain) by an electrode holder (Figure 6.1, panel C). As shown in Figure S6.1, panel D, the square wave voltammetry measurements were performed in a laptop computer operated by the battery, in which the portable bipotentiostat was connected by a universal USB port.

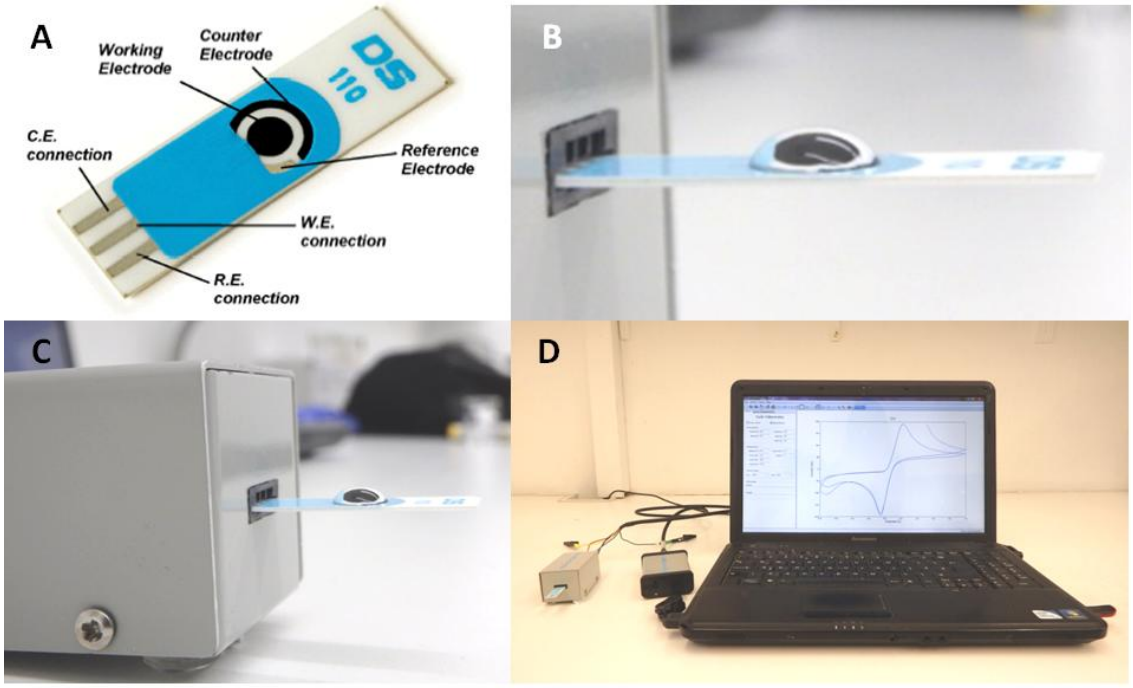

Figure S6.1. Set-up for the electrochemical readout. Panel A shows the configuration of the commercial screen-printed electrodes used in this work (image obtained from the following link: http://www.dropsens.com/en/screen_printed_electrodes_pag.html). 60 µL of the sample was dispensed on the surface of the electrode after the enzymatic reaction, as shown in detail in panel B. The electrode was connected to the portable bipotentiostat (DRP-STAT200, DropSens, Spain) by an electrode holder (panel C). The SWV measurements were performed in a laptop computer operated by the battery, under the DropView 2.2 software, in which the portable bipotentiostat was connected by a USB port (panel D).

The electrochemical readout was based on square wave voltammetry, in the presence of hydrogen peroxide as a substrate and hydroquinone as mediator and the horseradish peroxidase enzyme conjugated to the readout probes 2 and 4, which were used as electrochemical reporters. The sequences of these oligonucleotides are as follows:

Readout probe 2 (RCA)	HRP-TTTTTTTTTTGTGTATGCAGCTCCTCAGTA
Readout probe 4 (C2CA)	HRP-TTTTTTACTGAGGAGCTGCATACAC

While the readout probe 2 is complementary to the products of the rolling circle amplification, the sequence of the readout probe 4 was selected to be complementary to the circle-to-circle amplification products, and the specific binding of the readout probe is this achieved by hybridization, as shown in Figure S6.2, panels A and B.

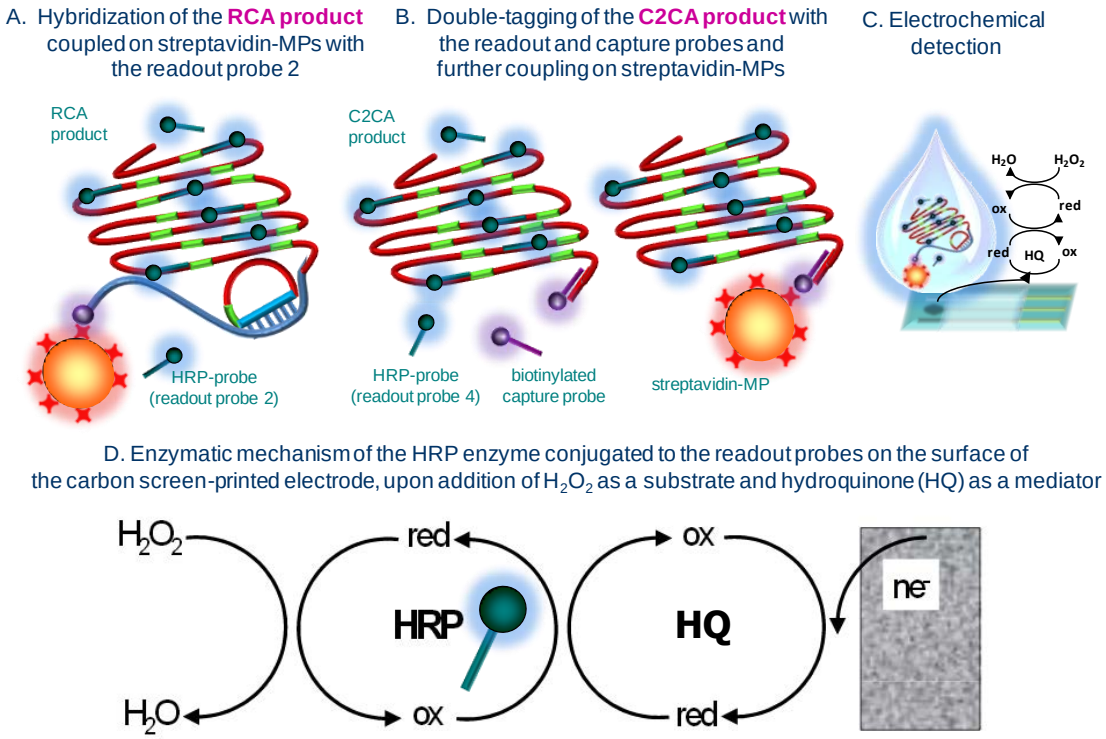

Figure S6.2. Panel A: Hybridization of the RCA products with the readout probe 2, labelled with HRP; Panel B: Hybridization of the C2CA products with the readout probe 4, labelled with HRP; Panel C: Enzymatic reaction and electrochemical readout on the surface of the screen-printed electrodes.

For the square wave voltammetry measurements, 60 µL hydrogen peroxide 0.25 mmol L^{-1} and hydroquinone 1 mmol L^{-1} was added to the sample as substrate and mediator for the HRP enzyme conjugated to the readout probes (as shown in Figure S6.2, panel C). After 2 min of enzymatic reaction, the solution was dispensed on the surface of the screen-printed electrode (Figure S6.1, panel B) connected by an electrode holder (Figure S6.1, panel C).

The fundamentals of the mechanism of the horseradish peroxidase-based enzymatic reaction is shown in detail in Figure S6.2, panel D. Horseradish peroxidase catalysed the oxidation of hydrogen peroxide to water, in the presence of a hydrogen donor, in this instance, hydroquinone. Upon addition of hydrogen peroxide as a substrate, the HRP is thus oxidized, while hydroquinone acts as mediator to shuttle electrons between the screen-printed electrode and the enzyme. The hydroquinone is thus oxidized, while HRP is reduced again, at

high turnover rate, being able to catalyze again the oxidation of new molecules of substrate, increasing the sensitivity of the approach and amplifying the electrochemical signal. The final readout at the surface of the screen-printed electrode is based thus on the reduction of the benzoquinone (the oxidized form of HQ) by SWV. To achieve that, the potential was ranged from was 0 to -0.7 V, with a potential step and amplitude of 10 mV, and frequency of 1 Hz, obtaining the maximal cathodic signal typically at potentials around -0.2 V (vs. Ag pseudo-reference electrode) (as observed in the raw SWV data in Figures 6.4, 6.5 and 6.6). The data were recorded and processed using DropView 2.2 software, and the maximal cathodic signals were used for the calibration plots shown in Figures 6.4, 6.5 and 6.6. It is important to highlight that this cathodic signal is directly proportional to the concentration of HRP, since saturated substrate conditions were used and the enzyme is thus working at saturation (Vmax, at zero kinetic order), being the Vmax directly proportional to the concentration of enzyme. The quantification of both the RCA and C2CA products is thus achieved since the higher the concentration of the amplified products, the higher the hybridization with the readout probes (Figure S6.2, panels A and B) and thus the higher the concentration of HRP.

As the screen-printed electrodes are disposable, one electrode was used in each measurement. The characterization and reproducibility study of the screen-printed electrodes by cyclic voltammetry is thus shown in Figure S6.3, and performed by adding 60 µL of hydroquinone 1 mmol L^{-1} in phosphate buffer pH= 7.0. The cyclic voltammograms were recorded in a potential ranging from -0.8 to +1.0V, using a scan rate of 100 mV s^{-1}.

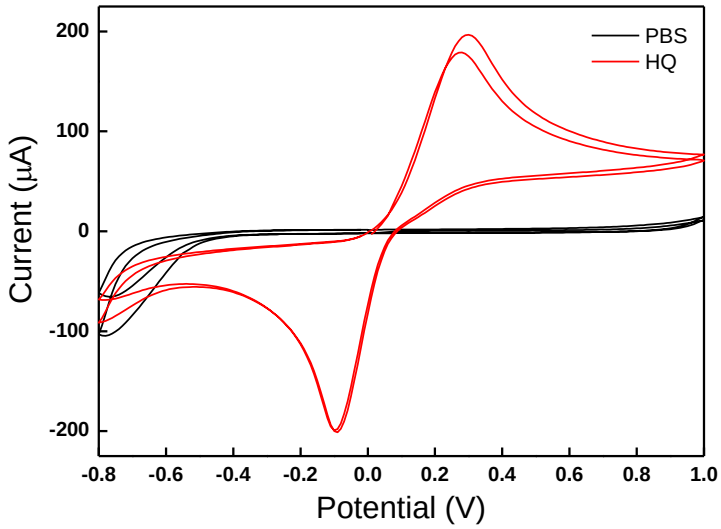

Figure S6.3. Cyclic voltammograms of screen-printed electrodes upon the addition of 1×10^{-3} mol L^{-1} of hydroquinone in phosphate buffer pH= 7.0. The scan rate was 100 mV s^{-1}. n=2.

As shown in Figure S6.3, no signal is observed in the absence of HQ, while the reduction peak (around -0.1 V) was obtained at a similar potential for SWV. Two cyclic voltammograms of two different electrodes are observed, showing outstanding reproducibility in the cathodic peak corresponding to the reduction of benzoquinone.

6.7.4 Ultra-sensitive Ebola detection by circle-to-circle amplification and fluorescence readout based on Q-linea

In order to compare the sensitivity of this electrochemical C2CA method with state-of-the-art fluorescent RCA quantification, a fraction of C2CA products were fluorescently labeled and analyzed by a commercially available amplified single molecule counting device (Q-linea, Sweden), as shown in Figure S6.4.

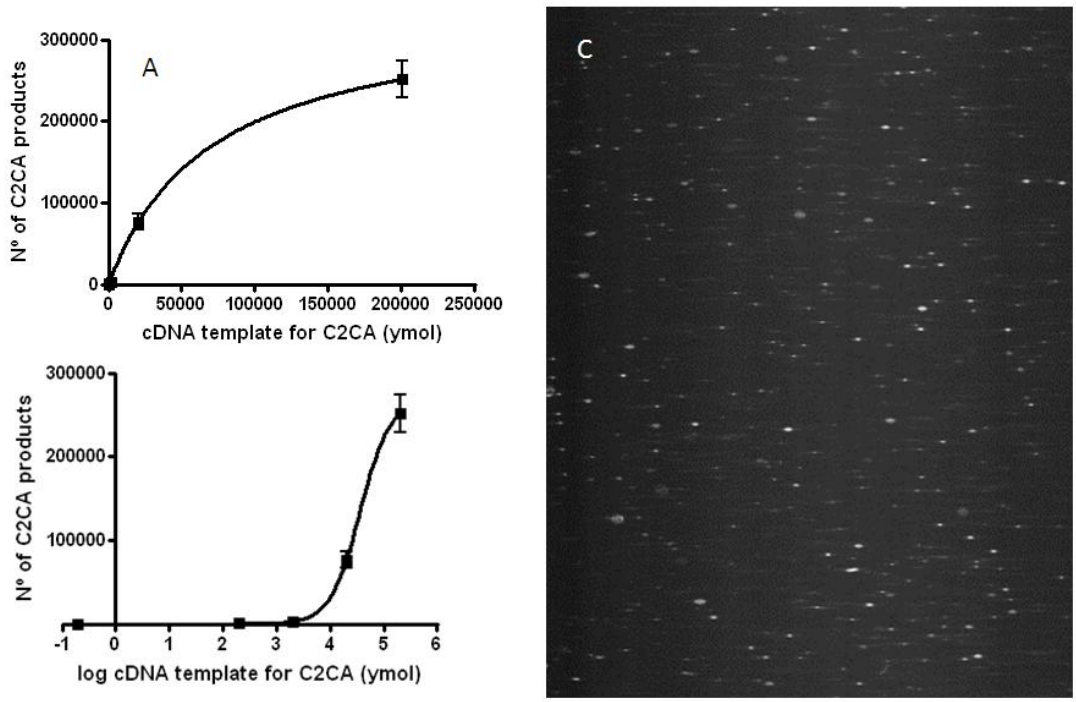

Figure S6.4. C2CA product quantification using state-of-the-art fluorescent RCA quantification using Aquila amplified single molecule counter (Q-linea, Sweden). The number of detected C2CA products is plotted against the number of target molecules added to the reaction. (X axis in logarithmic scale. The error bars show the standard deviation of the mean value. n=2.

The raw results are presented in Figure S6.4, panel A. The fluorescence signal was fitted using a nonlinear regression (One-site binding, Hyperbola– GraphPad Prism Software) (R^2= 0.9991). The LOD was estimated by fitting the raw data using a nonlinear regression (Four Parameter logistic Equation– GraphPad Prism Software) (R^2= 0.9999), as shown in Figure S6.4,

panel B, by processing the negative control samples (n=2) obtaining a mean value of 47 (N° of C2CA products) with a standard deviation of 19.67. The cut-off value was then determined with a one-tailed t test at a 95% confidence level (t=6.314), giving a value of 171 cDNA molecules (N° of C2CA products). Additionally, Figure S6.4, panel C, shows the bright fluorescence dots corresponding to each C2CA entities which were count with the Q-linea system.

6.8 References

[1] Mullis, K. B., Faloona, F. A. (1987). Specific synthesis of DNA in vitro via a polymerase-catalyzed chain reaction. Methods in Enzymology, 155, 335–350.

[2] Saiki, R. K., Gelfand, D. H., Stoffel, S., Scharf, S. J., Higuchi, R., Horn, G. T., Mullis, K. B., Erlich, H. A. (1988). Primer-directed enzymatic amplification of DNA with a thermostable DNA polymerase. Science, 239(4839), 487-491.

[3] Pividori, M. I., Merkoci, A., Barbe, J., Alegret, S. (2003). PCR-genosensor rapid test for detecting salmonella. Electroanalysis, 15(23-24), 1815-1823.

[4] Lermo, A., Campoy, S., Barbe, J., Hernandez, S., Alegret, S., Pividori, M. I. (2007). In situ DNA amplification with magnetic primers for the electrochemical detection of food pathogens. Biosensors and Bioelectronics, 22(9-10), 2010-2017.

[5] Brasil de Oliveira Marques, P. R., Lermo, A., Campoy, S., Yamanaka, H., Barbe, J., Alegret, S., Pividori, M. I. (2009). Double-tagging polymerase chain reaction with a thiolated primer and electrochemical genosensing based on gold nanocomposite sensor for food safety. Analytical chemistry, 81(4), 1332-1339.

[6] Liébana, S., Lermo, A., Campoy, S., Barbé, J., Alegret, S., Pividori, M. I. (2009). Magneto immunoseparation of pathogenic bacteria and electrochemical magneto genosensing of the double-tagged amplicon. Analytical chemistry, 81(14), 5812-5820.

[7] Liébana, S., Spricigo, D. A., Cortés, M. P., Barbé, J., Llagostera, M., Alegret, S., Pividori, M. I. (2013). Phagomagnetic separation and electrochemical magneto-genosensing of pathogenic bacteria. Analytical chemistry, 85(6), 3079-3086.

[8] Carinelli, S., Martí, M., Alegret, S., Pividori, M. I. (2015). Biomarker detection of global infectious diseases based on magnetic particles. New biotechnology, 32(5), 521-532.

[9] Urdea, M., Penny, L. A., Olmsted, S. S., Giovanni, M. Y., Kaspar, P., Shepherd, A., Wilson, P., Dahl, C.A., Buchsbaum, S., Moeller, G., Hay Burgess, D. C. (2006). Requirements for high impact diagnostics in the developing world. Nature, S1, 73-79.

[10] Niemz, A., Ferguson, T. M., Boyle, D. S. (2011). Point-of-care nucleic acid testing for infectious diseases. Trends in biotechnology, 29(5), 240-250.

[11] Li, J., Macdonald, J. (2015). Advances in isothermal amplification: novel strategies inspired by biological processes. Biosensors and Bioelectronics, 64, 196-211.

[12] Vincent, M., Xu, Y., Kong, H. (2004). Helicase-dependent isothermal DNA amplification. EMBO reports, 5(8), 795-800.

[13] Notomi, T., Okayama, H., Masubuchi, H., Yonekawa, T., Watanabe, K., Amino, N., Hase, T. (2000). Loop-mediated isothermal amplification of DNA. Nucleic acids research, 28(12), e63-e63.

[14] Lizardi, P. M., Huang, X., Zhu, Z., Bray-Ward, P., Thomas, D. C., & Ward, D. C. (1998). Mutation detection and single-molecule counting using isothermal rolling-circle amplification. Nature genetics, 19(3), 225-232.

[15] Baner, J., Nilsson, M., Mendel-Hartvig, M., Landegren, U. (1998). Signal amplification of padlock probes by rolling circle replication. Nucleic acids research, 26(22), 5073-5078.

[16] Tomita, N., Mori, Y., Kanda, H., & Notomi, T. (2008). Loop-mediated isothermal amplification (LAMP) of gene sequences and simple visual detection of products. Nature protocols, 3(5), 877-882.

[17] Demidov, V. V. (2002). Rolling-circle amplification in DNA diagnostics: the power of simplicity. Expert review of molecular diagnostics, 2(6), 542-548.

[18] Dahl, F., Banér, J., Gullberg, M., Mendel-Hartvig, M., Landegren, U., Nilsson, M. (2004). Circle-to-circle amplification for precise and sensitive DNA analysis. Proceedings of the National Academy of Sciences of the United States of America, 101(13), 4548-4553.

[19] Nilsson, M., Malmgren, H., Samiotaki, M., Kwiatkowski, M., Chowdhary, B. P., Landegren, U. (1994). Padlock probes: circularizing oligonucleotides for localized DNA detection. Science, 265, 2085-2088.

[20] Banér, J., Isaksson, A., WaldenstroÈm, E., Jarvius, J., Landegren, U., Nilsson, M. (2003). Parallel gene analysis with allele-specific padlock probes and tag microarrays. Nucleic acids research, 31(17), e103.

[21] Mezger, A., Öhrmalm, C., Herthnek, D., Blomberg, J., Nilsson, M. (2014). Detection of rotavirus using padlock probes and rolling circle amplification. PloS one, 9(11), e111874.

[22] Hartman, A. L., Towner, J. S., Nichol, S. T. (2010). Ebola and marburg hemorrhagic fever. Clinics in laboratory medicine, 30(1), 161-177.

[23] Gire, S. K., Goba, A., Andersen, K. G., Sealfon, R. S., Park, D. J., Kanneh, L., Jalloh, S., Momoh, M,. Fullah, M., Dudas, G., Wohl, S., Moses, L. M., Yozwiak, N. L., Winnicki, S., Matranga, C. B., Malboeuf, C. M., Qu, J., Gladden, A. D., Schaffner, S. F., Yang, X., Jiang, P. P., Nekoui, M., Colubri, A., Coomber, M. R., Fonnie, M., Moigboi, A., Gbakie, M., Kamara, F. K., Tucker, V., Konuwa, E., Saffa, S., Sellu, J., Jalloh, A. A., Kovoma, A., Koninga, J., Mustapha, I., Kargbo, K., Foday, M., Yillah, M., Kanneh, F., Robert, W., Massally, J. L., Chapman, S. B., Bochicchio, J., Murphy, C., Nusbaum, C., Young, S., Birren, B. W., Grant, D. S., Scheiffelin, J.S., Lander, E. S., Happi, C., Gevao, S. M., Gnirke, A., Rambaut, A., Garry, R. F., Khan, S. H., Sabeti, P. C. (2014). Genomic surveillance elucidates Ebola virus origin and transmission during the 2014 outbreak. Science, 1259657.

[24] World Health Organization. (2014). Urgently Needed: Rapid, Sensitive, Safe and Simple Ebola Diagnostic Tests. Geneva: WHO. Available in http://www.who.int/mediacentre/news/ebola/18-november-2014-diagnostics/en/.

[25] Jarvius, J., Melin, J., Göransson, J., Stenberg, J., Fredriksson, S., Gonzalez-Rey, C., Bertilsson S., Nilsson, M. (2006). Digital quantification using amplified single-molecule detection. Nature methods, 3(9), 725-727.

[26] Kühnemund, M., Nilsson, M. (2015). Digital quantification of rolling circle amplified single DNA molecules in a resistive pulse sensing nanopore. Biosensors and Bioelectronics, 67, 11-17.

[27] Towner, J. S., Rollin, P. E., Bausch, D. G., Sanchez, A., Crary, S. M., Vincent, M., Lee, W. F., Spiropoulou, C. F., Ksiazek, T. G., Lukwiya, M., Kaducu, F., Downing, R., Nichol, S. T. (2004). Rapid diagnosis of Ebola hemorrhagic fever by reverse transcription-PCR in an outbreak setting and assessment of patient viral load as a predictor of outcome. Journal of virology, 78(8), 4330-4341.

[28] Mezger, A., Öhrmalm, C., Herthnek, D., Blomberg, J., Nilsson, M. (2014). Detection of rotavirus using padlock probes and rolling circle amplification. PloS one, 9(11), e111874.

Chapter 7

FINAL CONSIDERATIONS AND CONCLUDING REMARKS

This dissertation addresses the design of novel diagnosis methods based on the integration of magnetic particles in order to improve the features of the diagnostic tests of communicable diseases. Infectious diseases are becoming a major threat worldwide due to the dissemination and adaptation of pathogens favored by cultural globalization and increasing migration and traveling. The design of diagnostic tests for the rapid identification of the infectious agent enables to improve human health and to save economic resources, by the selection of an appropriate treatment and following-up. In this field, clinical diagnosis has evolved in two different directions. On the one hand, the progress is focused on the development of complex and automatized benchtop instrumentation, resulting in powerful and efficient technologies. These innovative instruments opened the door for diagnostic procedures more accurate, less invasive, and safer for the patients. However, these technologies imply, in many cases, high complexity centers, high maintenance requirements and skilled personnel.

On the other hand, clinical diagnosis has led to the development of simple, portable, cost-effective devices which provides rapid results at point-of-need in low resource settings. At the level of primary care, particularly in rural areas, reliable transport of samples to centralized laboratory is a challenge that has to face with. The long distances from rural hospitals to central laboratories, and the low number of this kind of facilities result in the saturation of analytical laboratories and the delay in the results back. Point-of-Care (POC) devices are simple procedures that can be performed in small healthcare centers and regional laboratories with limited facilities. Therefore, new methodologies are needed for low-resource settings, to address the ASSURED recommendation published by the World Health Organization, being defined as Affordable, Sensitive, Specific, User-friendly, Rapid and Robust, Equipment-free, and Delivered to those who need it.

Among them, electrochemical sensors are devices that might solve many issues by reducing test complexity in a platform that would be useful in low resource settings. These devices possess a great potential for many applications, ranging from continuous in-line monitoring to rapid and in situ detection of an analyte in different fields such as environmental, agriculture, pharmaceutical, food-safety, healthcare, among others.

Along this dissertation, electrochemical readout was explored for biosensing devices for biomarkers detection of communicable diseases. Mass production of robust and reproducible transducers has allowed the fabrication of disposable and easy-to-hand electrodes at a very low cost. Solid electrodes based on carbon material were described along different sections. The procedure for the fabrication of magneto-actuated graphite-epoxy composite (m-GEC) electrode, involving the graphite-epoxy composite preparation, the integration of a magnet

and the paste into the transducer body, the curing, and the renewal of the surface was extensively explored. The m-GEC electrodes have demonstrated remarkable performance in different applications in biosensing strategies based on amperometric detection coupled with magnetic particles. All the results have shown the good characteristic of m-GEC electrodes in terms of reproducibility and reusability by a simple renewal of the electrode surface.

The integration of micro and nano magnetic particles has provided a remarkable improvement in the biosensing performance. Magnetic particles consist of a magnetic core coated with non-conducting polymers that prevent the formation of aggregates and facilitates the functionalization of the surface. Superparamagnetic particles are especially attractive due to their capability to magnetize by applying an external magnetic field. Magnetic particles conjugated to biomolecules can bind to specific ligands, making its separation by magnetic actuation highly selective. The bound material can be rapidly and efficiently separated from the rest of the sample by removing the unbound material, and resuspending it in a clean solution, avoiding thus interferences. Moreover, due to the magnetism, MPs can be used as solid support for sample immobilization on the magnetic surface by magnetic actuation. The electrodes used in this dissertation have incorporated a magnet inside the body of the transducer. This procedure allowed the simple and rapid immobilization of biomolecules on the electrode without the need of chemical modification of the transducer and further regeneration. Magnetic particles can be integrated to different procedures such as immunoassays, nucleic-acid amplification, and platforms including microfluidics and biosensors. The integration of the MPs on diagnostic tests for the most important infectious diseases (including HIV, Dengue, Influenza virus, Mycobacterium, and Malaria) was extensively described in "*Biomarker detection of global infectious diseases based on magnetic particles*" (New biotechnology, 2015, 32(5), 521-532).

In this dissertation, iron oxide-based MPs modified with specific antibodies, affinity proteins such as streptavidin and oligonucleotides were combined with different platforms for the detection of communicable diseases. Its implementation involved the preconcentration of the sample such as the cell isolation described in chapter 3 and 4, and nucleic-acid sequences purification, in chapter 5 and 6. The performance of magnetic separation was studied and evaluated in all cases. The immunomagnetic separation of lymphocytes from whole blood showed an outstanding efficiency. In the case of polydT-MPs, the efficiency in the mRNA purification was accordingly compared with the gold standard RNA extraction methods using ethanol precipitation and column purification, showing no significant differences among both procedures. The integration of polydT-MPs and the magnetic actuation simplified the mRNA

isolation procedure, avoiding precipitation and centrifugation steps. Furthermore, streptavidin-MPs were incorporated in biosensing strategies for the specific binding of biotinylated targets based on the high affinity of biotin-streptavidin interaction. It is widely known that streptavidin-biotin binding are unaffected by temperature, change in the pH, the presence of denaturing agents, among others. Taking advantage of this property, streptavidin-MPs were satisfactorily implemented as solid support in the nucleic acid isothermal amplification techniques for Ebola virus detection. Moreover, these particles were integrated for the IFN-γ detection based on the immobilization of the double-tagged amplicons on the electrode surface.

Moreover, in this dissertation, two different magneto-actuated strategies for HIV monitoring, integrating magnetic particles were presented. Since the first report of HIV infection, tens of millions of people have been infected with HIV and died. HIV preferentially destroys CD4 T lymphocyte. Therefore, CD4 counting can be considered an important biomarker of the progress of the infection. Flow cytometry is still considered the gold standard for CD4 count. This technique presents a high accuracy, precision, sample throughput, and reproducibility. However, its main drawback is the relative high cost of the instruments, reagents, as well as the instrument maintenance. Unfortunately, the most affected areas by HIV are resource-limited countries, wherein the availability of CD4 count by flow cytometry is limited. The core of the problem is that current CD4 technology is too sophisticated and inappropriate in the context in which it should be mainly used.

To achieve low-cost and reliable point-of-care HIV monitoring test for resource-constrained communities, two alternatives were developed based on magneto actuated platforms with optical and electrochemical readouts for CD4 quantification in whole blood. Both strategies used a double recognition, based on both CD3 and CD4 receptors, for the immunomagnetic separation and for the labeling and readout, respectively. As not only T lymphocytes express CD4 receptors, the strategy based on a dual biorecognition avoids interferences of other immunological cells expressing CD4 receptors, for instance, monocytes, macrophages, and dendritic cells. The CD4 quantification relied on peroxidase conjugated antibodies to obtain either the absorbance or the electrochemical signal to a number of CD4 cells. Both tests were validated in spiked leukocyte depleted whole blood samples, showing that the presence of any CD4 protein in the soluble fraction or other CD4 cell populations did not interfere in the test performance. Optical and electrochemical interferents present in whole blood such as red cells, salicylic acid, dopamine, bilirubin, heme group, cholesterol, creatinine, uric acid, among others, are avoided due to the use of magnetic particles. Therefore, due to the high specificity

of the antibodies, all the components of the matrix were removed during magnetic actuation and washing, eliminating all the interfering compounds. Both approaches are promising alternatives for the costly standard method based on flow cytometry. The magneto-actuated ELISA was able to reach the whole CD4 counting range of medical interest, being the limit of detection as low as 50 CD4+ cells per µL of whole blood. On the other hand, the limit of detection for the CD4 counting magneto-actuated biosensor in whole blood was as low as 44 cells μL^{-1} with a logistic range from 89 to 912 cells μL^{-1}, which spans the whole medical range for CD4 counts in AIDS patients. These methods are highly suitable alternative diagnostic tools at the community and primary care level, providing sensitive methods, but by using instrumentation widely available in low-resource settings laboratories, as is the case of a microplate reader or by using simple biosensors.

Another approach which was explored was for the detection of latent tuberculin infection (LTBI) and other intracellular infections. Tuberculosis is an infectious disease caused by the bacteria *Mycobacterium tuberculosis*. Identifying LTBI is fundamental to establish the diagnosis and treatment, reducing the risk of progression to active tuberculosis and the transmission within the population. The challenge of identifying LTBI-infected individuals lies in the lack of a diagnostic gold standard test. Tuberculin skin test (TST) and interferon-gamma release assays (IGRA) are the two tests that currently support this diagnosis. TST is based on the injection under the skin of tuberculin derived proteins and subsequent identification of an immune reaction at the site of injection several weeks later. A limitation of the TST is that the mixture of antigens used are not specific for *M. tuberculosis*, and therefore it is unable to differentiate between an existing immune response elicited by either, previous bacille Calmette-Guérin vaccination, exposure to nontuberculous *Mycobacterium*, or *M. tuberculosis* infection.

In this dissertation, this challenging goal was addressed by the design of a novel IGRA test based on electrochemical for the detection of IFN-γ transcripts produced by isolated T lymphocytes. To the extent of our knowledge, this was the first time that a biosensor for the detection of IFN-γ transcripts produced by isolated T cells was reported. The approach combined the advantages of the integration of MPs for immunomagnetic separation of the T cells on antiCD3-MPs, the multiplex amplification and double-tagging of the IFN-γ transcript (and GAPDH as housekeeping control) on polydT-MPs, and finally, the electrochemical genosensing on magneto electrodes using streptavidin-MPs as solid support.

The amplification of target nucleic-acid sequences using techniques such as Polymerase Chain Reaction can improve the test sensitivity up to 100-fold over immunoassays, such as ELISA or ELISPOT test. The electrochemical genosensor was able to quantify the transcripts

produced by as low as 150 cells for IFN-γ and only 3 cells for the housekeeping transcript used as positive control. An advantage of this method compared with the commercial IGRA test was that the T cells producing IFN-γ were specifically separated from whole blood by immunomagnetic separation, increasing the sensitivity of the assay and removing potentially interfering substances that can affect the test results. In the IGRA approach presented here, the PCR was used not only for the amplification of specific transcripts, but also for double-labeling of the amplicon with biotin/fluorescein and biotin/digoxigenin for IFN-γ and GAPDH transcript, respectively. The double-tagging PCR allowed the amplification of the analytical signal by amplifying the IFN-γ transcript in a rapid way, instead of detecting the IFN protein secreted by stimulated lymphocytes. The biotinylated tag was used for the rapid immobilization of the amplicons on the streptavidin-MPs, while the fluorescein and digoxigenin tags, for the labeling and detection with the specific antibodies, antifluorescein-HRP and antidigoxigenin-HRP, coding for IFN-γ and GAPDH, respectively, and performed in two separated reaction chambers. Moreover, available IGRA tests require up to 4-5 mL of blood obtained by extraction, while the detection of IFN-γ transcripts was performed from only 100 μL of whole blood, which can be potentially obtained by fingerprick, demonstrating a clear advantage over commercial test. In addition, the electrochemical genosensor can detect the IFN-γ mRNA in contrast to the other methods that are based on the detection of IFN-γ protein.

The specificity of the genosensing approach was conferred by both the antibody in the immunomagnetic separation of lymphocytes and the set of primers used during the double-tagging PCR. This analytical parameter was accordingly studied by the detection of a specific gene in the presence of the other amplicon. The electrochemical genosensing showed a great capability to clearly distinguish among the two different transcripts and its single and binary combinations. Finally, the performance of this approach was evaluated in whole blood from anonymized sample of healthy donors by stimulating the isolated lymphocytes with phytohemagglutin. Phytohemagglutin is a protein that simulates the event which occurs during intracellular infection such as the stimulation of cell division and the induction of de novo synthesis of cytokines as IFN-γ. Thus, the electrochemical genosensor was able to determine the functional production of cytokines by the lymphocytes upon stimulation, converting it into a potential candidate for the detection of inflammatory proteins. The same approach could also be designed for other clinical applications by selecting the appropriate antigen for T cell stimulation or by selecting a specific pair of primers to amplify and quantify other inflammatory biomarker. The electrochemical genosensor for IFN-γ transcript detection results in a promising alternative to the current IGRA test in the market for being used to screen-out

population at primary health care in low-resource settings. Furthermore, the electrochemical genosensor has the advantage of combining high sensitivity/specificity as well as simplicity of instrumentation, and can be easily expanded into multiplex detection platform. Therefore, the development of the electrochemical sensing platform is a significant step towards a low cost, sensitive, and specific transcript detection of IFN-γ.

Over the last decade, the development and application of molecular diagnostic techniques have initiated a revolution in the diagnosis and monitoring area. PCR is the gold standard for nucleic acid detection in laboratory analysis due to its well-standardized methodology, its extensively validated operation procedure and its availability of reagent and equipments. However, PCR has limited use at point-of-care, although some portable equipments able to be operated by batteries are currently being developed. Isothermal amplification methods are also emerging as good candidates to replace PCR-based amplification, since these techniques are compatible with POC test and can be applied in low resource settings where the lack of reliable power supply, trained personnel and specialized facilities are critical barriers. Isothermal amplification prevents the use of thermal cycler since the amplification reactions occur at a single temperature.

During the 2014 Ebola outbreak, the priority in controlling this epidemic was the rapid identification and isolation of infected individuals. A prompt Ebola diagnosis decrease the time a suspected patient spends in an Ebola health facility, and therefore the chances of infection with Ebola virus while waiting for the test result. On the other hand, highly accurate tests decrease the possibility of false negative results, and consequently, the dissemination of the disease due to misdiagnosis.

The design of an Ebola test as an alternative to the gold standard PCR-based method involving low technology, specific and highly sensitive procedure using an isothermal amplification method and magnetic particles with electrochemical readout was presented. The strategy combined isothermal DNA amplification, based on rolling circle amplification (RCA) and circle-to-circle amplification (C2CA), with electrochemical genosensing. In our strategy, biotinylated capture oligonucleotides were immobilized on magnetic particles by biotin-streptavidin interaction. The oligonucleotide was designed such that it binds to a specific sequence closer to the 5´- regarding the target sequence, allowing specific target isolation by magnetic force. Moreover, high concentration of padlock probes was required to achieve a full ligation efficiency in a short time. However, high concentrations of unreacted padlock probe interfere with the RCA reaction. The integration of magnetic particles in the assay allowed

washing steps to remove all the unreacted padlock probes and significantly reduced the assay time from several hours to several minutes.

Padlock probes were designed to specifically detect *L-gene* sequences present in *Ebolavirus*. Padlock probes are linear oligonucleotide probes that have the target recognition sequences situated at both 5´- and 3´- end connected by an intervening sequence that include detection elements. The simultaneous hybridization of two primer segments and the ligation reaction to close the padlock probe ends provide a high specificity and selectivity to the identification and detection of specific nucleic acid sequences. Furthermore, the circularization by ligation requires that both target complementary probe arms hybridize to the target sequence perfectly, increasing the specificity of the assay.

During the rolling circle amplification reaction, a circular template is continuously amplified by the polymerase enzyme creating multiple concatenated copies. As the amplification products contain a detection sequence, it can be labeled by using tag-oligonucleotides that hybridized to detection sequences introduced in the padlock probe backbone. Most of DNA detection methods rely on fluorescent labels. RCA/C2CA products can be detected as bright fluorescent spot when labeled with fluorescent-labeled oligonucleotide probes. However, these systems depend on expensive and sophisticated instruments to achieve a high sensitive readout. The electrochemical detection of amplified product using peroxidase-oligonucleotides was accordingly compared with the state-of-art fluorescent RCA/C2CA quantification showing similar limit of detection. This fact demonstrated the high sensitivity of the electrochemical detection system, achieved by the combination of enzymatic labeling.

The electrochemical genosensing strategy presented a limit of detection of 966 zmol of *L-gene* sequences, corresponding to ≈ 6×10^5 molecules of cDNA targets with a single RCA. In order to improve the limit of detection, C2CA amplification has been evaluated. In C2CA, the generated RCA products were enzymatically digested into monomers, religated forming new circles and further reamplified in a second round of RCA. The electrochemical genosensor combined with C2CA was thus able to reach a LOD of as low as 33 molecules of cDNA target, corresponding to 1.65×10^4 molecules of cDNA target mL^{-1}. The number of C2CA products generated during amplification depends on the amount of monomers generated in the first RCA and, in consequence, on the time of the reaction. The boost in the number of amplimers was achieved at the expense of increasing the assay time and the complexity of it. Despite several advantages of C2CA over conventional PCR assays its major drawback is that the C2CA assay consists of several manual steps which are cumbersome and time consuming. Nevertheless, rolling circle amplification reached an acceptable limit of detection for Ebola

virus diagnosis, where high levels of viremia were reported (ranging from 10^6 to 10^{10} RNA copies per mL).

Finally, Ebola test based on immunoassays requires blood transportation to BSL-4 laboratories to be tested. Blood sample analyzed by molecular diagnosis can be rapidly inactivated using strong detergents or physical method to destroy Ebola virus, keeping intact the viral RNA for their analysis. Thus, the test can be performed at BSL-2 facilities or mobile laboratories, reducing the risk of infection during the sample manipulation and reducing the requirement of BSL-4 facilities. The electrochemical genosensing approach has demonstrated to be a powerful combination for highly specific and sensitive nucleic acid detection that can be applied in clinical diagnosis. To the best of our knowledge, it was the first time that rolling circle/circle-to-circle amplification on magnetic particles was integrated in the same strategy with electrochemical readout.

Summarizing, electrochemical biosensors hold in a distinct position to cover the current demand of modern point of care technologies. Due to the robustness, simplicity, and its easy integration in different platforms, biosensing strategies in combination with MPs showed as a promising alternative for the detection of a wide number of analytes, from single and small molecules such as DNA/RNA to complex biological targets such as T lymphocytes.

Chapter 8

SCIENCE COMMUNICATIONS

8.1 List of Publications

The work carried out during this dissertation was published in different international journals.

- **Carinelli, S.**, Martí, M., Alegret, S., & Pividori, M. I. (2015). Biomarker detection of global infectious diseases based on magnetic particles. *New biotechnology*, *32*(5), 521.

- **Carinelli, S.**, Ballesteros, C. X., Martí, M., Alegret, S., & Pividori, M. I. (2015). Electrochemical magneto-actuated biosensor for CD4 count in AIDS diagnosis and monitoring. *Biosensors and Bioelectronics*, *74*, 974-980.

- **Carinelli, S.**, Xufré, C., Alegret, S., Martí, M., & Pividori, M. I. (2016). CD4 quantification based on magneto ELISA for AIDS diagnosis in low resource settings. *Talanta*, *160*, 36-45.

- Pividori, M. I., Aissa, A. B., Brandao, D., **Carinelli, S.**, & Alegret, S. (2016). Magneto actuated biosensors for foodborne pathogens and infection diseases affecting global health. In *Biosensors for Security and Bioterrorism Applications* (pp. 83-114). Springer International Publishing.

- **Carinelli, S.**, Kühnemund, M., Nilsson, M., & Pividori, M. I. (2017). Yoctomole electrochemical genosensing of Ebola virus cDNA by rolling circle and circle to circle amplification. *Biosensors and Bioelectronics*, *93*, 65-71.

- **Carinelli, S.**, Ballesteros, C. X., Martí, M., & Pividori, M. I. (2018). Interferon gamma transcript detection on T cells based on magnetic actuation and multiplex double-tagging electrochemical genosensing. *Biosensors and Bioelectronics, 117,* 183-190.

8.2 Conferences and congresses

The work carried out during this dissertation was also presented in numerous congresses and conferences, both national and international.

8.2.1 Oral communications

- Biosensor 2016. 26th Anniversary World Congress on Biosensor. 25-27 May 2016. Gothenburg, Sweden.
- XX SIBEE "XX Simpósio Brasileiro de Eletroquímica e Eletroanalítica". 17-21 August 2015. Uberlandia, Brasil.
- Diatech: Novel technologies for in vitro diagnostics. 6-8 October 2014. Leuven, Belgium.
- Summer school "Magnetic particles based platforms and bioassays". 30th June-3rd July 2014. Bellaterra, Spain.
- XVIII Trobada Transfrontera de Sensors I Biosensors Conference. 19-20 September 2013. Alès, France.
- VII International Workshop on Sensors and Molecular Recognition. 4-5 July 2013. Valencia, Spain.
- XVII Trobada Transfronterera on Sensors and Biosensors. 20-21 September 2012. Tarragona, Spain.

8.2.2 Poster presentations

- 12th International Conference on the Scientific and Clinical Applications of Magnetic Carriers. 22-26 May 2018. Copenhagen, Denmark.

- Biosensor 2016. 26th Anniversary World Congress on Biosensor. 25-27 May 2016. Gothenburg, Sweden.

- Jornades del Departament de Biologia Cel·lular Fisiologia i Immunologia. 3rd June 2015. Bellaterra, Spain.

- CEITEC (Central European Institute of Technology) Annual conference Frontiers in Life and Materials Science. 21-24 October 2014. Brno, Czech Republic.

- 3rd International Conference on Bio-Sensing Technology. 12-16 May 2013. Sitges, Spain.

- Ibero-American Congress on Sensors-Ibersensors. 16-19 October 2012. Carolina, Puerto Rico.

- First Workshop on Nanomedicine UAB-CEI. 5th June 2012. Universitat Autònoma de Barcelona, Spain.

- 9th International Conference on the Scientific and Clinical Applications of Magnetic Carriers. 23-26 May 2012. Minneapolis, USA.

8.3 Workshops and courses

The following workshops and courses were organized during this PhD thesis, including parts of the work and techniques developed in this dissertation:

- 4th Bioanalytical Nanotechnology school (www.bantschool.org). 25-29 January 2016. São Luís, Maranhão, Brasil.

- Summer school "Magnetic particles based platforms and bioassays". 30th June-3rd July, 2014. Bellaterra, Spain.

- 3rd Bioanalytical Nanotechnology school (www.bantschool.org). 29th January-1st February 2014. Manila, the Philippines.

- Seminars in highschool. Project “Parla, experimenta I xateja amb algú que fa ciencia a Barcelona… i a Catalunya”, Observatori de Difusió de la Ciència at Universitat Autònoma de Barcelona (www.odc.cat). 2012-2013.

The following courses were attended during this PhD thesis, as part of the training in new research areas or technical expertise.

- Microfabrication/Microfluidics. 24th June 2013. Lausanne, Switzerland.
- Advance techniques in Molecular Medicine. 24-26 October 2012. Uppsala, Sweden.
- Systems architecture of integrated biosensors. 13-15 February 2012. Eindhoven, Netherlands.

8.4 Scientific awards

- 2015. Award for Scientific Photography contest. “El hijo prodigo”. VII Jornada del Departament de Biologia Cel·lular, Fisiologia i Immunologia.

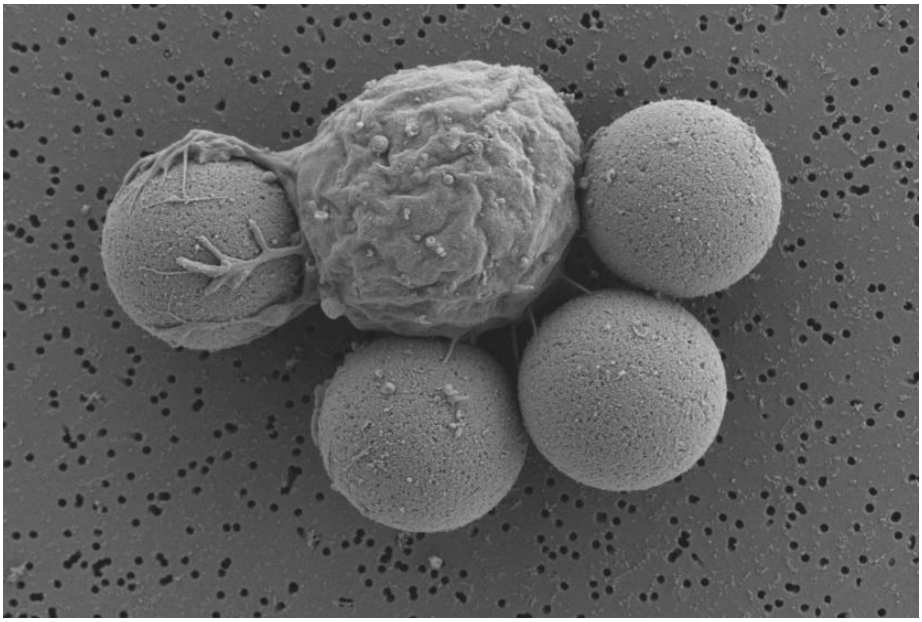

- 2013. Award for outstanding Poster Presentation. Authors: S. Carinelli, C. Xufré Ballesteros, M. Martí, S. Alegret, M.I. Pividori. Title: Biosensor for AIDS diagnosis and monitoring. 3rd International Conference on Bio-Sensing Technology. 12-16 May 2013. Sitges, Spain.